Insights into mechanisms of resistance to apoptosis in Epstein-Barr virus-associated T and NK cell lymphomas

by

NENAD SEJIC

A thesis submitted to

The University of Birmingham

for the degree of

DOCTOR OF PHILOSOPHY

Institute of Immunology and Immunotherapy

College of Medical and Dental Sciences

The University of Birmingham

September 2018

UNIVERSITY OF
BIRMINGHAM

University of Birmingham Research Archive

e-theses repository

This unpublished thesis/dissertation is copyright of the author and/or third parties. The intellectual property rights of the author or third parties in respect of this work are as defined by The Copyright Designs and Patents Act 1988 or as modified by any successor legislation.

Any use made of information contained in this thesis/dissertation must be in accordance with that legislation and must be properly acknowledged. Further distribution or reproduction in any format is prohibited without the permission of the copyright holder.

Abstract

Ectopic Epstein-Barr virus (EBV) infection of T or NK cells is associated with several aggressive diseases including extra-nodal NK/T cell lymphoma (ENKTL) and chronic active EBV (CAEBV). Resistance to standard chemotherapy results in extremely poor patient prognosis. This thesis aimed to uncover the cellular and viral mechanisms behind such resistance, and to identify vulnerabilities for therapeutic targeting. An extensive collection of patient-derived cell lines demonstrated an EBV latency II phenotype and exhibited resistance to clinically administered genotoxic compounds. Importantly, apoptotic cell death could be consistently induced following treatment with the BH3 mimetic, A-1331852, that inhibits the BCL-2 pro-survival protein, BCL-X_L. Furthermore, A-1331852 proved effective in 1 of 3 newly developed xenograft NSG mouse models. In the two non-responder cell lines, it was shown that BCL-X_L dependency was potentially maintained by viral LMP1 in an IL-2-dependent manner. IL-2 withdrawal in vitro, emulating the in vivo environment, led to a survival dependency switch from BCL-X_L to MCL-1, and ultimately a reduced response to A-1331852. Finally, to identify novel cytotoxic drugs for ENKTL and CAEBV, a high-throughput screen of 4079 compounds was performed. This identified a shortlist of effective hits for further study in these severe diseases where targeted treatment options are unexplored.

Acknowledgements

Firstly, I would like to thank my supervisors at the University of Birmingham, Dr. Claire Shannon-Lowe and Dr. Heather Long, and at WEHI, Dr. Gemma Kelly and Prof. Andreas Strasser. I am forever very grateful for the contribution each of them has made to my development as a scientist and for the opportunities they have given me.

For their expertise, discussions and technical help, I would like to thank the many members of the EBV research groups in Birmingham, particularly Dr. Andy Bell, Dr. Rosemary Tierney and Dr. Leah Fitzsimmons. I would also like to thank the Molecular Genetics of Cancer Division at WEHI for their assistance in the laboratory and for training in cell death research, particularly Ms. Catherine Chang, Ms. Margs Brennan and Dr. Robyn Schenk. I was very lucky to work with such talented people.

I would also like to thank the many WEHI services such as Bioservices, FACS facility and Histology. In particular, thanks to Dr. Kate Jarman and Dr. Helene Jousset of the Screening laboratory. Additionally, many thanks to the laboratories of A/Prof. Guillaume Lessene and Prof. David Huang for always providing compounds upon request.

This research was made possible thanks to funding from Universitas 21.

Finally, I would like to thank my friends for their encouragement, particularly during the writing of this thesis. I would like to thank my sister, Sonja, for making my life easy while I lived partially in Melbourne and partially in Birmingham. Mostly, I would like to thank Josephine for her love, her support and her ability to help with weekend tissue culture on occasion.

Contents

1. Introduction 1

1.1 Epstein-Barr virus 1

1.1.1 Discovery, classification and structure 1

1.1.2 EBV infection and cellular tropism 4

1.1.3 Lytic replication 8

1.1.4 Latent cycle 9

1.1.5 Latent genes 11

1.1.6 B cell malignancies 17

1.1.7 Epithelial cell malignancies 19

1.1.8 T cell and NK cell lymphoproliferative diseases 20

1.2 EBV-associated T and NK lymphoproliferative diseases 21

1.2.1 Extra-nodal NK/T cell lymphoma 21

1.2.2 Chronic active EBV 25

1.2.3 EBV infection of T and NK cells 26

1.2.4 Models of disease 32

1.2.5 Current and emerging therapies 35

1.3 Cell death and targeted therapy 39

1.3.1 Overview of apoptosis 39

1.3.2 Anti-apoptotic members of the BCL-2 family 48

1.3.3 Pro-apoptotic members of the BCL-2 family 57

1.3.4 Therapeutic targeting of the BCL-2 family 67

1.4 Aims of thesis 74

2. Materials and Methods 75

2.1 Cell culture 75

2.1.1 EBV-positive T and NK cell lines 75

2.1.2 EBV-negative T and NK cell lines 76

2.1.3 B cell lines 76

2.1.4 Generation of CAEBV cell line from patient blood 76

2.1.5 Cell cryopreservation and recovery 77

2.1.6 Revival of cryopreserved cells 77

2.2 RNA analysis 78

2.2.1 RNA purification 78

2.2.2 cDNA synthesis 78

2.2.3 Taqman qPCR for gene expression 79

2.2.4 High throughput qPCR 80

2.3 DNA analysis 81

2.3.1 DNA purification 81

2.3.2 *TP53* sequencing 81

2.3.3 Taqman qPCR for viral load 83

2.3.4 EBV typing 84

2.4 Western blotting 85

2.4.1 Protein preparation 85

2.4.2 Electrophoresis and blotting 86

2.4.3 Immunostaining 86

2.5 Flow cytometry 89

2.5.1 Cell surface staining 89

2.5.2 Rhodamine-123 staining 90

2.6 Cell death analysis 91

2.6.1 Apoptosis assays 91

2.6.2 Analysis 92

2.7 High throughput drug screen 93

2.7.1 Cells and compound libraries 93

2.7.2 Assay plate preparation 94

2.7.3 Drug treatment 94

2.7.4 Viability staining 95

2.7.5 Viability analysis 95

2.8 *In vivo* studies 96

2.8.1 Mice and disease monitoring 96

2.8.2 Drug treatments 96

2.8.3 *Ex vivo* cell culture 97

2.8.4 Histology 97

2.8.5 Haematology 97

2.9 Cytokine analysis 98

2.10 Statistical analysis 98

3. Results I: Characterisation of EBV-positive T and NK cell lines 100

3.1 Introduction 100

3.2 Cellular phenotype 102

3.2.1 Cell type lineage 102

3.2.2 γδ T cell and NK cell subtype markers 106

3.3 Cytokine, chemokine and growth factor production 110

3.4 Detection of EBV 115

3.4.1 Viral load 115

3.4.2 EBV subtyping 115

3.5 Viral gene expression 119

3.5.1 Latent gene expression 119

3.5.2 Expression of Latent membrane proteins 123

3.5.3 Lytic gene expression 125

3.6 Discussion 128

4. Results II: Resistance to chemotherapy and apoptotic evasion 135

4.1 Introduction 135

4.2 *In vitro* response to clinically relevant cytotoxic agents 138

4.3 Genotoxic drug tolerance via p-glycoprotein 142

4.3.1 *ABCB1* expression 142

4.3.2 Functional p-glycoprotein 143

4.4 Genotoxic drug resistance due to p53 pathway defects 147

4.4.1 Expression of p53 and MDM2 147

4.4.2 p53 gene sequencing 150

4.4.3 Non-genotoxic p53 activation 151

4.5 Evasion of apoptosis due to deregulated expression of BCL-2 family members 154

4.5.1 Expression of BCL-2 family members 154

4.5.2 BH3 mimetic drugs 159

4.5.3 Treatment with combinations of BH3 mimetic drugs 162

4.6 Establishment of a mouse model of disease 166

4.7 BH3 mimetic drug mediated inhibition of BCL-X_L *in vivo* 170

4.7.1 Subcutaneous models 170

4.7.2 Intraperitoneal models 176

4.7.3 Tumour cell dissemination in intraperitoneal models 183

4.8 The effect of IL-2 depletion on the sensitivity to BH3 mimetic drugs 186

4.8.1 Expression of BCL-2 family members and LMP1 186

4.8.2 Response to BH3 mimetic drugs 189

4.9 Discussion 192

5. Results III: Towards the development of novel therapies 198

5.1 Introduction 198

5.2 Assay optimisation 200

5.2.1 Cell number 200

5.2.2 DMSO tolerance 201

5.2.3 Assay variability 201

5.2.4 Control compounds 202

5.3 Primary screen: Data quality 207

5.4 Primary screen: Hit analysis 209

5.6 Discussion 217

6. Final discussion and future directions 221

7. References 230

8. Appendices 263

8.1 Appendix I 263

8.2 Appendix II 264

8.3 Appendix III 265

8.4 Appendix IV 266

8.5 Appendix V 267

List of Figures

Figure 1.1 Structure of EBV genome with gene and promoter positions. 3

Figure 1.2 EBV life cycle. 7

Figure 1.3 EBV latent gene expression. 10

Figure 1.4 Differentiation of T lymphocytes 28

Figure 1.5 Differentiation of Natural Killer cells. 30

Figure 1.6 Structural homology within the BCL-2 family. 43

Figure 1.7 Binding specificities of BCL-2 family members 46

Figure 1.8 Distinct apoptotic stimuli for different BH3-only proteins 58

Figure 2.1 Annexin V/PI assay gating strategy. 93

Figure 2.2 Plate map of compounds for drug screen. 94

Figure 3.1 Antibody testing for phenotyping panel #1 104

Figure 3.2 Analysis of ENKTL and CAEBV cell lines by phenotyping panel #1 105

Figure 3.3 Antibody testing for phenotyping panel #2 108

Figure 3.4 Analysis of ENKTL and CAEBV cell lines by phenotyping panel #2 109

Figure 3.6 Summary heat map of supernatant cytokines 114

Figure 3.7 EBV copies per cell 117

Figure 3.8 EBV typing of T and NK cell lines 118

Figure 3.9 Heat map summarising expression of latent viral transcripts 122

Figure 3.10 LMP1 mRNA expression 124

Figure 3.11 Heat map summarising the expression of lytic viral transcripts. 126

Figure 3.12 BHRF1 and BALF1 mRNA expression 127

Figure 4.1 Induction of cell death in T and NK cell lines..... 141

Figure 4.2 Background expression of the ABCB1 gene in T and NK cell lines..... 145

Figure 4.3 Detection of functional p-glycoprotein in EBV-positive T and NK cells 146

Figure 4.4 Expression of p53 and MDM2 protein in unstressed cells 148

Figure 4.5 Expression of p53 in T and NK lymphoma cell lines following genotoxic treatment 149

Figure 4.6 Non-genotoxic activation of p53 by nutlin3a 153

Figure 4.7 Expression of BCL-2 family members in T and NK cell lines in the absence of stress 157

Figure 4.8 Comparison of the expression of BCL-2 family members with the expression of LMP1 158

Figure 4.9 Cell survival analysis of EBV-positive T and NK cells following treatment with BH3 mimetic drugs 160

Figure 4.9 Cell survival analysis of EBV-positive T and NK cells following treatment with BH3 mimetic drugs 161

Figure 4.10 Cell survival analysis following combination treatments with BH3 mimetic drugs 164

Figure 4.11 Cell survival analysis following combination treatments with BH3 mimetic drugs 165

Figure 4.12 NSG xenograft protocol optimisation using EBV-positive T and NK cell lines. 169
Figure 4.13 Tumour latency of A-1331852-treated NSG mice in subcutaneous transplant models..... 173
Figure 4.14 Haematological analysis of A-1331852-treated NSG mice with subcutaneous SNK6 tumours 174
Figure 4.15 Haematological analysis of A-1331852-treated NSG mice with subcutaneous SNT15 tumours..... 175
Figure 4.16 Tumour latency of A-1331852-treated NSG mice in intraperitoneal models 180
Figure 4.17 Haematological analysis of A-1331852-treated NSG mice with subcutaneous SNK6 tumours 181
Figure 4.18 Haematological analysis of A-1331852-treated NSG mice with subcutaneous SNT15 tumours..... 182
Figure 4.19 Histological analysis of A-1331852-treated NSG mice with intraperitoneal injection of SNK6 or MEC04 tumours..... 185
Figure 4.20 Expression of pro-survival BCL-2 family members and viral LMP1 after IL-2 withdrawal 188
Figure 4.21 Cell survival analysis of IL-2 deprived SNK6 cells and SNT15 cells following treatment with BH3 mimetic drugs..... 191
Figure 5.1 Cell number optimisation..... 203
Figure 5.2 DMSO tolerance 204

Figure 5.3 Plate variability 205

Figure 5.4 Combination of the BH3 mimetic drugs A-1331852 and S63845 induces extensive killing of ENKTL and CAEBV cell lines 206

Figure 5.5 Control compounds successfully induce killing of ENKTL and CAEBV cell lines in the primary screen 209

Figure 5.6 Comparison of hits between cell lines 211

Figure 5.7 JAK2 inhibitors induce cell killing across the cell line panel 216

Supplementary figure 1 Viability of MEC04 cells following methotrexate treatment. 263

Supplementary figure 2 Expression of pro-survival BCL-2 family members following IL-2 removal. 264

Supplementary figure 3 Correlation between first and second replicates of primary screen for all compounds. 265

List of Tables

Table 2.1 List of qPCR assays. 80

Table 2.2 *TP53* primers 82

Table 2.3 Viral load primers 84

Table 2.4 EBV subtyping primers 85

Table 2.5 List of antibodies used for Western blot experiments 88

Table 2.6 List of antibodies used for flow cytometry analysis. 90

Table 2.7 List of drugs used for in vitro treatment of cell lines. 92

Table 4.1 Potency of genotoxic agents on T/NK cell lines 142

Table 4.2 p53 mutation status EBV-positive T and NK cells. 150

Table 4.3 Summary of mice excluded from analysis 178

Table 5.1 Primary screen: Z prime and robust Z prime values 208

Table 5.2 Hits per cell line. 212

Table 5.3 Total primary screen hits 212

Table 5.4 Most effective compounds from global hit list. 215

Supplementary table 1 Detection of functional p-glycoprotein in EBV-positive T and NK cells 266

Supplementary table 2 Binding affinities of BH3 mimetics to pro-survival BCL-2 family members 267

Abbreviations

AID	Activation-induced cytidine deaminase	CD	Cluster of differentiation
AIDS	Acquired immune deficiency syndrome	cDNA	Complementary DNA
AML	Acute myeloid leukaemia	CLL	Chronic lymphocytic leukemia
ANKL	Aggressive NK leukaemia	CLP	Common lymphoid progenitor
AQ	Absolute quantification	CML	Chronic myeloid leukaemia
ATP	Adenosine triphosphate	CMP	Common myeloid progenitor
B2M	Beta-2-microglobulin	COSMIC	Catalogue of Somatic Mutations in Cancer
BAC	Bacterial artificial chromosome	CRISPR	Clustered Regularly Interspaced Short Palindromic Repeats
BART	BamHI-A rightward transcript	CSA	Cyclosporin A
BCL	B cell lymphoma	Ct	Threshold cycle
BCR	B cell receptor	CTAR	C-terminal activating region
BL	Burkitt lymphoma	CTG	CellTiter-Glo
bp	Base-pair	CTL	Cytotoxic T lymphocytes
BSA	Bovine serum albumin	CYP	Cytochrome P450
CAD	Caspase activated DNAse	DISC	Death-inducing signalling complex
CAEBV	Chronic active EBV	DLBCL	Diffuse large B-cell lymphoma
CARD	Caspase recruitment domain	DMSO	Dimethyl sulphoxide

DNA	Deoxyribonucleic acid	GMP	Granulocyte-macrophage progenitor
dNTPs	Deoxynucleotide triphosphates	gp	Glycoprotein
EA	Early antigen	GSB	Gel sample buffer
EBER	Epstein-Barr virus-encoded small RNA	HDAC	Histone deacetylase inhibitors
EBNA	Epstein-Barr nuclear antigen	HDT	High-dose therapy
EBV	Epstein-Barr virus	HIV	Human immunodeficiency virus
EDTA	Diaminoethanetetraacetic acid	HL	Hodgkin's Lymphoma
EGFR	Epidermal growth factor receptor	HLA	Human leukocyte antigen
ENKTL	Extra-nodal NK/T cell lymphoma	HLH	Haemophagocytic lymphohistiocytosis
FACS	Fluorescence activated cell sorting	HRP	Horseradish peroxidase
FADD	Fas-associated protein with death domain	HSCT	Haematopoietic stem-cell transplantation
Fc	Fragment crystallisable region	HTS	High-throughput screen
FCS	Foetal calf serum	HV	Hydroa vacciniforme
G-CSF	Granulocyte colony-stimulating factor	IAP	Inhibitor of apoptosis protein
GAPDH	Glyceraldehyde-3-phosphate dehydrogenase	IE	Immediate early
GC	Gastric carcinoma	IFN	Interferon
GFP	Green fluorescent protein	Ig	Immunoglobulin
GM-CSF	Granulocyte-macrophage colony-stimulating factor	IHC	Immunohistochemistry

IL	Interleukin	miR	microRNA
IM	Infectious mononucleosis	MOMP	Mitochondrial outer membrane permeabilisation
IP	Intraperitoneal	NF-κB	Nuclear factor kappa B
IRF	Interferon regulatory factor	NIK	NF-kB inducing factor
kbp	Kilobase pair	NK	Natural killer
kDa	KiloDalton	NOD	Non-obese diabetic
KIR	Killer immunoglobulin-like receptor	NPC	Nasopharyngeal carcinoma
KO	Knock-out	NS	Nodular sclerosing
LCL	Lymphoblastoid cell line	NSCLC	Non small cell lung carcinoma
LD	Lymphocyte depleted	NSG	NOD-SCID-IL2rg$^{-/-}$
LMP	Latent membrane protein	ORF	Open reading frame
LP	Leader protein	oriP	Origin of plasmid replication
mAb	Monoclonal antibody	OS	Overall survival
MACS	Magnetic activated sorting	PAGE	Polyacrylamide gel electrophoresis
MC	Mixed cellularity	PBMC	Peripheral blood mononuclear cell
MFI	Median fluorescence intensity	PBS	Phosphate buffered saline
MHC	Major histocompatibility complex	PCR	Polymerase chain reaction

PGK1	Phosphoglycerate kinase 1	SE	Standard error
PI	Propidium iodide	SLE	Systemic lupus erythematosus
PS	Phosphatidyl serine	SOT	Solid organ transplant
PTLD	Post-transplant lymphoproliferative disease	TCR	T cell receptor
PVDF	Polyvinylidine difluoride	TM	Transmembrane
Q-PCR	Quantitative PCR	TNF	Tumour necrosis factor
QVD-OPH	Quinoline-Val-Asp -difluorophenoxymethylketone	TNFR	Tumour necrosis factor receptor
RBC	Red blood cell	TPO	Thrombopoietin
RPMI	Roswell Park Memorial Institute medium	TR	terminal repeats
RS	Reed Sternberg	TR-FRET	Time-resolved fluorescence energy transfer
RT	Reverse transcription	TRADD	Tumour necrosis factor receptor type 1-associated death domain
SC	Subcutaneous	UTR	Untranslated region
SCGM	Stem Cell Growth Medium	VCA	Viral capsid antigen
SCID	Severe combined immunodeficiency	WBC	White blood cell
SCLC	Small cell lung carcinoma	WHO	World Health Organisation
SD	Standard deviation	WT	Wild type
SDS	Sodium dodecyl sulphate	XIAP	X-linked inhibitor of apoptosis protein

1. Introduction

1.1 Epstein-Barr virus

1.1.1 Discovery, classification and structure

Epstein-Barr virus (EBV) is a B lymphotropic γ-herpesvirus ubiquitous within the human population. It was first discovered in Burkitt's lymphoma samples from patients from sub-Saharan Africa in the early 1960s (Epstein et al., 1964). Although this was the first human virus to be associated with the pathogenesis of cancer, most of the world's population carry the virus completely asymptomatically. However, there are several associations between EBV infection and disease. Most people become infected with EBV early in life, but if primary infection is delayed until early adulthood it can frequently result in the onset of infectious mononucleosis (IM). Primary EBV infection in children is generally sub-clinical and incidences of IM are rare events (Chan et al., 2003). A combination of a highly coordinated T cell mediated immune response and downregulation of viral genes allows the virus to exist silently for the lifetime of the host in most people. On the more severe end of the disease scale, in patients with immune defects EBV can drive aberrant proliferation of lymphoid cells and cellular changes that lead to malignancy. EBV-associated cancers can be of lymphocyte origin, including Burkitt's Lymphoma (BL), Hodgkin's lymphoma (HL), extra-nodal NK/T cell lymphoma (ENKTL), post-transplant

lymphoproliferative disease (PTLD), or of epithelial cell origin, including nasopharyngeal carcinoma (NPC) and gastric carcinoma (GC).

At the molecular level, EBV contains a linear 170 kbp double stranded DNA genome within the virion (Baer et al., 1984) (**Figure 1.1**). At either end of the linear genome are the terminal repeats that recombine by homologous recombination during early infection to form a circular episome. These terminal repeats vary following recombination and are often used to determine viral clonality. An infectious particle is encapsidated, enveloped and expresses surface glycoproteins (gp) that mediate host cell attachment and entry, reviewed in (Shannon-Lowe and Rowe, 2014).

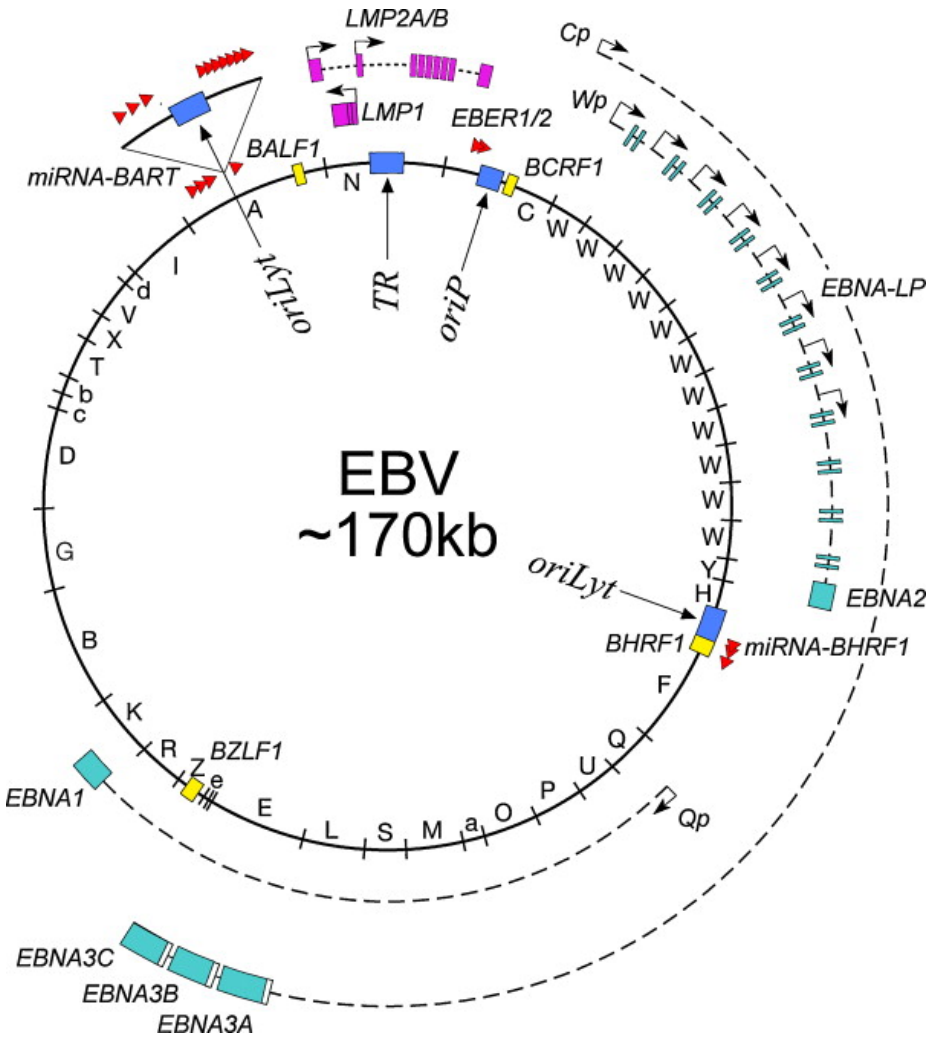


Figure 1.1 Structure of EBV genome with gene and promoter positions. The schematic represents the B95.8 laboratory strain of EBV. Coloured boxes indicate gene locations: EBNA genes (turquoise). LMP genes (magenta) and lytic genes (yellow). Origin of lytic replication (oriLyt), the plasmid origin of DNA replication (oriP) and terminal repeat (TR) are shown as blue boxes. Black arrows represent promoter sites and alternative splice sites are indicated by dotted lines. Single letters indicate DNA fragments produced by the BamHI restriction enzyme. Red triangles represent the location of non-coding RNAs (EBERs and microRNAs). Figure from (Kalla and Hammerschmidt, 2012).

1.1.2 EBV infection and cellular tropism

EBV is acquired orally and infection is believed to occur in the lympho-epithelium of the oropharynx. EBV is a naturally B lymphotropic virus which establishes latency in the memory B cells of healthy carriers. EBV can infect both naïve and memory B cells *in vitro*, giving rise to continuously proliferating lymphoblastoid cell lines (LCLs) that are useful for many studies (Henderson et al., 1977). EBV entry into B cells is mediated by a sequential set of interactions between viral glycoproteins and cellular surface molecules, enabling the initial attachment then endocytosis, fusion and release of the virus into the cellular cytoplasm. The major viral glycoprotein, gp350, initially interacts with the B cell specific surface marker CD21 (also known as complement receptor 2, CR2) (Fingeroth et al., 1984). CD21 deficient cells exhibit a lower susceptibility to viral infection, however this can partially be compensated for by the expression of CD35 which can act as a substitute and this surface marker is expressed during early B cell development (Ogembo et al., 2013). Binding of EBV to these surface proteins allows for the interaction between the viral gp42 and HLA class II that is critical for the infection of B cells (Wang and Hutt-Fletcher, 1998). Although this interaction initiates fusion between the viral envelope and the plasma membrane, it is not sufficient to complete the fusion process. Therefore, EBV employs three further glycoproteins, gH/gL and gB for this process. Specifically, the gp42 forms a complex with gH and gL, triggering a conformational change whereby the gp42 hydrophobic pocket widens allowing interaction with the highly conserved viral fusogenic protein, gB. Insertion of the gB binding loop into the plasma membrane triggers a

conformational change in gB whereby this protein effectively folds over to bring the viral envelope and the endosomal membrane into close proximity, thereby triggering fusion between the two membranes and generating a pore in the membranes through which the virus capsid can be delivered into the cytoplasm, reviewed in (Shannon-Lowe and Rowe, 2014).

Infection of epithelial cells is less well understood. Epithelial cells do not express the viral receptor CD21; therefore, EBV binds to epithelial cells in a CD21-independent manner. Furthermore, given the lack of HLA class II on epithelial cells, EBV does not require gp42 to enter these cells. However, the gH/gL complex binds to the epithelial cell surface integrins $\alpha_v\beta_5$, $\alpha v\beta_5$ and $\alpha_v\beta_5$ via the KGD integrin-binding motif. A conformational change then occurs within the gH/gL complex that allows the binding of gB, which initiates fusion (Chesnokova et al., 2009).

With regard to T and NK cell infection, EBV has rarely been found in these cell types of healthy individuals (Hudnall et al., 2005). Importantly, EBV infection of NK cells and T cells, is always associated with various lymphoproliferations, such as chronic active EBV (CAEBV), EBV-associated haemophagocytic lymphohistiocytosis (HLH) and hydroa vacciniforme (HV) or with two highly aggressive T/NK cell malignancies, aggressive NK leukaemia (ANKL) and extra-nodal NK/T cell lymphoma (ENKTL). It is currently unclear how EBV enters T cells and NK cells given their lack of the viral receptor CD21. However, it is thought the virus must enter a common T cell/NK cell progenitor due to the following lines of evidence: (i) The demonstration that clonal EBV was found in both the T cells and NK cells of individual

patients with CAEBV and EBV-HLH (C. Fox and C. Shannon-Lowe, unpublished); (ii) The virus receptor, CD21, is expressed during T cell/NK cell differentiation in the thymus before the point of lineage commitment, triggered by Notch-ligation of the precursor cells (C. Shannon-Lowe, unpublished); (iii) Rare somatic mutations have been identified in both the EBV infected T cells and NK cells from CAEBV patients with dual T/NK cell infection, strongly implying a common infected precursor (H. Kimura, Unpublished). However, in 2004, Isobe and colleagues reported infection of a mature NK cell line with EBV (Isobe et al., 2004), although these results have not yet been widely replicated.

Once within target cells, EBV does not undergo immediate lytic replication as is observed with many other herpesvirus infections. Instead EBV establishes a latent infection where only limited viral genes are expressed. Viral replication, or the lytic cycle, has been demonstrated in both differentiated epithelial cells and in terminally differentiated plasma cells (Temple et al., 2014, Laichalk and Thorley-Lawson, 2005). Depending on the cellular background in which the lytic replication takes place, the tropism of the virus can change. For example, in B cells, intracellular gp42 can bind to MHC class II and is subsequently degraded in the proteasome (Borza and Hutt-Fletcher, 2002). Virions emerging from B cells will therefore express fewer gp42/gH/gL trimers and more gH/gL dimers, which increases the likelihood of epithelial cell entry as this process does not require gp42. Conversely, epithelial cells do not express HLA class II, therefore gp42 is able to reach the cell surface and be incorporated into the virion and is therefore significantly more infectious for the B cell, where gp42 is absolutely required.

Viral transmission from person to person is thought to occur via transmission of epithelial cell-derived virus through saliva. As mentioned above, primary infection of naïve B cells occurs in the oropharyngeal cavity. From here, the virus can either: 1) enter the lytic cycle — where more virions are produced for transmission into a new host or 2) enter latent cycle — which is the state in which the virus exists throughout the lifetime of the host (**figure 1.2**).

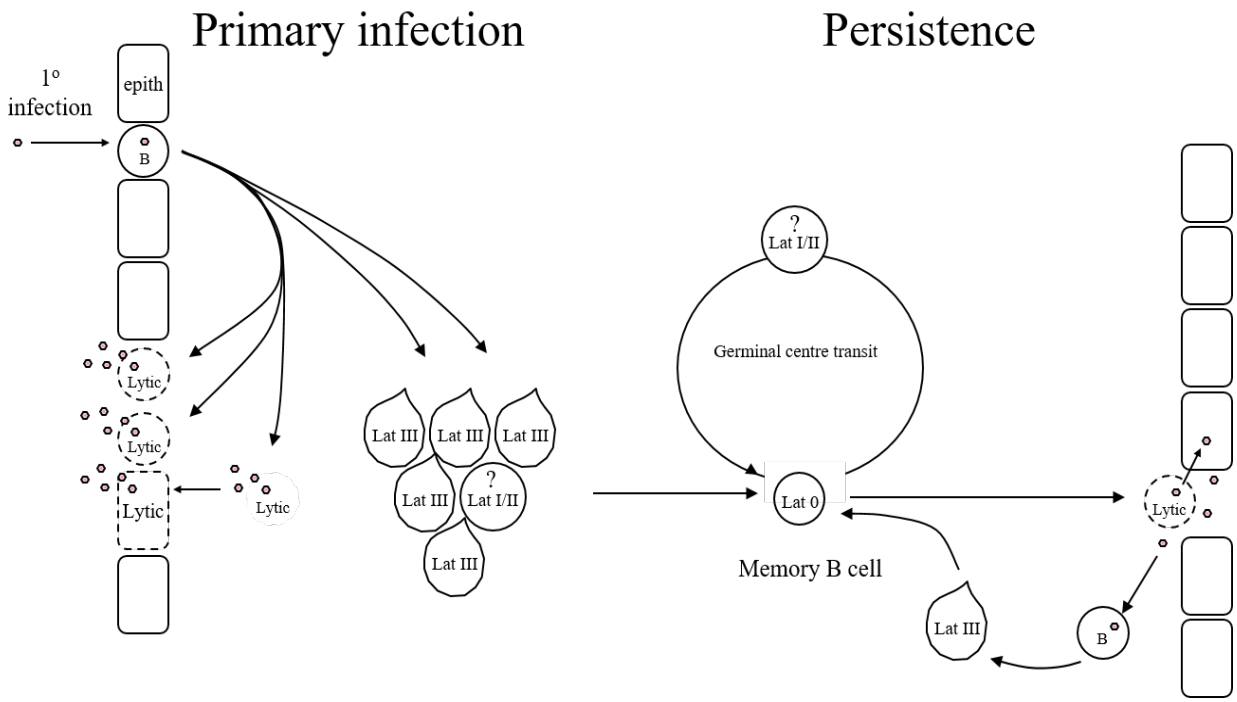


Figure 1.2 EBV life cycle. A model for EBV primary infection and persistence. EBV infects naïve B cells in the oropharynx where the virus initially expresses the latency III gene expression programme. Viral gene expression is eventually restricted to the latency 0 programme. Infected cells migrate to the germinal centre and then exist as memory B cells for the life time of the host. The differentiation of infected memory B cells into plasma cells facilitates entry into the lytic cycle where new infectious particles are produced which can then enter previously uninfected B cells, or epithelial cells by transfer infection. (Figure provided by A. Rickinson)

1.1.3 Lytic replication

In order to generate new infectious particles, the virus must enter the lytic cycle. This is the process of viral DNA replication, packaging the viral DNA into viral capsids and finally envelopment upon budding of the virus from the cell into the extracellular space. Lytic replication is a highly ordered cascade of viral gene expression, with each of the immediate early (IE), early (E) and late (L) gene replication phases dependent upon the preceding phase. Three subsets of IE, E and L lytic genes regulate this process and encode viral transcription factors, DNA replication machinery and structural proteins, respectively.

EBV encodes two immediate early (IE) genes, BZLF1 and BRLF1. Expression of the transcription factor Zta (also known as Z or ZEBRA) by BZLF1 is the key event in the switch from latent to lytic cycle (Rooney et al., 1989). Zta binds the promoters of downstream early and late lytic genes to initiate their activity, and this process is synergistically enhanced by Rta — the viral transcription factor expressed by BRLF1 (Liu and Speck, 2003). The early (E) lytic genes, of which there are over 30 with known functions, are subsequently expressed. Within this gene subset, EBV encodes proteins necessary and sufficient to replicate its own DNA, a feature conserved among all herpesviruses. Finally, the late (L) genes encode proteins such as the tegument proteins, capsid proteins and glycoproteins required for the formation of a new infectious virus particle. The large linear concatemeric DNA molecules produced during viral DNA replication are cleaved at the terminal repeats during packaging into viral capsids, resulting in one copy of the viral DNA per capsid. The capsids are then transported to the cell surface where they bud out of the plasma

membrane, taking membrane with them to form the new viral envelope (Daikoku et al., 2005).

1.1.4 Latent cycle

In newly infected B cells, EBV initially establishes a form of latent infection termed Latency III (Lat III), which involves the expression of all latent antigens. Following a combination of T cell exerted control of the EBV-infected population (discussed later) and influences from the microenvironment, such as Notch signalling, viral gene expression eventually becomes a highly restricted form of latency, termed Latency 0 (Lat 0). In Lat 0, only non-coding RNAs are expressed. This enables the virus to remain immunologically silent within the memory B cell compartment where the virus can reside for the lifetime of the host.

In total, there are four patterns of latent infection: Lat III, II, I and 0. The latency subtype is determined by the expression pattern of the latency genes, which include six nuclear antigenic proteins (EBNA1, 2, 3A, 3B, 3C and LP), three latent membrane proteins (LMP1, 2A and 2B) plus the non-coding RNAs: EBERs (Epstein-Barr virus-encoded small RNAs) and BARTs (gene regulatory miRNAs) (Young and Rickinson, 2004). Importantly, the latency subtyping is typically used to categorise EBV-associated diseases based upon gene expression (**figure 1.3**). Below I will discuss the function of each of these genes and their contribution to the pathogenesis of cancer.

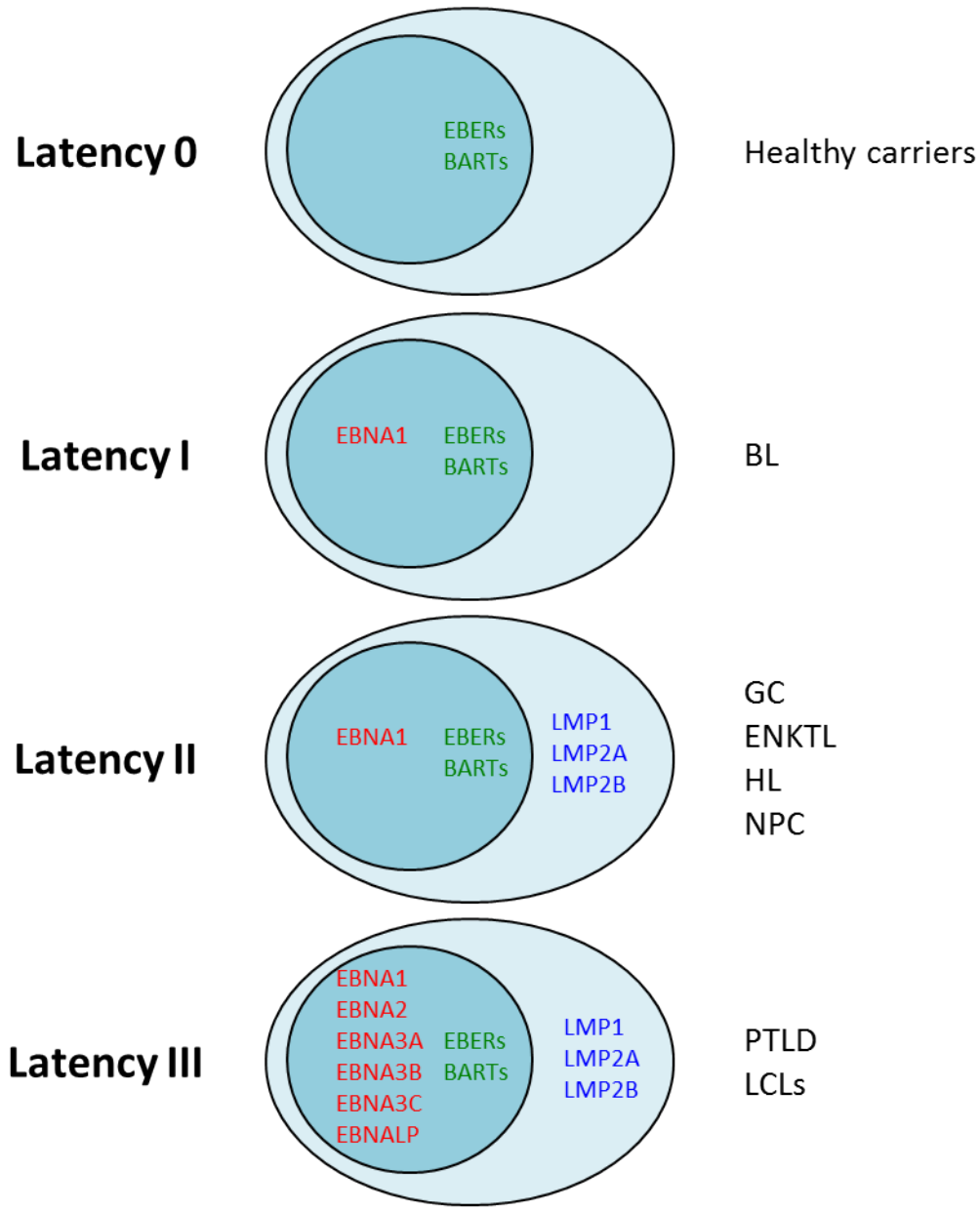


Figure 1.3 EBV latent gene expression. Diagram representing EBV latent genes and to which latency pattern their expression is restricted. Dark blue circles represent cell nuclei and light blue ovals represent the cell cytoplasm. The right-hand column contains a list of states of health, disease or laboratory models where these subtypes of latency can be detected. BL, Burkitt's lymphoma; GC, gastric carcinoma; ENKTL, extra-nodal NK/T cell lymphoma; HL, Hodgkin's lymphoma; NPC, nasopharyngeal carcinoma; PTLD, post-transplant lymphoproliferative disease; LCLs, lymphoblastoid cell lines.

1.1.5 Latent genes

EBNA1

EBNA1 functions as the viral genome maintenance protein and is essential in all EBV infected cells during cellular DNA replication (Leight and Sugden, 2000). EBNA1 functions by binding to the plasmid origin of replication (OriP) on the viral episome and tethering the episome to the cellular DNA to replicate the viral genome during cellular DNA replication and ensure equal division of the replicated episomes into daughter cells following mitosis. EBNA1 expression can be upregulated by cellular transcription factors, such as E2F, IRF1 and IRF2 (Schaefer et al., 1997) suggesting it is, at least in part, under cell cycle control. Furthermore, EBNA1 can restrict its own expression by binding downstream of the EBNA1 (Qp) promoter to prevent fully formed transcripts. The EBNA1 amino acid sequence contains an extensive Gly-Ala repeat (separating the N- and C-terminal regions), which inhibits the proteasome-mediated degradation of this protein and thereby limits presentation of antigenic peptides to circulating immune cells (Levitskaya et al., 1995).

Experimental evidence suggests that EBNA1 can also directly contribute to the development of cancer. The earliest evidence to support this idea was the demonstration that enforced EBNA1 expression could induce B cell lymphoma development in transgenic mice (Wilson et al., 1996). One mechanism in which EBNA1 could achieve this is by interfering with p53, where EBNA1 prevents the stabilisation of this tumour suppressive transcription factor. EBNA1 achieves this by outcompeting p53, and its regulator MDM2,

for the ubiquitin-specific protease USP7 (Saridakis et al., 2005). This prevents USP7 acting on p53 to remove ubiquitin chains, enhancing the proteasome mediated degradation of p53 (Sheng et al., 2006).

EBNA2 and EBNALP

EBNA2, a defining protein of latency III, is a driving force behind EBV driven neoplastic transformation, due to its ability to modulate the transcription of several viral and cellular genes. EBNA2 largely functions through disruption of the DNA binding Jκ recombination binding protein (RBP-Jκ) with gene promoters and its associated complex. RBP-Jκ forms a large complex with histone deacetylases (HDACs) and other transcriptional repressors in a virus-negative environment (Hsieh and Hayward, 1995). EBNALP assists EBNA2 by binding to its acidic activation domain and prevents the binding of the SMRT-HDAC complex (Sinclair et al., 1994). The recruitment of TFIIB, TFIIH and p300 (all critical components of the basal transcriptional machinery) leads to the switching-on of target genes under this regulation. Cellular genes under such control include CD23 and CD21 and viral genes regulated by EBNA2 include LMP1 and LMP2 (Kieff and Rickinson, 2007).

Differences within the EBNA2 gene contribute to a key difference between the two types of EBV, where EBV type 1 can more efficiently transform B cells *in vitro* compared to EBV type 2 strains (Rickinson et al., 1987). With respect to their nucleotide sequence, the two types of EBV are well known to largely differ in their EBNA2 sequence (53% identical in amino acid sequence) but significant differences within the EBNA3 family have also been

reported (Sample et al., 1990, Adldinger et al., 1985, Dambaugh et al., 1984, Rowe et al., 1989).

EBNA3 family

The EBNA3 family of proteins function as negative regulators of EBNA2 transcriptional activity by competing for binding to RBP-Jκ as demonstrated in transient reporter assays (Zhao et al., 1996). EBNA3A and EBNA3C, the more extensively studied family members, have been shown to be essential for B cell transformation with EBNA3C in particular showing immortalisation properties similar to those exerted by the adenovirus E1A and papillomavirus E7 proteins. EBNA3C can cooperate with EBNA2 to drive LMP1 expression and is also involved in the deregulation of cell cycle check points, which allows progression of cellular replication (Young and Rickinson, 2004). The function of EBNA3B is less well understood, but its knockout does lead to decreased EBNA3C expression and a decreased growth rate of LCLs. However neoplastic transformation is still possible in the absence of EBNA3B, indicating that this protein is not essential for tumorigenesis (Chen et al., 2006).

LMP1

Recombinant virus studies have shown that LMP1 is necessary for efficient transformation of B cells and the long-term growth of infected cells (Kaye et al., 1993). LMP1 is a highly important protein for sustained proliferation and cell survival in latency II and latency III backgrounds and is critical for EBV associated growth transformation. LMP1, with an open reading frame of 1.3 kbp, is expressed roughly 36 hours after primary B cell infection *in*

vitro (Alfieri et al., 1991). The 63 kDa protein is composed of an N-terminal cytoplasmic tail (amino acids 1-23) followed by six transmembrane domains (aa 24-186), responsible for its distribution at the cellular plasma membrane, plus a larger cytoplasmic domain at the C-terminal region (aa 187-386) (Eliopoulos and Young, 2001). The two key signalling features of LMP1 lie within the C-terminal cytoplasmic domain and are known as C-terminal activation regions 1 and 2 (CTAR1 and CTAR2).

LMP1 mimics the activity of a constitutively activated CD40 molecule without the need for ligand stimulation and can also act as a functional substitute for CD40 (Uchida et al., 1999). Nuclear-factor κB (NF-κB) activation occurs from CTAR1 and CTAR2 interactions with TNFR associated factors (TRAFs) and the death domain-containing protein TRADD, respectively. This results in the recruitment of the catalytic kinases that contain NF-κB-inducing kinase (NIK) and IκB kinases (IKKs) leading to the activation of the IκBα-driven NF-κB pathway. Via NF-κB, LMP1 mediates the upregulation of the pro-survival BCL-2 family members, BCL-2 (Henderson et al., 1991), MCL-1 (Wang et al., 1997) and BFL-1/A1 (D'Souza et al., 2000). Through TRAFs, LMP1 also mediates activation of the mitogen activated protein kinase kinase kinase (MAPKKK) and phosphatidylinositol 3-kinase (PI3K) pathways (Young and Rickinson, 2004).

LMP2A and LMP2B

LMP2A and LMP2B transcripts are alternatively spliced from the same gene and consist of 9 exonic regions only differing at the first exon, known as either exon 1A or exon 1B. These

first exons are separated from the rest of the coding DNA by the terminal region, meaning that this gene can only be expressed once the viral genome has circularised. Therefore, detection of LMP2 protein or gene expression is a marker for successful episome formation. Both LMP2 proteins contain 12 hydrophobic transmembrane domains and a C-terminal cytosolic tail (Laux et al., 1988), but LMP2A is 119 amino acids longer at the N-terminal end of the sequence as exon 1B is non-coding.

The LMP2 proteins are not considered vital for transformation. However, due to its B cell receptor (BCR) signalling mimicry, LMP2A is required for the transformation of germinal centre B cells that lack the BCR (Mancao and Hammerschmidt, 2007). Like LMP1, LMP2A can initiate activation of the Ras/Akt/PI3K pathway and increase the expression of several pro-survival members of the BCL-2 family (Fukuda and Longnecker, 2004). LMP2A has also been identified as a major contributor to EBV associated epithelial cancers, such as NPC, due to its ability to promote cell motility and migration (Chen et al., 2002). LMP2B is largely thought to be a negative regulator of LMP2A but does have some function in evading interferon (IFN) responses by inducing degradation of IFN receptors together with LMP2A (Shah et al., 2009).

Non-coding viral RNAs: EBERs and miRNAs

In all forms of latency, EBV expresses its non-coding RNAs — EBERs and EBV miRNAs — with varying degrees of contribution to disease. EBER1 and EBER2 are both highly abundant in all latent cells and have highly conserved sequences or structures with non-coding RNAs

from other lympho-cryptoviruses (Moss and Steitz, 2013). EBER1 has been shown to promote the proliferation of BL cells by binding ribosomal protein L22, mediating its transport from the nucleolus to the nucleoplasm (Houmani et al., 2009). A major function of EBER2 is to repress the activity of LMP1, LMP2A and LMP2B by direct binding at the viral terminal repeat and indirectly in the case of the B cell transcription factor PAX5 (Lee et al., 2015a).

The EBV miRNAs have the ability to regulate the expression of both viral and cellular genes. Viral miRNAs originate from either the BHRF1 (miR-BHRF1) or BART (miR-BART) microcluster regions. Other than regulating the viral gene BHRF1, miR-BHRF1s are implicated in the control of the cell cycle and cell death by regulating cellular genes, including PTEN, BACH1 and KDM4B (Bernhardt et al., 2016, Skalsky et al., 2012). Knock-out studies have demonstrated that viruses lacking either miR-BHRF1, miR-BHRF-2 or miR-BHRF-3 have substantial deficiencies in the transformation of B cells (Feederle et al., 2011a). Primary B cells infected with viruses lacking miR-BHRF1-1, miR-BHRF-2 and miR-BHRF-3 showed higher levels of apoptosis and the resulting cell lines were less proliferative (Feederle et al., 2011b). Strikingly, the combined deletion of both the BHRF1 protein and all miR-BHRF1s produced a completely transformation-deficient virus (Bernhardt et al., 2016).

miR-BARTs are also capable of regulating BHRF1 as well as the major oncogene, LMP1. The cellular targets of miR-BARTs are largely implicated in cell growth or cell death and include c-Myc, BIM and caspase-3 (Riley et al., 2012). However, the analysis of viruses lacking the

miR-BART region, such as the common laboratory strain B95.8, revealed that these genes are dispensable for cellular transformation (Raab-Traub et al., 1980).

1.1.6 B cell malignancies

Burkitt's lymphoma

There are three recognised forms of BL with varying degrees of association with EBV infection. Endemic Burkitt's lymphoma (eBL) is the most common childhood cancer in sub-Saharan Africa where virtually all cases are EBV positive and typically such patients present with a tumour of the jaw (Molyneux et al., 2012). Sporadic Burkitt's lymphoma (sBL) can be found worldwide where the EBV association is rare in North America and Europe although sBL cases in Brazil can reach 80% EBV positivity (Queiroga et al., 2008). Thirdly, incidences of immunodeficiency-, including AIDS-related BL occur and these are EBV associated in 30-40% of cases (Molyneux et al., 2012).

EBV associated BL commonly presents with a latency I gene expression pattern with readily detectable expression of the BARTs and EBER transcripts and EBNA1 protein. The defining genetic aberration of BL is a chromosomal translocation which places the c-Myc gene under the control of the IgH or IgL regulatory regions resulting in constitutive overexpression of c-MYC in the B cell lineage (Guikema et al., 2008). In line with this, BL is a cancer of germinal centre origin and has a defined phenotype of $CD10^+$, $CD77^+$ and $BCL6^+$. In terms of cooperating oncogenic lesions, in line with many cancers, mutations in the *p53* tumour

suppressor gene and other constituents of the p53 pathway are detected frequently in BL and contribute to the pathogenesis of the disease.

Hodgkin's lymphoma

Hodgkin's lymphoma (HL) is characterised by the presence of bi-nucleated malignant Reed-Sternberg (RS) cells and can be subtyped into nodular sclerosis (NS), mixed cellularity (MS), lymphocyte-depleted (LD) and lymphocyte-rich classical HL (Kuppers, 2009). Based on Ig typing data, the RS cells are believed to originate from a germinal centre B cell (Braeuninger et al., 1997). Unusually, these RS cells form only a minority of the tumour. Approximately 40% of HL cases are EBV associated and they display a latency II EBV infection, where the viral genes are predicted to play a pivotal role in the disease (Brauninger et al., 2006). The expression of LMP1 allows the activation of the CD40 signalling pathway and LMP2A expression promotes cell survival through activation of PI3K/AKT signalling, as described above (Fukuda and Longnecker, 2004). The contribution of EBV at the late malignant stage has been questioned due to the lack of an established EBV-positive RS cell line *in vitro*.

Post-transplant lymphoproliferative disorder

Post-transplant lymphoproliferative disorder (PTLD) is an abnormal B cell proliferation that may occur following either a solid organ transplant (SOT) or haematopoietic stem cell transplantation (HSCT) and immune-suppression. In 50-80% of cases, EBV is the major pathogenic driver in the immunosuppressed host (Dharnidharka et al., 2016). Suppression of the function of EBV-specific T cells allows the expansion of infected B cells where the

virus expresses its full latent gene repertoire. Therefore, a latency III phenotype is observed in the vast majority of EBV-positive cases of PTLD (Dharnidharka et al., 2016). EBV gene expression can be more restricted, or even EBV-negative, in later onset tumours, particularly in SOT.

1.1.7 Epithelial cell malignancies

Nasopharyngeal carcinoma

The most common EBV-associated neoplasm of epithelial cell-origin is nasopharyngeal carcinoma (NPC). Here, the virus exists in a latency II state, although with only around 50% of cases expressing detectable LMP1 but over 98% expressing LMP2A (Fahraeus et al., 1988, Brooks et al., 1992). LMP1 has been shown to induce pro-inflammatory cytokines (such as IL-1α, IL-β, IL-6, IL-8, TNF-α, RANTES and GM-CSF) found in inflamed hyper-proliferative epithelium and also facilitates epithelial-mesenchymal transition by the downregulation of E-cadherin (Huang et al., 1999, Tsai et al., 2002). Monoclonal virus can be detected in NPC tissues which is an indication that infection is an early event in malignant expansion. EBV associated NPC is found with high incidence in far-east Asia and is as common as 20-30 cases per 100,000 population (Raab-Traub, 2015). There is a high incidence of NPC in men of Chinese descent, indicating that genetic factors are involved in the pathogenesis of this disease. However, environmental factors, such as highly salted fish as a significant part of the diet, have also been implicated in the development of NPC (Raab-Traub, 2002).

Gastric carcinoma

Gastric carcinoma (GC) is associated with EBV in 10% of cases (Camargo et al., 2011, Matsusaka et al., 2011). EBV is detected in either a latency I or II pattern in GC, with LMP2A the most commonly expressed latent membrane protein found in over 50% of cases (Luo et al., 2005). Studies on GC derived cell lines demonstrated that LMP2A contributes to cell proliferation by upregulating survivin via the NF-kB pathway and also promotes cell migration by upregulating dynamin-related protein 1 through Notch signalling (Hino et al., 2008, Pal et al., 2014). Interestingly, the EBV-associated subset of GC has been shown to be correlated with increased overall survival and reduced lymph node (LN) metastasis compared to EBV-negative GC (Camargo et al., 2011, van Beek et al., 2004).

1.1.8 T cell and NK cell lymphoproliferative diseases

Although not considered to be part of the natural lifecycle of the virus, EBV infection of T cells and NK cells represents a significant clinical problem. EBV infection of these cell types is always associated with lymphoproliferations or malignancies for which treatment options are extremely limited. These diseases include chronic active EBV (CAEBV), EBV-associated haemophagocytic lymphohistiocytosis (HLH), hydroa vacciniforme (HV), aggressive NK leukaemia (ANKL) and extra-nodal NK/T cell lymphoma (ENKTL). The viral and non-viral contribution to these diseases is not yet fully understood and further work in this area is urgently required. The focus of this thesis will be on ENKTL and CAEBV, discussed in more detail in the following sections.

1.2 EBV-associated T and NK lymphoproliferative diseases

1.2.1 Extra-nodal NK/T cell lymphoma

Classification

ENKTL is defined as $CD2^+$, $CD56^+$, surface $CD3^-$ and cytoplasmic CD3ε chain-positive (Au et al., 2009). In addition to these markers, EBV infection is a requirement for a positive diagnosis due to the previously reported association of the virus with this cancer (Swerdlow SH et al., 2008). EBV infection is determined by the presence of EBERs and clonality is determined by the presence of exactly matching terminal repeat regions within every infected cell.

Epidemiology

ENKTL is found with greatest frequency in Eastern Asia and South America (4-6% of all non-Hodgkin's lymphomas) compared to the Western world (roughly 0.5% of all non-Hodgkin's lymphomas). It is thought this geographic variation is due to a combination of genetic factors, viral strains and as yet unidentified environmental factors (Au et al., 2009). The median age of disease is 55 years old with males being more frequently affected than females at a ratio of 2:1 (Haverkos et al., 2017). It is possible that there may be an HLA subtype predisposition, but this is currently unproven. The incidence of ENKTL is much higher in native Asians compared to USA-based Asians, and this provides evidence for an environmental contribution to the development of this disease (Bassig et al., 2016).

Clinical features

ENKTL is an aggressive malignancy that typically presents as a necrotic lesion around the nasopharynx, classified as nasal-type ENKTL (Harabuchi et al., 2009). Patients suffer from ulceration and necrosis within the nasal cavity and tumours protruding into local paranasal sinuses and lymph nodes (Haverkos et al., 2016). Non-nasal ENKTL occur at a much lower frequency and are typically found in the skin, lung, liver and spleen (Suzuki et al., 2010).

Viral contribution to pathogenesis

The presence of EBV within every malignant cell that provided the infected T/NK cell can maintain the virus, the virus has powerful transformation capabilities similar to that identified in B cells. Viral load analysis of tumours has proved to be a prognostic marker of disease (Hsieh et al., 2007). The virus present in ENKTL is usually clonal with every malignant cell containing approximately 20 copies of the virus per cell and each cell exhibiting a latency I or II gene expression profile (Hsieh et al., 2007).

Although functions of the viral genes within these tumours have not been fully characterised, informative experiments have been performed investigating LMP1 in particular. A study of primary ENKTL tumour samples showed that in 22 of the 30 cases investigated, LMP1 was present and that its expression was associated with a more favourable prognosis (Kanemitsu et al., 2012). This is possibly due to the ability of LMP1 to increase MHC I expression, which increases the likelihood of immune detection of infected malignant cells. However, other studies reported that LMP1 is responsible for the

downregulation of miR-15a, in order to promote proliferation, and is a prognostic marker of potential disease progression (Komabayashi et al., 2014). The regulation of LMP1 partially occurs through a positive feedback loop that involves IL-15 secretion from tumour-infiltrating macrophages that induce LMP1 expression. In turn, LMP1 induces IP-10 cytokine expression and secretion from the tumour cells, which acts as a chemoattractant for such macrophages (Ishii et al., 2012). IL-2, and to a lesser extent IL-10, have been shown to also regulate LMP1 expression in the SNK6 and KAI3 cell lines (Takahara et al., 2006). LMP1 can also be controlled by viral miR-BART9, impacting upon cellular growth and proliferation (Ramakrishnan et al., 2011).

Other latency II viral genes and non-coding RNAs have been studied to a lesser extent. LMP2 function has not been thoroughly investigated in T and NK cells but LMP2 mRNA transcripts have been detected in approximately 40% of ENKTL tumours (Chiang et al., 1996). LMP2A protein could not be detected in ENKTL derived cell lines despite the presence of low numbers of LMP2A transcripts (Fox et al., 2010). Furthermore, LMP2B transcripts were detected but there are no antibodies available to detect LMP2B protein. Importantly LMP2 protein expression has been indirectly identified by LMP2-specific cytotoxic T cell recognition. Given the lack of LMP2A protein expression, a novel LMP2 transcript was identified that is initiated from a promoter in the terminal repeat region of the EBV genome. This novel transcript (termed LMP2-TR) was also identified in primary ENKTL samples in which no LMP2A or LMP2B transcripts were detectable (Fox et al., 2010). Expression of LMP2 in ENKTL tumours could have implications for therapeutic targeting.

It has also been demonstrated that EBNA1 promotes cell cycle progression in the ENKTL cell line HANK1 by reducing the expression of the cyclin dependent kinase inhibitor, p27 (Ian et al., 2008). Investigation into viral miRNA expression by Illumina deep sequencing has revealed the possible extent to which the miR-BARTs could be contributing to disease (Alles et al., 2016). Strikingly, the miR-BARTs constitute 31.4% and 14.7% of the total miRNA repertoire in SNK6 and SNKT16 cells, respectively. The same report also investigated selected viral miRNAs and reached the conclusion that miR-BART16 can downregulate the expression of sphingosin-1-phosphate receptor 1 (S1PR1) in cooperation with EBERs. No expression of the miR-BHRF1 family was observed.

Non-viral contribution to pathogenesis

The literature is limited on genetic analysis of primary tumour material. Although deletions of the long arm of chromosome 6 have been reported, no known specific gene loss has been designated a critical feature in the pathogenesis of ENKTL. It has been suggested that the frequent loss of the chromosomal region 6q21 — containing the PRDM1 gene — may contribute to disease (Iqbal et al., 2009). PRDM1 encodes the tumour suppressor BLIMP1, which is commonly mutated or lost in B cell lymphomas (Mandelbaum et al., 2010, Huang et al., 2010). The KHYG1, SNK1 and SNK6 cell lines showed hypermethylation in the PRDM1 gene promoter region (Iqbal et al., 2009). Another methylation study using cell lines and a small number of primary samples identified 95 genes that had been markedly silenced, including *Bcl2l11* which encodes the pro-apoptotic protein BIM (Kucuk et al., 2015).

1.2.2 Chronic active EBV

Classification and clinical features

Chronic active EBV (CAEBV) is an EBV-positive lymphoproliferative disease that clinically presents with defined symptoms of fever, splenomegaly and lymphadenopathy lasting 6 months or more. Patients have no known immunodeficiencies and present with high antibody responses against viral capsid antigen (VCA) and viral early antigen (EA-D) (Straus, 1988). Clinically, patients can be separated based on whether T cells or NK cells are the dominant carriers of EBV. NK cell carriers tend to present with high levels of IgE and a hypersensitivity to mosquito bites whereas T cell carriers suffer from high fevers and have high levels of EBV-specific antibodies (Kimura et al., 2001). Severe and persistent cases of CAEBV have been reported to develop into ENKTL, indicating that CAEBV can be considered a pre-malignant state (Jones et al., 1988).

Viral contribution to pathogenesis

High viral load within the peripheral mononuclear cells of patients is considered a negative prognostic marker. This can range from 10^3 to 10^7 genomes per million PBMC prior to therapy (Kimura et al., 2001). T and NK cell lines established from CAEBV patients have been shown to express a latency II viral gene expression pattern but primary samples have not yet been thoroughly investigated (Iwata et al., 2010). EBV can be found clonal or oligoclonal in both the T and NK cell compartments within these patients and this indicates that infection can be an early event in the development of CAEBV.

Non-viral contribution to pathogenesis

Attempts to delineate the genetic contribution to disease in CAEBV have only recently commenced. A whole genome sequencing analysis of 83 patient samples revealed great variation across the cohort. Only 58% of samples were found to carry one somatic mutation or more (Okuno et al., 2017). The most common mutation (16.8% of patients) was found within the DDX3X gene — encoding a DEAD-box helicase — a mutation resulting in the reduced global translation in various cancer types (Valentin-Vega et al., 2016). CAEBV patients carrying the DDX3X mutation had a worse overall survival at 5 years (40.6% vs 78.6% for all other cases). The second most common gene mutation found was in KMT2D (4.8% of patients) — a histone methyltransferase — and this was also associated with a worse overall survival at 5 years (50% vs. 73.9% for all other cases). The lack of a genetic aberration common to a majority of patient samples indicates that infection with EBV is the dominant driver of disease.

1.2.3 EBV infection of T and NK cells

The infection of T or NK cells with EBV and the viral contribution to disease are poorly understood mechanisms. Attempts have been made to infect T and NK cells *in vitro*, establish cell lines and to phenotype EBV infected cells. However, these have all been achieved to varying degrees of success as described below.

Infection of T cells

The first description of ENKTL appeared in 1988 by Jones et al. In this report, three patients suffered from chronic illness presenting with fever, haematological abnormalities and high antibody titres against EBV capsid antigen. All three patients developed fatal T cell lymphoma (Jones et al., 1988). These tumours contained detectable viral DNA and were judged to be monoclonal proliferations based upon T cell receptor gene rearrangement.

The key steps in the development of T cells are outlined in **figure 1.4** with detail of surface marker expression at each step. The stage of T cell differentiation where EBV infection can occur is under debate. The identification of rare somatic mutations in both the EBV infected T cells and NK cells from CAEBV patients with dual T/NK cell infection, indicate infection occurs at a progenitor stage (H. Kimura, Unpublished). However, others have demonstrated that mature T cells are able to be infected but the virus type is key to the process. It has been proposed that the geographical distribution of EBV type 2 — which is more common in East Asia than in Western countries — may be able to more readily infect mature T cells than EBV type 1 (Coleman et al., 2017, Coleman et al., 2015). This hypothesis would also partially account for the geographical distribution of ENKTL. EBV type 2 has been reported to readily infect isolated $CD8^+$ T cells *in vitro* causing proliferation (Coleman et al., 2015). In the same experiments, it was shown that cytokine production was induced — including IL-8, RANTES and MIP1-α — which have all been previously shown to be regulated by LMP1 and this is consistent with the stable expression of LMP1 following primary T cell infection. In EBV-negative T cell lines, the overexpression of LMP1 has been

shown to downregulate expression of the SH2D1A gene, which encodes signalling lymphocyte activation molecule (SLAM)-associated protein (SAP), through the transcription factor ATF5 (Chuang et al., 2005, Chuang et al., 2008). LMP1 was therefore able to indirectly induce, via TRAF2/5 and NF-kB, secretion of cytokines such as IFN-γ and TNF-α (Chuang et al., 2005).

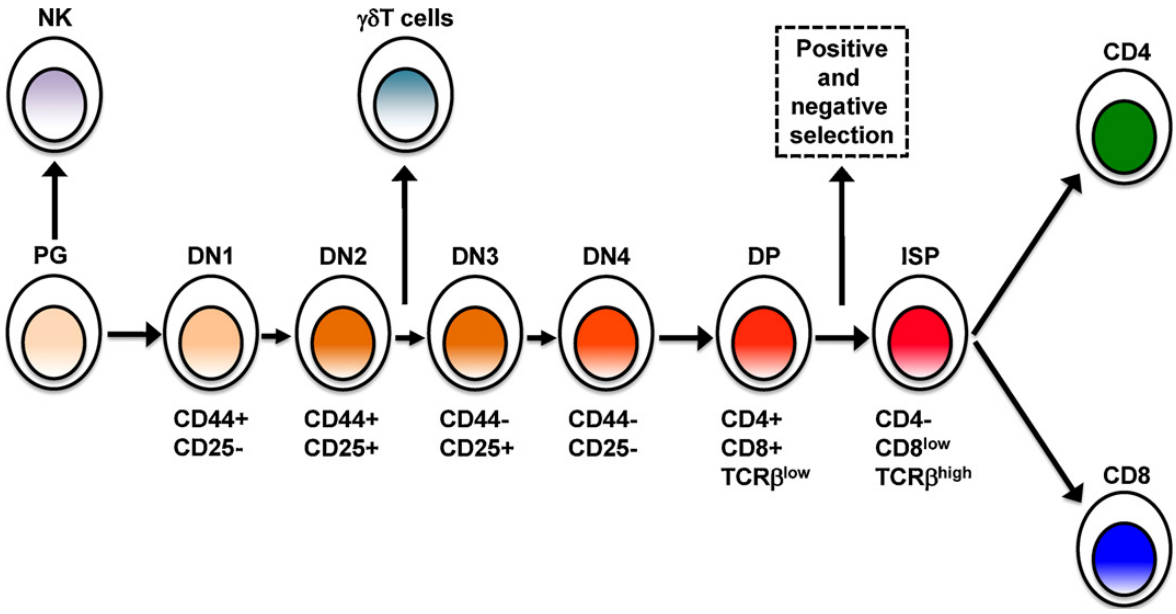


Figure 1.4 Differentiation of T lymphocytes. Progenitor cells (PG) migrate from the bone marrow to the thymus where commitment to either NK cell or T cell lineage occurs. Cells entering T cell lineage commitment undergo multiple double-negative (DN) stages, a double-positive (DP) stage, an immature single-positive (ISP) stage followed by either CD4 or CD8 single-positive stage commitment. Commitment to γδ T cell lineage occurs at the DN2/DN3 stage. Adapted from (D'Acquisto and Crompton, 2011).

Infection of NK cells

From clinical samples, it has been learned that the vast majority of ENKTL cases involve the infection of NK cells with a minority of cases involving infection of T cells (Au et al., 2009). CAEBV cases in East Asia and South America typically arise from an EBV infection of $CD16^+$ NK cells (Kasahara et al., 2001). In North America, it has been suggested that most cases of CAEBV are of B cell origin highlighting an interesting and unexplained geographical difference between the US and East Asia/South America (Cohen et al., 2011).

Phenotypic studies of ENKTL have been limited by the rare nature of the disease. Current understanding is that roughly 85% of cases are of NK cell origin where surface marker profile is expected to be $CD56^+$, $CD16^{-/dim}$, surface $CD3^-$, cytoplasmic $CD3\epsilon^+$, $CD57^-$ and $CD2^+$ (Au et al., 2009, Lima, 2015). The differentiation state of an NK cell (NK precursor, functional NK cell or memory NK cell) can be determined by surface marker expression (detailed in **figure 1.5**). However, large-scale studies using multicolour flow cytometry to confirm the NK differentiation state of ENKTL has yet to be performed. For intracellular markers, perforin and granzyme B expression are found frequently (Schwartz et al., 2008). Further investigation into the cytokine and cytokine receptor expression profile would be informative regarding the maturation and activation stage of these NK cells. It could then be determined whether these infected NK cells were likely to be responding to EBV-infected cells or whether they had come into contact with the virus through an entirely different circumstance.

The first description of an *in vitro* infection model in NK cells was reported by Isobe et al., 2004. They successfully infected isolated peripheral blood NK cells, the NK-92 cell line and the NKL cell line with a type 1 recombinant EBV containing a GFP tag. Cell-free virus was used to infect the cells comparable to common B cell infection protocols. They confirmed infection by GFP positivity and detection of viral mRNA of latency I and II genes by reverse transcriptase PCR. However, the establishment of an immortalised NK cell line carrying EBV was not achieved as most infected cells died via apoptosis within one week.

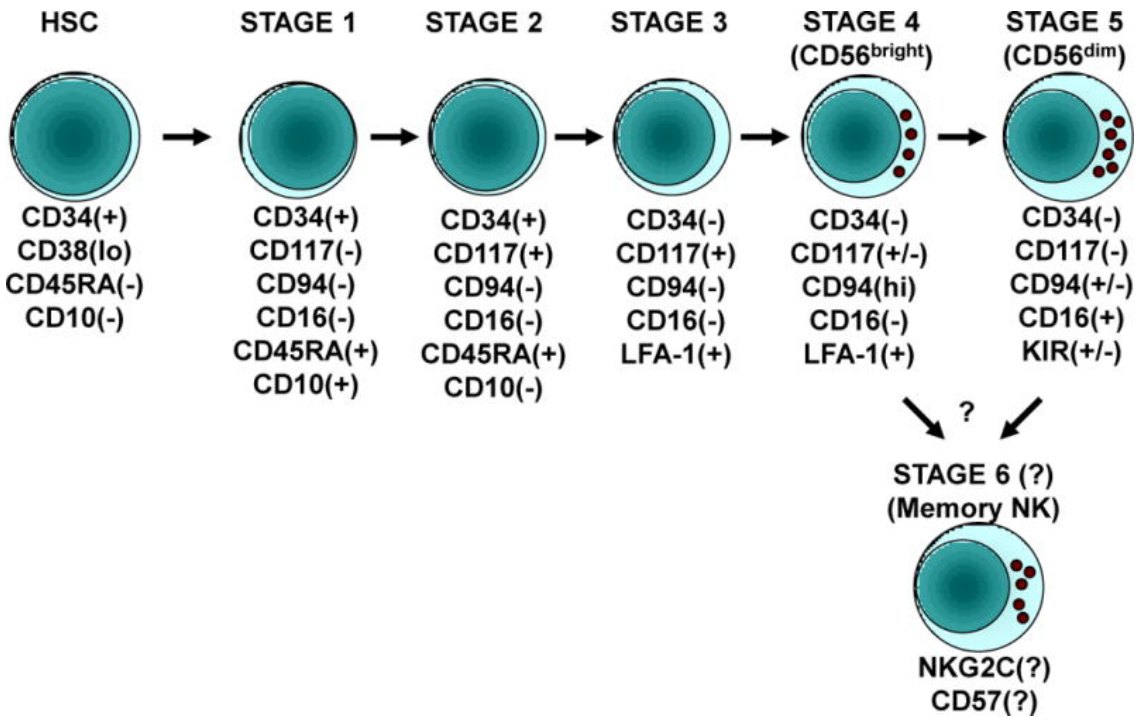


Figure 1.5 Differentiation of Natural Killer cells. Haematopoietic stem cells (HSCs) can enter the NK cell developmental path which can be divided into 6 stages defined by the expression or lack of expression of indicated cell surface markers. Stages 1 to 3 represent immature NK cells. Stages 4 to 6 represent the late stages of NK cell differentiation where memory NK cells (stage 6) can be derived from either $CD56^{bright}$ (stage 4) or $CD56^{dim}$ (stage 5) cells. Adapted from .(Yu et al., 2013).

Immune control of EBV

EBV is not found within the T or NK cell compartment of healthy carriers but these subsets of the immune system are important in the control of the virus during the EBV life cycle. Understanding T and NK cell control of EBV infection can perhaps reveal clues to how infection of such cells may occur, although the EBV-specificity of infected cells is unknown.

Following primary infection, activated NK cells have been shown to be present as an expanded population in the peripheral blood of IM patients compared to that of healthy individuals (Williams et al., 2005, Hislop et al., 2007). The role of NK cells in the control of viral infection is further exemplified by their ability to inhibit EBV transformation of primary B cells *in vitro* (Lunemann et al., 2013). However, evidence exists showing that NK cells provide an incomplete protection against EBV. Haematopoietic stem cell transplanted patients who develop an EBV driven PTLD have recovered levels of NK cells by the onset of disease (O'Reilly et al., 1997). The importance of NK cell control of EBV infection perhaps occurs during early events of the lytic cycle. During the lytic cycle, EBV downregulates MHC class I molecules to remain immunologically silent which removes the stimulus to NK cell inhibitory receptors, such as killer-cell immunoglobulin-like receptors (KIRs) (Keating et al., 2002). During the lytic cycle of the virus, NKG2D ligand expression is induced due to cellular stress. Collectively, these initiate killing of EBV infected cells as an early event in the control of virus spread.

Primary infection in asymptomatic individuals is controlled by antigen-specific $CD4^+$ and $CD8^+$ T cells that force the virus into latency 0 where it expresses only non-coding RNAs. Memory T cells remain for long-term protection against viral reactivation. Primary EBV infection resulting in IM is associated with a large increase in $CD8^+$ T cells in the peripheral blood, reviewed in (Rickinson et al., 2014). Due to high levels of virus replication and therefore presence of large amounts of EBV antigens, unsurprisingly, most of these T cells are EBV antigen-specific with a majority recognising immediate early and early lytic proteins over latent antigens but this dominance settles with time after infection, reviewed in (Hislop et al., 2007). T cells recognising an individual lytic peptide can account for up to 40% of the overall $CD8^+$ population and T cells recognising a single latent peptide can account for up to 5% of all $CD8^+$ T cells with a bias towards the EBNA3 family of proteins. These expanded T cell populations have been shown to be competent in cytotoxic function (i.e. expression of perforin) and show markers of T cell activation, including CD38, and Ki-67, a marker of cell proliferation.

1.2.4 Models of disease

Models for EBV

Since its discovery, EBV has been studied *in vitro* by the use of cell lines derived from primary tumours to investigate the contribution of the virus to B cell and epithelial cell derived neoplastic disease. The *in vitro* transformation of B cells into LCLs by EBV has proved to be a useful model for primary infection, immune response to disease and latent

gene function. The common laboratory strain of EBV, known as B95.8, was cloned into a BAC system in a 293T cell background where lytic replication can be readily induced and studied (Delecluse et al., 1998).

The investigation of EBV and EBV-associated diseases *in vivo* has proved to be more challenging. As stated earlier in this introductory chapter, EBV is a human-specific gamma-herpesvirus with a highly coordinated binding and entry mechanism. Importantly, such mechanisms deny the virus the ability to infect cells of non-human origin — therefore, a direct mouse model of EBV infection has not been established. Since the late 1980s, BL has been extensively studied using the *Eμ-Myc* transgenic mouse model which recapitulates the disease by placing the *c-Myc* gene under the control of the *IgH* gene enhancer (Harris et al., 1988). However, this is not informative for investigating EBV as the transformed cells do not contain viral DNA nor do they express the latency I genes that contribute to EBV-positive BL cases — i.e. EBNA1, BHRF1 and viral non-coding RNAs. Xenografts of either BL cell lines or cells derived directly from a human tumour into immune-deficient mice — such as the NOD-SCID IL-2rγ$^{-/-}$ (NSG) mice — have provided the background for many drug studies (Chu et al., 2017, Ghetie et al., 1996, Lee et al., 2015b). Humanised mouse models have massively contributed to the field of EBV immunology (Munz, 2017). Although not a perfect model, the irradiation of mice followed by reconstitution with a human immune system prior to EBV exposure has become a highly utilised *in vivo* model for studying EBV infection, the associated tumorigenesis and immune control. In another EBV transgenic mouse model, the enforced expression of LMP1 in the B cell compartment — combined

with defective T cell surveillance — was shown to be sufficient to induce B cell lymphoma development (Zhang et al., 2012). It is proposed in this context that LMP1 was the driver of further oncogenic events by inducing further chromosomal aberrations by eliciting the expression of activation-induced cytidine deaminase (AID).

Models for ENKTL and CAEBV

Big challenges still await the field of ENKTL as many hurdles are yet to have been overcome. Beginning with *in vitro* models, the obvious hurdle for establishing a model for T and NK cell disease is the lack of an infection/transformation model akin to that of LCLs for B cells. The kinetics of viral gene expression during early, intermediate and late phases of infection and immortalisation are well understood in B cells but virtually unexplored in T and NK backgrounds. Due the lack of a T or NK cell transformation model, the limited number of cell lines that are available have become the standard model for studying ENKTL and EBV-positive aberrant T/NK cell proliferations.

In terms of challenges for *in vivo* models, again research on ENKTL lags behind the field of B cell neoplastic disease. It is not known whether EBV infection alone is sufficient to transform T or NK cells *in vivo* (or *in vitro*). It is also unlikely that LMP1-alone would be sufficient to induce T and NK proliferations. As a bona fide driver of tumourigenesis has yet to be identified, a genetic mouse model of disease does not yet exist. Therefore, some studies have focused on using ENKTL cell lines, particularly SNK6, in xenograft models using NSG mice, but such experimentation is not yet widely used (Siddiquey et al., 2014, Suzuki

et al., 2015). Xenograft models have been adopted in CAEBV where the transplant of patient-derived cells showed that $CD4^+$ T cells were required for successful engraftment of EBV-positive T or NK cells (Imadome et al., 2011).

1.2.5 Current and emerging therapies

Classical treatments for ENKTL and CAEBV have been adopted from treatment regimens of other haematological diseases. Given these diseases are rare, clinical trials have been equally rare. Currently, ENKTL is treated empirically with no real knowledge about whether these regimens will actually be efficacious, leading to the present low success rates. The lack of cell lines and animal models has so far limited the understanding of the disease and the development of new effective treatment regimens. Below is a description of how such diseases have been treated in the past and how the field may advance the development of targeted therapies in the future.

Classical therapy

Patients diagnosed with either ENKTL or CAEBV have typically been treated with standard chemo-radiation although there is great variation in the treatment protocols used across the globe (Kim et al., 2001, Lee et al., 2006, Tse and Kwong, 2013, Okano, 2002). ENKTL has a median survival of 7.8 months whereas the survival rate for patients with CAEBV is reportedly 58% at 10 years (Vose et al., 2008, Kimura et al., 2003). Radiotherapy appears to be initially successful in reducing ENKTL tumour burden but only in around 50% of patients (Liang, 2009, Li et al., 2006). This initial success is temporary with many patients

relapsing within 1 year of treatment. With regards to chemotherapy, the CHOP regimen — cyclophosphamide, hydroxydaunorubicin, onvocin (vincristine) and prednisone — commonly used for the treatment of non-Hodgkin's lymphomas (NHLs) and many solid tumours, has only little impact on ENKTL (Kim et al., 2003).

In an effort to improve survival rates, high-dose chemotherapy has been combined with haematopoietic stem cell transplantation in the treatment of ENKTL. Reports are limited but a pooled analysis study focusing on NK cell neoplasms identified a significant increase in survival of ENKTL patients when treated with this combination as opposed to patients treated with chemotherapy alone (Suzuki et al., 2006). However, this study analysed a relatively small cohort with 22 patients in the combination arm *vs* 127 patients in the chemotherapy-only arm. As this was a multi-institutional study, the authors acknowledge that variance in the criteria for inclusion of patients in these trials may have contributed to the differences. A study involving 29 CAEBV patients reported high levels of success when combining chemotherapy with allogeneic haematopoietic stem cell transplantation; 18 of the 29 patients were placed on fludarabine, melphalan, cyclophosphamide, low dose radiation plus allogeneic haematopoietic stem cell transplantation and showed an overall survival rate of 95% ±4.9% (S.E) (Kawa et al., 2011). Cohen and colleagues have suggested that CAEBV in the USA — where most cases are of B cell origin, unlike in East Asia — can be curable when patients are also treated with allogeneic haematopoietic stem cell transplantation (Cohen et al., 2011). The stage of disease and age of the patient greatly

determines the success of such treatment as younger patients with early stage disease can more easily handle such therapy.

Improved chemotherapy

Immunohistochemistry staining of primary ENKTL tumours has suggested that high levels of the multidrug efflux pump, p-glycoprotein, may be responsible for resistance to chemotherapy (Wang et al., 2008). P-glycoprotein is an ATP-dependent cell surface protein that functions to decrease the concentration of substances that may be toxic to the cell as an important mechanism for cell survival (Lin and Yamazaki, 2003). P-glycoprotein has a normal tissue distribution in the brain, kidney, intestine and liver, to name a few tissues. However, the upregulation of p-glycoprotein as a method of evading the killing by chemotherapeutic drugs is found in various epithelial cell carcinomas, multiple myeloma and certain other cancers. Despite the presence of p-glycoprotein in ENKTL tumours, a direct contribution of this to chemoresistance has yet to be proven. *In vitro* studies on SNT16 and SNT8 cells indicated that the increase in p-glycoprotein in these cell lines may be mediated by EBV and potentially driven by LMP1 (Yoshimori et al., 2015). The chemotherapy regimen known as SMILE — steroid (dexamethasone), methotrexate, ifosphamide, L-asparaginase and etoposide — has been developed specifically by using drugs with a reduced p-glycoprotein susceptibility. Although a large scale assessment of patient response to SMILE therapy versus CHOP therapy is yet to be performed, clinical trials have shown encouraging results in patients with ENKTL (Yamaguchi et al., 2008, Yamaguchi et al., 2011, Kwong et al., 2012).

Immunotherapy

LMP1 and LMP2 proteins provide an attractive target for immunotherapy as their expression discriminates between malignant and non-malignant cells. The field of immunotherapy has exploded over recent years with the use of cytotoxic T lymphocyte (CTL) mediated therapy and monoclonal antibody therapy. The patient-specific process of generating LCLs and LMP-expressing dendritic cells to generate autologous LMP-specific CTLs has led to positive outcomes in EBV-associated lymphomas (Bollard et al., 2011). Using such methodology, a study focusing on EBV-positive NHLs achieved complete responses (follow-up time ranging from 2 to 5 years) in 4 out of 7 ENKTL patients who had previously demonstrated resistance to chemoradiation (Bollard et al., 2014). Even more encouragingly, 5 out 5 ENKTL patients identified as high risk for relapse showed a complete response (follow up time ranging from 2 to 4 years). The identification of the novel LMP2-TR transcript in ENKTL cell lines and primary tumours provides a rationale for continuing with such trials, especially considering the progress made with targeting LMP2 with CTL driven therapy in Hodgkin's lymphoma (Fox et al., 2010, Bollard et al., 2004).

A large contributor to the emergence of immunotherapy is the development of monoclonal antibodies that inhibit the immune checkpoint effector PD-1 and its ligand PD-L1, that are found on the CTLs and tumour cells, respectively (Pardoll, 2012). A study investigating primary ENKTL tumours identified 41 out of 73 analysed tumours to be PD-L1 positive (with a cut-off of 10% tumour cell positivity) (Kim et al., 2016). Interestingly, patients expressing

PD-L1 on their tumour cells exhibited a favourable response, indicating that PD-L1 expression could serve as a positive prognostic marker.

Tumour evasion of cytotoxic therapy

The ability of the above therapies to be effective is dependent on their ability to induce tumour cell death and the ability of the tumour cells to activate appropriate cell death pathways. The evasion of apoptosis is a recognised hallmark of cancer (Hanahan and Weinberg, 2000, Hanahan and Weinberg, 2011). The next section of this introduction will describe the apoptotic pathway with particular focus on how the evasion of programmed cell death can contribute to the development of cancer as well as the resistance of malignant cells to anti-cancer therapy and how this may be overcome.

1.3 Cell death and targeted therapy

1.3.1 Overview of apoptosis

The term 'apoptosis' was first coined in 1972 by Kerr and colleagues. Here, apoptosis was described as a biological phenomenon of cell elimination that was morphologically characterised by the condensation of chromatin and cell membrane fragmentation (Kerr et al., 1972). Apoptosis is a highly conserved genetically encoded process of cell suicide that plays a critical role in tissue homeostasis, embryonic development, immunity and tumour development. Below is a mechanistic description of the two distinct pathways to

apoptosis (the intrinsic and extrinsic pathways) with focus on the BCL-2 protein family which regulates this process.

Intrinsic apoptotic pathway

Apoptosis can be initiated by DNA damage (e.g. elicited by γ-irradiation), hypoxia, cytokine deprivation, oncogenic stress and many other stimuli (Norbury and Zhivotovsky, 2004). Downstream of these stimuli, the BCL-2 family function as a group of proteins that regulate the cell death switch and they can be divided into two broad categories: pro-apoptotic (BH3-only or effector proteins) and anti-apoptotic members. The anti-apoptotic BCL-2-like proteins include BCL-2 itself, BCL-X_L, BCL-W, MCL-1 and BFL-1/A1 (Kelly and Strasser, 2011). The primary function of this subclass is to maintain cell survival by preserving the integrity of the outer mitochondrial membrane to prevent the release of apoptogenic molecules, such as cytochrome c and Smac/DIABLO. They perform their pro-survival function by inhibiting the action of pro-apoptotic effector proteins BAK and BAX (and possibly BOK) which when activated, oligomerise to form pores in the mitochondrial outer membrane (MOMP: mitochondrial outer membrane permeabilisation). With regards to their amino acid sequences, the anti-apoptotic and the pro-apoptotic BAX and BAK proteins discussed so far show high similarity; all contain 4 regions of homology known as the BCL-2 homology domains 1-4 (BH1 – BH4) and a transmembrane domain that tethers them to the outer mitochondrial membrane (**figure 1.6**) (Youle and Strasser, 2008). The third subclass of the BCL-2 protein family, known as the pro-apoptotic BH3-only proteins, function to overcome the action of the BCL-2-like anti-apoptotic proteins. There are 8 major BH3-only family

members that are activated in response to diverse cell death-inducing stimuli: BIM, BID, PUMA, NOXA, BAD, BMF, BIK and HRK. A critical feature of these proteins is that they contain only one of the BCL-2 homology domains, BH3, hence why they are collectively named the BH3-only proteins. The BH3-only proteins use their BH3 domains to insert themselves into the hydrophobic pocket of the BCL-2-like pro-survival proteins and thereby block their ability to restrain the pro-apoptotic functions of BAK and BAX, reviewed in (Youle and Strasser, 2008).

In normal healthy cells in the absence of an apoptotic stimulus, the pro-survival BCL-2 like proteins restrain BAK or BAX to prevent MOMP and the induction of apoptosis. Translocation and structural conformational changes in BAK and BAX are key steps leading up to MOMP to allow eventual apoptosis, reviewed in (Kalkavan and Green, 2018). BAX and BAK can be activated when they are unleashed from their restraint by the pro-survival BCL-2-like proteins when those are blocked by an increase in BH3-only proteins, the initiators of apoptosis. In addition, it is thought that certain BH3-only proteins, such as BIM, PUMA and caspase-8 cleaved, activated BID, called truncated BID (tBID) (see below), can also directly bind to and thereby activate BAX and BAK. In an initial activation step, BAX and BAK monomers undergo a conformational change to expose their C-terminal latch, thereby allowing homodimerisation (Dewson et al., 2008, George et al., 2007). In a second activation step, such BAK or BAX homodimers can aggregate into oligomers that form pores in the outer mitochondrial membrane (MOMP), thereby allowing the release of

apoptogenic factors (e.g. cytochrome c, Smac/DIABLO) from the inter-mitochondrial space (Kim et al., 2009).

Cytochrome c initiates dATP-dependent oligomerisation of the adaptor protein, Apaf-1, that is central to the formation of the apoptosome — the platform for the activation of the initiator caspase, caspase-9, and downstream activation of the caspase cascade that causes cell demolition. The caspase-recruitment domains (CARD) of the Apaf-1 molecules form a ring structure at the centre of the apoptosome which can interact with the enzymatically inactive zymogen for caspase-9, called pro-caspase-9 (Riedl and Salvesen, 2007). The apoptosome recruits pro-caspase-9 proteins and consists of a 7:2 ratio of Apaf-1:pro-caspase-9 proteins (Malladi et al., 2009). Recruitment forces a conformational change in pro-caspase-9 that unleashes its proteolytic activity, which does not necessitate its auto-catalytic cleavage. However, enzymatic activation of caspase-9 is often followed by such self-processing which generates a large fragment of ~20 kDa (p20) and a small fragment of ~10 kDa (p10). These fragments assemble as $p20_2p10_2$ hetero-tetrameric fully active proteases. Active initiator caspase-9 proteases can proteolytically process the zymogens of the so-called effector caspases, caspases-3, -6 and -7. This releases p20 and p10 fragments that assemble into the $p20_2p10_2$ hetero-tetrameric fully active effector caspases. The effector caspase can cleave hundreds of substrates and this causes the demolition of the cell and the classical morphology of apoptosis (Parrish et al., 2013). For example, effector caspase-mediated cleavage of iCAD (inhibitor of the DNAse CAD, caspase activated DNAse) unleashes the inter-nucleosomal DNA cleavage that is a hallmark of apoptosis. Moreover,

effector caspases cause externalisation of phosphatidyl-serine (PS) to the outer leaflet of the plasma membrane, a marker of apoptosis exploited by staining with Annexin V (which binds PS) to identify cells undergoing apoptosis, by proteolytic activation of a PS scramblase and proteolytic inactivation of a PS translocase (Verhoven et al., 1995, Segawa et al., 2014).

XIAP, a member of the inhibitors of apoptosis family (IAPs) can impede the activation of caspase-9 and can also bind to the active site of executioner caspases and thereby block their activity (Deveraux et al., 1997). The presence or absence of XIAP was shown to impact the sensitivity of cells to FASL, which activates the death receptor FAS (see below) (Jost et al., 2009). XIAP itself is inhibited by Smac/DIABLO and Omi/HtrA2, two proteins that are released alongside cytochrome c (the activator of the apoptosome, see above) from the inter-mitochondrial space following MOMP (Chai et al., 2000).

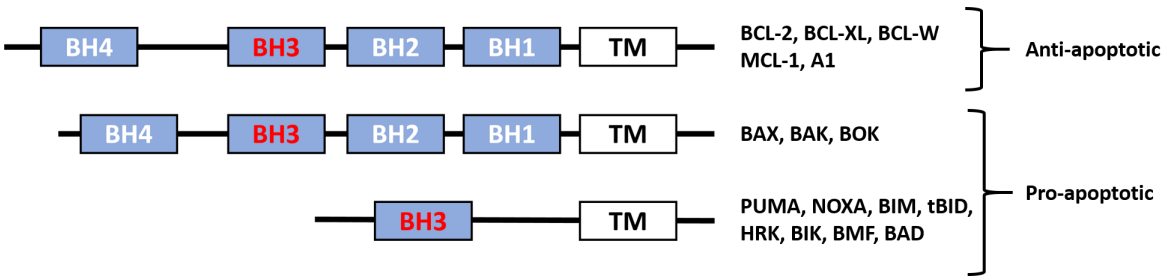


Figure 1.6 Structural homology within the BCL-2 family. The family can be divided into several subgroups. The anti-apoptotic proteins contain all four BCL-2 homology domains (BH1-4)**.** The pro-apoptotic proteins can be further subdivided into two functionally distinct groups — the multi-domain (effector) proteins and the single domain (BH3-only) proteins.

Interactions between members (binding specificities)

Cell death through the intrinsic apoptotic pathway is proposed to occur through two mechanistic models that are not mutually exclusive: the neutralisation model and the direct activation model. The neutralisation model states that for BAK and/or BAX mediated MOMP to occur, the BCL-2-like pro-survival proteins need to be blocked by the BH3-only proteins (Adams and Cory, 2007). Certain BH3-only proteins, such as BAD, HRK and NOXA, can only bind to a subset of the BCL-2-like anti-apoptotic proteins. BAD, BMF, HRK and BIK have specificity for BCL-2, BCL-X_L and BCL-W and NOXA binding is restricted to MCL-1 and A1. In contrast, BIM, PUMA and tBID (caspase-8 cleavage activated BID downstream of death receptor stimulation; see below) are capable of binding all five BCL-2-like pro-survival proteins (**figure 1.7**). This complexity of interactions between different members of the BCL-2 family and their highly regulated expression patterns allow for a controlled response that is tailored to the distinct apoptosis-inducing stimuli and specific cell types. For example, a cell that relies on MCL-1 for its survival would not undergo apoptosis if only BAD expression was induced or, in another example, NOXA may not necessarily induce death in a cell expressing both MCL-1 and BCL-X_L without the help of BAD or BIM for instance.

The direct activation model suggests that certain BH3-only proteins can directly interact with BAK and/or BAX to induce their conformational change leading to their activation and ultimately MOMP. Such BH3-only proteins are classified as direct activators whereas the other BH3-only proteins that are only capable of inducing apoptosis by blocking the BCL-2-

like pro-survival proteins are classified as sensitizers. Initially, only BIM and tBID were assigned to the direct activator category and were shown to interact directly with the effector proteins although weakly (Letai et al., 2002, Westphal et al., 2014). Subsequently, PUMA, NOXA and BMF have also been shown to interact directly with BAX and BAK (Cartron et al., 2004, Dai et al., 2011). Thus, the boundaries between the two models of BAX/BAK activation to cause apoptosis are becoming rather blurred. A mutant of BIM protein that lacks the ability to interact with BAX was shown to still be able to induce apoptosis, indicating a combination of the two models likely contributes to apoptotic cell death (Merino et al., 2009).

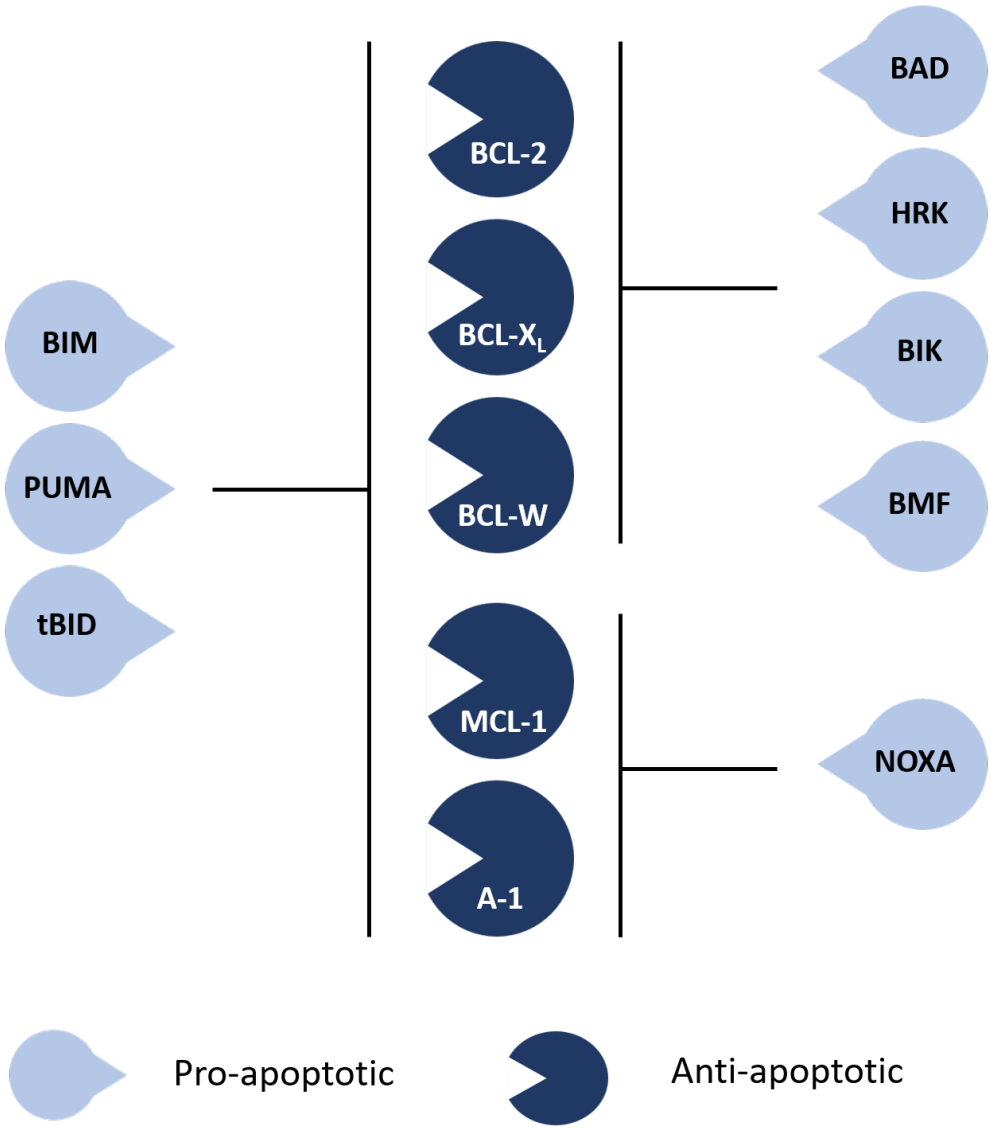


Figure 1.7 Binding specificities of BCL-2 family members. The promiscuous BH3-only proteins BIM, PUMA and tBID can bind all pro-survival members of the BCL-2 family. The remaining BH3-only proteins all exhibit a restricted binding profile. BAD, HRK, BIK and BMF can all bind BCL-2, BCL-X_L and BCL-W whereas NOXA can only bind A1 (BFL-1) and MCL-1.

The extrinsic apoptotic pathway

The extrinsic pathway to apoptosis can be initiated by cytotoxic T cells and NK cells interacting with surface molecules on target cells known as death receptors. Death receptors are members of the tumour necrosis factor (TNF) receptor gene superfamily where the encoded transmembrane proteins contain an intra-cellular death domain responsible for transducing the extracellular signal into an intracellular event. CD95 (also known as FAS or APO-1) is a transmembrane protein expressed across a variety of tissues and its ligand, CD95L (or FASL), is produced by cytotoxic T cells and NK cells (Peter et al., 2015). Other well characterised receptors include TNFR1 and TNF-related apoptosis-inducing ligand receptor 1 and 2 (TRAIL-R1 and TRAIL-R2), with their respective ligands being TNF and TRAIL (de Miguel et al., 2016). Ligand binding triggers aggregation of preformed trimers of death receptors and the FAS-associated death domain (FADD) protein and the zymogen for caspase-8 (pro-caspase-8) are then recruited to the cytosolic aspect of FAS to form the so-called death inducing signalling complex (DISC) — the apoptosome equivalent for the extrinsic apoptotic pathway. Recruitment into the DISC forces a conformational change in pro-caspase-8 that unleashes its activation, which as for caspase-9, can lead to its autoproteolytic processing, generating p20 and p10 fragments that assemble into $p20_2p10_2$ hetero-tetrameric active proteases. Similar to caspase-9, active caspase-8 can proteolytically activate the executioner caspases-3, -6 and -7. In certain cell types, called type 1 that are mostly lymphoid ones, this direct death receptor > FADD > caspase-8 > effector caspase pathway is sufficient for cell killing, but in so called

type 2 cells, including hepatocytes and pancreatic cells, cell killing necessitates amplification of the caspase cascade (Strasser et al., 1995, Scaffidi et al., 1998, Jost et al., 2009). This is achieved by caspase-8 mediated proteolytic activation of the BH3-only protein BID into its active form, tBID, that unleashes activation of the BAX/BAK dependent intrinsic apoptotic pathway (Fulda and Debatin, 2006, Li et al., 1998, Luo et al., 1998).

1.3.2 Anti-apoptotic members of the BCL-2 family

Bcl-2 was the first oncogene to be discovered that prevents cell death rather than promoting cell growth or proliferation, such as the previously described oncogenes *Ras*, *Myc* or *Src* (Vaux et al., 1988). Over the last 30 years since the discovery of its function, BCL-2 has been joined by other members of this protein family in promoting cell survival. These anti-apoptotic proteins and their genes have been extensively studied, primarily using knockout mouse strains generated by gene-targeting in ES cells. Below I describe the roles of the different pro-survival BCL-2 family members in embryonic development, tissue homeostasis in adult life and tumour development.

BCL-2

During embryogenesis, the *Bcl-2* gene is switched on much later compared to the other major pro-survival members of the family, *Bcl2l1* (encoding BCL-X_L) and *Mcl*-1 (Metcalfe et al., 2004). Bcl-2-deficient mice surprisingly showed little neuronal impairment considering the high expression of *Bcl-2* in cells of the early central nervous system and late peripheral nervous system (Veis et al., 1993, Nakayama et al., 1994). However, BCL-2 deficient mice

exhibit major defects within other organs and systems. These mice have a reduction in size of the thymus and spleen due to decreased levels of mature resting B and T lymphocytes despite an initially normal haematopoiesis (Kamada et al., 1995, Bouillet et al., 2001). The *Bcl-2*-deficient mice also suffer from loss of melanocytes producing a grey coat and critically these mice succumb to renal failure before 16 weeks of age due to polycystic kidney disease because BCL-2 is required for renal epithelial cell survival during embryogenesis.

The frequent t(14;18) reciprocal chromosomal translocation is present in nearly all cases of human follicle centre B cell lymphoma. This chromosomal aberration subjugates the *Bcl-2* gene under the control of the immunoglobulin heavy chain gene enhancer, and this discovery was the first indication that BCL-2 has a role in cancer (Tsujimoto et al., 1984). The first indication of the function of BCL-2 came when transfection with a BCL-2 expression vector was found to prevent the death of the IL-3 dependent FDC-P1 mouse myeloid progenitor cell line following cytokine deprivation (Vaux et al., 1988). It was later shown that BCL-2 alone was not sufficient to induce tumours in mice but could dramatically accelerate MYC-driven lymphomagenesis (Strasser et al., 1990). High levels of BCL-2 have been observed in an array of haematological cancers and solid tumours, including follicle centre B cell lymphoma (see above), chronic lymphocytic leukaemia (CLL), diffuse large B cell lymphoma (DLBCL), mantle cell lymphoma, neuroblastoma and small cell lung carcinoma (SCLC) (Hanada et al., 1993, Kitada et al., 1998, Ikegaki et al., 1994, Castle et al., 1993). In addition to chromosomal translocations involving the *Bcl-2* gene, overexpression

of BCL-2 has been attributed to promoter hypomethylation and chromosomal loss at 13q14.3 which contain the BCL-2 regulating micro RNAs, miR-15a and miR-16-1 (Calin et al., 2005, Cimmino et al., 2005).

BCL-X_L

The expression of the *Bcl2l1* gene (which encodes BCL-X_L) is switched on at the two-cell stage during embryonic development and mice lacking *Bcl2l1* are not able to develop past embryonic day 13.5 (Motoyama et al., 1995). This embryonic lethality has been attributed to the aberrant apoptosis in the neuronal and erythroid compartments. The examination of the *Bcl-x* gene-targeted mice revealed that BCL-X_L is required for the survival of post-mitotic immature neuronal cells in the developing brain, spinal cord and dorsal root ganglia and erythroid progenitors in the foetal liver (Motoyama et al., 1995). Studies of chimaeric mouse models identified a critical role for BCL-X_L in the survival of thymocytes. Of note, the differentiation from $CD4^-CD8^-$ double negative (DN) progenitors into $CD4^+CD8^+$ double positive (DP) thymocytes is accompanied by a substantial increase in BCL-X_L levels. Single positive (SP) thymocytes ($CD4^+CD8^-$ or $CD4^-CD8^+$) express only relatively low levels of BCL-X_L and instead rely on BCL-2 and also MCL-1 for their survival. The loss of BCL-X_L in the haematopoietic system causes a substantial reduction in the DP thymocyte population and this curtails the production of cells at the next stage of differentiation, i.e. the mature single positive $CD4^+$ and $CD8^+$ T cells (Ma et al., 1995). The survival of red blood cells is also reported to be BCL-X_L-dependent (see above). In addition to the analysis of the BCL-X_L deficient E13.5 embryos, this was demonstrated by conditional deletion of *Bcl2l1* in

erythroid cells leading to highly anaemic adult mice (Wagner et al., 2000). The pro-apoptotic protein mediating this cell death has not been confirmed as this anaemic phenotype was not rescued by the co-deletion of *Bcl2l1* with the genes encoding BIM or PUMA. BCL-X_L has also been shown to be the major survival factor in the platelet producing megakaryocytes where its expression is largely regulated by thrombopoetin (TPO) (Kirito et al., 2002). Loss of *Bcl2l1* has resulted in a marked depletion of megakaryocytes and platelets. This was exacerbated when loss of BCL-X_L was combined with the additional loss of *Mcl-1* with compound deficient mice succumbing to massive internal bleeding (Debrincat et al., 2012, Josefsson et al., 2011).

With respect to cancer, BCL-X_L has been implicated in the survival of malignant cells of multiple myeloma (Peeters et al., 2005). These tumours are neoplastic counterparts of antibody secreting plasma cells and they arise from B cells undergoing immunoglobulin class switching and hypermutation where BCL-X_L is required to maintain survival in such situations where apoptotic stimuli come in the form of excessive DNA damage (Fang et al., 1996). Multiple myeloma is often driven by the acquirement of a chromosomal translocation activating the *Myc* gene which — when combined with apoptotic protection from BCL-X_L — drives oncogenic transformation (Cheung et al., 2004). Chronic myelogenous leukaemia (CML) positive for the fusion gene Bcr/Abl exhibit dependency on BCL-X_L for survival. Bcr/Abl has been shown to induce activation of the STAT5 transcription factor which then drives the expression of BCL-X_L (Gesbert and Griffin, 2000). BCL-X_L was

also shown to be key in both the development and progression of colorectal cancer in an inflammation-driven *in vivo* model (Scherr et al., 2016).

MCL-1

Although *Mcl-1* expression is turned on at the same time as *Bcl2l1* during embryonic development, it would appear that *Mcl-1* plays a more critical role during early embryogenesis. Deletion of the *Mcl-1* gene causes embryonic lethality in mice at the peri-implantation stage (Rinkenberger et al., 2000). This suggested a role for MCL-1 in the adhesion of the embryo to the uterine wall in early pregnancy. Conditional *Mcl-1* knockout studies in mice investigating neuronal development have identified *Mcl-1* as a critical survival factor for both proliferating and post-mitotic neuronal cells. Mice lacking *Mcl-1* in the neuronal compartment do not survive past embryonic day 16 (Arbour et al., 2008). Ablation of *Mcl-1* in the haematopoietic compartment leads to rapid apoptosis of diverse cell types in the bone marrow. Repression of *Mcl-1* either due to the deprivation of cytokines (such as SCF, the ligand for c-KIT) or loss of one allele of *Mcl-1*, increases the sensitivity of bone marrow haematopoietic progenitors to diverse stress stimuli and therefore causes bone marrow failure after exposure to doses of γ-irradiation or 5-fluorouracil from which wild-type mice are able to recover. Experiments using different types of CRE transgenic strains to delete the *Mcl-1* gene in a cell type restricted manner have shown that MCL-1 is critical for the survival of all stages of lymphoid cell differentiation, starting from the common lymphoid progenitor (CLP) to mature B, T and NK cells, activated B cells and Ig secreting plasma cells (Opferman et al., 2003, Vikstrom et

al., 2010, Peperzak et al., 2013). Dependency on MCL-1 is also seen in the myeloid cell compartment where conditional deletion of the *Mcl-1* gene at the common myeloid progenitor stage (CMP) or the granulocyte-monocyte progenitor (GMP) stage causes a depletion of immature myeloid cells in the bone marrow (Opferman et al., 2005). Such aberrant cell death has not been reported for the deletion of either *Bcl-2* or *Bcl2l1* (BCL-X_L) within the same compartment. *Mcl-1* deletion also causes a decrease in the numbers of mature neutrophils. The GMP are the precursor for neutrophils and macrophages so it was no surprise when a reduction of neutrophils resulted from *Mcl-1* deletion. However, it appears that the expression of BCL-2 and/or BCL-X_L also safeguards the survival of macrophages which likely explains why *Mcl-1* deletion does not cause a reduction of macrophages *in vivo*. In addition, inducible loss of MCL-1 was shown to cause death of cardiomyocytes, leading to fatal heart or liver failure, respectively (Thomas et al., 2013, Weber et al., 2010).

There is strong evidence that MCL-1 plays a major role in tumorigenesis and the response of malignant cells to diverse anti-cancer therapeutics. A genome wide analysis of over 3000 human cancers across 26 subtypes found that the locus encoding MCL-1 had undergone somatic amplification in around 11% of tumours (Beroukhim et al., 2010). Increasing severity of disease in non-Hodgkin's lymphoma has been associated with increasing levels of MCL-1 as demonstrated by immunohistochemistry in a study of 151 clinical samples (Cho-Vega et al., 2004). Other malignancies displaying high levels of MCL-1 protein include cholangiocarcinoma, multiple myeloma and acute myeloid myeloma (Kobayashi et al.,

2005, Le Gouill et al., 2004). Experimentally, the overexpression of MCL-1 in the haematopoietic compartment in transgenic mouse studies generated lymphomas, primarily of B cell origin, in 85% of mice but over a 2-year period (Zhou et al., 2001). When *Mcl-1* was placed under the control of the potent pan-haematopoietic promotor *vav,* most transgenic mice developed leukaemias and/or lymphomas within 20 months of age, mostly of either stem cell progenitor or pre-B cell origin (Campbell et al., 2010). In the *Eμ-Myc* transgenic mouse model of MYC driven lymphomas, such as BL, the deletion of even a single allele of *Mcl-1* was shown to abrogate the sustained growth of such tumours *in vivo*, unless they had acquired a mutation in the tumour suppressor p53, when only the loss of both alleles of *Mcl-1* stopped such tumour growth (Kelly et al., 2014). Moreover, the inducible deletion of MCL-1 also impaired the sustained growth of human BL cell lines *in vitro* and reduced tumour and in xenograft mouse models *in vivo* (Aubrey et al., 2015), as well as the growth of BCR-ABL driven pre-B ALL as well as T cell lymphomas driven by the loss of p53 or mutations in *Notch* (Koss et al., 2013, Grabow et al., 2014, Spinner et al., 2016).

BFL-1/A1

The pro-survival member A1 (termed BFL-1 in humans) is encoded by the *Bcl2a1* gene. In mice the genomic locus is relatively complex compared to the other pro-survival BCL-2 family genes, comprising 4 genes with one being a pseudogene (Hatakeyama et al., 1998). The complete knockout of all functional *Bcl2a1* gene isoforms — A1-a, -b and -d — in mice caused only minor defects to the haematopoietic system or any other organ system. The

defects in the haematopoietic compartment included a modest decrease in the γδT cells, $CD4^+$ T cells and dendritic T cells (Schenk et al., 2017). Despite the rapid induction of A1 expression seen upon TCR stimulation in $CD4^+$ and $CD8^+$ T cells, *Bcl2a1*-deleted mice did not show any impairment in the generation of cytotoxic T cells, the generation of antigen-specific memory T cells and viral clearance (Tuzlak et al., 2017). These studies suggest that A1 exhibits substantial functional overlap with other anti-apoptotic members of the BCL-2 family.

With respect to cancer, the knockdown of BFL-1 by shRNAs has been shown to sensitise certain malignant human B leukaemia/lymphoma cells to apoptosis triggered by treatment with the chemotherapeutic agents, vincristine and cisplatin, or by the CD20 targeting monoclonal antibody, rituximab (Brien et al., 2007). A1 has also been demonstrated to contribute to IL3-independent survival and growth of Bcr/Abl-positive CML cells (Nieborowska-Skorska et al., 2002). Moreover, a screen of primary tumour samples and cancer derived cell lines revealed BFL-1 expression in multiple malignancies but particularly in gastric and colon cancers (Park et al., 1997). High levels of BFL-1 have also been associated with melanoma metastasis (Riker et al., 2008, Cruz-Munoz et al., 2012, Hind et al., 2015) and chemoresistance in certain haematological malignancies, such as AML (Morales et al., 2005). More recently, BFL-1 has been associated with resistance to certain BH3 mimetic drugs (see section 1.3.4 below). Up-regulation of BFL-1 was shown to render CLL derived cell lines resistant to even high concentrations of ABT-737, a potent inhibitor of BCL-2, BCL-X_L and BCL-W (Vogler et al., 2009). Of note, knockdown of BFL-1 was able to

overcome the resistance of double-hit B lymphoma derived cell lines to the BCL-2 specific BH3 mimetic drug, ABT-199 (Esteve-Arenys and Roue, 2018). Given that loss of A1 causes essentially no abnormalities in mice, targeting BFL-1 for cancer therapy would be anticipated to cause only few or no on-target side-effects.

BCL-W

Mice deleted for the *Bcl2l2* gene that encodes BCL-W are born normal, indicating loss of BCL-W does not impact on embryogenesis (Ross et al., 1998, Print et al., 1998). The only abnormality reported for BCL-W deficient mice is male infertility due to a defect in spermatogenesis that may be due to the aberrant apoptosis of Sertoli and Leydig cells, which function to support the developing sperm cells.

In regard to a role for BCL-W in cancer, it was reported that loss of BCL-W causes a marked delay in lymphoma development in *Eμ-Myc* mice. In human cancers, an analysis of 57 BL samples and 319 DLBCL samples revealed overexpression of BCL-W relative to normal B cells (Adams et al., 2017a). A further analysis of 6 subtypes of B cell lymphoma showed consistent overexpression of BCL-W compared to normal B cells, and this was inversely correlated to BCL-2 expression in some lymphoma types (Adams et al., 2017b). The authors of these studies suggested that BCL-W may be as important as BCL-2 in lymphoma cell survival.

1.3.3 Pro-apoptotic members of the BCL-2 family

If the anti-apoptotic members of the BCL-2 family can be described as oncogenes, then the pro-apoptotic BH3-only proteins can be considered tumour suppressors by the nature of their action. The varying stimuli that can induce the transcriptional or post-transcriptional activation of the different BH3-only proteins have been summarised in **figure 1.8**. Below I describe the experimental and epidemiological evidence that has given insight into the roles of the pro-apoptotic BCL-2 family members in normal development, homeostasis and in tumorigenesis.

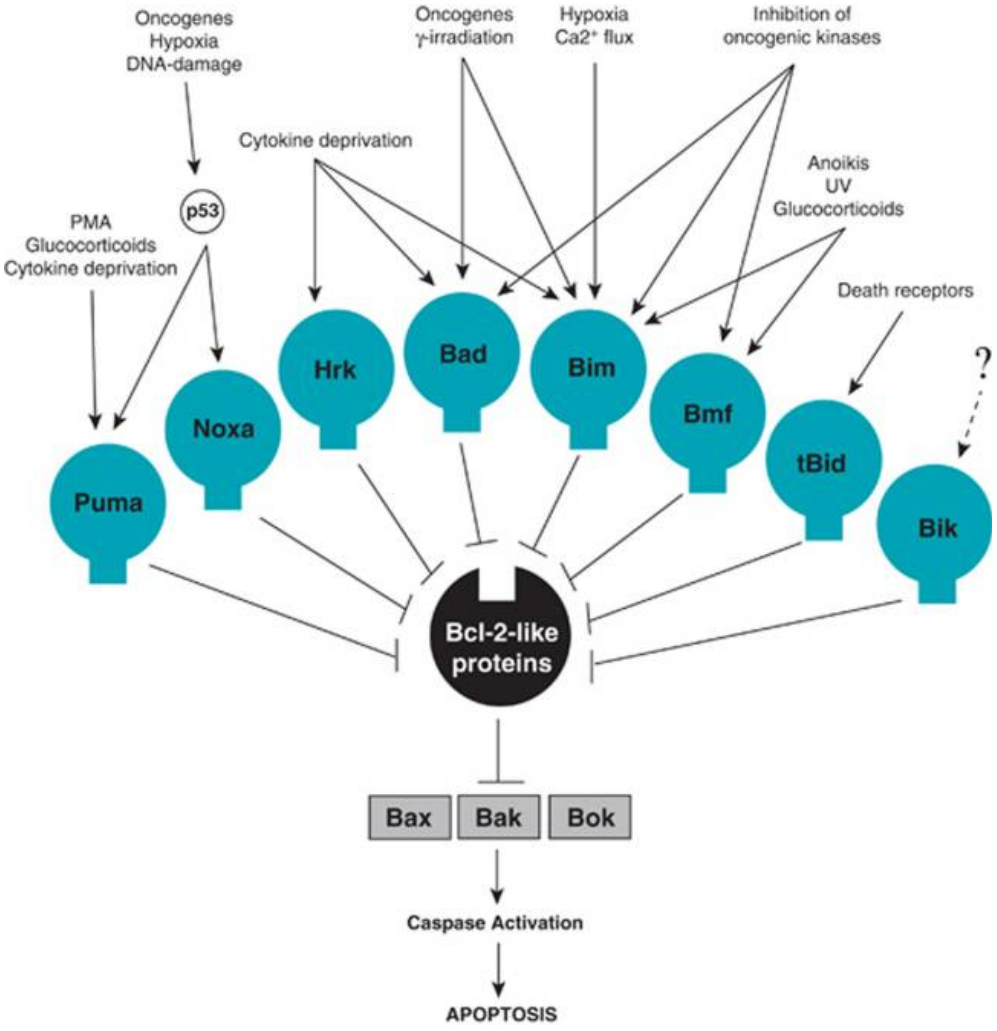


Figure 1.8 Distinct apoptotic stimuli for different BH3-only proteins. The activation of BH3-only proteins is mediated by different apoptotic stimuli including DNA damage, oncogene activation and anoikis. The activation of certain BH3-only proteins, such as BIM, can occur through multiple stimuli including cytokine deprivation, hypoxia and Ca2+ flux. The activation of other BH3-only proteins can be more restricted for example the activation of tBID that occurs only after death receptor engagement. (Adapted from Kelly and Strasser, 2011)

BIM

BIM is encoded by the *Bcl2l11* gene. The importance of BIM as the major member in its class is perhaps best demonstrated by the ability of *Bcl2l11* gene deletion to rescue the defects observed in BCL-2-deficient mice, including the polycystic kidney disease, loss of melanocytes and loss of mature B and T lymphocytes (Bouillet et al., 2001). BIM plays a major role in the hematopoietic system as demonstrated by the observation that BIM deficient mice alone develop lymphoid and myeloid hyperplasia and on a mixed C57BL/6 x 129SV genetic background fatal SLE-like autoimmune disease. The BIM-deficient lymphocytes are resistant to diverse apoptotic stimuli, including cytokine removal, deregulated calcium ion flux, DNA damage and glucocorticoids (Bouillet et al., 1999). Loss of BIM also impairs the negative selection of autoreactive T cells in the thymus (Bouillet et al., 2002).

Loss of BIM, even loss of one allele of *Bim*, significantly accelerates lymphoma development in *Eμ-Myc* transgenic mice (Egle et al., 2004). This was the first demonstration that BIM can function as a tumour suppressor. Typically, more than half of *Eμ-Myc* tumours are selected for a mutation in the p19Arf/p53 pathway (Eischen et al., 1999). Interestingly, 0% of tumours from *Bim*$^{-/-}$ Eμ-Myc mice contained such mutations, suggesting that loss of BIM acts as an alternative mechanism to loss of p53 activity during tumour development. Reduced *Bim* expression is frequently observed in human cancers of various origins, including Burkitt's lymphoma and diffuse large B cell lymphoma and mantle cell lymphoma where homozygous deletions have been reported (Mestre-Escorihuela et al., 2007).

Homozygous loss of 2q13, the region encoding the *Bcl2l11* gene, was found to occur in 17% of mantle cell lymphoma samples analysed in a genome-wide array (Tagawa et al., 2005). In epithelial cell tumours with a constitutively active H-Ras/ERK pathway, proteasome-dependent degradation of BIM was shown to mediate paclitaxel resistance (Tan et al., 2005).

Bim expression is mediated through a complex network of transcriptional, post-transcriptional and post-translational regulation. Transcriptionally, c-MYC can bind the *Bim* promoter to induce expression and sensitise cells to BIM-mediated apoptosis (Muthalagu et al., 2014). Additionally, *Bim* expression can be induced by E2F1, a transcription factor highly involved in the activation of genes associated with cell cycle progression (Hershko and Ginsberg, 2004). At the post-transcriptional level, *Bim* mRNA can be targeted at its UTR by miRNAs such as by members of the miR-17-92 cluster (Ventura et al., 2008). At the protein level, c-Jun N-terminal kinase (JNK) can phosphorylate BIM in order to potentiate its proapoptotic activity following trophic factor deprivation (Putcha et al., 2003).

PUMA and NOXA

PUMA and NOXA are the major effectors of p53-mediated apoptosis, which is activated in response to death stimuli including DNA damage and cytokine withdrawal. Single or double-stranded DNA breaks (induced by ultraviolet light, gamma irradiation and topoisomerase inhibitor treatment) can lead to p53 activation and subsequent *Puma* and *Pmaip1* (NOXA) transcriptional upregulation (Yu and Zhang, 2008, Ploner et al., 2008).

Additionally, both PUMA and NOXA can be upregulated in hypoxic conditions where PUMA remains under the control of p53 but hypoxia-inducible factor 1-alpha mediates the induction of NOXA (Kim et al., 2004).

Mice deleted for the gene *Bbc3* that encodes PUMA are born normal and exhibit no developmental defects. Consistent with PUMA and NOXA being the major effector of p53-mediated apoptosis, PUMA/NOXA double deficient thymocytes and mature B as well as T cells are completely protected from gamma irradiation both *in vitro* and *in vivo*. Interestingly, loss of PUMA also affords lymphoid cells protection from certain p53-independent stimuli, including cytokine deprivation or treatment with glucocorticoids or phorbol esters (e.g. PMA) (Jeffers et al., 2003, Villunger et al., 2003a).

Many studies have provided evidence that PUMA can function as a tumour suppressor. Knockdown of *Puma* expression by shRNA synergised with enforced expression of E1A plus Ras or Myc in the transformation of primary mouse fibroblasts in culture (Hemann et al., 2004). Furthermore, loss of PUMA, even loss of one allele of *Puma*, substantially accelerated lymphoma development in Eμ-Myc transgenic mice and reduced the pressure to inactivate the p53 tumour suppressor in this tumour model (Michalak et al., 2009). Mice lacking both BIM and PUMA develop more severe lymphadenopathy and splenomegaly than those lacking only BIM, and some appear to develop malignancies of plasma cells (Erlacher et al., 2006). In human malignancies, chromosomal loss at 19q, which harbours the *Puma* gene, has been reported in multiple cancer types, including glioma, neuroblastoma, head and neck squamous cell carcinoma, lung cancer and malignant

melanoma (Yong et al., 1995, Mora et al., 2001, Hoque et al., 2003, Karst et al., 2005). Moreover, the PUMA gene is frequently epigenetically silenced in B cell malignancies, such as Burkitt's lymphoma (Garrison et al., 2008).

NOXA is more limited in its function when compared to PUMA. Mice deleted for *Pmaip1* are born normally and do not display any abnormalities even in adulthood (Villunger et al., 2003a). Despite being a p53 target gene, loss of NOXA alone provided little to no protection to cells from p53-dependent apoptotic stimuli. However, loss of NOXA alongside PUMA protected primary mouse embryonic fibroblasts (MEFs) from apoptosis induced by etoposide to a greater extent than loss of PUMA alone. Furthermore PUMA/NOXA knockout thymocytes were as protected from γ-radiation induced killing as p53-deficient thymocytes both *in vitro* and *in vivo*. The binding specificity of NOXA is limited to only MCL-1 with high affinity and to A1 with low affinity (Willis et al., 2005). An example of the effect of this limited binding spectrum has been demonstrated in mouse embryonic fibroblasts where both MCL-1 and BCL-X_L are required for survival. The overexpression of NOXA in such cell types is not sufficient to induce significant cell killing as it cannot neutralise BCL-X_L, and therefore for efficient killing the function of NOXA must be complemented by the action of BAD (targeting BCL-2, BCL-X_L and BCL-W) or by a BH3-only protein that can target all anti-apoptotic BCL-2 family members, such as PUMA or BIM (Willis et al., 2005). Loss of NOXA alone, even when combined with loss of PUMA, does not induce tumours in mice up to one year of age (Villunger et al., 2003a). However, when combined with loss of PUMA, loss of NOXA caused a significant acceleration in lymphoma development in the Eμ-Myc

transgenic mice (Michalak et al., 2009). In human cancers, loss or mutation of *Pmaip1* has not been considered a common event in tumorigenesis (Lee et al., 2003).

BAD

Knockout mice lacking *Bad* develop normally (Ranger et al., 2003). However, around 20% of aged mice go on to develop germinal centre B cell lymphomas suggesting a role for BAD in suppression of lymphoid tumour. The pro-apoptotic function of BAD can be inhibited by its phosphorylation. MAPK signalling to phosphorylate serine residue 112 of BAD and PI3K/Akt mediated phosphorylation at serine 136 of BAD has been detected in cancers and is reported to prevent the binding of BAD with the anti-apoptotic BCL-2 family members (Blume-Jensen et al., 1998, Zha et al., 1996).

BIK

BIK is one of the lesser studied members of the BH3-only proteins perhaps because its loss in knockout mice causes no notable abnormalities in any of the tissues examined, including the haematopoietic system (Coultas et al., 2004). Moreover, the decrease in haematopoietic cells induced by loss of *Bcl-2* could not be rescued by the concomitant loss of *Bik*. These data point towards some functional overlap between BIK and other BH3-only proteins. Consistent with this idea, the combined loss of BIK and BIM caused severe defects in spermatogenesis and male infertility, whereas loss of either BH3-only protein alone did not cause such defects.

With respect to a role of BIK in cancer, the loss of BIK did not impact lymphoma development in Eμ-Myc mice, even when combined with loss of NOXA (Happo et al., 2012). Possible evidence for BIK as a tumour suppressor can be found in human gliomas and renal cell carcinomas where chromosomal loss at 22q, containing the *Bik* gene, is observed (Bredel et al., 2005, Kim et al., 2006, Sturm et al., 2006). However, the genomic region lost in these cancers contains not only *Bik* but many more genes.

HRK

Hrk$^{-/-}$ mice are indistinguishable from WT mice with respect to weight, appearance, behaviour and histological appearance of major organs suggesting a lack of requirement for HRK during normal development (Coultas et al., 2007). HRK has been demonstrated to induce apoptosis in neuronal cells and haematopoietic cells upon growth factor removal *in vitro* (Imaizumi et al., 1997, Sanz et al., 2000). The epigenetic silencing of HRK or chromosomal loss at 12q13.1 has been proposed to be exploited by glioblastomas and anaplastic astrocytomas as a mechanism of evading apoptosis (Nakamura et al., 2005). Again, it must be noted that this chromosomal region contains not only *Hrk* but many additional genes.

BMF

Mice lacking the *Bmf* gene do not exhibit any phenotypic abnormalities during development (Labi et al., 2008). However, B cell-restricted lymphadenopathy and accelerated γ-irradiation induced lymphoma development have been observed in Bmf-

deficient mice. Apoptosis induced by HDAC inhibitors was shown to be dependent in part on BMF in thymocytes and in certain cancer derived cell lines (Labi et al., 2008, Zhang et al., 2005). Cytokine withdrawal causes an increase in the expression of *Bmf* as demonstrated in bone marrow-derived granulocytes (Villunger et al., 2003b). Similarly, to the loss of *Bcl2l11* (BIM), the loss of *Bmf* accelerates lymphoma development in Eμ-Myc mice and reduces the pressure for acquiring mutations in the Arf/p53 pathway (Frenzel et al., 2010). In human cancers, loss of heterozygosity at 15q14-15 (which contains the *Bmf* locus) has been associated with breast and lung cancer development but this has not been directly attributed to *Bmf* loss (Schmutte et al., 1999).

BID

The BH3-only protein BID is the linker between the extrinsic and intrinsic apoptotic pathways as described above. *Bid*-deficient mice develop normally, with no apparent abnormalities in any major organs (Yin et al., 1999). The loss of *Bid* rendered type 2 cells, such as hepatocytes, resistant to Fas- or TNFR1-mediated killing, both *in vitro* and *in vivo*, but so-called type 1 cells, such as thymocytes or mature T cells, remained normally sensitive to FAS ligand (Yin et al., 1999, Kaufmann et al., 2007). Studies with *Bid*-knockout mice have suggested an important role for BID in myeloid homeostasis due to the development of myeloproliferative disorder in aged mice (Zinkel et al., 2003). These mice developed chromosomal aberrations which led to the suggestion that BID had a role in apoptosis induced by DNA damage (Zinkel et al., 2005). However, these findings in *Bid*-deficient mice were not replicated by others who showed no tumour development in such

mice and failed to identify differences between *Bid*-deficient and WT cells when treated with multiple DNA damage-inducing stimuli (Kaufmann et al., 2007). In humans, it has been reported that ~6% of gastric carcinomas contain a frameshift mutation in the *Bid* gene that mediates resistance to 5-fluorouracil chemotherapy demonstrating the role of BID as a tumour suppressor (Lee et al., 2004).

BAK / BAX / BOK — the effectors of apoptosis

The overlapping functions of BAK and BAX have been demonstrated through the analysis of *Bax* and *Bak* gene knockout mice. BAX knockout mice develop normally and show only limited abnormalities, including relatively mild lymphadenopathy with age and a defect in spermatogenesis that causes male infertility (Knudson et al., 1995). The BAK knockout mice also develop normally and exhibit no abnormalities with the exception of a mild albeit significant increase in blood platelet levels (Lindsten et al., 2000). However, most mice lacking both *Bak* and *Bax* die on the day of birth, mostly due to cleft palate, with fewer than 10% surviving into adulthood (Ke et al., 2018). Cells deficient for both BAX and BAK are completely resistant to many (and possibly all) apoptotic stimuli (Lindsten et al., 2000) including the enforced expression of BH3-only proteins (e.g. BIM, PUMA) (Zong et al., 2001).

The function of BOK, which shares substantial amino acid sequence similarity and structural similarity with BAX and BAK, is less well understood (Ke et al., 2018, Zheng et al., 2018). BOK has been shown to bind MCL-1 and can induce mitochondrial apoptosis (Hsu et

al., 1997). BOK protein stability was reported to be regulated by endoplasmic reticulum-associated degradation rather than having its activation regulated positively by the pro-apoptotic BH3-only proteins and negatively by the BCL-2-like pro-survival proteins (Llambi et al., 2016). Triple knockout of *Bak*, *Bax* and *Bok* in the haematopoietic system has shown similar phenotypes to *Bak* and *Bax* double knockouts with respect to survival due to autoimmune disease but the additional loss of *Bok* led to increased numbers of peripheral blood lymphocytes (Ke et al., 2015). Interestingly, the BAX/BAK/BOK triple knock embryos present with substantially more severe developmental defects compared to the BAX/BAK double knockout embryos (Ke et al., 2018). Although mutations in the *Bak* and *Bax* genes are rare, two missense mutations reported in the Catalogue of Somatic Mutations in Cancer (COSMIC) catalogue (Kim et al., 2012, Forbes et al., 2015) were shown to over-stabilise the BAX homodimer thereby preventing proper oligomerisation and pore formation (Zhang et al., 2016). *Bax* mutations are most associated with colorectal cancer (Miquel et al., 2005, Pryczynicz et al., 2014) but low levels of both *Bak* and *Bax* have been detected in AML samples (Glaser et al., 2012).

1.3.4 Therapeutic targeting of the BCL-2 family

The possibility to develop small molecules that could bind to the BCL-2-like pro-survival proteins and disrupt protein-protein interactions in order to specifically kill cancer cells became possible through advances in structural biology and medicinal chemistry that opened the door to screening-based techniques and rational drug design. Below I provide

a description of selected compounds targeting distinct pro-survival members of the BCL-2 family with the experimental and clinical data supporting their use as anti-cancer agents.

Early inhibitors of pro-survival BCL-2 family members

The first agent to be considered for BCL-2 targeting action was the (-) enantiomer of the polyphenolic compound gossypol. Originally used as a contraceptive agent, gossypol was found to have BCL-2 and BCL-X_L binding ability and could induce cell death in Jurkat cells overexpressing these anti-apoptotic proteins more effectively than the chemotherapeutic agent etoposide (Oliver et al., 2005). Gossypol demonstrated its ability to induce cytochrome c release, caspase activation and inhibition of tumour growth in models of DLBCL (Mohammad et al., 2005). However, gossypol kills cells lacking both BAX and BAK as efficiently as their BAX/BAK proficient parental cells. This demonstrates that this compound kills cancer cells in a manner independent of the intrinsic apoptotic pathway and hence independent of targeting any pro-survival BCL-2 family members (van Delft et al., 2006). Despite this, the drug entered clinical trials but 14 out of 14 patients with recurring extensive-stage SCLC failed to show any response to the drug in a phase II study (Baggstrom et al., 2011).

The small molecule known as obatoclax, or GX15-070, was identified in a library screen to inhibit BCL-2, BCL-X_L, BCL-W and MCL-1 (Konopleva et al., 2008) and was demonstrated to be efficacious in inducing NOXA-mediated apoptosis in laboratory models of mantle cell lymphoma (Perez-Galan et al., 2007). Although obatoclax was initially well tolerated in

patients with SCLC, the drug ultimately failed during phase II trials because no responses were observed in patients with SCLC, even when obatoclax was combined with chemotherapy (Paik et al., 2010, Paik et al., 2011). Moreover, like gossypol, obatoclax was found to kill cells in a BAX/BAK independent manner and therefore does not work on-target (van Delft et al., 2006).

Development of BH3 mimetic compounds

The successful development of small molecule inhibitors of the BCL-2-like pro-survival proteins was achieved through rational drug design. Resolution of the structure of BCL-X_L using nuclear magnetic resonance (NMR) spectroscopy techniques led to the development of ABT-737 which binds with sub-nM affinity to the hydrophobic pocket of BCL-X_L, BCL-2 and BCL-W but has negligible binding to MCL-1 or A1 (K_i > 1 uM) (Muchmore et al., 1996, Oltersdorf et al., 2005). ABT-737 kills tumour cells in a BAK/BAX-dependent manner and thus functions on-target. Treatment with ABT-737 was shown to inhibit tumour growth in xenograft mouse models of SCLC (Oltersdorf et al., 2005). A limitation of ABT-737 is its low solubility and poor oral bioavailability but this was improved upon and led to the development of its derivative, ABT-263 (navitoclax), which also binds with high affinity to BCL-X_L, BCL-2 and BCL-W but has markedly improved pharmacological properties. Navitoclax was the first BH3-mimetic to progress into the clinic and showed promising results in patients, including those with blood cancers, such as CLL. However, the patients developed thrombocytopenia due to a dependency of platelets on BCL-X_L and this has

limited the clinical application of Navitoclax (Roberts et al., 2012, Wilson et al., 2010, Mason et al., 2007).

Targeting BCL-2

To overcome the problems with platelet toxicity, a BCL-2 specific inhibitor was developed. Souers and colleagues reported ABT-199/Venetoclax which bound with high affinity to BCL-2 ($K_i \leq 0.01$nM) and killed cells in a BAK/BAX-dependent manner (i.e. through an on-target mechanism) (Souers et al., 2013). ABT-199 demonstrated efficient killing in NHL cell lines with a 100-fold lower EC50 values in cells expressing high BCL-2 versus cells expressing low levels of BCL-2. Efficient killing of CLL cells *in vivo* in patients was also observed in early clinical trials. Importantly, due to the absence of significant binding of ABT-199 to BCL-X_L, no thrombocytopenia was observed. Following the success of phase I clinical trials where the drug was well tolerated, phase II trials reported a 79% overall response rate and 20% complete response in CLL patients (Roberts et al., 2016). In 2016, ABT-199 was granted FDA approval in the USA for the treatment of refractory CLL. Many clinical trials combining Venetoclax with standard anti-cancer therapies for the treatment of diverse human cancers are now underway.

Targeting BCL-X_L

Using similar rational drug design approaches based upon structural data, an array of BCL-X_L-specific inhibitors have been developed. Such inhibitors include WEHI-539, A-1155463 and A-1331852, all with sub-nM binding affinities to BCL-X_L and lack of significant binding

to all other pro-survival BCL-2 family members (Lessene et al., 2013, Tao et al., 2014, Leverson et al., 2015a). A-1155463, developed as a more potent binder of BCL-X_L than WEHI-539, was reported to induce marked platelet killing *in vivo,* as is observed with ABT-737, however, platelet numbers recovered within 96 hours of initial treatment (Tao et al., 2014). A-1155463 was shown to inhibit tumour growth in subcutaneous xenograft mouse models of SCLC although the effects were modest. The most promising of the BCL-X_L inhibitors is A-1331852 with a $K_i \leq 0.01$nM and, as expected, it kills cells in a BAK/BAX-dependent manner and is orally bioavailable (Lessene et al., 2013). A-1331852 was shown to significantly inhibit tumour growth in xenograft models of SCLC, breast and ovarian cancer. However, the treated mice also show markedly decreased platelet levels and this on-target effect of this compound could become dose-limiting and limit its future clinical development.

Targeting MCL-1

The first MCL-1-specific BH3 mimetic reported is known as A-1210477 with $K_i = 0.454$ nM as determined by time-resolved fluorescence energy transfer (TR-FRET) (Leverson et al., 2015b). In MCL-1 dependent cell lines, A-1210477 was able to disrupt the MCL-1:BH3-only protein interaction, induce cytochrome c release and apoptosis. Furthermore, the killing of fibroblasts by this compound was shown to be BAK/BAX dependent. However, this compound has severe limitations due to high absorption by serum, poor membrane permeability and poor bio-availability. Subsequently, Servier revealed their MCL-1 inhibitor, S63845, that could bind MCL-1 with a 20-fold higher affinity than A-1210477 and

exhibits more favourable pharmacological properties (Kotschy et al., 2016). S63845 induces apoptosis via BAK/BAX-dependent killing and is able to efficiently induce cell death in an array of haematological malignancies *in vitro* and in xenograft models of disease *in vivo*. In mouse models, the drug was well tolerated at doses that could induce lymphoma regression, with no overt damage to healthy tissues. This is surprising considering the high reliance on MCL-1 for survival in many subsets of lymphocytes and other cell types, including hepatocytes and cardiomyocytes (Thomas et al., 2013, Weber et al., 2010, Opferman et al., 2003, Opferman et al., 2005). MCL-1 inhibitors have now entered phase I clinical trials for blood cancers, including AML and multiple myeloma.

The future of BH3 mimetic drugs

There are still some limitations with regard to the clinical application of BH3 mimetics. The effectiveness of ABT-199 has led to tumour lysis syndrome in several cases in early clinical trials and milder side effects have included neutropenia with a risk of respiratory infections (Roberts et al., 2016, Flinn et al., 2015). However, such issues have been addressed by dose control and co-treatment with granulocyte colony stimulating factor (G-CSF). The dependency of platelet survival on BCL-X_L has been demonstrated by BH3 mimetics that target this pro-survival protein, such as ABT-737 and A-1331852. Although there is evidence for platelet recovery following treatment, perhaps combining BH3 mimetics at lower doses with other chemotherapeutics or targeted agents could allow BCL-X_L specific BH3 mimetic drugs to enter clinical practice.

Evidence in support of combining BH3 mimetics with other anti-cancer drugs is rapidly emerging, suggesting synergistic tumour cell killing can be achieved, presumably because the latter cause an increase in BH3-only proteins, such as BIM and PUMA. In subcutaneous xenograft models of various solid tumours, A-1331852 was most efficacious when combined with the chemotherapy agent docetaxel (Leverson et al., 2015a). The combined treatment achieved 74% tumour growth inhibition in 6 of 7 tumour models whereas A-1331852 alone ranged from 34-67%. Another rationale for the use of BCL-X_L inhibitors in combination therapies is that *Bcl2l1* copy numbers have been reported to be upregulated in tumours resistant to cytotoxic agents and therefore A-1331852 could be used in an effort to overcome such chemoresistance (Amundson et al., 2000). The combination of ABT-737 with epidermal growth factor receptor (EGFR) inhibitors, such as gefitinib, have proven efficacious in non-small cell lung cancer (NSCLC) cell lines (Cragg et al., 2007). ABT-737 has also been combined with MEK inhibitors to induce BIM-dependent apoptosis in solid tumours harbouring BRAF mutations (Cragg et al., 2008). Combining BH3 mimetics that target different pro-survival BCL-2 family members has been shown to be an effective strategy against tumour cells which can adapt and switch their dependency from one anti-apoptotic protein to another. However, it is predicted that blocking two or more pro-survival BCL-2 family members will have the risk of causing substantial damage to healthy tissues.

The usefulness of BH3 mimetic drugs stretches beyond the treatment of well-understood cancers and they have great utility as research tools. Regulation of the BCL-2 protein family

of apoptosis contains complexities and redundancies that can prove challenging to pick apart in a cancer cell. BH3 mimetics now allow for the precise identification of dependencies of different cell types on different pro-survival BCL-2 family members and such information can be used for deciding on treatment strategies. The use of BH3 mimetics will therefore accelerate our understanding of less well investigated cancer types, such as ENKTL, where neither cellular nor virus-mediated mechanisms of apoptotic evasion have been identified.

1.4 Aims of thesis

1) To characterise, validate and critique the use of currently available ENKTL and CAEBV cell lines as the primary disease model within the field. This will be achieved by assessing the immunophenotype of these cell lines and determining their EBV expression profile.

2) To determine the mechanism of resistance of ENKTLs and CAEBVs to current chemotherapeutics. This will be achieved by assessing the response of ENKTL and CAEBV derived cell lines to clinically relevant genotoxic treatments and assessing the apoptotic pathway within these cells *in vitro* and *in vivo*.

3) To identify novel susceptibilities of ENKTL and CAEBV derived cell lines that could be exploited therapeutically in the future. This will be achieved by performing a high-throughput drug screen to identify potential compounds for therapeutic use and to identify molecular pathways critical for the survival of these malignant cells.

2. Materials and Methods

2.1 Cell culture

All human cell lines were grown in tissue culture-grade plates or flasks and maintained in a humidified incubator at 37°C with 5% CO_2. All cell lines were passaged 2-3 times per week, depending on starting cell density and proliferation rate, to a final density ranging from 0.5-1x10^6 cells per mL in relevant media, as described below.

2.1.1 EBV-positive T and NK cell lines

EBV-positive cell lines SNK1, SNK6, SNT8, SNT13, SNT15, SNT16, MEC04 (Zhang et al., 2003, Nagata et al., 2001, Oyoshi et al., 2003, Coppo et al., 2009) and NKC1 (see **section 2.1.4**) were grown in 'NK/T media' - RPMI-1640 media (Sigma, USA) supplemented with 10% v/v heat-inactivated and sterile-filtered human serum (Sigma), 100 U/mL penicillin (Invitrogen, USA), 100 μg/mL streptomycin (Invitrogen), 6 mM L-glutamine (Invitrogen), 1mM sodium pyruvate (Sigma), 700 U/mL IL-2 (Novartis, Switzerland). NKC1, SNT8, SNT13 and SNT15 cells were grown in 12-well plates with 3mL media per well. SNK1, SNK6, SNT16 and MEC04 cells were grown in 25 cm^3 flasks with 10mL media.

2.1.2 EBV-negative T and NK cell lines

Jurkat and MOLT4 cells were grown in 'standard media' - RPMI-1640 media supplemented with 10% v/v foetal calf serum (FCS) (ThermoFisher, USA), 100 U/mL penicillin, 100 µg/mL streptomycin, and 6mM L-glutamine. NKL cells were grown in standard medium with 400 U/mL IL-2. KG-1 cells were grown in standard medium adjusted to 20% v/v FCS.

2.1.3 B cell lines

Burkitt lymphoma cell lines BL2, BL41, Kem-BL and Sav-BL were grown in standard media with 1 mM sodium pyruvate, 8 µg/mL gentamycin (Sigma), 20 nM bathocupronine disulphonic acid (Sigma) and 50 µM α-thioglycerol (Sigma).

2.1.4 Generation of CAEBV cell line from patient blood

Peripheral blood from a post-treatment CAEBV patient was received from University Hospitals Leicester NHS Trust for research purposes under ethics number 07/H1208/62. Mononuclear cells from the patient blood sample were first isolated. To do this, blood was diluted 1:1 with phosphate-buffered saline (PBS) then, in 50 mL Conical Centrifuge Tubes (Falcon), 25 mL of diluted blood was overlaid onto 15 mL Lymphoprep (Axis-Shield, UK). Samples were then centrifuged at 652 g at room temperature with no brake for 30 minutes at room temperature. Human peripheral blood mononuclear cells (PBMCs) were isolated from the interface and washed twice in PBS. To promote growth of EBV-positive NK cells, PBMCs were grown in CellGro SCGM (stem cell growth medium – CellGenix, Germany)

supplemented with 10% v/v heat-inactivated and sterile-filtered human serum (Sigma), 100 U/mL penicillin (Invitrogen), 100 μg/mL streptomycin (Invitrogen), 6 mM L-glutamine (Invitrogen), 1 mM sodium pyruvate (Sigma) and 700 U/mL IL-2 (Novartis). Cell viability and growth were monitored until the establishment of a continuously proliferating NK cell line as determined by flow cytometry and described later.

2.1.5 Cell cryopreservation and recovery

Human PBMCs, cell lines and mouse tumour cells were centrifuged at 453 g at room temperature for 5 minutes and the supernatant was removed. The cell pellet was resuspended in 'freezing media' – RPMI-1640, 20% v/v FCS and 10% dimethyl sulfoxide (DMSO) – to a final density of $10x10^6$ cells per mL and were aliquoted at 1 mL per cryovial (ThermoFisher). Cryovials were stored at -80°C overnight in a Mr Frosty Freezing Container (Nalgene) with isopropanol to allow gradual temperature decrease at 1°C per minute. Frozen cells were then transferred to liquid nitrogen storage for long term cryopreservation.

2.1.6 Revival of cryopreserved cells

Cryovials were placed in a 37°C water bath for the minimum time required for thawing of the cells. Cell lines were then washed in 50 mL of appropriate media then resuspended at $0.5\text{-}1x10^6$ cells per mL and then maintained in a humidified incubator at 37°C with 5% CO_2.

2.2 RNA analysis

2.2.1 RNA purification

Cells were pelleted (3500 g at room temperature) and washed once in PBS prior to total RNA extraction. For each RNA preparation, between 0.5-5x10^6 cells were processed to ensure optimal yields. Samples were processed according to the manufacturer's instructions using the RNeasy kit (Qiagen, Germany) and eluted with 50 µL nuclease-free water. RNA was quantified by UV spectroscopy using the Nanodrop 1000 (ThermoFisher). Concentration was determined by absorbance at 260 nm and purity was determined by the 260:280 nm ratio. RNA was stored at -80°C and kept on ice when in use.

Precise quantification of RNA transcripts relies upon minimal DNA contamination within the sample. This is particularly important for quantitative-PCR reactions (qPCR) involving a probe that does not span an exon-exon boundary. To ensure minimal DNA contamination, eluted RNA samples were DNAse I treated (Turbo DNase kit, ThermFisher) according to the manufacturer's instructions.

2.2.2 cDNA synthesis

The generation of cDNA from RNA was achieved using QScript cDNA Supermix (Quantabio, USA), according to the manufacturers' instructions. Briefly, for each reaction, up to 1 µg RNA was incubated with 4uL of 5x master mix (containing reverse transcriptase (RT), $MgCl_2$, dNTPs, RNAse inhibitor protein and random primers) and nuclease-free water to a final

volume of 20 µL. The cDNA synthesis protocol was as follows: 5 minutes at 25°C; 30 minutes at 42°C; 5 minutes at 85°C. Negative controls (no-reverse transcriptase enzyme (RT) controls) were prepared in the same way but in the absence of the master mix. cDNA was stored at -20°C and kept on ice when in use.

2.2.3 Taqman qPCR for gene expression

QPCR assays were used to determine the expression of both EBV and cellular genes from generated cDNA. Assays were set up in 96-well optical plates (Geneflow, UK) and performed using an Applied Biosystems 7500 real-time PCR system (ThermoFisher). For each reaction, 25 ng cDNA was added to 12.5 µL TaqMan qPCR master mix (2x) (ThermoFisher) (containing DNA polymerase, $MgCL_2$ and dNTPs), 1.25 µL pre-mixed gene-specific primers and probes (ThermoFisher) (Tierney 2015 and **table 2.1**) and nuclease-free water to a final volume of 25 µL. Gene of interest probes were FAM labelled with a TAMRA quencher. Housekeeping gene probes used a VIC label to allow assay multiplexing. All assays were performed with no-template and no-RT controls.

For cellular transcripts, relative quantification was calculated against a reference sample using the ΔΔCt method and normalised to PGK1 expression. For EBV transcripts, absolute quantification was calculated against a standard curve generated by serial dilution (range of 1 copy to 10^5 copies per µL) of the absolute quantification (AQ) plasmid and also normalised to PGK1 expression. The AQ plasmid, containing 45 EBV amplicons and 3

cellular amplicons, is used to determine the total number of copies of a gene transcript normalised to a control housekeeping gene (e.g. PGK1).

Table 2.1 List of qPCR assays. Reverse transcriptase qPCR assays used to detect cellular genes provided as pre-mixed primers and probes at a 20X concentration (obtained from Thermo Fisher).

Gene	Assay number
BCL2L11 (BIM)	Hs00197982_m1
BID	Hs00609632_m1
BCL-2	Hs00608023_m1
Phosphogycerate kinase 1	Hs99999906_m1
β-2-microgobulin	Hs00187842_m1
GAPDH	Hs99999905_m1

2.2.4 High throughput qPCR

High throughput qPCR for the absolute quantification of EBV gene transcripts was performed using the Fluidigm Dynamic Array system as described by Tierney et al., 2015. Initially, specific target amplification was performed where 1.25 µL of AQ plasmid/sample cDNA (25 ng/µL) was incubated with 1.25uL of primer mix (primers for 45 EBV genes and the 3 cellular genes at 0.2x their respective final concentrations) and PreAmp Master Mix (Life Technologies) in DNA suspension buffer (10 mM Tris, pH 8.08, 0.1 mM EDTA) as per the manufacturers' instructions. The PCR protocol was as follows: 10 minutes at 95°C; 12 cycles of 15 seconds at 95°C, 4 minutes at 60°C. The specific target amplification step was

necessary as low amounts of cDNA template were used per reaction. Samples were then diluted 1 in 5 with nuclease-free water and loaded onto a 48:48 Dynamic Array IFC (Fluidigm, USA) with the 3 cellular qPCR assays (**table 2.1**) and all 45 EBV specific qPCR assays (Tierney et al., 2015) as per manufacturers' instructions, run in a Biomark HD machine and data analysed using Biomark Real-Time PCR Analysis Software Version 2.0.

2.3 DNA analysis

2.3.1 DNA purification

Cells were pelleted (3500 g at room temperature) and washed once in PBS prior to total DNA extraction. For each DNA preparation, between 1-5x10^6 cells were processed to ensure optimal yields. Samples were processed according to the manufacturer's instructions using the DNeasy kit (Qiagen) and eluted with 50 µL nuclease-free water. DNA was quantified by UV spectroscopy using the Nanodrop 1000 (ThermoFisher). Concentration was determined by absorbance at 260 nm and purity was determined by the 260:280 nm ratio. DNA was stored at -20°C and kept on ice when in use.

2.3.2 *TP53* sequencing

Sequencing of the *TP53* gene was performed on PCR products amplified from extracted genomic DNA. Due to the size of the region of interest (exons 5-8), three separate PCR reactions were performed on extracted genomic DNA. Primers were designed (**table 2.2**) to bind intronic regions using Primer-BLAST (NCBI) based upon the published human *TP53*

gene sequence (GenBank accession number U94788). Primers were obtained from Integrated DNA Technologies. For each reaction, 100 ng DNA was incubated with Quick-Load Taq 2X Master Mix (New England BioLabs, USA), forward and reverse primers (1 µM final concentration) and nuclease-free water to a final volume of 50 µL. The thermal cycling protocol was as follows: 5 minutes at 94°C; 32 cycles of 1 minute at 94°C, 1 minute at reaction-specific annealing temperatures (**table 2.2**), 30 seconds at 72°C; and a final extension step of 5 minutes at 72°C.

Table 2.2 *TP53* primers. PCR primer sequences used to amplify *TP53* exons 5-8.

Reaction	Gene	Exon	Annealing temp (°C)	Primer sequence	
1	*TP53*	5 & 6	53	Forward	CTGTTCACTTGTGCCCTGACT
				Reverse	TGACAACCACCCTTAACCCC
2	*TP53*	7	53	Forward	CCTCATCTTGGGCCTGTGTT
				Reverse	AGTGTGCAGGGTGGCAAG
3	*TP53*	8	51	Forward	TCCTTACTGCCTCTTGCTTCTC
				Reverse	TCCACTTGATAAGAGGTCCCA

PCR products were treated with ExoSAP-IT PCR Product Cleanup (ThermoFisher) in order to remove excess primers and unincorporated nucleotides that may interfere with sequencing. For each reaction, 5 µL PCR product was incubated with 2 µL ExoSAP reagent

for 15 minutes at 37°C followed by 15 minutes at 80°C. All Sanger sequencing was done using an Applied Biosystems 3730s Genetic Analyser by Micromon DNA Sequencing Services at Monash University, Victoria, Australia. Sequences were analysed and quality checked using DNASTAR software.

2.3.3 Taqman qPCR for viral load

QPCR assays were used to determine the viral load per cell from extracted genomic DNA. Assays were set up in 96-well optical plates (Geneflow) and performed using an Applied Biosystems 7500 real-time PCR system (ThermoFisher). For each reaction, 100 ng DNA was added to 12.5 µL TaqMan qPCR master mix (2x) (ThermoFisher) (containing DNA polymerase and dNTPs), gene-specific primers and probes (0.2 µM final concentration) (Junying et al., 2003) (**table 2.3**) and nuclease-free water to a final volume of 25 µL. The EBV BALF5 probe was labelled with FAM and the β-2-microgobulin (β2M) probe was VIC labelled to allow multiplexing of the qPCR assays. All assays were performed with no-template.

For quantification of EBV genomes per sample, a standard curve was generated by serial dilution (range of 2 to 4000 EBV genomes per µL) of genomic DNA extracted from Namalwa-BL cells, which have a known viral load of 2 (integrated) genomes per cell (Lestou et al., 1996). Test samples were then normalised to the housekeeping gene, β2M, to calculate the number of EBV genomes per cell.

Table 2.3 Viral load primers. Primers and probes for viral qPCR on genomic DNA. Sequences taken from Junying et al., 2003.

Gene	Primer/probe sequence	
BALF5 (EBV DNA polymerase)	Forward	CTTTGGCGCGGATCCTC
	Reverse	AGTCCTTCTTGGCTAGTCTGTTGAC
	Probe	CATCAAGAAGCTGCTGGCGGCC
β-2-microgobulin	Forward	GGAATTGATTTGGGAGAGCATC
	Reverse	CAGGTCCTGGCTCTACAATTTACTAA
	Probe	AGTGTGACTGGGCAGATCATCCACCTTC

2.3.4 EBV typing

PCR assays were performed on DNA extracted from the cell lines to determine the EBV subtype residing in the cells. To distinguish between subtypes, PCR primers were designed to target an EBNA2 gene region where the DNA sequence was specific to either EBV type 1 or type 2, as published (Aitken et al., 1994). The primer sequences and expected PCR product sizes are listed in **table 2.4**. For each reaction, 100 ng DNA was incubated with Quick-Load Taq 2X Master Mix (New England BioLabs), forward and reverse primers (1 µM final concentration of each) and nuclease-free water to a final volume of 50 µL. The PCR protocol was as follows: 5 minutes at 94°C; 32 cycles of 1 minute at 94°C, 1 minute at 48°C; 30 seconds at 72°C; and a final extension step of 5 minutes at 72°C. PCR products and 100 bp DNA ladder (New England Biolabs) were separated by electrophoresis (100V for 30

minutes) in 1% acrylamide gels with 1x TBE buffer (90 mM Tris-borate, 2mM EDTA) containing 0.5 µg/mL ethidium bromide.

Table 2.4 EBV subtyping primers. PCR primers targeting either EBV type 1 or type 2 EBNA2. Primer sequences taken from Aitken et al., 1994.

EBV subtype	Primer	Sequence	Product size
Type 1	Forward	AACTTCAACCCACACCATCA	115
	Reverse	TTCTGGACTATCTGGATCAT	
Type 2	Forward	TACTCTTCCTCAACCCAGAA	120
	Reverse	GGTGGTAGACTTAGTTGATG	

2.4 Western blotting

2.4.1 Protein preparation

Cells were washed and pelleted (3500 g at room temperature) once in PBS prior to protein extraction. For each protein preparation, between 2-10x10^6 cells were resuspended in 200 µL urea buffer (9 M urea, 5 mM Tris, pH 7.5) and then kept on ice before 2 x 20 seconds of sonication using an ultrasonic cell disrupter (Misonix, USA). The sonicated supernatants were centrifuged at 16,200 g for 20 minutes at room temperature to pellet remaining cellular debris and the supernatants removed to a clean tube. The protein-containing suspensions were quantified using the DC Protein Assay (Bio-Rad, USA) according to

manufacturer's instructions. Protein concentrations were calculated using a standard curve generated from known concentrations of bovine serum albumin (BSA). Samples were then diluted to 1 mg/mL in gel sample buffer (GSB) (9 M urea, 10% glycerol, 0.15 M β-mercaptoethanol, 10% SDS, 50 mM Tris pH 7.4, 0.1% bromophenol blue) and heated for 5 minutes at 100°C before gel loading.

2.4.2 Electrophoresis and blotting

Criterion TGX Precast 4-12% acrylamide gels were loaded with 20 µL protein sample (1 mg/mL) and SeeBlue Plus 2 prestained ladder (ThermoFisher) (diluted 1:1.5 in GSB). Gels were run in Tris/Glycine/SDS PAGE buffer (GeneFlow) at 120V until desired protein separation was achieved. Separated proteins were transferred from the acrylamide gel onto PVDF membranes using the TurboBlot system (Bio-Rad) as per manufacturer's instructions (7 minutes at 25V) and then stored at 4°C in PBS with 1% v/v Tween-20 (PBS-T) until immunostaining.

2.4.3 Immunostaining

Following transfer, membranes were incubated for 1 hour at room temperature with 5% w/v dry milk in PBS-T (blocking buffer) in order to block non-specific antibody binding. Membranes were then incubated overnight at 4°C with primary antibody (**table 2.5**) diluted in blocking buffer, then washed in PBS-T for 30 minutes at room temperature with fresh PBS-T every 5 minutes. Membranes were then incubated for 2 hours at room temperature with the appropriate secondary HRP-conjugated antibody diluted in blocking

buffer before being washed in PBS-T for 60 minutes at room temperature with fresh PBS-T every 10 minutes. For visualisation, membranes were incubated with Amersham ECL Western Blotting Detection Reagent (GE Healthcare, USA) for 1 minute at room temperature and then analysed using the ChemiDoc MP system with Image Lab software (Bio-Rad).

Table 2.5 List of antibodies used for Western blot experiments. Antibodies were either purchased from commercial companies or provided by collaborators at WEHI, UoB or Peter Mac. WEHI, The Walter and Eliza Hall Institute; UoB, University of Birmingham; Peter Mac, Peter MacCallum Cancer Institute.

Target	Clone	Species	Dilution	Supplier
BCL-2	Bcl-2-100	Mouse	1/2000	ThermoFisher
BCL-X_L	9C9	Rat	1/1000	WEHI/D. Huang
MCL-1	19C4-15	Rat	1/2000	WEHI
BIM	3C5	Rabbit	1/1000	Enzo Biochem
BID	2D1-3	Rat	1/1000	WEHI
BAK	7D10	Rat	1/2000	WEHI/D. Huang
BAX	ABC11	Rabbit	1/1000	Merck Millipore
P53	CM5	Rabbit	1/2000	Leica
P53	D.01	Mouse	1/100	UoB/R. Grand
MDM2	2A9	Mouse	1/1000	D. Lane
LMP1	CS1-4	Mouse	1/2000	M. Rowe
Calregulin	C4606	Rabbit	1/2000	Sigma
HSP70	N6	Mouse	1/10,000	Peter Mac/R. Anderson
Anti-Mouse Ig -HRP	1010-05	Goat	1/2000	Southern Biotech
Anti-Rabbit Ig -HRP	4010-05	Goat	1/5000	Southern Biotech
Anti-Rat Ig -HRP	3010-05	Goat	1/5000	Southern Biotech

2.5 Flow cytometry

All samples were run on an LSR-II or an Accuri C6 flow cytometer (both BD Biosciences, USA) and analysis was carried out using FlowJo software (Tree Star).

2.5.1 Cell surface staining

$1x10^6$ cells were counted, pelleted and washed once in PBS prior to cell surface staining. Cells were first stained with viability dye (violet stain or near-IR stain) (Invitrogen) according to manufacturer's instructions. Cells were then washed again in PBS and resuspended with relevant cell surface antibodies (**table 2.6**) diluted in MACS buffer (PBS, 2% BSA, 2 mM EDTA). Cells were stained for 30 minutes on ice then stained cells were washed and resuspended into 300 µL MACS buffer before analysis.

Table 2.6 List of antibodies used for flow cytometry analysis.

Target	Fluorochrome	Clone	Dilution	Manufacturer
CD3	APC-Cy7	SK7	1/40	BD Biosciences
CD4	PE-Cy7	RPA-T4	1/50	Biolegend
CD8	FITC	RPA-T8	1/25	BD Biosciences
CD16	BV650	3G8	1/500	Biolegend
CD56	PE-TexasRed	N901	1/40	Beckman Coulter
CD57	PE-Cy7	TB01	1/80	Biolegend
TCRγδ	PE	B1.1	1/30	Thermo Fisher
Vδ1	PE	REA173	1/12.5	Miltenyi Biotec
Vδ2	FITC	123R3	1/12.5	Miltenyi Biotec
NKG2A	APC	Z199	1/100	Beckman Coulter

2.5.2 Rhodamine-123 staining

The presence and functionality of the multidrug efflux pump, p-glycoprotein, was determined by measuring the relative intensity of cell staining using the fluorescent molecule rhodamine-123 (Rh-123) (Sigma) – a p-glycoprotein specific substrate. The staining procedure took place in two-steps (staining and efflux): firstly, for each sample and condition, $5x10^5$ cells were incubated for 30 minutes, at 37°C and 5% CO_2, in 0.5 µg/mL Rh-123 or equivalent volume of 100% ethanol (unstained control) in appropriate growth

medium then washed twice in PBS. Secondly, stained cells were resuspended in appropriate medium and incubated for 2 hours with the following differences in conditions: p-glycoprotein inhibition controls (2 µM cyclosporin A at 37°C); p-glycoprotein efflux controls (4°C); test samples (37°C). Unstained cells were resuspended in appropriate medium and incubated for 2 hours at 37°C. All samples were washed and resuspended in MACS buffer before flow cytometric analysis.

2.6 Cell death analysis

2.6.1 Apoptosis assays

Apoptosis assays were set up in 96-well flat bottom plates with $4x10^4$ cells seeded per well in a final volume of 200 µL. Rows and columns at the edge of the plates were not used and instead filled with 200 µL PBS to decrease loss of media-volume by evaporation. For drug treatment experiments, cells were treated with the indicated concentrations of drug (**table 2.7**) or DMSO-only treated negative controls for the indicated time periods. Positive controls for apoptosis for all experiments were Jurkat cells treated for 6 hours with 10 µM camptothecin (Sigma). For staining, cells were washed with PBS and stained with the APC or FITC Annexin V/propidium iodide (PI) Apoptosis Detection Kit (BD biosciences) according to manufacturer's instructions. Samples were run on an LSR-II or an Accuri C6 flow cytometer (both BD Biosciences).

Table 2.7 List of drugs used for in vitro treatment of cell lines.

Drug	Manufacturer
Etoposide	Sigma
Methotrexate	Sigma
Ionomycin	Sigma
Camptothecin	Sigma
ABT-199	Active Biochem
ABT-737	Active Biochem
A-1331852	AbbVie/G. Lessene
S63845	Active Biochem

2.6.2 Analysis

Analysis was carried out using FlowJo software (Tree Star) and statistical tests were calculated using GraphPad Prism software. Populations were gated as shown in **figure 2.1**. Cells that stained negatively for both Annexin V and PI, markers that can distinguish early and late apoptosis, were used to measure survival. All experiments included DMSO-treated cells (negative controls) to which the survival percentages of the drug treated cells were normalised.

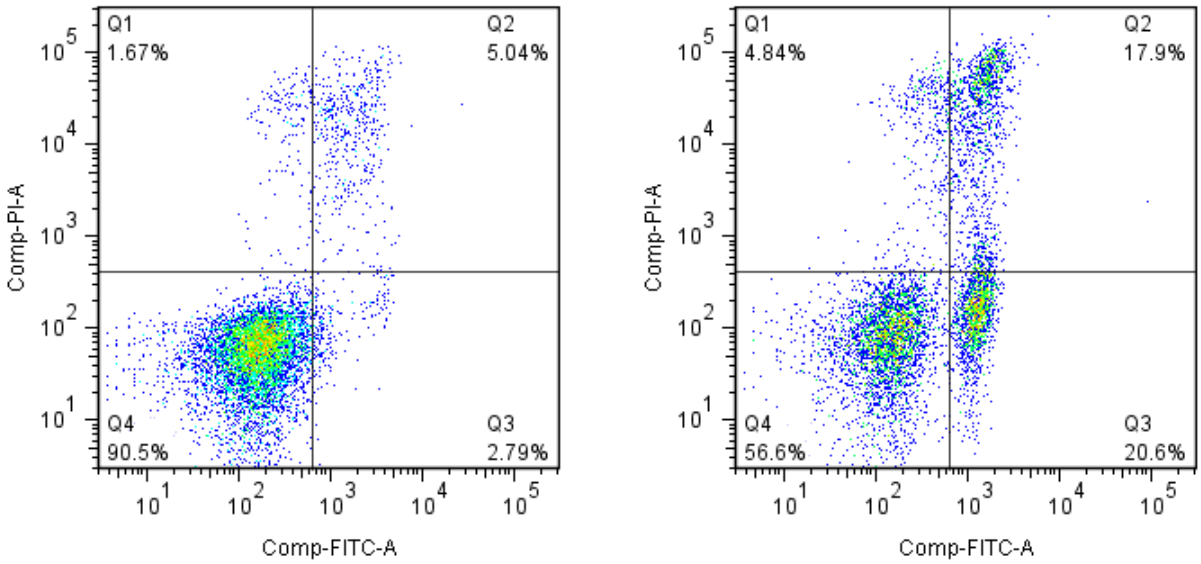


Figure 2.1 Annexin V/PI assay gating strategy. Left: DMSO-treated MOLT4 cells at 48 hours. Right: MOLT4 cells treated with 0.5uM etoposide at 48 hours. Value shown in bottom-left quadrant represents percentage of live cells.

2.7 High throughput drug screen

2.7.1 Cells and compound libraries

High throughput drug screening was performed under the supervision of Dr Kate Jarman and Dr Helene Jousset of the WEHI Screening Laboratory. Six of the eight EBV-positive T and NK cells (NKC1, SNK6, SNT8, SNT13, SNT15 and MEC04) were used in the drug screen. Three compound libraries were employed: Kinase library (276 compounds); Targeted agents library (73 compounds); and the Known drugs library (3707 compounds). Treated cells were tested for viability as described below.

2.7.2 Assay plate preparation

Assays were set up in Greiner LUMITRAC 200 384-well plates. Plates were loaded with test compounds, DMSO controls and positive controls (namely 10 µM A-1331852 and 10 µM S63845) (**table 2.7**), by Compounds Australia, Griffith University, Australia. Plates were shipped and stored at -20°C until use. To detect any row-specific loading inaccuracies when cells were added, DMSO and positive controls were seeded in the pattern shown in **figure 2.2**. All compounds were screened in duplicate on separate assay plates.

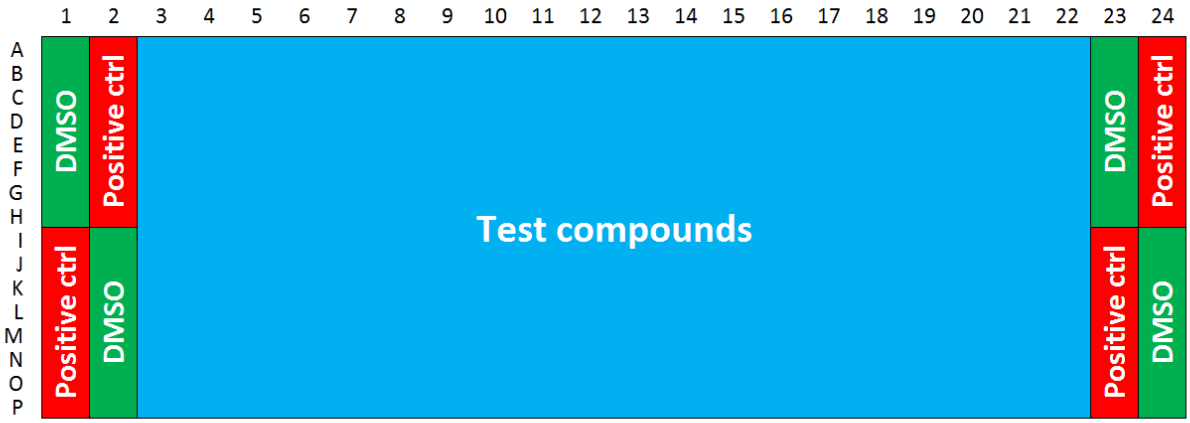


Figure 2.2 Plate map of compounds for drug screen. DMSO wells and positive control drug wells arranged to detect row-specific loading effects.

2.7.3 Drug treatment

Drug containing assay plates were thawed to room temperature before use. Cells were counted and resuspended in fresh NK/T media with 700 U/mL IL-2 at a density of $5x10^4$ cells per mL. 50 µL (2500 cells) were seeded per well using a Multidrop Combi Reagent

Dispenser (Thermo Fisher). Following addition of cells, all test compounds and positive control drugs were at a final concentration of 10 µM. Cells were then incubated, without stacking of the plates, for 48 hours at 37°C and 5% CO_2.

2.7.4 Viability staining

Viability was determined by quantitating relative amounts of ATP within cell cultures using the CellTiter-Glo 2.0 Luminescent Cell Viability Assay (CTG) (Promega, USA). Cells and CTG reagent were allowed to reach room temperature before staining. 25uL CTG was added per well using a Multidrop Combi Reagent Dispenser (ThermoFisher) and plates were covered with SealPlate film (Sigma). Plates were then then placed on a shaker for 2 minutes at 600RPM and then left at room temperature for 10 minutes without shaking. Luminescence readings were then taken using an EnVision Multilabel plate reader using EnVision Workstation software (Perkin Elmer, USA).

2.7.5 Viability analysis

Luminescence data generated from assay optimisation experiments were analysed using Graphpad Prism v10 software. Luminescence data generated from the primary screen were analysed and validated as described in **Chapter 5, Results III** using Spotfire (TIBCO, USA).

2.8 *In vivo* studies

2.8.1 Mice and disease monitoring

All experiments with mice were conducted in accordance with guidelines set out by The Walter and Eliza Hall Institute (WEHI) Animal Ethics Committee. Female NOD-SCID-IL2rg$^{-/-}$ (NSG) mice (Shultz et al., 2005) were used in all xenograft experiments. At the point of xenograft, mice were aged between 6 and 8 weeks old. Single cell suspensions, in 200 µL final volume of PBS, were delivered by subcutaneous (SC) or intraperitoneal (IP) injection. Mice were monitored at least 3 times per week for up to 180 days (experimental endpoint). Illness endpoint criteria included the development of a tumour up to a maximum size of 1cm^3 or the mouse exhibited signs of being unwell, such as visible weight loss, difficulty in breathing, hunched stance as detailed in guidelines set out by the WEHI Animal Ethics Committee. Animal wellbeing checks, injection of cells and administration of drug (see **2.8.2** below) were performed by trained animal technicians at WEHI. Upon the fulfilment of endpoint criteria, mice were culled by CO_2 exposure. Bleeds were taken for haematological analysis (see **2.8.5**) and organs were harvested for either histological analysis (**2.8.4**) or the establishment of cell lines (tumour samples only) (**2.8.3**).

2.8.2 Drug treatments

A-1331852 was formulated in 60% Phosal 50 PG (Lipoid, Germany), 27.5% Polyethylene glycol 400 (Sigma), 10% ethanol and 2.5% DMSO. 50 mg/kg of drug was administered by

oral gavage up to a maximum of 200 µL per mouse. Drug treatments were administered once per day for 7 consecutive days. For statistical analysis, Graphpad Prism v10 software was used to generate Kaplan-Meier plots with log-rank tests to compare tumour-free survival in drug-treated vs. vehicle-treated mice.

2.8.3 *Ex vivo* cell culture

Harvested tumours, derived from NSG mice xenografted with SNK or SNT cell lines, were processed by mechanical shearing into single cell suspensions and either frozen (as described in **2.1.5**) or placed into tissue culture with NK/T media (as described in **2.1.1**).

2.8.4 Histology

Tumour samples and organs including spleen, kidney, lung, heart, sternum, liver and lymph nodes (when enlarged), were surgically removed post-mortem and fixed in 10% formalin for 24 hours. Subsequent sectioning of material, staining with H&E and human-specific CD45 antibody (clone 2B11, DAKO, USA) were performed by Cary Tsui of the WEHI Histology Department.

2.8.5 Haematology

Blood samples were collected either by eye bleed or heart bleed and analysed using the ADVIA automated haematology system (Bayer, Germany). Morphological analysis was used to determine the following parameters: red blood cell, platelet, white blood cell,

neutrophil, monocyte and lymphocyte counts per μL of blood. Statistical analysis was performed using Graphpad Prism v10 software.

2.9 Cytokine analysis

Human cytokines were measured from cell culture supernatants (SNK1, SNK6, SNT8, SNT13, SNT15, MEC04, NKC1 and SNT16 cells) at 48 hours post passaging. The Bio-Plex Pro Human Cytokine 17-plex Assay (Bio-Rad) was used to measure cytokine concentrations according to manufacturer's instructions and performed by Dr Yifan Zhan, Immunology Division, WEHI. Briefly, the assay was performed in a 96-well plate where cytokine-specific detection antibodies and streptavidin-PE were used to generate a luminescence read-out using the BioPlex 2200 Multiplex Testing system (Bio-Rad). Luminescence readings were recorded from provided control samples with known concentrations of cytokines to generate standard curves from which test sample cytokine concentrations were calculated.

2.10 Statistical analysis

GraphPad Prism version 7 software and TIBCO Spotfire software were used for statistical analysis. Experiments were performed with either two or three technical replicates as indicated in figure legends. Mean values (with error bars showing standard deviation or standard error as indicated) from independent experiments are shown. Two-group comparisons – for *in vitro* drug treatments (Annexin V / PI assays and CTG luminescence assays), Rh-123 efflux assays, mouse organ weight comparisons and haematological

analysis – were made using 2-tailed *t* tests. Mouse survival data were plotted using Kaplan-Meier curves and statistical comparisons between groups were made using log-rank (Mantel-Cox) test. Statistical differences where *P* values were less than 0.05 were considered significant. Z prime (Z') and robust Z prime (RZ') values were calculated for high throughput drug screening data from the mean and standard deviation of the positive and negative controls for each assay plate. For both measures, assays with scores above 0 were considered acceptable and values above 0.5 were considered a good assay (Zhang et al., 1999).

3. Results I: Characterisation of EBV-positive T and NK cell lines

3.1 Introduction

We have very little understanding of the factors that drive the pathogenesis of ENKTL and CAEBV due to multiple limiting factors. Firstly, these diseases have very low incidence rates thereby limiting the availability of primary material to analyse. ENKTL is most prevalent in East Asia and South America (4-6% of all non-Hodgkin's lymphomas) whereas in the Western world the incidence rate is much lower (0.5% of all non-Hodgkin's lymphomas) (Au et al., 2009). Case reports of CAEBV have been sporadic and incidence rates are not confidently known (Park and Ko, 2014). Secondly, the establishment of immortalised cell lines has been difficult to achieve. For ENKTL, this can partially be attributed to the necrotic nature of the tumours (Harabuchi et al., 2009). Thirdly, a successful and reproducible method for the *in vitro* infection of primary T or NK cells with EBV has not been determined. Collectively, these limitations mean that investigations focusing on ENKTL and CAEBV disease development and sustained pathogenesis have centred on only a limited number of available cell lines.

Many of the frequently studied ENKTL and CAEBV cell lines were established by the Shimizu laboratory (Tokyo, Japan) and are referred to as the SNK and SNT cell lines (Zhang et al., 2003, Nagata et al., 2001, Oyoshi et al., 2003). For our experiments, we have collected 7 of these cell lines plus the MEC04 cell line derived from an ENKTL tumour of NK cell origin (NK-ENKTL) reported by Coppo et al., 2009. These cell lines represent an assortment of NK cell, αβ T cell and γδ T cell backgrounds as later described in further detail.

Unlike other EBV-associated diseases like BL where contributing cellular factors are known (such as abnormal c-MYC expression), for ENKTL the cellular drivers of transformation have not been formally proven. Although cytogenetic analysis has revealed deletions in chromosome 6 in small patient cohorts and in the SNK1 cell line (Zhang et al., 2003, Tien et al., 1997) the precise genetic factors that may lead to transformation are not known. The lack of known and universal contributing cellular genes, together with the fact that almost all incidences of ENKTL are EBV-positive highlights the potential importance of the virus in the pathogenesis of these diseases (Au et al., 2009, Vose et al., 2008). Therefore, there is a need to fully understand the role of EBV in such diseases.

As mentioned above, there are a limited number of ENKTL and CAEBV cell lines available and the suitability of these cell lines for assessing the role of EBV in the disease pathogenesis is questionable. Tumour-derived cell lines are grown in laboratory tissue culture conditions for prolonged periods of time. This essentially produces a monoclonal population where differences between individual cells are minimised. Furthermore, the prolonged growth of cell lines under laboratory conditions can induce gene expression changes over time, possibly through the acquisition of additional mutations over the course of multiple cell divisions. Therefore, it is conceivable that phenotypic diversion from the originally isolated cells has occurred over time.

This chapter focuses on assessing the suitability of the currently available ENKTL and CAEBV cell lines to behave as disease models for functional studies in later results chapters. There are three major subcategories to this study. Firstly, to what extent are the cell lines phenotypically representative of primary tumours? This can be determined by analysing the

expression of cell surface molecules by flow cytometry and then comparing this with both epidemiological studies and the original reports in which they were first characterised. Secondly, what is the EBV status of these cells? This can be achieved by assessing the cells for EBV-positivity and analysing the expression of multiple viral transcripts from genes of interest. Finally, which cytokines and signalling factors are these cell lines capable of producing? The local release of signalling factors may influence gene expression and cellular activity. To investigate this, cell supernatants can be screened for cytokine secretion by a multiplex immunoassay.

3.2 Cellular phenotype

3.2.1 Cell type lineage

In order to examine the T or NK cell lineage of each of the cell lines, cells were stained with a phenotyping panel of antibodies and assessed by flow cytometry. The cell surface markers used to resolve T cell lineage were the pan T cell marker CD3, plus the markers of functional T cell subsets CD4, CD8, TCRγδ. To resolve NK cell lineage, the pan NK cell marker CD56 was included in the panel alongside CD16 and killer-cell immunoglobulin-like receptors (KIRs) as markers of differentiated NK cells.

The phenotyping panel was initially tested on healthy donor PBMCs that contained all subtypes of lymphocyte. The gating strategy, used throughout this experiment, was as follows: i) singlet gating, ii) exclusion of CD14-positive cells (marker of monocytes) and dead cells by a viability dye (dump channel), iii) removal of debris determined by FSC and SSC (**figure 3.1A**). These gated lymphocytes (termed 'total lymphocyte population') were then

used to test the staining of antibodies targeting T cell markers (**figure 3.1B** and **C**) and NK cell markers (**figure 3.1D**). From the total lymphocyte population, $CD3^+$ cells and $TCR\gamma\delta^+$ cells were identified (**figure 3.1B**). Single positive $CD4^+$ and $CD8^+$ cells and also small numbers of $CD4^+CD8^+$ double positive cells were identified from the total lymphocyte population (**figure 3.1C**). For NK cell markers, $CD56^{dim}CD16^+$ and $CD56^{bright}CD16^-$ cells were successfully identified where positive KIR^+ cells were identified within the $CD56^{dim}CD16^+$ population (**figure 3.1D**).

All 8 EBV-positive T and NK cell lines were stained with the lineage panel of antibodies and the results presented in **figure 3.2**. Gates were set based on unstained samples for each cell line. All 8 cell lines appeared to positively stain, to varying degrees, with the TCRγδ antibody. This was unexpected as previously only SNT8, SNT13 and SNT15 had exhibited TCRγδ-positivity in their respective original reports (Zhang et al., 2003, Nagata et al., 2001, Oyoshi et al., 2003, Coppo et al., 2009). Generally, cells were low for CD3 surface expression with the exception of SNT15 which stained double positive for TCRγδ and CD3. All cell lines were negative for CD8 and all cell lines, with the exception of SNT16, did not express CD4. The observation that SNT16 cells were CD4 positive in the absence of CD3 is unusual and unexpected.

With respect to the NK cell lineage markers, the results were less clear as many cell lines exhibited a non-monoclonal pattern of expression for CD56, therefore demonstrating a degree of heterogeneity within each cell population. No CD56 expression was detected in SNK1 or SNT16 cells. For SNK6, MEC04 and NKC1, the majority of the cell populations showed high CD56 expression. However, SNT8, SNT13 and SNT15 cells appeared to contain populations both positive and negative for the NK marker CD56. The $CD56^+$ cells were then

stained for CD16 and KIRs but no expression of these NK markers was detected in any of the cell lines.

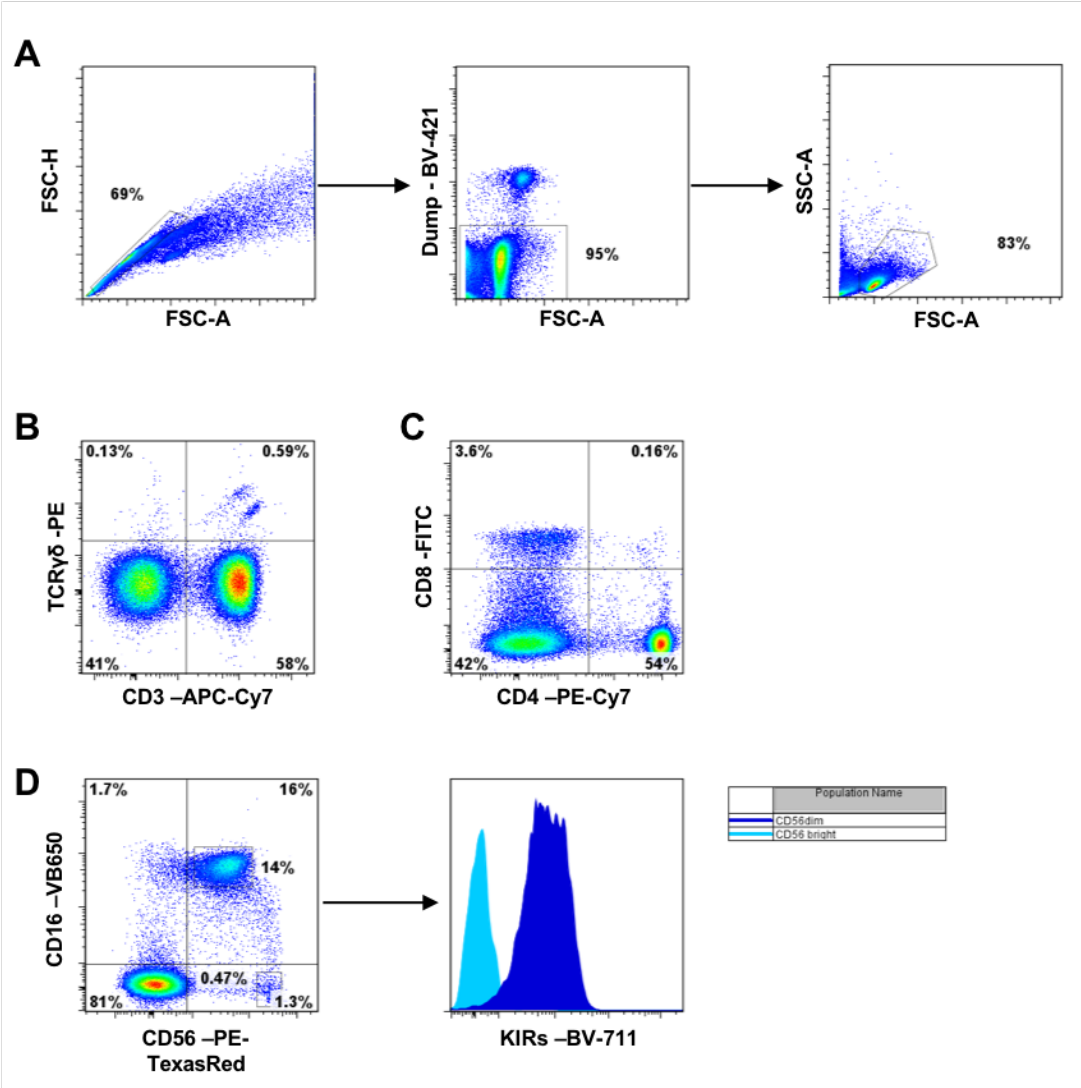


Figure 3.1 Antibody testing for phenotyping panel #1. The designed panel was tested on healthy donor PBMCs. **A)** Gating strategy used to isolate lymphocytes: Singlets were isolated; dump channel used for the removal of dead cells (viability dye-positive cells) and monocytes (CD14-positive cells); removal of debris by forward and side scatter. **B-D**) Analysis of T cell and NK cell markers. PBMC, peripheral blood mononuclear cells

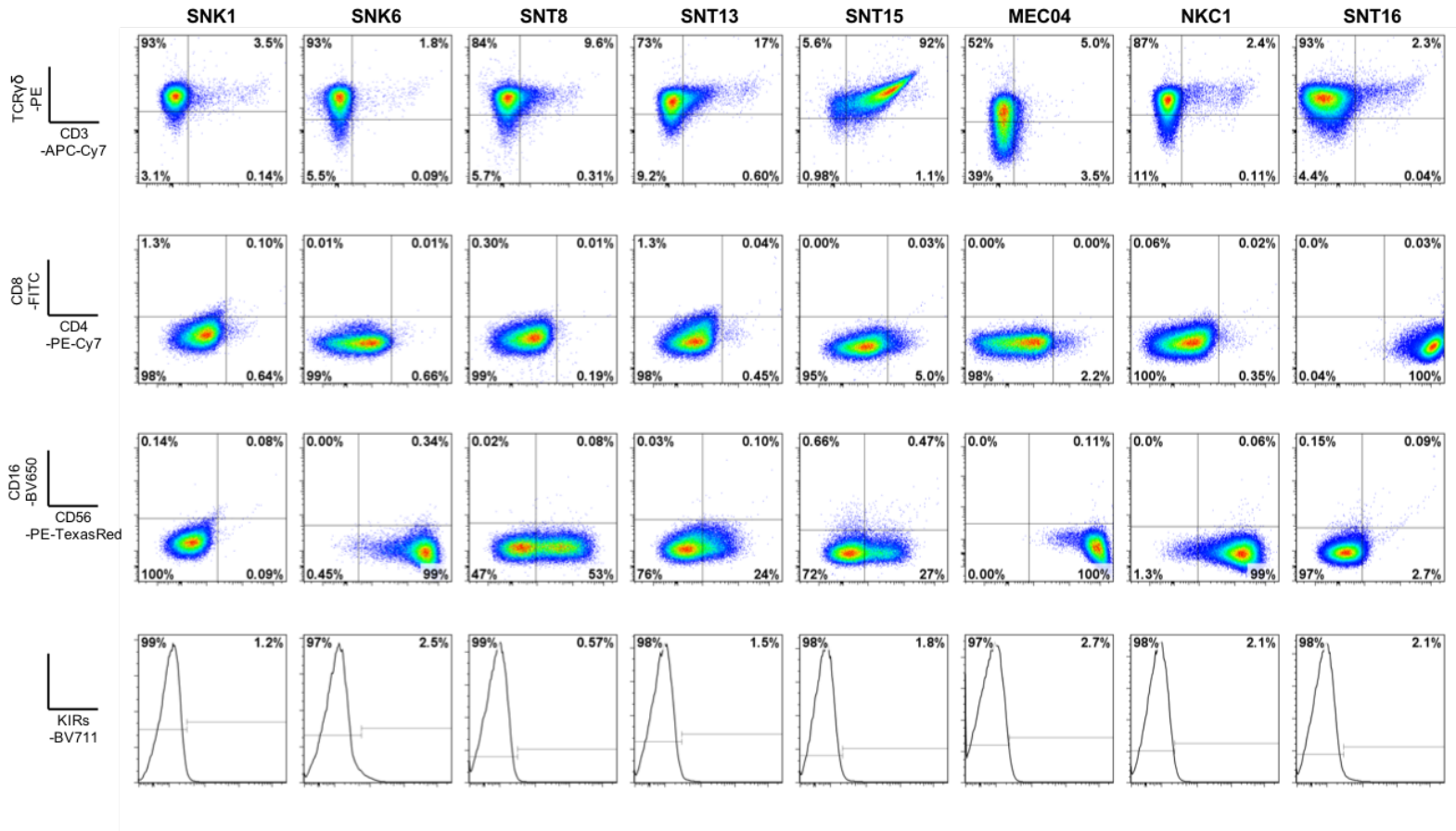


Figure 3.2 Analysis of ENKTL and CAEBV cell lines by phenotyping panel #1. Cells were gated as demonstrated in **figure 3.1A**. Cells were then analysed for T cell subset markers CD3, TCRγδ, CD4 and CD8. Cells were also analysed for NK subset markers CD16, CD56 and killer-cell immunoglobulin-like receptors (KIRs).

3.2.2 γδ T cell and NK cell subtype markers

The data presented in **figure 3.2** highlighted two features of the cell line panel that warranted further investigation. Firstly, the positivity for TCRγδ in all 8 cell lines was unexpected. Secondly, the apparent heterogenous CD56 expression in some of the cell lines (SNT8, SNT13 and SNT15) that were established from T cell proliferative disease, since staining positive for CD56 opens up the possibility of such cells being of NK cell origin instead of T cell origin.

To address the first question surrounding the TCRγδ status of the cell lines, a second phenotyping panel was designed which included antibodies specific for either Vδ1 or Vδ2, the two major subsets of peripheral blood γδ T cells. To address the second question surrounding the T or NK cell lineage of the SNT8, SNT13 and SNT15 cells, further NK cell markers were included into the second phenotyping panel. These additional markers were CD57, a marker of NK cell terminal differentiation, and NKG2A, an NK cell inhibitory receptor which detects surface human leukocyte antigen (HLA) molecules.

This second phenotyping panel was also initially tested on healthy donor lymphocytes. In **figure 3.3A,** the live cell gating strategy was applied as previously described. Positive staining was identified for both Vδ1 and Vδ2-specific antibodies at 0.3% and 0.91%, respectively. The entire γδ T cell population typically comprises 1-4% of the total lymphocyte population (**figure 3.3B**) (Kaufmann, 1996).

With respect to NK cell markers, within the total lymphocyte population, $CD56^{-}$, $CD56^{dim}$ and $CD56^{bright}$ cell populations were observed (**figure 3.3C**). Using these markers, NK cells can be categorised into discrete differentiation stages of NK cell development: stages 1-3

(developmental intermediates); stage 4 (functional NK cells, $CD56^{bright}$), stage 5 (functional NK cells, $CD56^{dim}$) and stage 6 (memory NK cells) as outlined by Yu and colleagues (Yu et al., 2013). Identification of functional NK subsets was demonstrable by the second phenotyping panel. NKG2A positivity was found on $CD56^{bright}$ cells (stage 4 NK cells) and a subset of $CD56^{dim}$ cells (stage 5 NK cells). The late stage NK cell differentiation marker CD57 was found on a subset of $CD56^{dim}$ cells (stage 6 NK cells).

All 8 cell lines were then assessed using the second cell lineage marker panel of antibodies. Although all cell lines appeared to positively stain with the pan-TCRγδ antibody in **figure 3.2**, the data shown here appear contradictory. No cell lines demonstrated positivity for Vδ1 and only three cell lines, SNT8, SNT13 and SNT15, stained positively for Vδ2, confirming the status of these three cell lines as γδ T cells. However, SNT8, SNT13 and SNT15 demonstrated heterogeneity with respect to Vδ2 expression where positive populations ranged from 30% to 99%. With respect to the NK cell markers, SNT8, SNT13 and SNT15 cell lines retained heterogeneous staining for CD56, despite their γδ T cell nature. One cell line, SNK6, stained positive for the late stage NK cell marker CD57 but only 30% of the population were positive. Around 20% of SNK6 cells also stained positive for NKG2A. These data suggest that the cell lines in our panel are either of an early NK cell (NKC1 and MEC04), late stage NK cell (SNK6), $CD4^{+}$ T cell (SNT16) or γδ T cell (SNT8, SNT13 and SNT15) phenotype. However, SNK1 cells could not be assigned to such categories from the experiments performed here. Improved gating strategies for the experiments described above, for example the inclusion of isotype controls, would allow for a higher degree of confidence when interpreting these data. For

confirmation of the apparent heterogeneity observed within cell lines here will require further robust analysis.

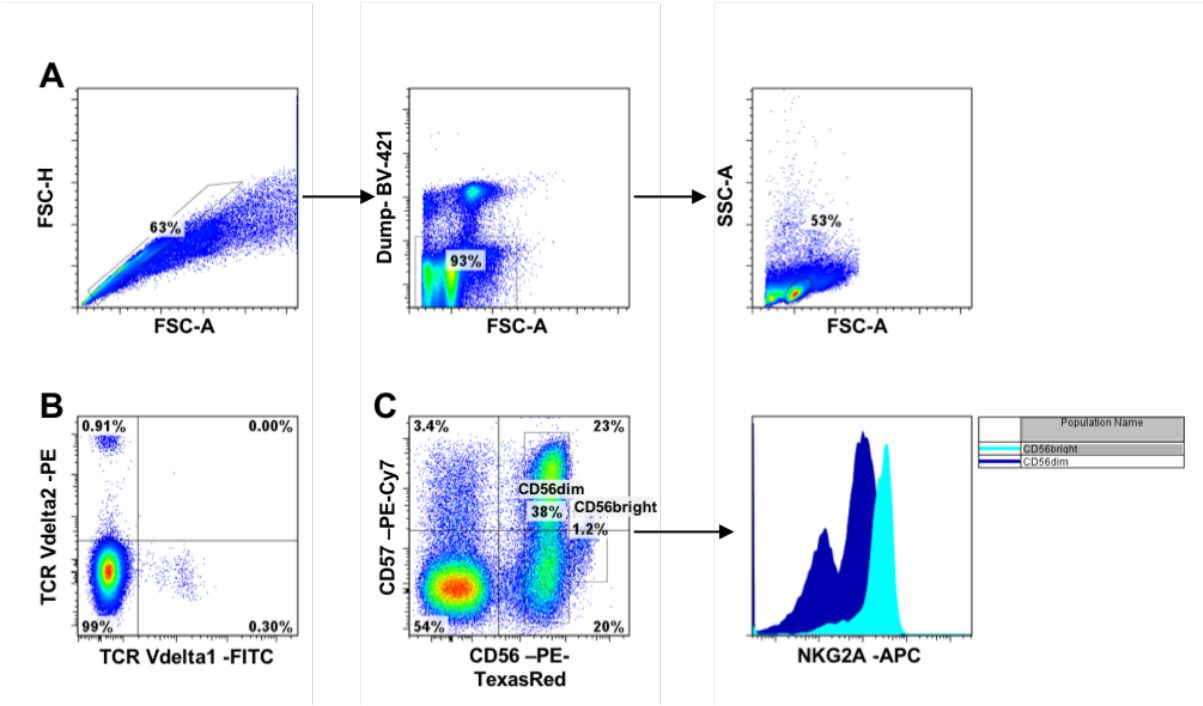


Figure 3.3 Antibody testing for phenotyping panel #2. The designed panel was tested on healthy donor PBMCs. **A)** Gating strategy used to isolate lymphocytes: Singlets were isolated; dump channel used for the removal of dead cells (viability dye-positive cells) and monocytes (CD14-positive cells); removal of debris by forward and side scatter. **B** and **C)** Analysis of γδ T cell and NK cell markers.

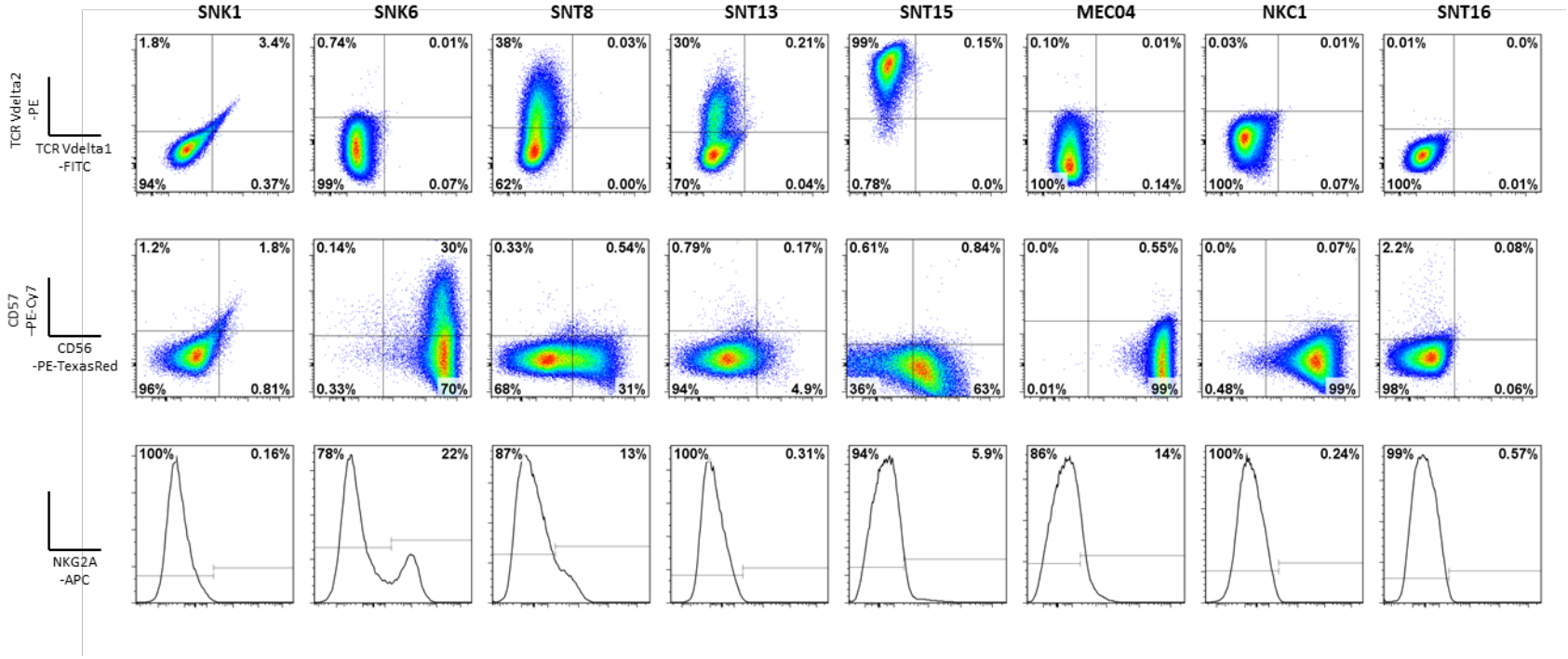


Figure 3.4 Analysis of ENKTL and CAEBV cell lines by phenotyping panel #2. Cells were gated as demonstrated in **figure 3.3A**. Cells were then analysed for γδ T cell subsets markers Vδ1 and Vδ2. Cells were also analysed for NK subset markers CD56, CD57 and NKG2A.

3.3 Cytokine, chemokine and growth factor production

To further characterise the panel of ENKTL and CAEBV cell lines, we next explored their cytokine profiles. A multiplex assay quantitating 27 human cytokines and signalling factors was performed on cell supernatants. Cytokine production was measured in ng/mL and plotted in **figure 3.5** then summarised as a heat map in **figure 3.6**. The broad spectrum of signalling factors measured provide insights into potential cellular functions. Signalling factors such as inflammatory cytokines, immunosuppressive cytokines and cytotoxic factors are examined and described in further detail below. The interpretation of absolute concentrations was limited as only test cell lines were included in the assay. Therefore, the analysis was focused on comparing the level of a particular cytokine between cell lines as opposed to drawing conclusions about the relative levels of different cytokines within an individual cell line. Cytokine concentrations ≥1ng/mL were considered to be of an appreciable concentration. In certain circumstances, as indicated in the summary heat map shown in **figure 3.6**, cytokine production exceeded the maximum detectable concentration, as determined by the luminescence-based immunoassay.

The summary data highlights several differences between the cell lines, for example with IL-5 and IL-13 — both reported to be primarily secreted by $CD4^+$ T_H2 cells (Zhu et al., 2010). IL-5 was not detected in 3 of 4 T cell lines (SNT8, SNT13 and SNT15) and the concentration only just reached the 1 ng/mL threshold in the fourth T cell line, SNT16 cells (1.48 ng/mL). Variable amounts of IL-5 were secreted from the cells of NK-origin ranging from below the threshold level in SNK6 cells (0.38 ng/mL) up to detectable levels of 18.9ng/mL in SNK1

cells. IL-13 concentrations exceeded detectable concentrations (>10.1ng/mL IL-13) for 5 of 8 cell lines (SNK1, SNK6, SNT8, SNT13 and SNT16). NKC1 cells also secreted high concentrations of IL-13 at 5.36ng/mL but barely detectable concentrations were observed for SNT15 and MEC04.

Production of the multifunctional immunomodulatory cytokine IL-6 evenly splits the cell line panel into those cell lines that express very low levels that are below the threshold (SNK6, SNT15, MEC04 and SNT16; mean average of 170pg/mL) and those that produce approximately 15-100 fold higher amounts (SNK1, SNK6, SNT13 and NKC1). IL-6 can be regulated by IL-17 activity, however such obvious division was not mirrored in the panel with respect to IL-17 production.

The common-gamma chain family of cytokines were also examined. IL-2 has been excluded from the analysis as all cell lines are IL-2-dependent and were grown in exogenous IL-2. Therefore IL-2 readings in this assay were not indicative of endogenously produced cytokine. IL-4 and IL-7 were detected at low concentrations in the cell lines, ranging from 0.06-0.1 ng/mL and 0.3-0.44 ng/mL, respectively. IL-9 levels varied dramatically across the cell lines, with concentrations from 0.96-17.1 ng/mL observed. This was exclusive of SNT13 which exceeded measurable concentrations (>33.2ng/mL of IL-9). IL-15, involved in homeostasis of both T and NK cells, was produced consistently in all the cell lines (range 1.45-2.21ng/mL) and no obvious differences between cells of NK or T cell origin was observed.

The production of the immunosuppressive cytokine IL-10 separated the cell lines into two groups: IL-10-high (SNT15 and MEC04) and IL-10-low (SNK1, SNK6, SNT8, SNT13, SNT16). The mean concentration of IL-10 detected in the IL-10-low group was 1.61ng/mL whereas the IL-10 high group, consisting of SNT15 and MEC04 cells, had supernatant concentrations of IL-10 that were approximately 10-fold and 20-fold higher, respectively. Although primarily produced by macrophages, monocytes, neutrophils and dendritic cells as opposed to T or NK cells, 7 of 8 cell lines produced detectable concentrations of IL-12 that just reached the 1 ng/mL level.

TNF-α is produced by a large number of cell types where receptor engagement can lead to inflammation or cell death (Kalliolias and Ivashkiv, 2016). All cell lines produced TNF-α in the 1-6 ng/mL range. IFN-γ is typically secreted by cytotoxic and Th1 lymphocytes. In the cell line panel IFN-γ was produced at low levels that were below the threshold concentration in MEC04, NKC1 and SNT16 cells and at detectable levels that ranged from 6.2-25.4ng/mL in the remaining 5 cell lines. The IFN-γ inducible factor and pro-inflammatory chemokine, RANTES, was detected at concentrations that exceeded the maximum measureable limit (>36.3ng/mL) for all 8 cell lines.

These data sets show that each of the examined ENKTL and CAEBV cell lines have a variable cytokine profile. An inflammatory phenotype could be proposed based upon consistent detection of factors such as TNF-α and RANTES. Interestingly, large differences between cell lines are observed with the immunosuppressive cytokine, IL-10, and the multifunctional cytokine IL-6. Although these data require validation as only a single

experiment was performed to assess the cytokine profile, they may serve as a useful future reference when deciphering the functional capabilities of these cell lines.

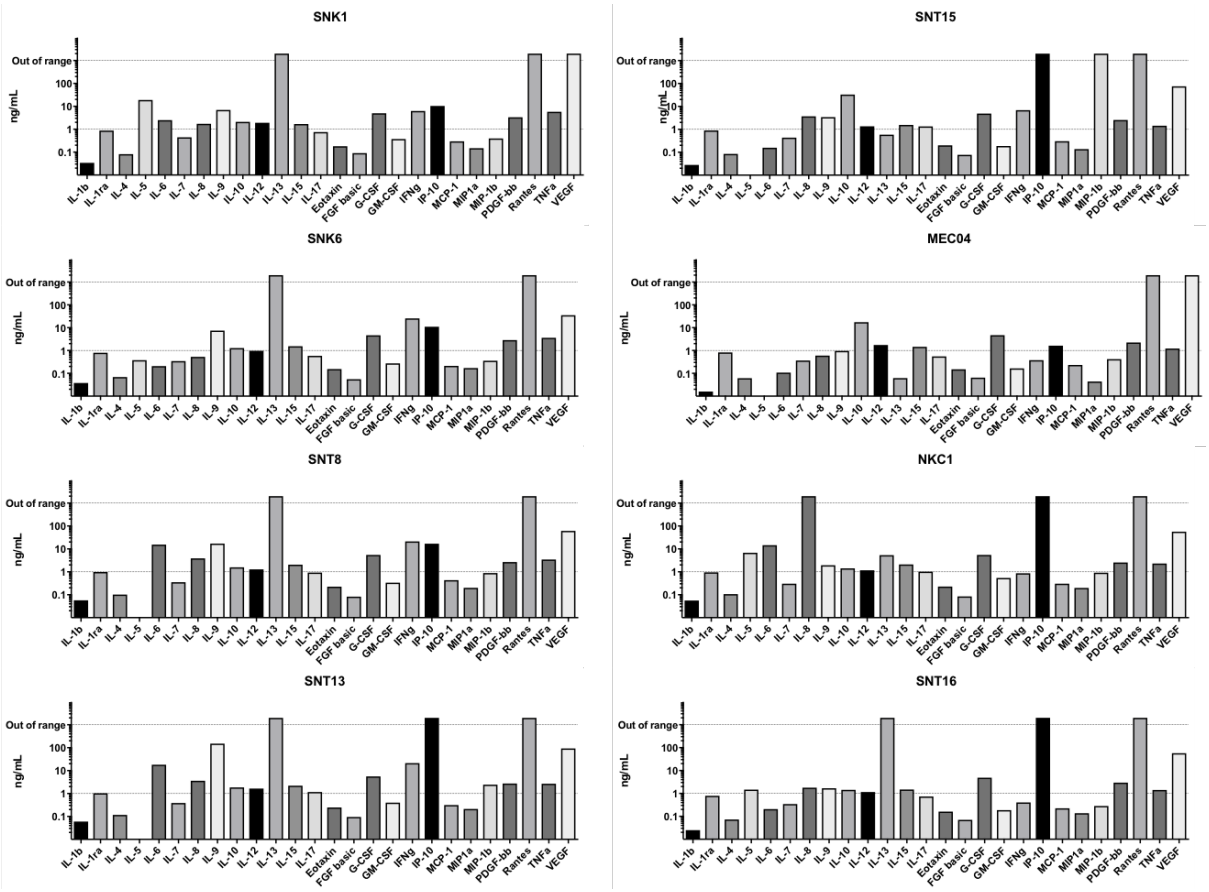


Figure 3.5 Cytokine production by ENKTL and CAEBV cell lines. Cell culture supernatants were harvested 48 hrs after routine passaging, screened for cytokine secretion by a multiplex immunoassay detecting 27 human cytokines and plotted on a log scale. A measurement of 1 ng/mL was considered an appreciable concentration. Readings above the measurable concentration are indicated as out-of-range. Data shown is of a single experiment performed in duplicate.

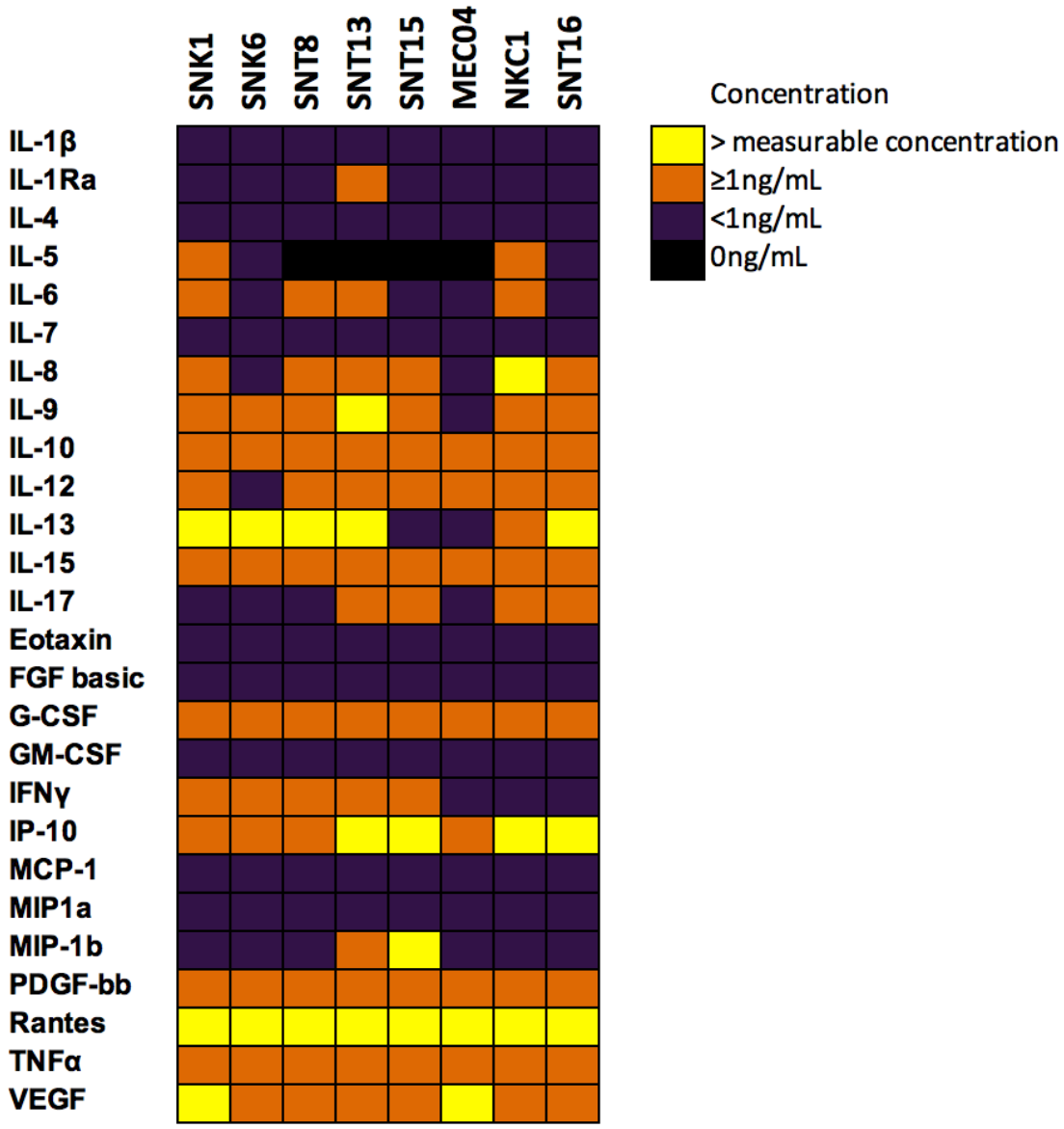


Figure 3.6 Summary heat map of supernatant cytokines. Data from **figure 3.5** is presented here as a heat map as indicated by the scale bar. Cytokines for each cell line were categorised according to concentration: Negative (0 ng/mL), positive low (<1ng/mL), positive high (≥1ng/mL) and above measurable concentration. Data shown is of a single experiment performed in duplicate.

3.4 Detection of EBV

3.4.1 Viral load

Following confirmation that the examined cell lines are of either T or NK cell lineage, the EBV-infection status remained to be determined. To detect the presence of EBV and measure the viral load per cell, a qPCR assay was performed (**figure 3.7**). DNA was extracted from the ENKTL and CAEBV cells and subjected to an assay that quantifies the number of copies of the viral POL gene (BALF5), using the cell line Namalwa-BL that has two integrated copies of EBV as a reference (Matsuo et al., 1984). The POL gene is a single copy lytic gene and its nucleotide sequence is highly conserved across viral strains. An additional assay to quantitate cellular beta-2-microglobulin DNA was performed. From these assay, average viral loads per cell were determined and comparisons made between the cell lines.

As expected, no viral DNA could be detected in the negative control cell line, Jurkat, an EBV-negative leukaemic T cell line. In the ENKTL and CAEBV cell lines, viral DNA was detected at varying levels ranging from 11 copies per cell (NKC1 cells) to 60 copies per cell (SNK6 cells) (**figure 3.7**). The values reported here are an average viral load within the cells. Viral copy number can vary between cells within a population.

3.4.2 EBV subtyping

For further characterisation purposes, we next determined whether the viruses harbouring within the T and NK cells were of EBV subtype 1 or 2. This question was answered by PCR

of EBV DNA. EBV subtypes 1 and 2 differ primarily through variation in the EBNA2 and EBNA3 sequences (Sample et al., 1990, Adldinger et al., 1985, Dambaugh et al., 1984, Rowe et al., 1989). Such differences have previously been exploited in order to perform viral typing in BL cell lines by PCR where primer pairs were designed to be complementary to either type 1 or type 2 EBNA2 sequences (Aitken et al., 1994). Such primers and reactions were used here to examine the ENKTL and CAEBV cell lines in addition to two control cell lines, Akata-BL (type 1 EBV) and Jijoye (type 2 EBV) (**figure 3.8**).

The PCR detecting type 1 or 2 strains was designed to perform amplification products of size 115 bp and 120 bp, calculated from the viral strain sequences of B95.8 (type 1) and AG876 (type), respectively (Aitken et al., 1994). The reaction performed with type 1-specific primers produced a band of approximately the correct size of 115 bp with DNA extracted from each T and NK cell line in addition to the known EBV type 1-infected cell line, Akata-BL (**figure 3.8, top**). The reaction performed with type 2-specific primers did not produce a band of the expected size of 120 bp in any of the T or NK cells but only in the known EBV type 2-infected cell line, Jijoye (**figure 3.8, bottom**). These experiments suggest that all members of the ENKTL/CAEBV cell line panel are infected with type 1 EBV.

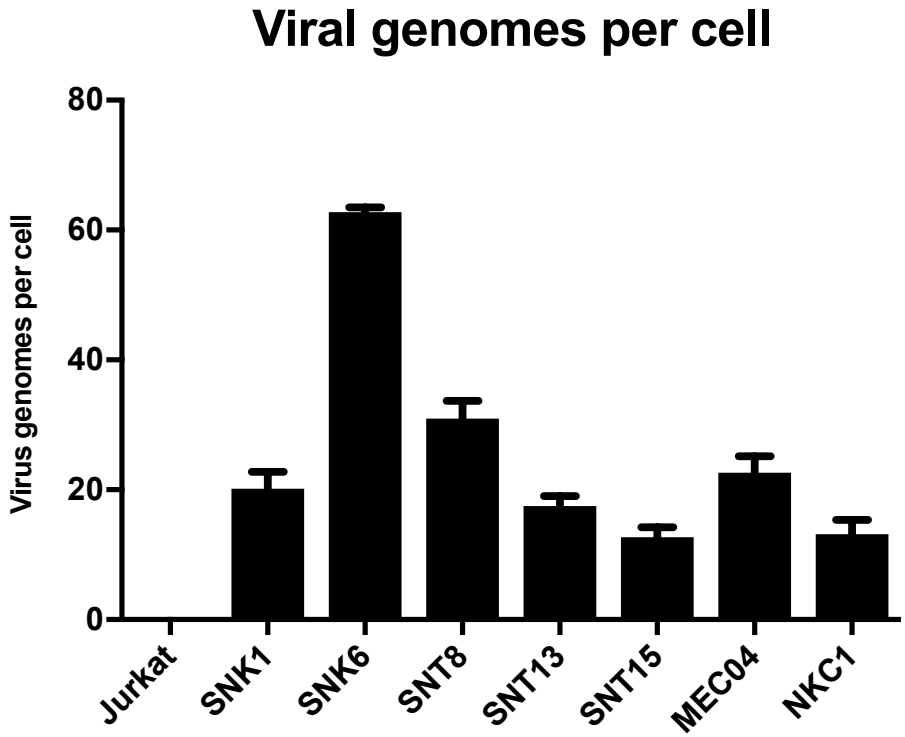


Figure 3.7 EBV copies per cell. Extracted DNA from ENKTL and CAEBV cell lines were subjected to qPCR. The qPCR assay detected the single copy viral POL gene. A standard curve was generated using DNA extracted from Namalwa-BL cells, which contain two integrated copies of DNA. The POL assay was multiplexed with a cellular β-2-microgobulin assay which was then used to calculate the number of EBV copies per cell. Data presented are mean ±SE of three independent experiments performed in triplicate.

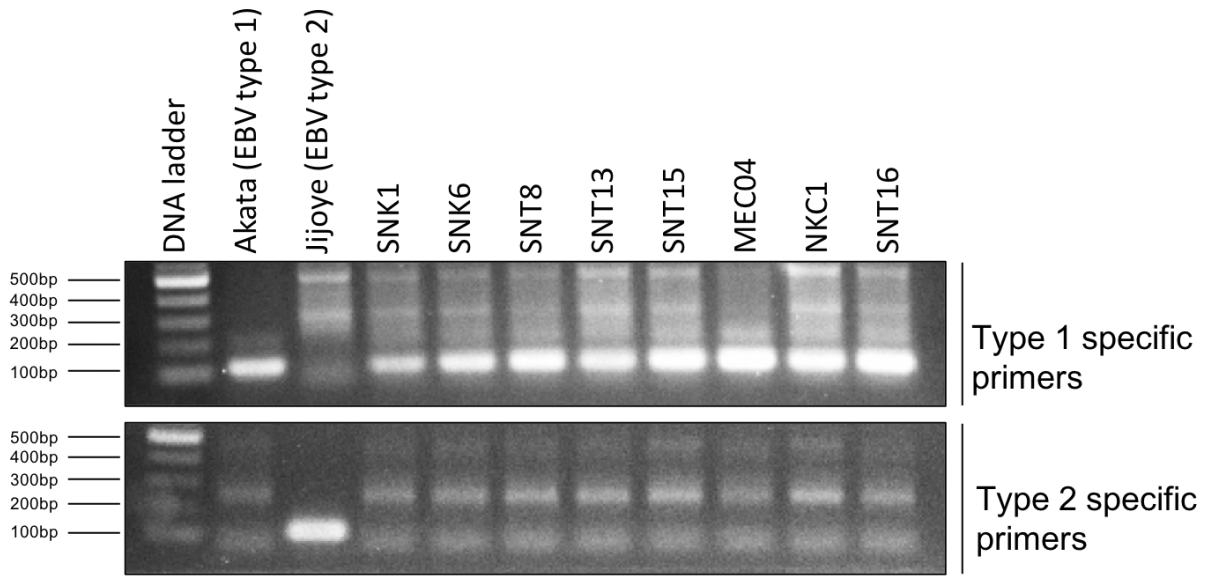


Figure 3.8 EBV typing of T and NK cell lines. Extracted DNA from ENKTL, CAEBV and control BL cell lines were subjected to a PCR with either EBV type 1 or type 2-specific primers. PCR amplification products and DNA ladder were separated by gel electrophoresis for visualisation. Data presented is representative of two independent experiments.

3.5 Viral gene expression

3.5.1 Latent gene expression

Following confirmation that the cell lines were EBV-positive, the expression levels of the different viral genes was assessed. To do this, a high-throughput qRT-PCR assay, termed Fluidigm, was performed as outlined in detail by Tierney et al., 2015. The Fluidigm system allows for the absolute quantification of viral mRNA by interpolation from a standard curve of Ct values generated by the serial dilution of a known number of template amplicons (from the absolute quantification (AQ) plasmid), as described in the materials and methods sections 2.2.3 and 2.2.4. The cellular housekeeping gene, PGK1, was used to normalise the data to allow for appropriate comparison between cell lines. DNA sequence variation has been accounted for in this assay by avoiding variable regions for primer and probe placement. Where it has not been possible to avoid such regions, multiple qPCR assays have been designed — e.g. assay LMP1 B95.8 and assay LMP1 CAO have two different probes to distinguish between the two common variants of this gene region. A heat map summary of latent viral gene expression in the T/NK cell lines, alongside B cell lines, is shown in **figure 3.9**.

The data for the B cell lines presented in the heat map in **figure 3.9** have been taken from published data (Tierney et al., 2015) and are used here for comparative purposes, as they act as representative expression profiles for different forms of latency and the lytic cycle. Latency I is represented by Rael-BL cells and is characterised by EBNA1 positivity expressed from the Qp promoter and no activity for the Latency III-associated promoters, Wp and Cp.

Latency III is represented by the cell lines AG876 and the 2089 LCL. AG876 is a Burkitt lymphoma cell line that carries type II EBV and 2089 LCL is a lymphoblastoid cell line that carries the type I EBV strain, B95.8. In both cell lines, EBV uses the Wp/Cp promoters to express EBNA1, EBNA2 and the EBNA3 family, and express LMP1 and LMP2 mRNAs from their own promoters. Salina-BL is a Wp-restricted Burkitt's lymphoma cell line characterised by high Wp activity leading to expression of EBNA1, EBNA3s and BHRF1 in the absence of EBNA2. The EBERs and BARTs were expressed in all forms of latency and were therefore detectable in all control B cell lines. Akata-BL cells (induced into the lytic cycle by IgG cross-linking) primarily act as a control for the lytic genes shown later in **figure 3.11**.

There was some variability in EBV gene expression across the individual lines but overall, the ENKTL and CAEBV cell lines carried EBV in a Latency II infection. This involves no activity from the Wp/Cp promoters and undetectable expression of EBNA2 and the EBNA3s. Instead, the Qp promoter is used to express EBNA1, and the LMP1 and LMP2 proteins are expressed from their own promoters. EBER1 and EBER2 transcripts are expressed at very low levels within the T and NK cell line panel when compared to the B cell lines, however the significance of this finding is not clear. The BART transcripts are precursors to the viral miRNAs, therefore further investigation is required to determine which miRNAs are expressed and functional. EBNA1 transcripts were detectable in all cell lines with the unusual exception of SNK1. The apparent absence of EBNA1 in SNK1 cells may be due to expression falling below the level of detection. It has been reported that in B cells the virus can express as little as a single EBNA1 transcript per cell (Tierney et al., 2015). Whilst no

EBNA2 or EBNA3 family genes were detected in the vast majority of cell lines, low numbers of transcripts of EBNA2 type 1, EBNA3A and EBNA3C were detected in SNT16 cells. This detection of Latency III gene transcripts is likely to be a false positive for two reasons. Firstly, EBNA2 and EBNA3 transcripts are driven by either Wp or Cp promoter activity which were not detected in SNT16. Secondly, EBNA2 type 1 transcripts were detected at a similarly low level in AG876 cells (which contain an EBNA2 type 2 sequence only), therefore such low levels can be considered background. All ENKTL or CAEBV cell lines express either LMP1, LMP2A or LMP2B, but interestingly, LMP1 and LMP2 levels showed great variability across the cell line panel in terms of relative expression and, in some incidences, absolute absence of detectable transcripts.

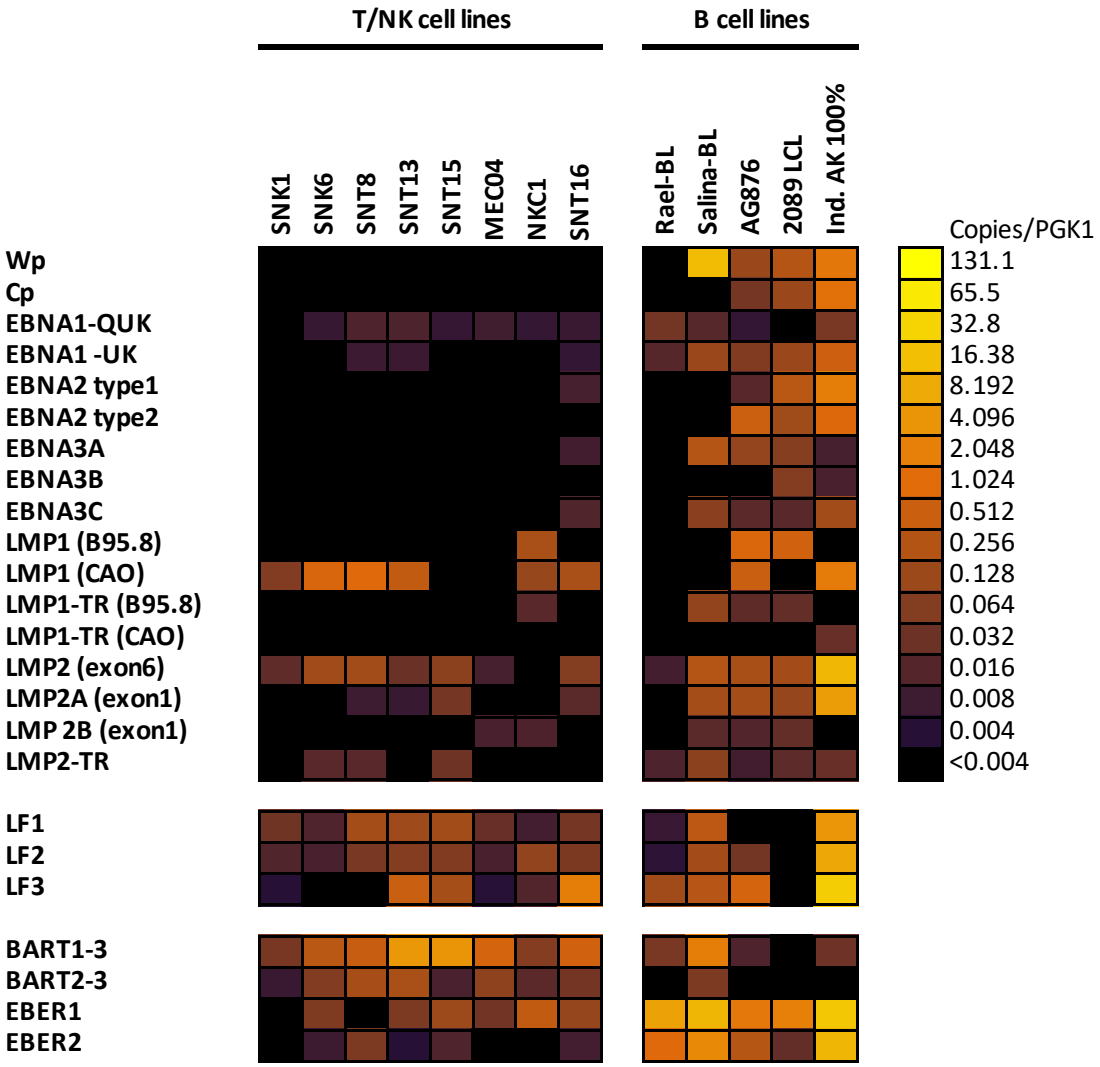
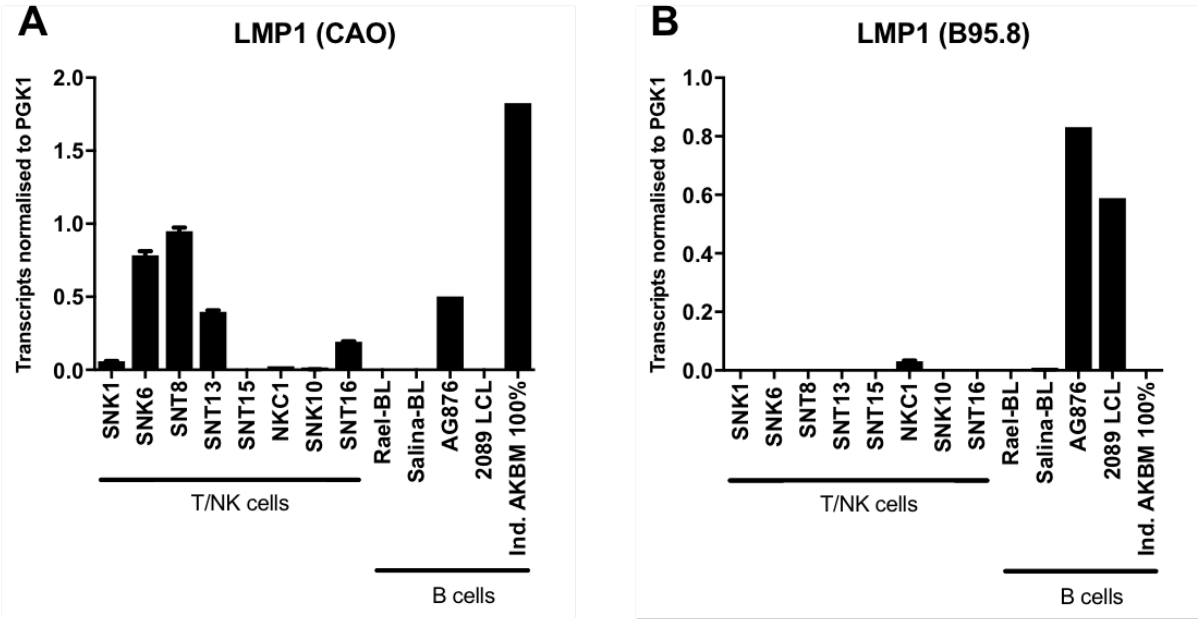


Figure 3.9 Heat map summarising expression of latent viral transcripts. High-throughput qPCR was used to detect latent transcript levels of EBV latent genes in T and NK cell lines which then have been normalised to cellular phosphoglycerate kinase-1 (PGK-1) expression level. Data are presented as a heat map with values indicated by the scale bar, where each colour change represents a two-fold change in transcript level. Data presented are mean of at least two independent experiments performed in duplicate. Data for B cell lines is taken from Tierney et al., 2015 as a comparative measure.

3.5.2 Expression of Latent membrane proteins

The presentation of gene expression data by heat map using a logarithmic scale has its limitations since low-level and high-level expressed genes are presented together on the same diagram/scale, making it difficult to compare the expression of an individual gene across multiple cell lines. Therefore, Fluidigm qPCR data from the two assays used to detect LMP1 are represented as bar charts in **figure 3.10**.

As mentioned above, some latent genes contain sequence variations that may affect the ability of a qPCR assay to accurately quantitate the number of transcripts. One such example of this can be found with LMP1. Two common strains of EBV — B95.8 and CAO — have sequence variations within the LMP1 gene and therefore two separate qPCR assays have been designed with different probe sequences but at the same location crossing the exon 2/3 boundary. LMP1 CAO transcripts were detected in 6 of 8 cell lines: SNK1, SNK6, SNT8, SNT13, NKC1 and SNT16 (**figure 3.10A**). Of note, B95.8 LMP1 transcripts were not detected in SNT15 and MECO4 but these cell lines retain a Lat II-restricted phenotype due to their expression of LMP2. Unusually though, LMP1 transcripts were detected in NKC1 cells with both the B95.8 sequence-specific assay and the CAO-specific assay (**figure 3.10B**). The LMP1 sequence of NKC1 was therefore sequenced and compared against the probe sequences for both LMP1 qPCR assays (**figure 3.10C**). The LMP1 sequence of NKC1 contains 1bp change and 2bp change compared to the LMP1 sequences of B95.8 and CAO strains, respectively. These bp differences suggest that both probes bind sub-optimally to the target DNA and therefore it is likely that both the B95.8 and CAO LMP1 assays underestimate the expression of LMP1 in NKC1 cells.



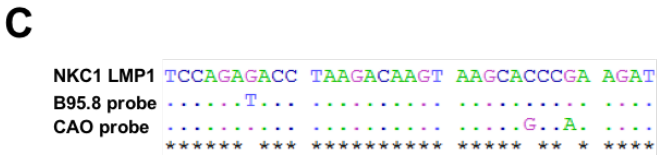


Figure 3.10 LMP1 mRNA expression. LMP1 expression data taken from high-throughput assay shown in **figure 3.9**. Transcripts detected by **A)** CAO sequence-specific assay and **B)** B95.8 sequence specific assays. **C)** LMP1 sequence from NKC1 cells at probe site. Data presented are mean of at least two independent experiments performed in duplicate. Error bars show standard deviation. Data for B cell lines is taken from Tierney et al., 2015 as a comparative measure.

3.5.3 Lytic gene expression

As in **figure 3.9**, the high throughput (Fluidigm) qPCR assays were also applied to assess which viral lytic genes were expressed in our cell line panel (**figure 3.11**). As before, standard curves generated by the AQ plasmid enabled the quantification of viral genes and were normalised against the housekeeping gene PGK1. The data are represented on a heatmap alongside the comparator cell lines of B cell origin, including Akata-BL cells induced into the lytic replication by Ig cross-linking.

Expression of the two immediate early genes, BZLF1 and BRFL1, were detected in only 4 of 8 T/NK cells but at extremely low levels that were approximately 2000-fold lower than lytic Akata-BL cells. A lack of immediate early gene activity was accompanied with expectedly low activity of early and late lytic genes. Across the cell line panel, SNT8, SNT13, SNT15, and SNT16 expressed the highest levels of lytic genes indicating they had the most lytic cycle activity. Looking at the different lytic cycle genes, the most highly expressed genes were BNLF2A and BNLF2B. However, the BNLF2A and BNLF2B transcripts are contiguous to the 3' UTR of LMP1 mRNA, therefore these results may not correlate directly with the lytic cycle and rather be due to LMP1 expression.

The results for the assays that detect the viral BCL-2 homologues, BHRF1 and BALF1, are represented as bar charts in **figure 3.12**. Three different splice variants of the BHRF1 gene are represented: H2-HF (transcribed from the Hp promoter during the lytic cycle), W2-HF and Y2-HF (transcribed from the Cp/Wp promoters in latent cycle) (Austin et al., 1988, Oudejans et al., 1995). All ENKTL and CAEBV cell lines were negative for the latent BHRF1

transcripts but SNT8, SNT13, SNT15 and SNT16 expressed low levels of BHRF1 H2-HF and BALF1, consistent with detection of the immediate early genes and lytic cycle activity in these cell lines. Despite detection of BHRF1 H2-HF and BALF1 transcripts, the expression levels were multiple orders of magnitude less than that of the positive controls Salina-BL and lytic Akata-BL.

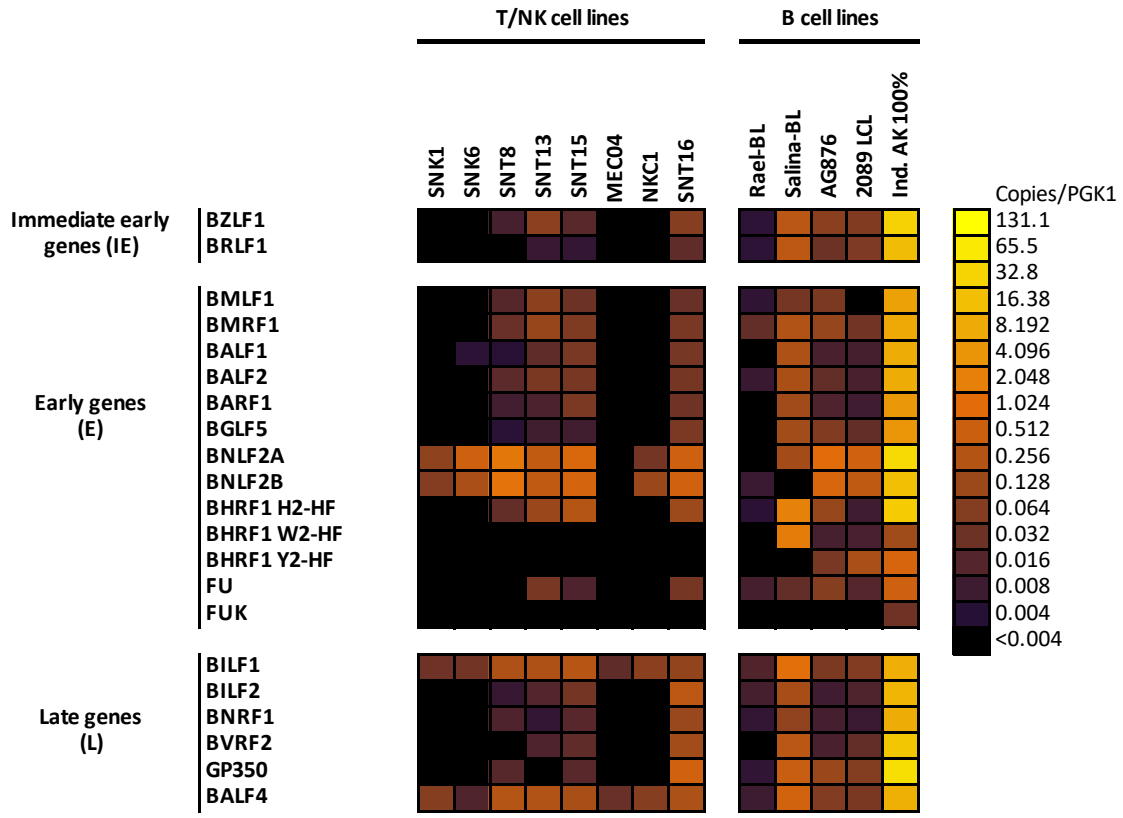


Figure 3.11 Heat map summarising the expression of lytic viral transcripts. High-throughput qPCR was used to detect transcript levels of EBV lytic genes in T and NK cell lines which then have been normalised to cellular phosphoglycerate kinase-1 (PGK-1) expression level. Data are presented as a heat map with values indicated by the scale bar, where each colour change represents a two-fold change in transcript level. Data presented are the mean of at least two independent experiments performed in duplicate. Data from B cells taken from Tierney et al., 2015 act as a comparative measure.

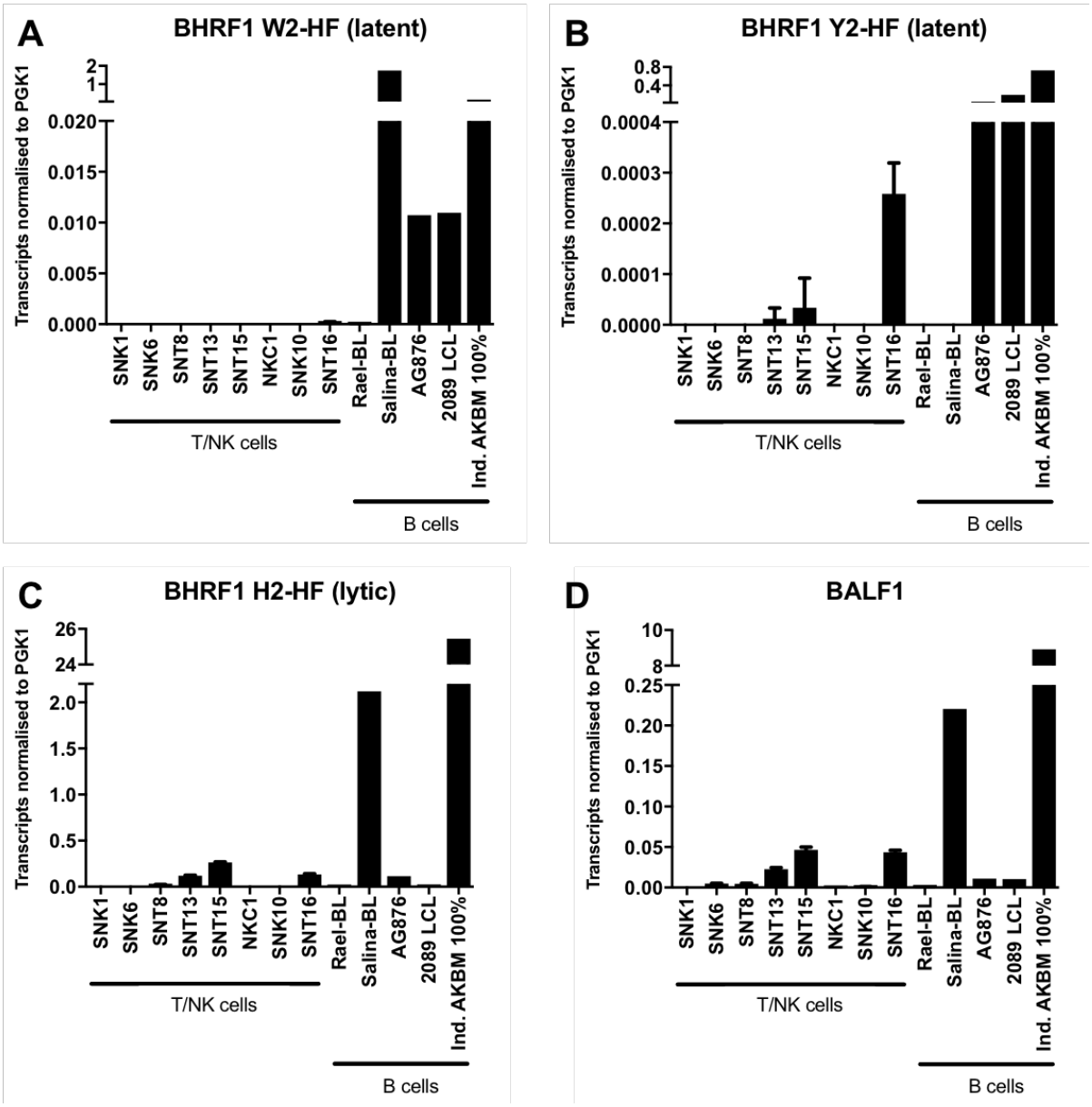


Figure 3.12 BHRF1 and BALF1 mRNA expression. Expression data taken from high-throughput QRT-PCR assays shown in the heatmap in **figure 3.11**. BHRF1 transcripts detected by **A)** W2-HF-specific, **B)** Y2-HF specific assays and **C)** H2-HF specific assays. **D)** BALF1 expression. Data presented are mean of at least two independent experiments performed in duplicate. Error bars show standard deviation. Data for B cell lines is taken from Tierney et al., 2015 as a comparative measure.

3.6 Discussion

This results chapter aimed to characterise the available ENKTL and CAEBV cell lines in order to determine their suitability as disease models for the subsequent experiments. As stated earlier, the limited availability of primary material, combined with the lack of an *in vitro* infection model, means that the few available ENTKL and CAEBV cell lines are the most commonly used models of such diseases. We have collected a comprehensive panel of cell lines to study EBV-associated T/NK cell lymphoproliferations, however, limited information on their immunophenotype and their EBV status is currently known. Here, we have extensively characterised these cell lines to report on such characteristics. This enables us to compare our data to the publications in which the cell lines were first described and also to epidemiological reports commenting on the phenotype of primary tumour samples.

The categorisation of each cell line into T or NK cell lineage based upon phenotypic markers and cytokine production was possible, but with clear exceptions, and a requirement for further analysis remains. Three T cell lines from the panel, namely SNT8, SNT13 and SNT15, proved to be of γδ T cell origin. All three cell lines were previously reported to contain a cell population of 75% or greater that were TCRγδ-positive, however we can only confirm such high expression of TCRγδ for SNT15 cells (Oyoshi et al., 2003). Only 30-40% of the SNT8 and SNT13 cell populations stained positive for TCRγδ. Interestingly, these same cell lines presented with heterogeneity with regards to the NK cell marker, CD56. CD56 was initially reported to be expressed on the surface of these cells following their establishment as cell lines, although no comment on heterogeneity was made (Oyoshi et al., 2003). The

expression of CD56 on γδ T cells was unexpected but such a phenotype has been reported in other cell lines. For example, it has been demonstrated by others that CD56 expression is induced by *in vitro* TCR activation where expression can be accentuated by the addition of IL-2 (Kelly-Rogers et al., 2006). Whereas other reports state the combination of IL-2 and IL-12 is sufficient to induce CD56 expression on either αβ T cells or γδ T cells (Satoh et al., 1996). Such reported $CD56^+$ T cells obtained cytolytic features and were capable of producing IL-4, IL-13 and IFN-γ but not IL-10. However, the EBV-positive γδ T cell lines (SNT8, SNT13 and SNT15) did deviate from this $IL\text{-}4^+$ $IL\text{-}13^+$ $IL\text{-}10^-$ phenotype (**figures 3.11 and 3.12**). IL-4 was only detected at <1 ng/mL in all three cell lines. Additionally, SNT15 cells produced high levels of IL-10 and low levels of IL-13. So whilst there are some parallels between some of our cell lines and the described $CD56^+$ γδ T cells (Satoh et al., 1996), there are also some differences. The impact on phenotype by IL-2 signalling in these reports may have consequence for the EBV-positive T/NK cell lines examined here. The establishment and sustained growth of SNT8, SNT13 and SNT15 cells required the addition of IL-2 to the culture media. It is not known whether the unusual CD56 expression observed on these TCRγδ-positive cells was enforced by IL-2 *in vitro* or was already present on the primary cells isolated from the patient and therefore a genuine disease marker. The original publication that reported the establishment of SNT13 and SNT15 (which also discussed SNT8) cell lines, made statements to confirm that the *in vitro* established SNT13 and SNT8 cell lines were phenotypically comparable to the primary tumour cells from which the lines were established, however, no such comment was made for SNT15 (Oyoshi et al., 2003). Currently, extensive gene expression analysis such as RNA-seq, of all the cell lines studied

here, has not been performed. This would provide insight into the remaining questions regarding the cell origin, the genetic factors contributing to pathogenesis and the overall aim of evaluating these cell lines as appropriate models of ENKTL/CAEBV disease. Short tandem repeat analysis on the cell lines would also provide confidence in their identity and prevent any future contamination issues.

It is widely accepted that the vast majority of ENKTL cases are of NK cell origin and therefore few studies have solely focused on the question surrounding the TCR status of such tumour cells beyond the investigation into clonality. In one study, a collection of 67 ENKTL tumours were investigated for TCR status and it was reported that only 5% expressed TCRγδ, 3% TCRαβ, 1% TCRγδ/αβ, 21% indeterminate, with the remaining 70% samples of NK origin (Pongpruttipan et al., 2012). Although this was a small cohort, it demonstrates that ENKTL can be of γδ T cell origin, as is the case with some of the cell lines we intend to use for our studies.

T cells are not the natural reservoir for EBV and therefore it is possible that characterising the T cell stage of the EBV-positive ENKTL cell lines may provide insights into how EBV infects the T cell lineage. The observation that SNT8, SNT13 and SNT15 are all $V\delta2^+$ T cells, could indicate that this cell type is susceptible to EBV infection. The point at which an EBV:γδ T cell interaction would occur in the virus life cycle remains unclear but a conceivable hypothesis would be that this interaction could occur during the early immune response to the virus. Although the immune control of EBV infected cells is primarily understood to occur through αβ T cells (Hislop et al., 2007, Long et al., 2011), a role for γδ

T cells has been suggested in early phases of infectious mononucleosis (De Paoli et al., 1990).

An alternative hypothesis is that the virus may have infected a precursor cell and EBV itself then drives the cell towards one of many mature phenotypes but with an inclination towards a Vδ2^{+} phenotype. Such events would explain the presence of EBV in other T cell types, such as the CD4^{+} SNT16 cells, and the incidences of CAEBV where EBV is found within both the T and NK cells compartment of the same patient (C. Shannon-Lowe, unpublished). The infection of a target cell type that would satisfy these criteria is the common lymphoid progenitor (CLP) cells. These cells are precursors to the stage of NK or T cell lineage commitment and, importantly, express CD21 which is a critical surface protein required for EBV entry into B cells (Fingeroth et al., 1984, Shannon-Lowe and Rowe, 2014).

Greater efforts have been taken to understand the phenotype of ENKTL tumour cells of NK cell origin. A meta-analysis published in 2015 investigated a total of 411 NK-ENKTL tumours in an effort to determine the normal counterpart of such malignant cells (Lima, 2015). The most frequent phenotype of NK-ENKTL cells was determined to be CD56^{bright}, CD94^{+} (KIR), CD57^{-}, CD16^{-} and also positive for the activation markers CD45RO and HLA-DR. From our cell line panel, MEC04 and the newly established CAEBV line NKC1 demonstrated a comparable phenotype of CD56^{+}, CD57^{-}, CD16^{-} but in contrast they did not express KIRs. SNK6 was the only CD56^{+} cell line that expressed KIRs and NKG2A (CD159a) in a subset of cells but this cell line also stained positive for the NK terminal differentiation cell marker, CD57. In the analysis performed by Lima and colleagues, CD57^{+} tumours were evident but were indicated to be rare. SNK1 cells, despite having been previously described as

$CD56^{+}CD16^{+}$ (Zhang et al., 2003), did not stain for any of the T or NK cell markers included in our panel. It is possible that this cell line has lost expression of the cell surface markers during serial passage. Interestingly, the CAEBV cell line NKC1, expressed the same phenotype as MEC04 (ENKTL cell line) of $CD56^{+}CD16^{-}CD159a^{-}$ along with the absence of KIR expression which is consistent with an early NK cell phenotype. Overall, the EBV-positive NK cell lines examined here exhibited phenotypes consistent with their original reports and were representative of NK-ENKTL tumours reported in the literature.

It is apparent that our panel represents a diverse combination of EBV infected T and NK cell subtypes. The characterisation studies revealed three cell lines of γδ T cell origin (SNT8, SNT13 and SNT15), one CD4+ T cell line (SNT16), one mature NK cell line (SNK6) and two early NK cell lines (MEC04 and NKC1). Further investigation into other cell differentiation markers are required to confirm this preliminary categorisation and it should be noted that some changes to cellular phenotype may have occurred during cell culture. From this analysis however, it can be argued that EBV can either infect an array of T and NK cell subtypes or that infection is an early event prior to cellular differentiation. The favoured hypothesis at this stage is that EBV gains entry into CD21-expressing common lymphoid progenitor (CLP) cells before the stage of NK or T cell lineage commitment. However, it remains uncertain as to which point within the life cycle of the virus that EBV would encounter such precursor cells that primarily reside in the bone marrow before migrating to the thymus for differentiation since neither the bone marrow nor the thymus are associated with normal EBV biology.

Besides the phenotype of the cells, another factor investigated by the ENKTL field, is the virus subtype. EBV strains can be divided into either type 1 or type 2, primarily based upon EBNA2 and EBNA3 sequences (Sample et al., 1990, Adldinger et al., 1985, Dambaugh et al., 1984, Rowe et al., 1989). Only recently has this bifurcation been considered to affect the cell types that the virus may be prone to infect. Coleman and colleagues showed that EBV type 2 virus could infect primary $CD8^+$ T cells and establish latency (Coleman et al., 2015, Coleman et al., 2017). Such reports favoured us to expect that the ENKTL cell lines would also be infected with type 2 EBV. However, in contrast to our predictions, the results from the typing PCRs indicated type 1 virus was present in all 8 cell lines.

In clinical samples, viral gene expression in EBV-infected T and NK tumour cells has been assessed to a limited degree. A small study of 23 ENKTL cases reported a latency II pattern of EBV gene expression, although EBV-infected cells that were also LMP-negative were noted to be present in multiple tumours (Chiang et al., 1996). A different study that examined 7 ENKTL patients of T cell origin detected LMP1 and/or LMP2 expression in 6 of 7 samples (van Gorp et al., 1996). Reports of CAEBV have shown typical latency II phenotypes (EBNA1, LMP1 and LMP2-positive, EBNA2-negative) with no lytic cycle activity as determined by a lack of BZLF1 transcript detection (Yoshioka et al., 2001, Kimura et al., 2005). Our findings from the high-throughput gene expression analysis on patient derived cell lines agree with previous conclusions from patient studies that EBV establishes a latency II phenotype in T and NK cells with variable expression of the LMP proteins and also negligible lytic activity. The data presented here are the most extensive EBV expression analysis of ENKTL and CAEBV cell lines.

The application of the technology described here to patient samples in order to assess EBV gene expression could prove insightful and would avoid the extensive costs associated with similar technologies, such as RNA-seq. It would be informative to correlate the expression of the different EBV genes to patient survival or treatment responses since this may reveal potential contributions of these viral genes to both tumorigenesis and chemosensitivity. Although the functions of the relevant latent genes, such as EBNA1, LMP1, LMP2A and LMP2B, are well studied in B cell and epithelial cell backgrounds, their impact on the pathogenesis of T or NK cell disease is less well understood. In this regard, LMP1 has been shown to induce Th1 cytokines, TNF-α secretion and PD-1 expression in relevant *in vitro* T cell models (Chuang et al., 2005, Chuang et al., 2008, Lay et al., 2003, Bi et al., 2016). Although we did not perform functional experiments to probe the contribution of the individual EBV genes in the ENKTL/CAEBV cell lines, we anticipate that the thorough analysis of EBV gene expression will provide a strong basis for subsequent investigations of this nature.

In conclusion, the data presented here is a comprehensive insight into EBV gene expression, cell phenotype and steady-state cytokine production within this extensive collection of ENKTL and CAEBV cell lines. Overall these cell lines provide a close representative of the respective diseases and are comparable to the original reports describing the tumour cells. Therefore, they can be deemed as suitable and informative *in vitro* models of T/NK cell disease and can be taken forward for further investigation into ENKTL and CAEBV.

4. Results II: Resistance to chemotherapy and apoptotic evasion

4.1 Introduction

Chemotherapy-based treatment regimens for patients with EBV-positive T and NK cell neoplasms leaves the vast majority of individuals with poor prognoses and low quality of life due to the side effects induced by cytotoxic chemotherapy (Au et al., 2009, Yamaguchi et al., 2011). The high rates of relapse in those that do initially respond suggest that the cancer cells are not completely cleared despite initial remission and therefore that a population of the malignant cells can evade such therapies. Therefore, there are a large number of patients who receive toxic treatments which are ineffective at eliminating their disease. Understanding how the tumour cells evade such therapies is a question that has not been satisfyingly answered.

Studies over the past 10 years have suggested that the evasion of cell death in EBV-positive T and NK cells is partially due to expression of the multi-drug efflux pump known as p-glycoprotein, or multidrug resistance protein 1 (MDR1), encoded by the *ABCB1* gene (Yamaguchi et al., 1995, Yoshimori et al., 2015). The expression of p-glycoprotein is found within normal tissue of the brain, kidney, liver and multiple other organs as a defence against toxins (Staud et al., 2010). P-glycoprotein has been reported to function as a drug resistance factor in various haematological and epithelial cancer types (Eadie et al., 2016, Eadie et al., 2014, Goldstein et al., 1989). Chemotherapy substrates of p-glycoprotein include docetaxel, vincristine and etoposide. The observation that p-glycoprotein is

expressed in ENKTL tumours — found by immunohistochemical staining of paraffin embedded tissue — led to the adjustment of therapy from the CHOP regimen to what is known as the SMILE treatment regimen — dexamethasone (steroid), methotrexate, ifosfamide, L-asparaginase and etoposide (Yamaguchi et al., 2008, Yamaguchi et al., 2011). However, SMILE therapy still includes etoposide and methotrexate despite reports that they can be exported by p-glycoprotein, preventing build-up of these drugs to efficacious concentrations in cancer cells (Sehested et al., 1992, de Graaf et al., 1996).

Another factor that may affect the apoptotic response to anti-cancer drugs is the major tumour suppressor gene, p53, that is known to be commonly mutated across most cancer types (Muller and Vousden, 2013). p53 is central to the activation of apoptosis in response to DNA damage — such as that induced by etoposide treatment. The mutation status of p53 in ENKTL or CAEBV has not been extensively studied and it is currently not known whether its dysregulation is a contributing factor to cellular transformation or survival during anti-cancer therapy in this context.

The induction of apoptosis by p53 is mediated by transcriptional upregulation of its direct target genes *Puma* and *Noxa,* which encode BH3-only proapoptotic members of the BCL-2 family (Oda et al., 2000, Nakano and Vousden, 2001). Dysregulation within the BCL-2 family commonly leads to evasion from apoptosis. Such evasion is typically mediated by overexpression of pro-survival members of the family or reduced expression of the pro-apoptotic BH3-only members of the family, but can also involve other factors including aberrant binding, regulation and protein modifications. The precise abnormality leading to apoptotic resistance can be difficult to delineate and it can take substantial effort using

classical techniques that analyse protein expression and interaction. However, more modern methodologies, including the use of BH3 profiling, have improved our understanding of which BCL-2 family members maintain survival in various cell types. BH3 profiling is a technique which in principle uses peptides derived from BH3-only proteins then applied to mitochondria isolated from cells of interest (Deng et al., 2007). This reveals which BH3-only proteins would be needed to kill a cell and thus can identify the pro-survival BCL-2 proteins that are essential for the sustained survival of a given cell. Other technical approaches include the use of BH3 mimetics (described in detail in **section 1.3.4**). Due to their specific binding profiles, BH3 mimetics can provide details on which pro-survival member is important for the maintained survival of a cell or cell type. BH3 mimetics have the added advantage of not only being a useful research tool but also having clinical relevance. The recent success of the BCL-2 specific inhibitor ABT199/Venetoclax has opened the door to the therapeutic inhibition of other pro-survival members (Souers et al., 2013, Roberts et al., 2016).

Animal models of ENKTL are limited. Whilst genetic aberrations, such as loss or mutations of tumour suppressors such as p53, BLIMP1 and BIM, have been identified with varying frequencies in ENKTL (Hongyo et al., 2005, Iqbal et al., 2009, Kucuk et al., 2015), a bona fide driver of tumorigenesis has yet to be confirmed in order to develop a genetic mouse model of ENKTL. Xenograft mouse models using patient-derived tumour cells have been successful, but this is limited by availability of primary material (Imadome et al., 2011). The successful xenograft of an ENKTL cell line into immunocompromised mice has also been reported and this avenue is currently the most attractive on a technical basis (Siddiquey et

al., 2014). Establishment of a reliable ENKTL disease model would enable efficacy studies and toxicity studies of novel drugs/compounds and therefore be a step closer towards bringing novel targeted therapies into the clinic.

The major aim of this results chapter is to investigate the effectiveness of SMILE therapy with *in vitro* disease models and to determine how EBV-positive T and NK cells resist the activation of apoptotic cell death. We investigated this by examining a panel of ENKTL cell lines for their response to etoposide and methotrexate — two clinically relevant genotoxic compounds. Subsequently, we investigated p-glycoprotein expression and function and the role of the p53 and BCL-2 pathways as potential mechanisms of chemoresistance. Finally, we assessed the therapeutic potential of the BCL-X_L specific BH3 mimetic, A-1331852, in xenograft mouse models of disease.

4.2 *In vitro* response to clinically relevant cytotoxic agents

To determine the effectiveness of currently used chemotherapy agents, the panel of EBV-positive T/NK cell lines were exposed to selected cytotoxic agents and cell survival analysis was performed. From the five agents included in the SMILE chemotherapy regimen, three are capable of direct cytotoxicity: etoposide, ifosfamide and methotrexate. Etoposide and methotrexate were taken forward for analysis as, unlike ifosfamide, they do not require metabolic activation by the cytochrome P450 (CYP) enzymes and were therefore more readily testable *in vitro* (Chang et al., 1993). Etoposide and methotrexate both activate the apoptotic pathway by inducing DNA damage (Fortune and Osheroff, 2000). Etoposide is a topoisomerase II inhibitor and therefore prevents DNA unwinding whereas methotrexate

is a dihydrofolate reductase inhibitor that interferes with synthesis of thymidine molecules and thereby prevents DNA synthesis.

Cells were treated with increasing concentrations of etoposide for 48 hours then stained with annexin-V and PI prior to analysis by flow cytometry. The percentage of PI-/annexin V- cells representing live cells, is plotted in **figure 4.1A**. The control EBV-negative T lymphoblastic leukaemia cell line, MOLT4, exhibited marked susceptibility to etoposide induced apoptosis with an IC50 of 0.33uM (**table 4.1**). The EBV-positive T and NK cell lines all exhibited much lower levels of sensitivity to etoposide-induced killing. The IC50 values exceeded the maximum tested dose of 10 uM in 4 of 8 cell lines, whereas for the remaining 4 cell lines the IC50 values ranged from 1.92 uM to 7.17 uM.

The response to methotrexate-induced killing is represented in **figure 4.1B**. Again, MOLT4 was used as a reference susceptible cell line, only 10% of cells remained viable following a 48 hour treatment with 0.1 uM of drug. The EBV-positive T and NK cell lines varied in their response to methotrexate to a greater extent compared to the response to etoposide. At 10 uM methotrexate, cell viability ranged from 50% (MEC04 cells) to 85% (SNT16 cells). All EBV-positive cell lines presented with an unusual dose-response curve following methotrexate treatment in which a small percentage of cells died at low doses but no additional cells were induced into apoptosis with increasing concentration of drug. This is indicative of at least two distinct subpopulations of cells - one of which is sensitive to killing even at low concentrations of drug, whereas the other subpopulation demonstrates

no/little susceptibility to killing (representative data for MEC04 cells shown in **supplementary figure 1**).

These data suggest that the EBV-positive T and NK cell lines do not readily undergo apoptosis in response to commonly used therapeutic agents that initiate signalling in the apoptotic pathway via the induction of DNA damage. This suggests that etoposide and methotrexate may not be suitable for the treatment of EBV-associated T and NK cell disease according to the *in vitro* disease model investigated here. Although these cell lines may be the closest disease model available, as discussed in chapter 3 of this thesis, there are limitations in comparing their response *in vitro* to that of patients and primary samples. Cell lines are likely like to acquire additional mutations after prolonged culture which may alter signalling pathways associated with cell survival. Also, these cancer cells may respond in an alternate manner to various stimuli outside the local microenvironment in which they developed. The resistance to apoptosis exhibited by these cell lines occurs through a currently unknown mechanism.

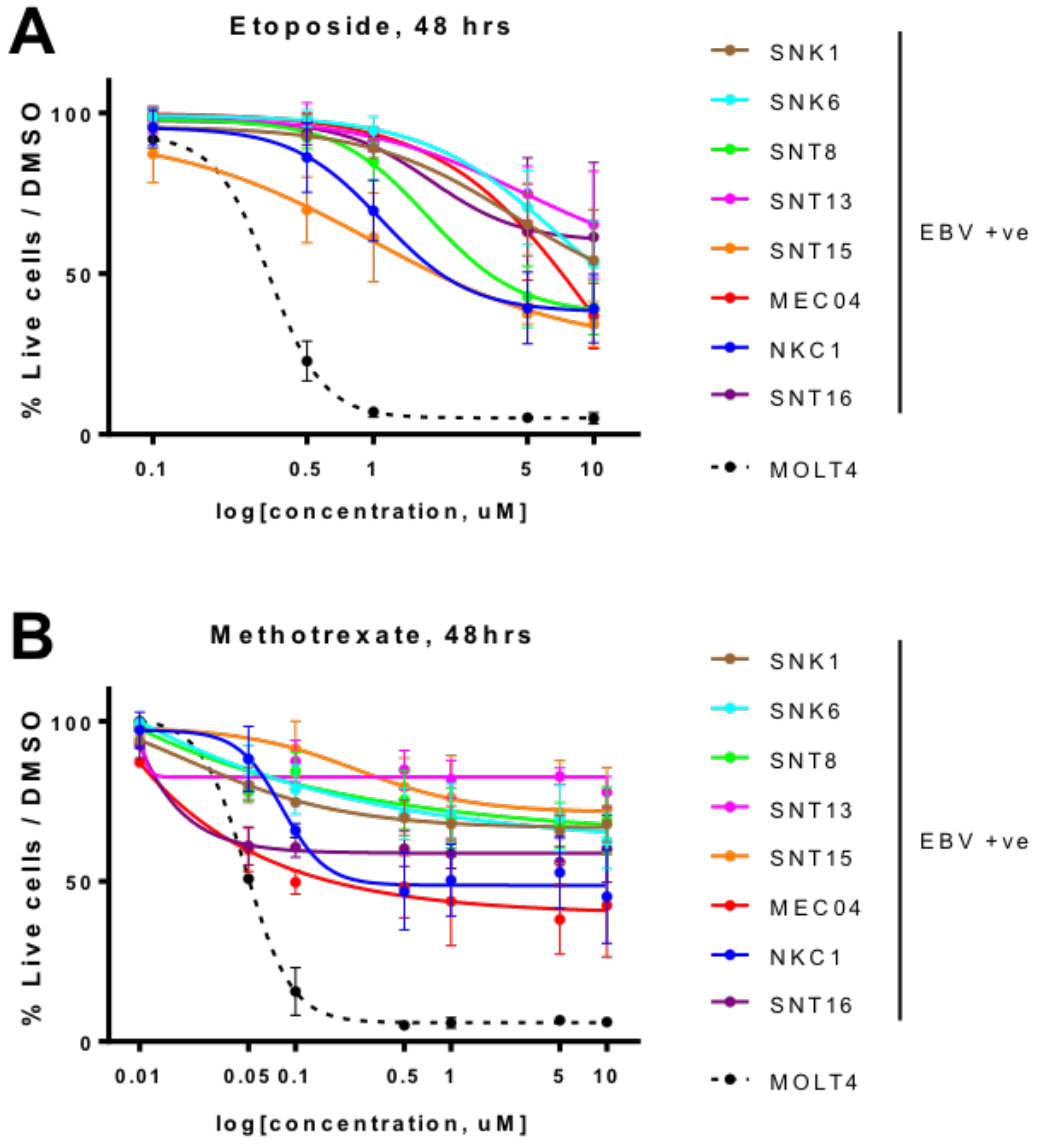


Figure 4.1 Induction of cell death in T and NK cell lines. EBV-positive cell lines (coloured curves) and the EBV-negative cell line MOLT4 (black, dotted curve) were treated with increasing concentrations of **A)** etoposide or **B)** methotrexate. Cells were stained with Annexin V and PI to determine survival where PI-/Annexin V- double negative populations (deemed live cells) were normalised to DMSO-only controls and then plotted. Data presented are mean ±SE of three independent experiments performed in duplicate. SE, standard error.

Table 4.1 Potency of genotoxic agents on T/NK cell lines. IC50 values for etoposide, methotrexate and ionomycin calculated from dose-response curves.

	Etoposide	Methotrexate
SNK1	>10	>10
SNK6	>10	>10
SNT8	3.35	>10
SNT13	>10	>10
SNT15	1.92	>10
MEC04	7.17	1.22
NKC1	2.01	1.53
SNT16	>10	>10
MOLT4	0.33	1.13

4.3 Genotoxic drug tolerance via p-glycoprotein

4.3.1 *ABCB1* expression

As mentioned above, the high expression of p-glycoprotein (encoded by the *ABCB1* gene) identified in ENKTL tumours by IHC has led to the suggestion that chemoresistance is mediated by drug efflux. To test this hypothesis, the panel of EBV-positive T and NK cells were first assessed for expression for *ABCB1* by qRT-PCR. KG-1 cells, an acute myelogenous leukaemia cell line, were used as controls due to their reportedly high expression of *ABCB1* (Bailly et al., 1995). As shown in **figure 4.2,** the expression of *ABCB1* formed a dichotomy across the panel as transcripts were detected in 4 of 8 cell lines — SNK1, SNK6, MEC04 and

NKC1. MEC04 cells expressed the highest levels at approximately 2-fold greater than control KG-1 cells whereas substantially lower levels were detected in the remaining *ABCB1*-positive cells. The remaining 4 cell lines (SNT8, SNT13, SNT15 and SNT16) did not show detectable expression of *ABCB1*. Expression of the housekeeping gene, *PGK1*, was detectable in all cell lines, which confirmed the presence of viable cDNA.

4.3.2 Functional p-glycoprotein

To further investigate the hypothesis that p-glycoprotein is a contributing factor towards resistance to cell death induced by genotoxic agents, its function in EBV-positive T and NK cells was assessed in a rhodamine-123 efflux assay (**figure 4.3**). Rhodamine-123 is a fluorescent molecule that is a specific substrate of the p-glycoprotein efflux pump (Twentyman et al., 1994). Therefore, high fluorescence or retention of rhodamine-123 by a cell indicates either the low/absent expression or low/absent functionality of p-glycoprotein. Following pre-incubation with rhodamine-123, a subsequent 2 h incubation under various conditions was performed during which rhodamine-123 would be exported by functional p-glycoprotein. In **figure 4.3A**, a shift of the red histogram from the grey histogram (maximum rhodamine-123 signal, rhodamine-123 retention due to cold incubation), on the right side of the plot, towards the black histogram (minimum rhodamine-123 signal, unstained cells), on the left side of the plot, indicates the presence of functional p-glycoprotein in KG-1 cells. This shift is not observed with the p-glycoprotein-negative control Jurkat cells. An additional negative control (blue histogram) was included where the efflux step took place at 37°C but in the presence of cyclosporin A (2 uM) – a

known inhibitor of p-glycoprotein (Cumber et al., 1991). This demonstrates that any observed efflux at 37°C has occurred due to p-glycoprotein activity. Rhodamine-123 efflux is observed in SNK1, SNK6, MEC04, and NKC1 cells but not in the remaining cell lines.

The mean fluorescence intensity (MFI) values for each histogram was used to quantitate the rhodamine-123 signal using the following formula: $(MFI_{red} \times 100) / (MFI_{grey} - MFI_{black})$ = % Maximum efflux (**figure 4.3B**). SNT8, SNT13, SNT15 and SNT16 cells exhibited low levels of rhodamine-123 efflux which were not significantly different from the p-glycoprotein-negative Jurkat cells of 17.2%. As Jurkat cells do not express p-glycoprotein/*ABCB1*, this background level of efflux is likely due to membrane leakiness.

The data presented here show that rhodamine-123 efflux, a feature exclusive to cells with functional p-glycoprotein, occurred in SNK1, SNK6, MEC04 and NKC1 cells consistent with their gene expression profiles. The hypothesis that p-glycoprotein mediates the observed chemoresistance observed in all EBV-positive T and NK cells disease cannot be accepted based upon these experiments, as p-glycoprotein activity was not consistent across all cell lines. Therefore, alternative mechanisms of chemoresistance require consideration.

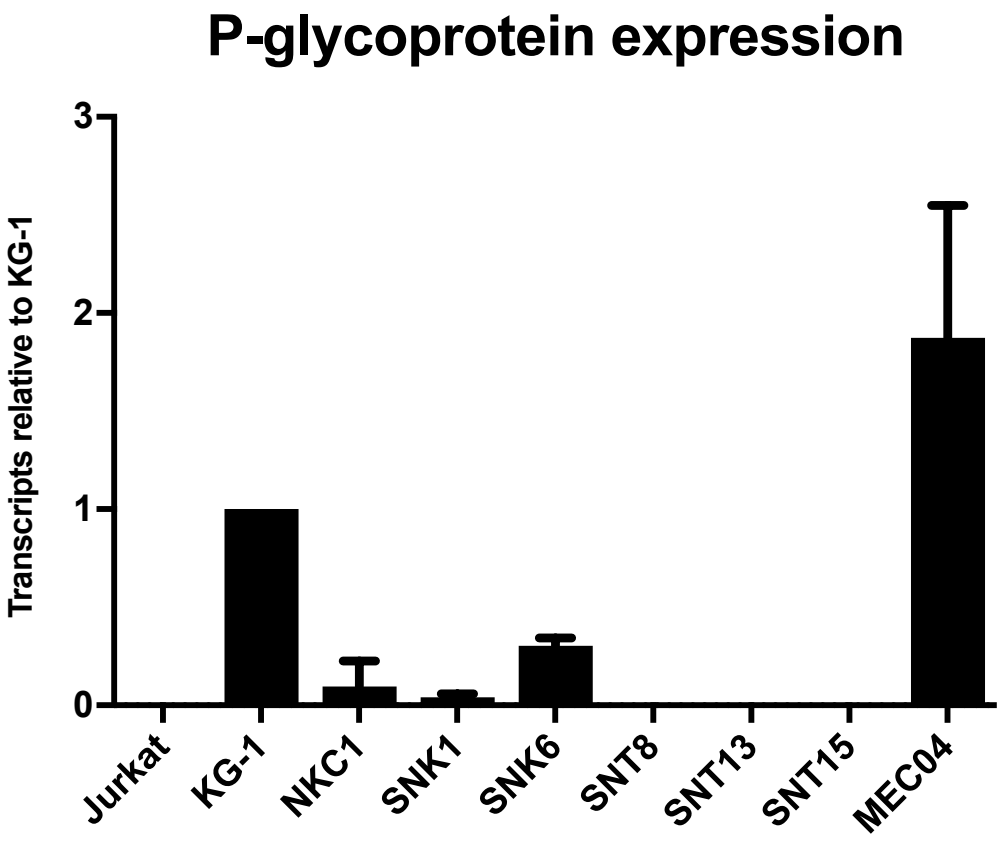


Figure 4.2 Background expression of the ABCB1 gene in T and NK cell lines. QRT-PCR analysis to detect *ABCB1* gene transcripts was performed on EBV-positive T and NK cells. KG-1 cells (positive control) and Jurkat cells (negative control) were included in the experiments due to their reported high *ABCB1* expression and lack of *ABCB1* expression, respectively. Values were normalised to PGK1 expression and subjected to ΔΔCt calculation and presented as relative to KG-1 cells. Data presented are mean ±SE of three independent experiments performed in duplicate (n=3).

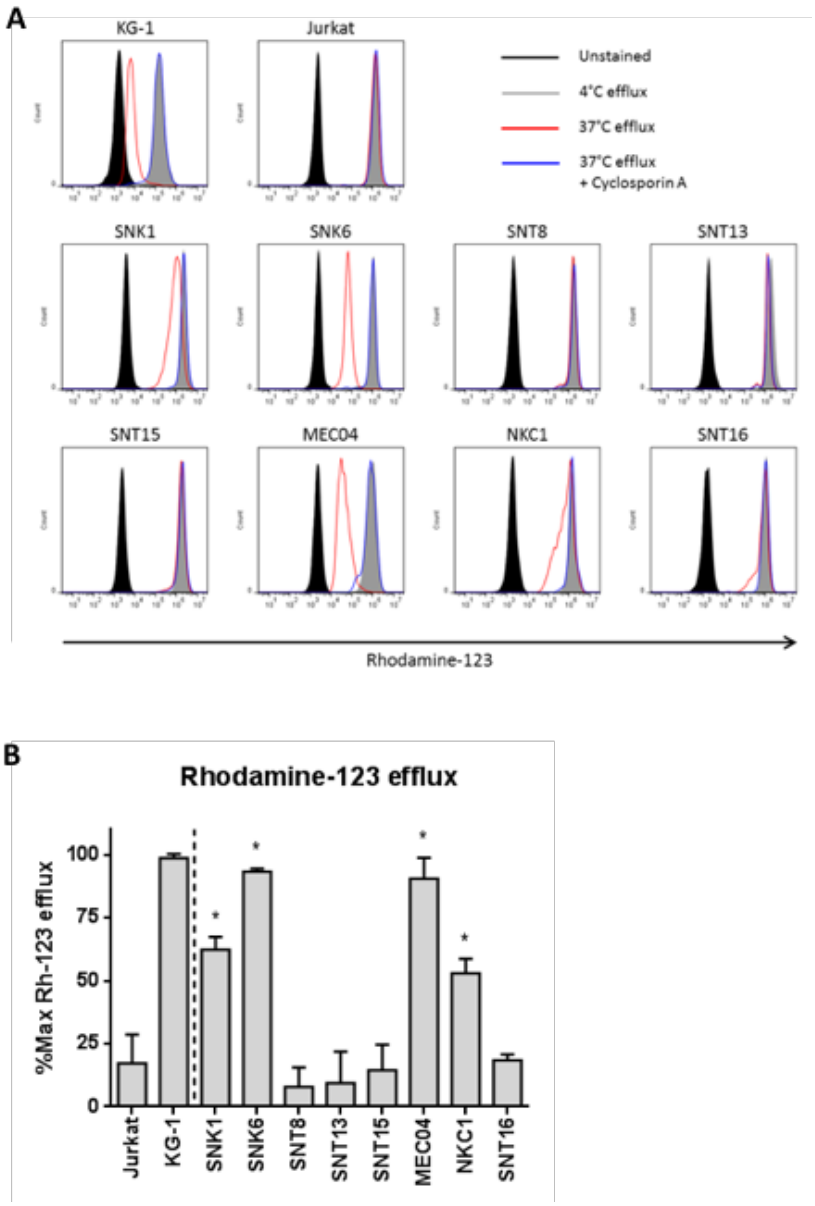


Figure 4.3 Detection of functional p-glycoprotein in EBV-positive T and NK cells. The functionality of p-gp was assessed by the efflux of fluorescent rh-123 as determined by flow cytometry. **A)** Cells were either left unstained or stained with rh-123 (black, filled histogram), stained with subsequent incubation at 4°C (grey, filled histogram), stained with subsequent incubation at 37°C (red, open histogram) or stained with subsequent incubation at 37°C in the presence of the p-gp inhibitor, CsA (blue, open histogram). **B)** Rh-123 efflux was quantified using the following formula: $(MFI_{red} \times 100) / (MFI_{blue} - MFI_{black})$. KG-1 cells (positive control) and Jurkat cells (negative control) were included in the experiments due to their reported high p-gp expression and lack of p-gp expression, respectively. Data presented are means ±SE of three independent experiments performed in triplicate (n=3). *p<0.05, vs. Jurkat. P-gp, p-glycoprotein; Rh-123, rhodamine-123; CsA, cyclosporin A; MFI, median fluorescence intensity.

4.4 Genotoxic drug resistance due to p53 pathway defects

4.4.1 Expression of p53 and MDM2

To investigate possible contributions of disturbances of the p53 pathway within the T/NK cell line panel, the levels of the proteins p53 and its negative regulator, the MDM2 E3 ubiquitin ligase (Honda et al., 1997), were assessed by Western blot analysis (**figure 4.4**). High levels of p53 protein can be indicative of a mutation in p53. Mutations in p53 frequently cluster within the DNA binding domain and these result in stabilisation of the p53 protein (Olivier et al., 2010, Wiech et al., 2012). By contrast, WT p53 protein is maintained at very low levels in unstressed cells, reviewed in (Harris and Levine, 2005). The basal levels of expression of p53 and MDM2 were assessed in the T/NK cell lines during steady state in comparison to selected BL cell lines where the p53 status is known: BL2, BL41, Kem-BL and Sav-BL. BL2 have a reported WT sequence of p53 (negative control) whereas BL41, Kem-BL and Sav-BL have mutant p53 sequences (positive controls).

Relative to WT and mutant p53 control cells, SNK1, SNT15 and SNT16 exhibited low levels of p53 protein consistent with WT p53 whereas MEC04 cells expressed the highest level among the T/NK panel, comparable to p53 expression in the control mutant p53 expressing cells, likely indicating a mutation within the p53 gene. The remaining cell lines expressed varied levels of p53 protein but levels were generally elevated compared to BL2, suggestive of some p53 activation. Expression of MDM2 was detected in all cell lines, with SNK1 and SNT13 expressing the highest levels.

To determine if p53 could respond to DNA damage inducing agents, selected cell lines, representing a range of p53 expression levels, were treated with either etoposide, methotrexate or ionomycin (the latter drug as an example of a non-DNA damage-inducing initiator of apoptosis) followed by protein analysis expression by Western blotting (**figure 4.5**). SNK1, SNK6 and SNT8 cells exhibited an increase in p53 expression after treatment with increasing concentrations of either etoposide or methotrexate but not with ionomycin, as expected. This suggests that these cells contain a WT p53 that is induced in response to DNA damage. However, MEC04 cells, which presented with the highest level of p53 expression in the steady state, showed only a modest increase in p53 expression after treatment with etoposide or methotrexate relative to the untreated control cells. This is consistent with the notion that this cell line contains mutant p53.

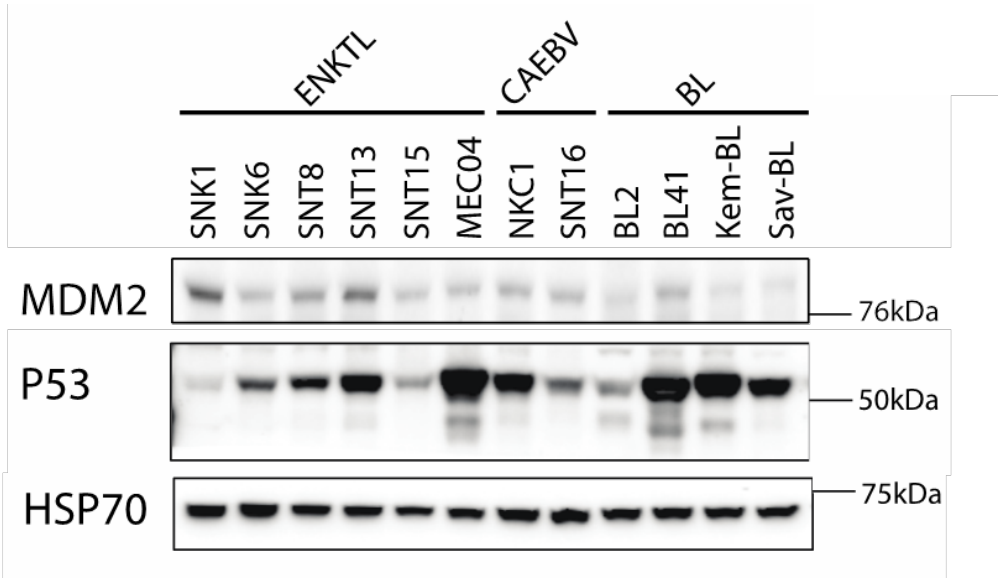


Figure 4.4 Expression of p53 and MDM2 protein in unstressed cells. Western blot analysis was performed in order to determine the levels of p53 and MDM2 protein in EBV-positive T and NK cell lines. HSP70 was used as a loading control. BL cell lines BL2 (wt p53), BL41 (mutant), Kem-BL (mutant) and Sav-BL (mutant) were included for comparison. Data presented are representative of three independent experiments. BL, Burkitt's lymphoma.

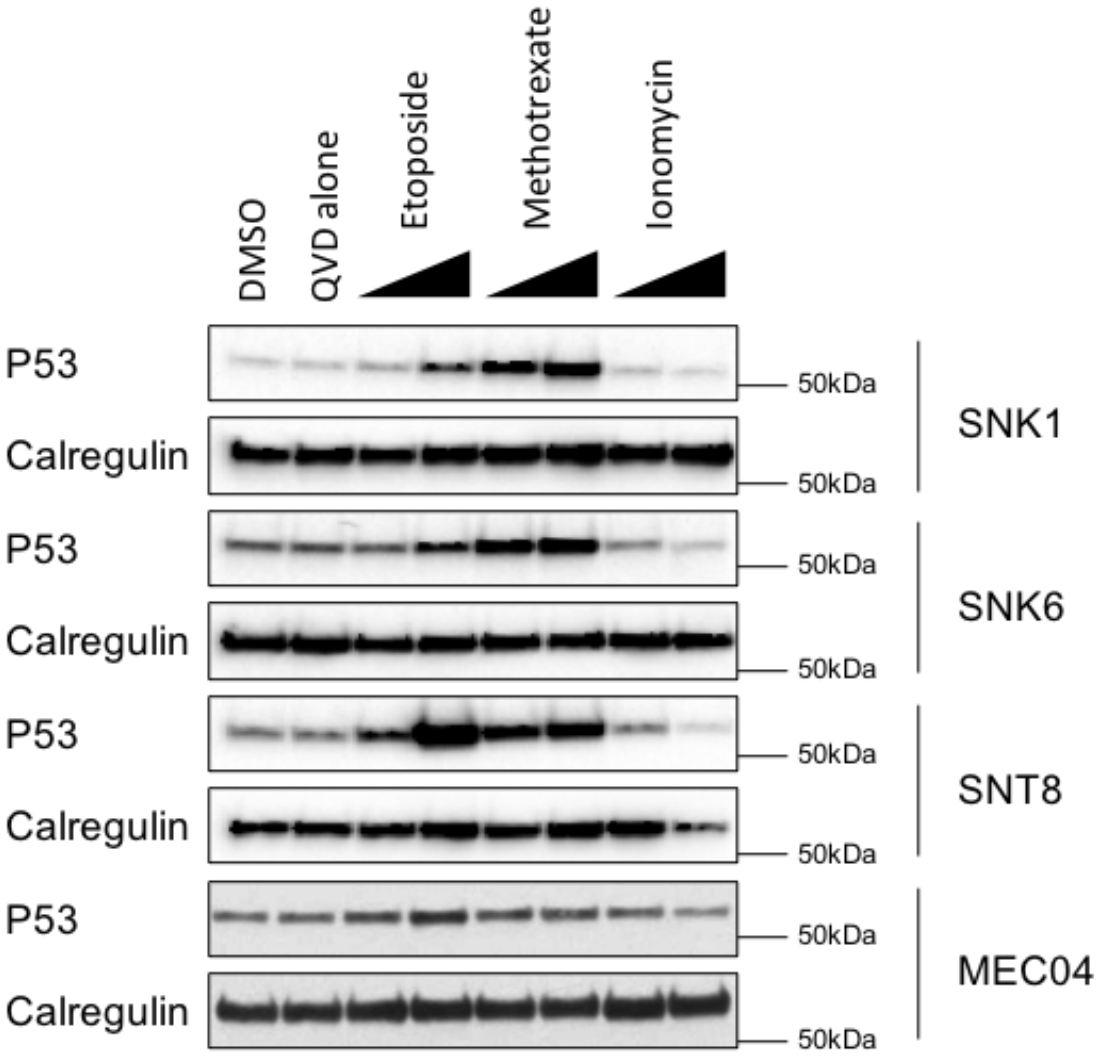


Figure 4.5 Expression of p53 in T and NK lymphoma cell lines following genotoxic treatment. Western blot analysis was performed in order to detect changes in the expression of p53 in response to treatment with genotoxic drugs in selected EBV-positive T and NK cell lines. Calregulin was used as a loading control as previously used by others (Zuo et al., 2011, Kelly et al., 2009). The genotoxic agents, etoposide and methotrexate, were utilised along with the non-genotoxic agent, ionomycin, that was included as a negative control. Indicated concentrations of drug are 0.5 uM and 5 uM and cells were examined at 48 hours. Cells were co-treated with 25 uM QVD-OPH (broad spectrum caspase inhibitor) with the exception of those in lane 1 labelled 'DMSO'. This was done to prevent the protein degradation that occurs during late stages of apoptosis due to the activity of caspases. Data presented are representative of three independent experiments.

4.4.2 p53 gene sequencing

To formally determine the p53 gene mutational status of the cell lines, the p53 sequence of all T/NK cell lines was determined by Sanger sequencing. Mutations within the p53 gene primarily occur within the DNA binding domain, which is encoded by exons 5 to 8 (Pavletich et al., 1993). Sequencing of this region revealed WT sequences in all the T and NK cell lines with the exception of MEC04 (**table 4.1**). Of note, within exon 7 of the MEC04 cells a C>T mutation was found, which leads to an Arg248Gln amino acid change in the protein sequence. This is reportedly sufficient to prevent p53 interaction with target DNA (Wong et al., 1999), and this likely explains the raised p53 protein levels and the lack of response to DNA damaging agents observed in this cell line.

Table 4.2 p53 mutation status EBV-positive T and NK cells.

Cell line	Exon 5	Exon 6	Exon 7	Exon 8
SNK1	WT	WT	WT	WT
SNK6	WT	WT	WT	WT
SNT8	WT	WT	WT	WT
SNT13	WT	WT	WT	WT
SNT15	WT	WT	WT	WT
MEC04	WT	WT	**Arg248Gln**	WT
NKC1	WT	WT	WT	WT
SNT16	WT	WT	WT	WT

4.4.3 Non-genotoxic p53 activation

Although only MEC04 cells contained a mutation in the hotspot region of the p53 gene, the apparent elevated p53 protein expression in a subset of the other cell lines in the absence of a p53 gene mutation warranted further investigation. To determine if the p53 pathway was functional, non-genotoxic activation of p53 was induced by the treatment of cells with the small molecule inhibitor of MDM2, nutlin-3a (Vassilev et al., 2004). Blockade of the E3 ubiquitin ligase function of MDM2 stabilises p53 protein expression and therefore leads to the transactivation of p53 target genes, such as PUMA and NOXA, to induce apoptosis. Thus, successful induction of apoptosis by nutlin-3a treatment is indicative of a functional p53 signalling pathway.

Treatment of the EBV-positive T and NK cells with increasing concentrations of nutlin-3a demonstrated an expected inconsistency across the panel (**figure 4.6A**). Nutlin-3a was used at an upper concentration limit of 20 uM as this was shown to sufficiently induce extensive cell death in lymphoma cell lines with verified functional p53 (Valente et al., 2016). As expected, the MEC04 cells, due to the p53 DNA binding domain mutation, did not respond to nutlin-3a and exhibited total resistance to apoptosis, even at later time points, such as 72 hours (**figure 4.6B**). The NKC1, SNT15 and SNT16 were all susceptible to nutlin-3a treatment albeit to varying degrees, which is consistent with the findings that they express a WT p53 protein. Interestingly though, the SNK1, SNK6, SNT8 and SNT13 cells, which also encode a WT p53 protein, all exhibited resistance to nutlin-3A treatment (**figure 4.6A** and -**B**). In the case of SNK1 and perhaps SNT13, this resistance is perhaps explained by the comparatively high MDM2 protein expression in these cells (**figure 4.4**).

The reason(s) why the SNK6 and SNT8 cells are insensitive to nutlin-3a induced, p53-mediated cell killing is still unclear but could reflect other aberrations within this pathway, such as loss of critical pro-apoptotic BH3-only proteins.

Collectively, these data suggest that deregulation within the p53 pathway plays an important role in maintaining the survival of EBV-positive T and NK cells in response to genotoxic treatment. However, since only 1 of 8 cell lines harboured a p53 mutation, our data suggest that resistance is not primarily mediated through mutations in the DNA binding domain of p53. This is in sharp contrast to the situation in many other human tumours where p53 mutations are common. Given the important implications for the clinical management of ENKTL and CAEBV patients, this requires further investigation to elucidate the underlying cause of the resistance to p53-mediated cell killing.

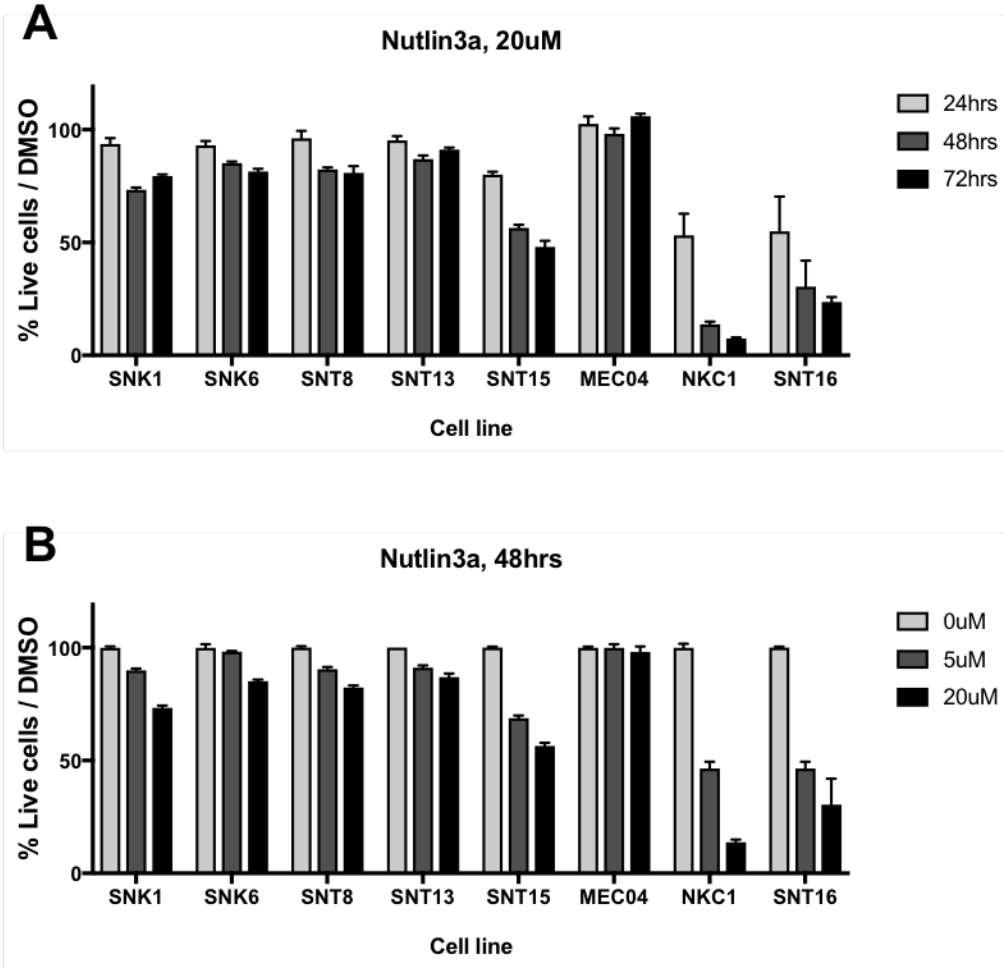


Figure 4.6 Non-genotoxic activation of p53 by nutlin3a. EBV-positive T and NK cells were treated with nutlin3a then stained with Annexin V and PI to determine survival where PI-/Annexin V-double negative populations were normalised to DMSO-only controls and then plotted. Cells were either **A)** treated with 20uM nutlin3a for 24-72 hours or **B)** treated with increasing concentrations of nutlin3a for 48 hours. Data presented are mean ±SE of three independent experiments performed in triplicate.

4.5 Evasion of apoptosis due to deregulated expression of BCL-2 family members

4.5.1 Expression of BCL-2 family members

Subsequent to extensive DNA damage, the activation of p53 leads to the transcriptional upregulation of target genes, such as *Puma* and *Noxa*, which are pro-apoptotic members of the BCL-2 family, which mediate the life/death switch of a cell (Villunger et al., 2003a). Resisting cell death is one of the hallmarks of cancer and mechanisms of evasion from apoptosis in numerous cancer types are detailed in **sections 1.3.2** and **1.3.3**.

In order to determine whether abnormalities within the BCL-2 family of proteins were contributing factors in EBV-positive T and NK cell pathogenesis, our cell line panel was initially subjected to Western blot analysis to assess the basal level of expression of major BCL-2 family proteins (**figure 4.7**). The BL cell lines BL2, BL41, Kem-BL and Sav-BL were selected as positive controls, as together these cell lines express the full set of proteins of interest.

Variable expression of pro-survival and pro-apoptotic (BH3-only proteins and BAX/BAK effector proteins) proteins were observed across the cell line panel. A high level of BCL-2 expression was consistently seen across the entire T and NK cell line panel, similar to the BL cells, BL2 and BL41. BCL-X_L expression was expressed at high levels in SNK1 and SNK6 cells but at only low/intermediate levels in the remaining lines. Weak MCL-1 expression was seen in all cell lines with SNK1 cells producing the strongest signal. The expression of full length BID fell below the level of detection in SNK6, SNT8, SNT13, SNT15 and MEC04

cells but BID was expressed in NKC1, SNT16 cells and most abundantly in SNK1 cells. The major BH3 only protein induced in response to multiple apoptotic stimuli, BIM, was found either at very low levels or was not detected (SNK6, SNT8 and SNT13 cells). Importantly for the ability of these cells to undergo MOMP, all T and NK cell lines contained readily detectable levels of both pro-apoptotic effector proteins BAK and BAX.

Since the protein expression of BIM and BID appeared low or absent in multiple cell lines (**figure 4.7**), we performed a qRT-PCR analysis in order to confirm either the presence or absence of *Bcl2l11* (BIM) and *Bid* gene transcripts (**figure 4.8**). The complete absence of *Bid* was confirmed in SNK6, SNT8 and SNT13 cells by a lack of gene transcript detection (**figure 4.8B**). Only SNT13 cells lacked *Bcl2l11* transcripts whereas SNK6 and SNT8 cells expressed low levels (relative to the control cell line, Jurkat). Since BCL-2 was expressed at the highest levels in the cell lines, we also performed Q-RT-PCR analysis to quantitate BCL-2 expression. Interestingly, although *Bcl-2* transcripts were detected in all cell lines (**figure 4.8A**), SNT15 and MEC04 cells expressed the highest levels of *Bcl2* transcripts, which was not similarly reflected at the protein level in **figure 4.7**.

Tumour cells typically exhibit high levels of pro-apoptotic members of the BCL-2 family and this is thought to be due to high cellular stress. However, this was not universally the case for the pro-apoptotic proteins examined here. The EBV-encoded oncogene LMP1 has a well-established relationship with the anti-apoptotic members of the BCL-2 family where it has been shown to induce expression of BCL-2, MCl-1 and BFL-1 (Henderson et al., 1991, Wang et al., 1997, D'Souza et al., 2000, Rowe et al., 1994). However, the contribution of LMP1 to the biology of T and NK cells is currently less wll understood. LMP1 transcripts

were therefore also measured in the same qRT-PCR experiments described above (**figure 4.8D**). As expected from reports in other cell types, LMP1 levels inversely correlated with the levels of *Bcl2l11* transcripts (**figure 4.8E**). Interestingly, LMP1 also held an inverse correlation with *Bid* levels but no such relationship with pro-survival *Bcl-2* was observed.

The BCL-2 family expression data described above suggest that low levels of pro-apoptotic BH3-only proteins could mediate the survival of these cells in the steady state. Low BIM expression associated with cancer progression was discussed in section 1.3.3 Pro-apoptotic members. However, it is not unexpected that cells express low BIM in the absence of an apoptotic stimuli. Alternatively, cell survival could be mediated by the activity of a pro-survival member of the BCL-2 family. Variable levels of MCL-1 and BCL-X_L were expressed across the cell line panel, however, high BCL-2 expression was consistent. It could therefore be predicted that BCL-2 is the conserved mediator of cell survival in EBV-positive T and NK cells.

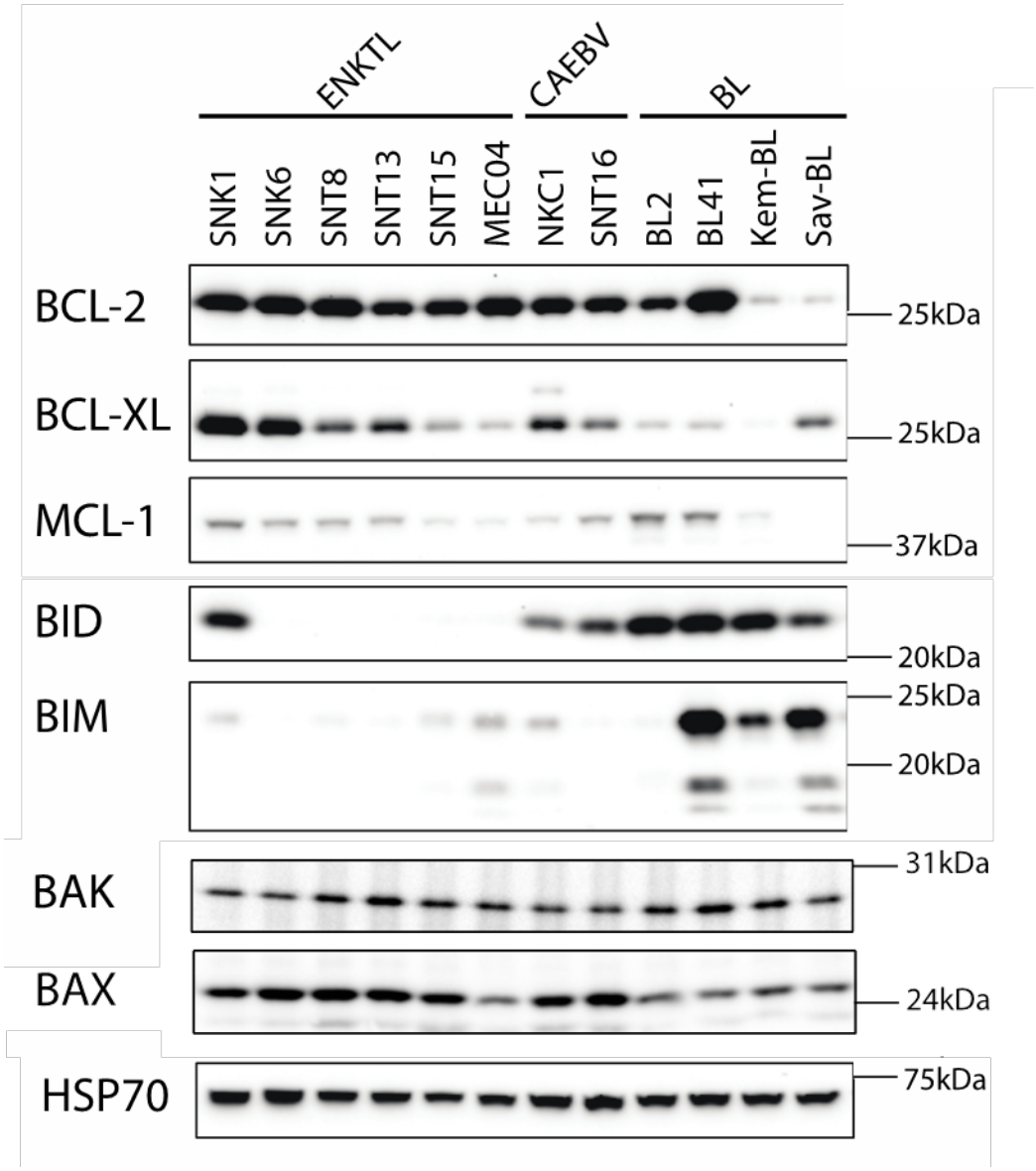
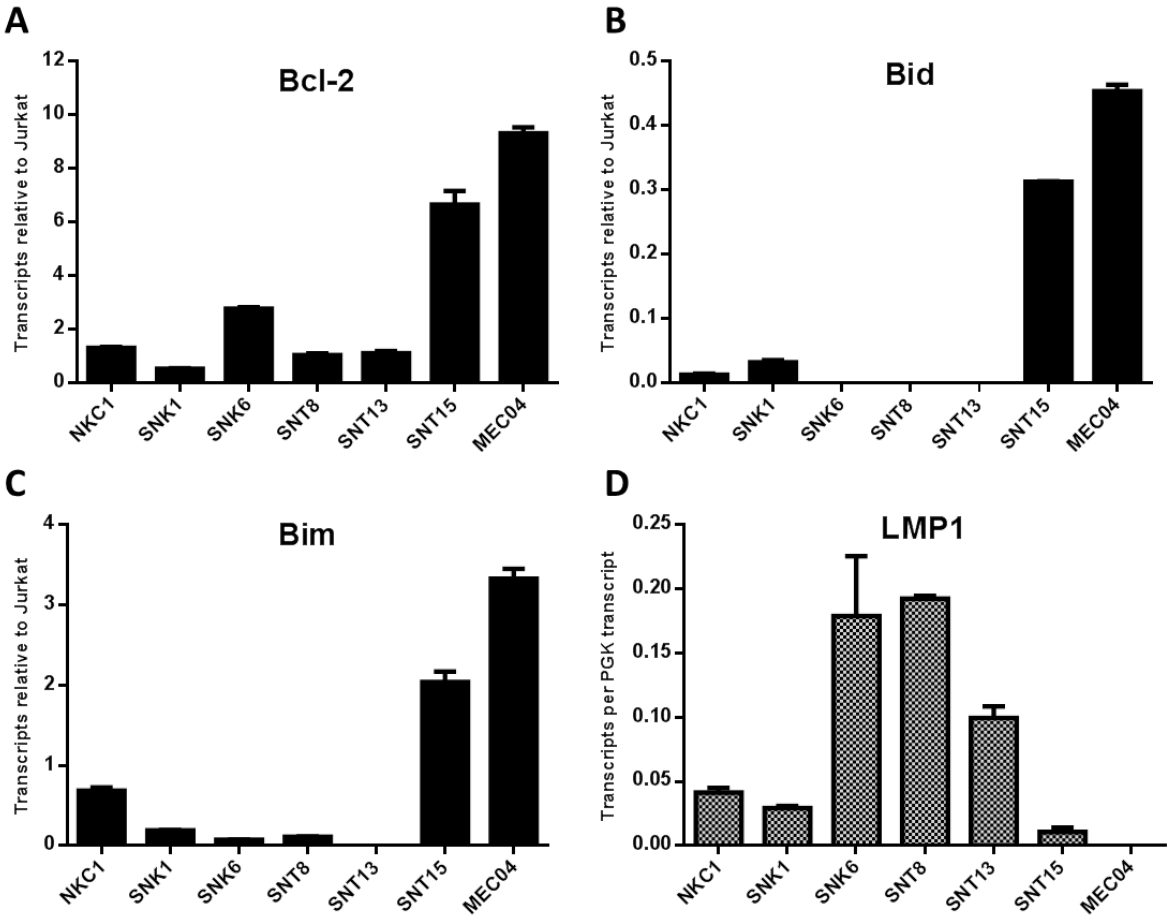


Figure 4.7 Expression of BCL-2 family members in T and NK cell lines in the absence of stress. Western blot analysis was performed in order to detect the presence of members of the BCL-2 family of apoptosis regulators at the protein level in EBV-positive T and NK cell lines. BL cell lines BL2, BL41, Kem-BL and Sav-BL were included as antibody controls. Data presented are representative of three independent experiments.



E

Correlations				
		Bcl-2	Bim	Bid
LMP1	Spearman correlation, r	-0.5357	-0.8214	-0.9636
	Sig. (2-tailed), p	0.2357	0.0341	< 0.0001
	N	7	7	7

Figure 4.8 Comparison of the expression of BCL-2 family members with the expression of LMP1. Expression of **A)** *Bcl-2*, **B)** *Bid*, **C)** *Bim* (*Bcl2l11*) and **D)** *LMP1* transcripts were measured by qRT-PCR during steady state. For cellular genes, raw Ct values were normalised to PGK1 expression and subjected to ΔΔCt calculation and presented as relative to Jurkat cells. *LMP1* transcripts were calculated based upon a standard curve generated from AQ plasmid serial dilutions. **E)** Spearman rank correlation coefficients of LMP1 expression compared against expression of *Bcl-2*, *Bid* and *Bim*. Data presented are representative of three independent experiments performed in duplicate. AQ, absolute quantification.

4.5.2 BH3 mimetic drugs

The survival and sustained growth of cells can be dependent on one pro-survival member of the BCL-2 family or on several. In tumour cells this dependency may reflect the normal dependency of the progenitor cells on a particular BCL-2 family protein or it can be associated with overexpression, post-translational deregulation or aberrant binding of pro-survival BCL-2-like proteins to pro-apoptotic members of this family. To determine functionally if the EBV-positive T and NK cells were reliant upon a particular pro-survival BCL-2 family member for their sustained growth, cells were treated with BH3 mimetic drugs of differing specificities (**figure 4.9A**) (**supplementary table 2**) and their survival determined using a flow cytometric assay (staining with PI plus Annexin V). Generally, across all cell lines, BH3 mimetic drugs targeting BCL-X_L proved most effective.

All 8 T and NK cell lines demonstrated little to no response to BCL-2 inhibition by ABT-199 (**figure 4.9B**), even at high doses of 5 uM. However, the inhibition of BCL-2, BCL-X_L plus BCL-W with ABT-737 led to notable induction of cell death in all cell lines (**figure 4.9C**), especially at the higher dose of 5 uM when cell viability was decreased to <60% in all but one of these cell lines. The greatest percentage of cell death was observed in the CAEBV cell lines NKC1 and SNT16 with the lowest effect observed in SNK6 cells — 90% and 71% viability at 0.5 uM and 5 uM, respectively. Single inhibition of BCL-X_L with A-1331852 (**figure 4.9D**) resulted in a similar rate of killing in the cell lines as treatment with ABT-737. This suggests that these cells are reliant on BCL-X_L rather than BCL-2 or BCL-W. Interestingly the low dose of 0.5 uM A-1331852 induced almost as much cell killing as the higher dose of 5 uM.

Treatment with the MCL-1 specific inhibitor, S63845, only produced measurable cell killing in SNT15 cells (**figure 4.9E**). The high dose of 5 uM S63845 only induced <20% cell death in all other cell lines tested. BH3 mimetics were tested at concentrations up to 5 uM at 24 hours as this was comparable to their previous use in the assessment of human cancer cell lines (Leverson et al., 2015a).

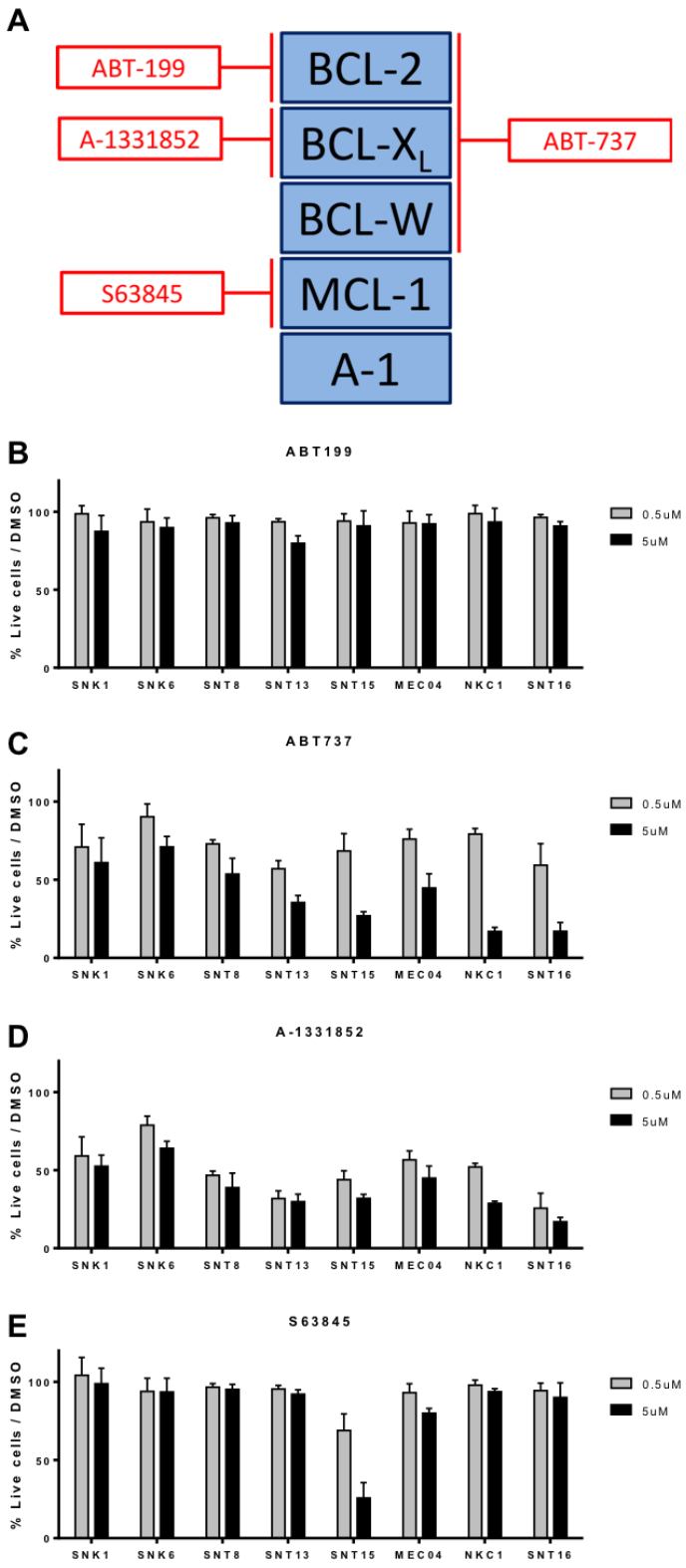


Figure 4.9 Cell survival analysis of EBV-positive T and NK cells following treatment with BH3 mimetic drugs. A) Specificities of the BH3 mimetic drugs used: ABT-199 (inhibitor of BCL-2), ABT-737 (inhibitor of BCL-2, BCL-X_L and BCL-W), A-1331852 (inhibitor of BCL-X_L) and S63845 (inhibitor of MCL-1). EBV-positive T and NK cells were treated as indicated then stained with Annexin V and PI to determine survival where PI-/Annexin V- double negative cells were normalised to DMSO-only controls and then plotted. Cells were treated with either **B)** ABT-199, **C)** ABT-737, **D**) A-1331852 or **E**) S63845 at the indicated concentrations for 24 hours. Data presented are mean ±SE of three independent experiments performed in triplicate.

4.5.3 Treatment with combinations of BH3 mimetic drugs

In order to determine whether inhibition of multiple pro-survival BCL-2 proteins could enhance apoptosis in the cell line panel, cells were treated with combinations of BH3 mimetic drugs (**figure 4.10** and **4.11**). As we had already inferred that BCL-X_L inhibition was an effective strategy, we focused on targeting BCL-X_L in addition to other BCL-2-like pro-survival proteins. We initially did this by comparing the effectiveness of A-1331852 (which targets BCL-X_L alone) against ABT-737 (which targets BCL-X_L in addition to BCL-2 and BCL-W). We predicted that ABT-737 would induce a greater percentage of apoptosis due to its ability to inhibit additional pro-survival proteins beyond BCL-X_L. However, cell killing was not significantly greater when compared to the single inhibition of BCL-X_L by A-1331852. This observation was made in 7 of 8 T/NK cell lines with the exception of NKC1 (**figure 4.11C**) where the apoptosis was slightly increased by additional inhibition of BCL-2 and BCL-W by utilising ABT-737 to treat the cells. The expression of BCL-W has been shown to contribute to survival in models of BL (Adams et al., 2017a) but has not been shown to be a factor of survival or to be expressed in T or NK cells. The absence of BCL-W in our T and NK cell lines of interest was assumed when interpreting the results in this chapter. From these data, we suspected that the additional inhibition of BCL-2 did not enhance the level of apoptosis.

ABT-737 and ABT-199/A-1337852 co-treatment both inhibit BCL-2 and BCL-X_L, therefore it could be predicted that both treatments would elicit similar levels of survival. Although not significantly different with the exception of SNK6 cells, the cell lines tolerated ABT-737 treatment better vs ABT-199/A-1331852 co-treatment. This is perhaps simply due to the

greater total amount of drug (5 uM of a single drug vs. 5 uM for each of two drugs) or it could be due to the greater efficiency of apoptotic induction by ABT-737 in BCL-2-dependent cells compared to BCL-X_L-dependent cells, as previously reported (Rooswinkel et al., 2012). As BCL-X_L appears to be the important pro-survival factor, the preferential binding to BCL-2 by ABT-737 could diminish its killing potency in cells that rely on BCL-X_L for survival.

We next investigated the potential of targeting MCL-1 in addition to BCL-X_L. We did this by treating cells with A-1331852 in combination with the MCL-1 specific BH3 mimetic, S63845. In all cell lines, this combination was the most effective inducer of apoptosis. SNT15 cells demonstrated the greatest susceptibility to this drug combination, with only 6.5% viability, and were also the only cell line susceptible to S63845 as a single agent (**figure 4.11A**).

Despite the lack of observed cell death in single treatments using ABT-199 or S63845, these compounds were used in combination to determine whether the inhibition of both BCL-2 and MCL-1 could induce apoptosis in the cell line panel. With the exception of SNK6 cells, this combination was a more effective inducer of apoptosis than single treatments with either ABT-199 or S63845 alone. However, despite targeting more pro-survival proteins, the combination of ABT-199 plus S63845 was generally not as effective as targeting BCL-X_L alone by A-1331852. These data suggest that EBV-positive T and NK cells demonstrate the highest reliance on BCL-X_L for survival followed by MCL-1.

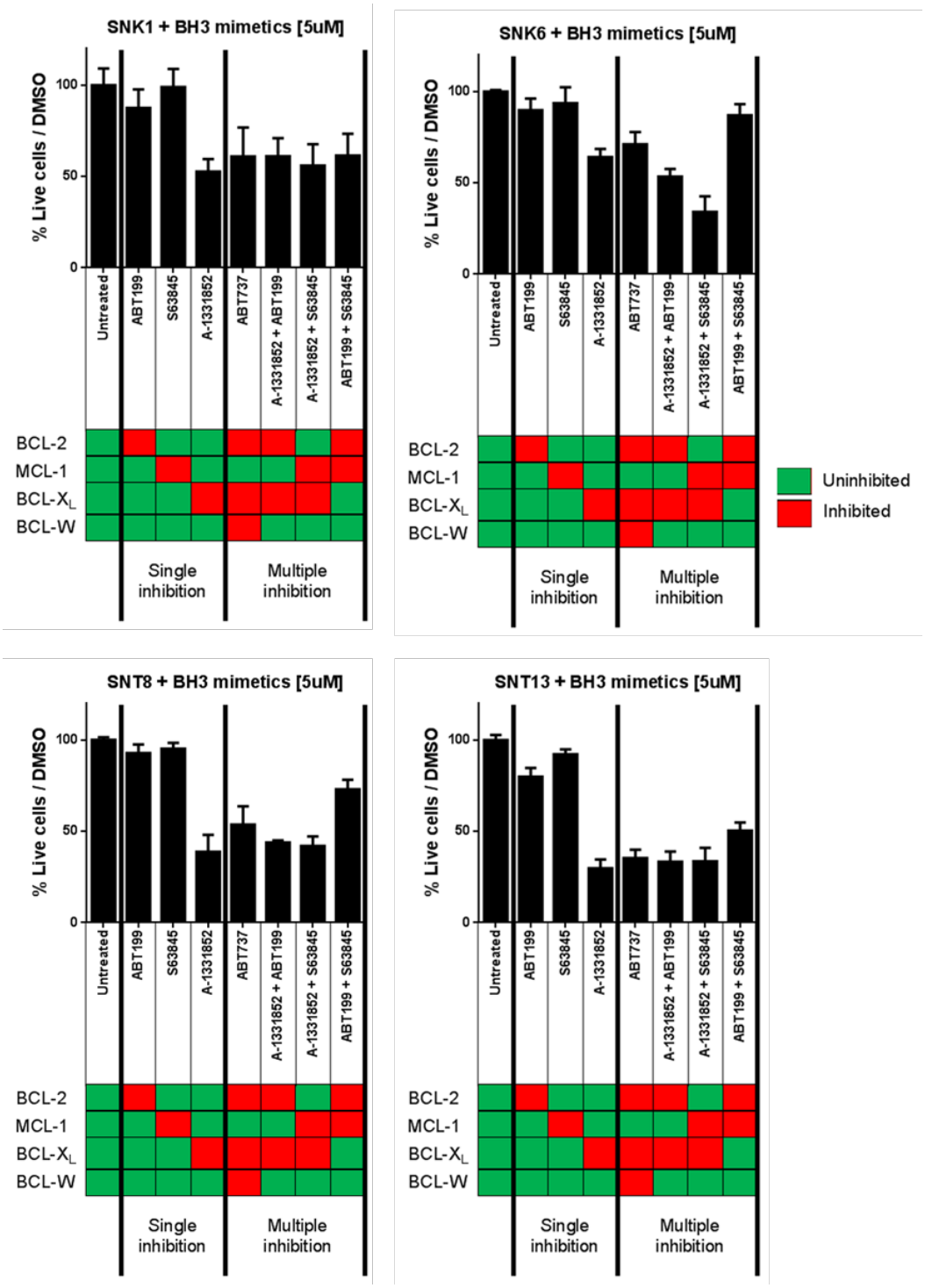


Figure 4.10 Cell survival analysis following combination treatments with BH3 mimetic drugs. A) SNK1, **B)** SNK6, **C)** SNT8 and **D)** SNT13 cells were treated with BH3 mimetic drugs, then stained with Annexin V and PI to determine survival where PI-/Annexin V- double negative cells were normalised to DMSO-only controls and then plotted. Cells were treated with 5 uM of the indicated drug for 24 hours. Data presented are mean ±SE of three independent experiments performed in triplicate.

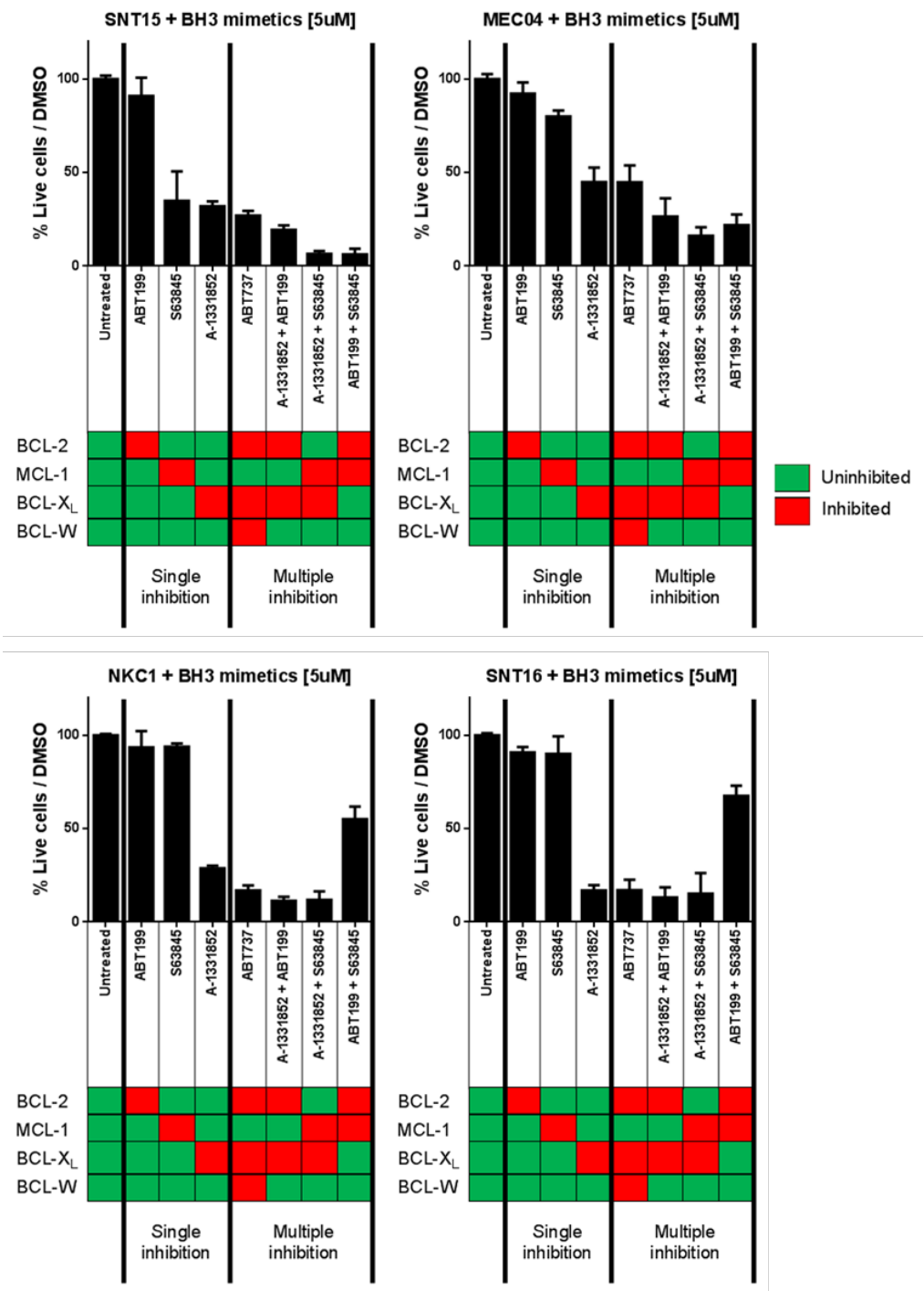


Figure 4.11 Cell survival analysis following combination treatments with BH3 mimetic drugs. A) SNT15, **B)** MEC04, **C)** NKC1 and **D)** SNT16 cells were treated with BH3 mimetic drugs, then stained with Annexin V and PI to determine survival where PI-Annexin V- double negative cells were normalised to DMSO-only controls and then plotted. Cells were treated with 5 uM of the indicated drug for 24 hours. Data presented are mean ±SE of three independent experiments performed in triplicate.

4.6 Establishment of a mouse model of disease

Therapeutic compounds identified by HTS need validation *in vitro* and *in vivo* as part of the pre-clinical examination process. With respect to EBV-positive T and NK cell disease, the *in vitro* efficacy can be determined by the ability of compounds of interest to induce apoptosis in patient derived cell lines. However, options for the examination of the efficacy and potential toxicity of such compounds *in vivo* remain limited. To develop an *in vivo* model of disease, we took the approach of developing a cell line-based xenograft model into immune-compromised mice.

To date, from our panel of T and NK cell lines, only SNK6 cells have been reported to successfully grow as xenotransplants in immune-deficient mice (Siddiquey et al., 2014). However, the ability of the remaining cell lines to be successfully transplanted into immune-deficient mice is currently unknown. To test this, the EBV-positive T and NK cell lines were xenotransplanted into NOD-SCID IL-2rγ$^{-/-}$ (NSG) mice which were then monitored for tumour growth and other illness endpoint criteria that may be indicative of tumour growth/dissemination. The aim of this was to obtain a consistent method of tumour cell transplantation that would most efficiently and reproducibly lead to tumours in mice using a variety of T/NK cell lines.

The route of injection of human cell lines into mice can influence how readily the cells grow as transplants. Generally speaking, injection of human cells into the tail vein, as is done for mouse lymphoma cells, does not work well and often leads to the tumour cells lodging in the lungs or being cleared before they can grow (G.L. Kelly, personal communication).

Instead, xenotransplants are often established through transplantation of cells by subcutaneous or intraperitoneal injection.

Initially we decided to transplant the cells into the NSG mice by subcutaneous injection as these tumours are more readily palpable versus intraperitoneal tumours — therefore leading to less subjectivity in determining the experimental endpoint. Due to the irregular kinetics of tumour growth in early studies, tumour size over time was not recorded but only the number of days required to reach maximal tumour size (tumour latency).

SNK6 and SNT15 cells (**figure 4.12B** and **E**) successfully formed subcutaneous tumours, following injection of $2x10^6$ cells, in all 3 mice at 47 days and 33 days, respectively. This establishes their suitability for *in vivo* experimentation. In three other cell lines — SNT8, SNT13 and MEC04 (**figure 4.12C, D** and **F**) — subcutaneous tumours were formed in 1 of 3 recipient mice. Unfortunately, SNK1, NKC1 and SNT16 cells (**figure 4.12A, G** and **H**) did not form tumours in any of the subcutaneously injected mice and did not cause any visual signs of tumour growth or significant weight loss. These three cell lines were therefore not taken forward into any further experiments due to a lack of any indication that they could be grown in NSG mice.

In an effort to increase the efficiency of transplantation with the SNT8, SNT13 and MEC04 cell lines, the number of cells injected was increased to $5x10^6$ cells (from $2x10^6$ cells) per subcutaneous injection. With SNT8 cells (**figure 4.12C**), the success of tumour formation remained at 1/3 mice, whereas the success rate increased to 3/3 mice for the SNT13 and MEC04 cell lines (**figure 4.12D** and **E**).

An alternative approach to the above experiments is to deliver the cells via intraperitoneal administration. This increases the potential number of sites for the injected malignant cells to establish growth and often produces more representative tumour models, since cells can track to microenvironments that are more conducive for growth. For this reason, intraperitoneal injections of human cells into NSG mice were attempted with selected cell lines. Tumour cells could be expected to spread throughout the animal body, into primary and secondary lymphoid organs in particular. Intraperitoneally injected mice that received $5x10^6$ SNK6 or MEC04 cells developed tumours with a success rate of 3 from 3 mice per cell line (**figure 4.12B** and **F**). However, SNT15 cells when transplanted by intraperitoneal injection did not produce tumours in any of the recipients, despite successful transplantation via subcutaneous injections (**figure 4.12E**).

Collectively, the findings from these experiments show that under appropriate conditions (injection route and cell number) SNK6, SNT13, SNT15 and MEC04 cells can consistently form tumours in NSG mice. Within an experimental timeframe of 50 days, tumours can be formed using SNK6 cells (subcutaneous or intraperitoneal administration), SNT15 cells (subcutaneous) and MEC04 cells (intraperitoneal). Although it would have been preferable to repeat these experiments to increase the number of mice and give greater confidence in the latency times, this could not be done due to time restraints. Therefore, these models were taken forward for the *in vivo* assessment of the BH3 mimetic drug, A-1331852, that had previously demonstrated *in vitro* activity.

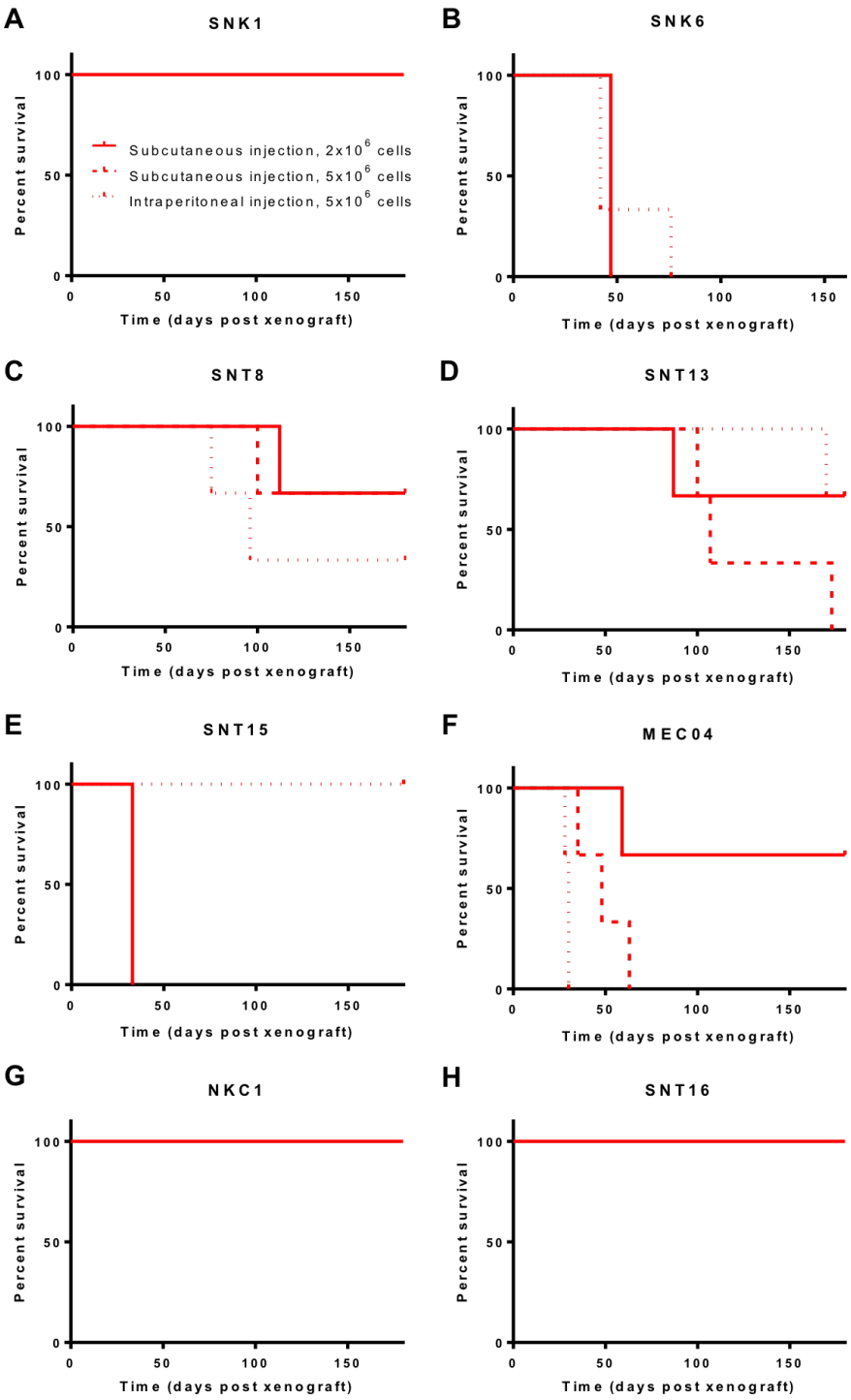


Figure 4.12 NSG xenograft protocol optimisation using EBV-positive T and NK cell lines. Cells were injected either subcutaneously or intraperitoneally at doses of either $2x10^6$ or $5x10^6$ cells, as indicated. Recipient mice were monitored for tumour burden and other illness endpoint criteria for 180 days. Indicated survival represents tumour-free survival. Each experimental arm included 3 recipient mice.

4.7 BH3 mimetic drug mediated inhibition of BCL-X_L *in vivo*

4.7.1 Subcutaneous models

The development of a mouse model of EBV-positive T and NK cell disease above was a significant progression and enabled *in vivo* testing of BH3 mimetic drugs of interest that had shown *in vitro* efficacy. As outlined in **figure 4.9**, BCL-X_L inhibition was most effective at killing T and NK cell lines *in vitro*. This BCL-X_L inhibition could be mediated by the BH3 mimetics A-1331852 and ABT-737 but only A-1331852 was investigated further due to its exclusive specificity for BCL-X_L. Thus far, we have only demonstrated A-1331852 to act as a research tool in identifying BCL-X_L dependency, whereas in the experiments described below focus on the therapeutic potential of this compound in an animal model of disease.

In order to examine the possibility that BCL-X_L inhibition by A-1331852 may be of therapeutic value for EBV-associated T and NK cell disease, xenotransplanted NSG mice were treated with this drug and monitored for disease burden. The experiment was performed as presented in **figure 4.13A**. Here, SNK6 or SNT15 cells were subcutaneously injected before daily delivery of A-1331852 or vehicle between 7 and 13 days post-xenografting.

A delay in tumour latency was observed in the drug-treated group compared to the vehicle-treated group in SNK6 cell-transplanted mice with median tumour latencies of 56 and 37 days, respectively (**figure 4.13B**). However, no significant difference between the two treatment groups was observed for SNT15 cell-transplanted mice (**figure 4.13E**). Comparable tumour burden, as determined by tumour weight, at time of sacrifice was

confirmed in the drug vs vehicle treated mice (**figure 4.13C** and **F**). For both vehicle and drug treated mice, transplanted with either cell line, no observable difference between spleen weight was detected in the sick mice (**figure 4.13D** and **G**). However, SNT15 cells appeared to more efficiently disseminate into lymphoid organs compared to SNK6 cells, as indicated by the approximate 4-fold difference in spleen weights between the two cell lines — mean weights 0.045 g (SNK6) vs 0.125 g (SNT15) — although the increased weight was not confirmed to be tumour infiltrate. The tumour latency for the SNT15 cell transplanted mice was more variable in this experiment (range 39-81 days, for both groups) than in the previous experiment shown in **figure 4.12** (33 days, all mice). The SNT15 cell xenotransplant model is very sensitive to differences in cell number, as shown in **figure 4.12C** where transplantation of $2x10^6$ cells did not give rise to tumours whereas transplantation of $5x10^6$ cells gave tumours in all injected mice at 33 days. Therefore, any slight discrepancy in cell number or fitness of the cells at the time of injection may account for the difference in tumour latency observed.

Immediately before sacrifice of tumour burdened mice, bleeds were taken for haematological analysis. Total white blood cell (WBC) counts were recorded — including lymphocyte, monocyte and neutrophil counts — as well as red blood cell (RBC) and platelet counts. This analysis was performed to monitor the tumour burden in the peripheral blood of mice and could also be used to determine whether the drug treatment had exerted a long-term impact on specific blood cell types. For both SNK6-transplanted mice (**figure 4.14**) and SNT15-transplanted mice (**figure 4.15**), no significant differences were found in any of the analysed cell types. Due to the association of BCL-X_L inhibition with

thrombocytopenia (Roberts et al., 2012, Wilson et al., 2010), platelet counts were of keen interest. Interestingly, no significant difference was observed in platelet counts between vehicle-treated vs drug-treated mice in SNK6 or SNT15 cell transplanted mice (**figure 4.14B** and **4.15B**). However, there was a trend towards higher platelet counts in the drug treated mice, perhaps suggesting that there was a compensatory effect at these later time points due to loss of platelets at earlier time points after A1331852 treatment. This indicated that, whilst not lethal to the mice, future experiments should monitor the platelet counts at earlier time points following A1331852 treatment. Overall, these experiments show that mice could tolerate A-1331852 treatment and that BCL-X_L inhibition could significantly delay tumour growth, resulting in a longer tumour latency in mice transplanted with SNK6 cells, but not in mice transplanted with SNT15 cells.

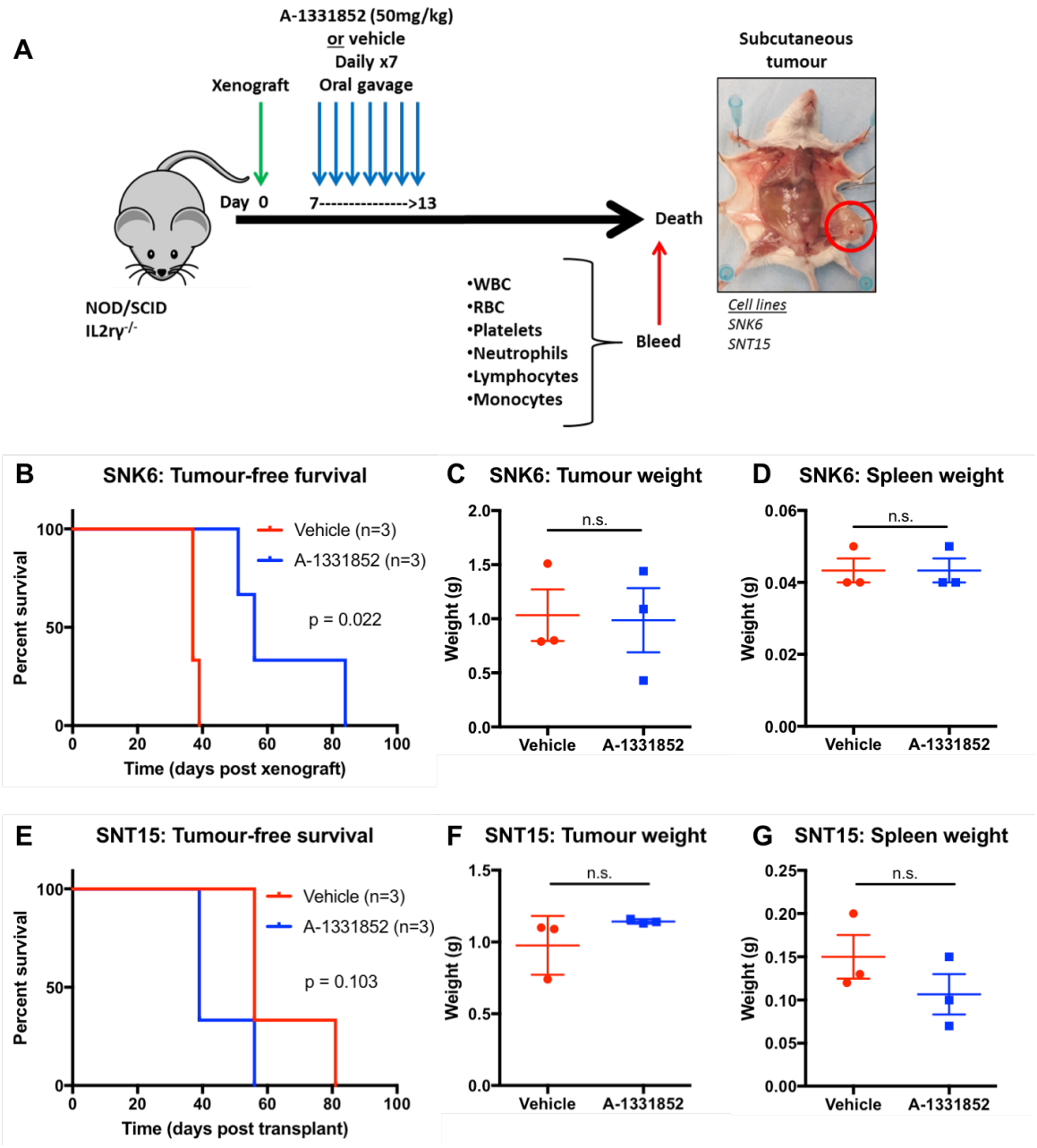


Figure 4.13 Tumour latency of A-1331852-treated NSG mice in subcutaneous transplant models.

NSG mice were injected with $2x10^6$ SNK6 or SNT15 cells in 200 uL PBS at day 0. Oral gavage delivery of either A-1331852 (50 mg/kg body weight) or DMSO occurred daily between day 7 and 13 inclusive. Mice were monitored for endpoint illness criteria for up to 180 days. Mice were bled immediately before sacrifice for haematological analysis. Tumour and spleen were surgically harvested and weighed post-mortem. N = 3.

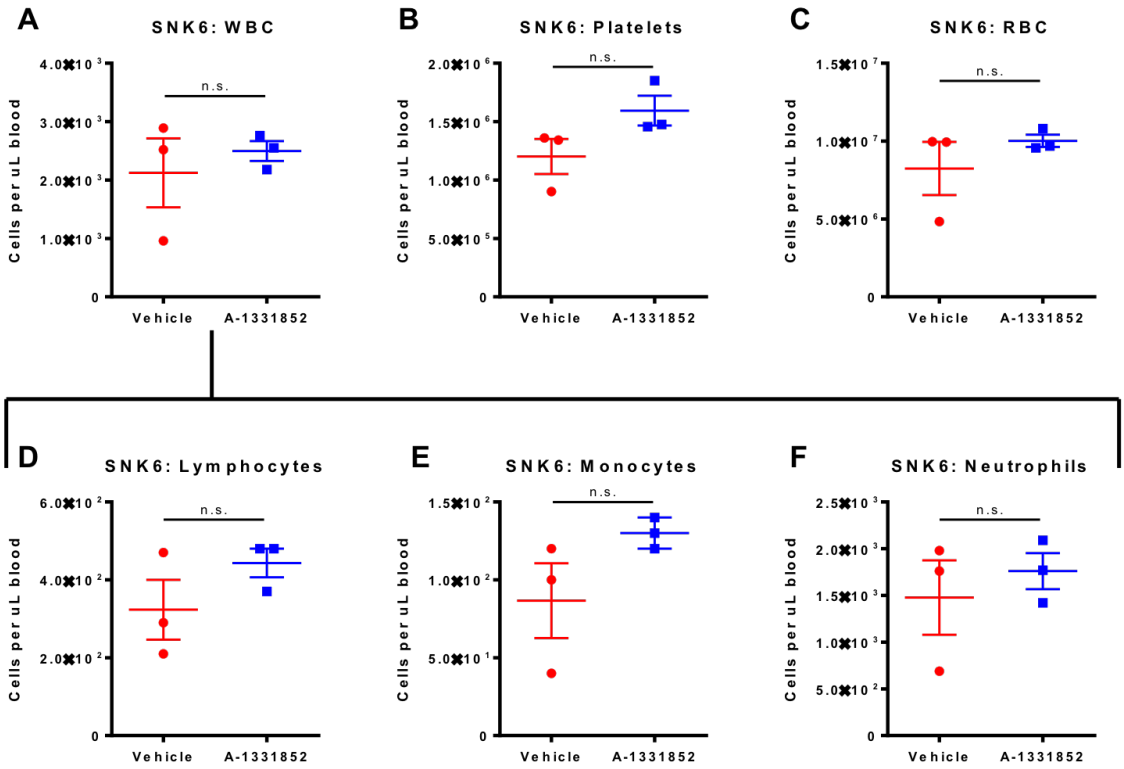


Figure 4.14 Haematological analysis of A-1331852-treated NSG mice with subcutaneous SNK6 tumours. The experiment was performed as outlined in **figure 4.13A.** Blood samples were taken immediately prior to sacrifice of tumour-burdened NSG mice xenotransplanted with SNK6 cells. Peripheral blood cell populations were determined by the ADVIA blood analyser system. Each experimental arm included 3 mice.

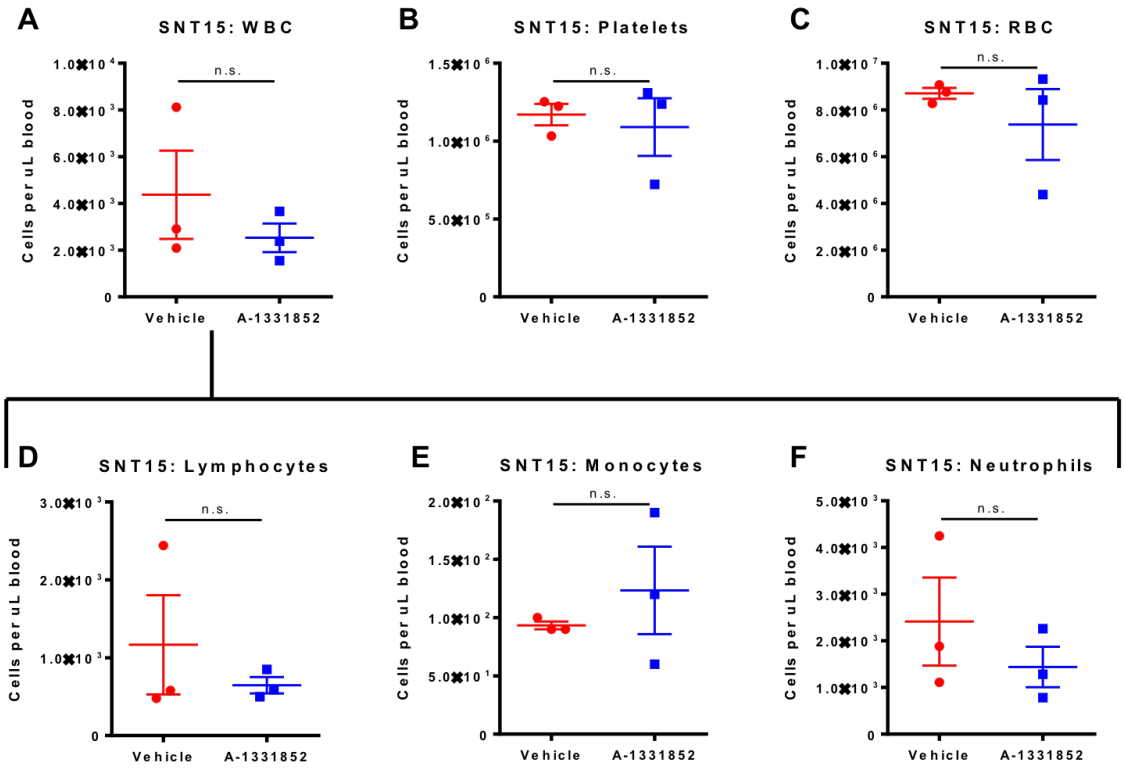


Figure 4.15 Haematological analysis of A-1331852-treated NSG mice with subcutaneous SNT15 tumours. The experiment was performed as outlined in **figure 4.13A.** Blood samples were taken immediately prior to sacrifice of tumour-burdened NSG mice xenotransplanted with SNT15 cells. Peripheral blood cell populations were determined by the ADVIA blood analyser system. Each experimental arm included 3 mice.

4.7.2 Intraperitoneal models

The experiments described above demonstrated successful application of subcutaneous engraftment models of EBV-positive T and NK cell disease. We were able to assess the effectiveness of the BCL-X_L inhibitor A-1331852 as a clinical compound to treat such diseases where we saw a delay in tumour latency with SNK6 cell engrafted mice, whereas no significant difference was observed with SNT15 cell engrafted recipients. However, we were interested to examine whether intra-peritoneal tumours were more accessible, and therefore more susceptible, to treatment with the BCL-X_L inhibitor A1331852 than sub-cutaneous tumours.

A xenograft drug treatment experiment was performed with intraperitoneal tumour transplanted mice as described in **figure 4.16A**. Cohorts of NSG mice were transplanted with either $5x10^6$ SNK6 cells or $5x10^6$ MEC04 cells. Both cell lines had previously been shown to readily form tumours under these conditions (**figure 4.12B** and **-F**). Tumour latency, endpoint illness criteria and changes in blood cell compartments were monitored. The experiment was modified to obtain peripheral blood from mice for haematological analysis throughout the transplant and drug treatment protocol to monitor the impact of BCL-X_L inhibition on the normal blood cells, in particular the platelet counts.

A delay in tumour latency in A-1331852-treated mice was statistically significant vs control mice (median latency of 60 days vs 40 days) upon transplantation with SNK6 cells (**figure 4.16B**) but not in mice transplanted with MEC04 cells (**figure 4.16E**). Spleen and tumour weights were recorded post-mortem with no difference between the two treatment

groups at endpoint in mice engrafted with either cell line suggesting mice were sacrificed with comparable disease burden. A delay in tumour latency in SNK6 mice treated with A-1331852 has now been observed in both subcutaneous and intraperitoneal models (**figure 4.13A** and **4.16A**).

Analysis of survival, tumour weight, spleen weight or haematology had required the exclusion of mice in certain incidences (summarised **table 4.3** below). The survival curve depicted in **figure 4.16E,** representing A-1331852-treated vs vehicle control treated mice transplanted with MEC04 cells, excludes two mice that died without tumour formation. Mouse #1162, treated with vehicle, died of unknown causes after 13 days post xenotransplant. Post-mortem analysis was not possible due to the late discovery of the animal. Mouse #1163, treated with A-1331852, was sacrificed 14 days after xenotransplant due to rapid weight loss and breathing difficulty. Post-mortem analysis of mouse #1153 revealed that the cause of this suffering was due to an overdistended large intestine that was filled with air, although no blockage could be found. The inclusion of mice #1162 and #1163 into survival analysis did not affect the previous outcome of no statistical difference between the two treatment groups (**figure 4.16H**). Additionally, the spleen weights for mice #1145 (SNK6, control group) and #1161 (MEC04, control group) were not recorded due to a researcher not being available at the time of sacrifice (**figure 4.16D** and **G**).

Table 4.3 Summary of mice excluded from analysis.

Mouse number	Cell line	Treatment group	Excluded analysis	Reason
1145	SNK6	Vehicle	Spleen weight	Researcher not available
1161	MEC04	Vehicle	Spleen weight	Researcher not available
1162	MEC04	Vehicle	Tumour-free survival Tumour weight Spleen weight Haematology (death)	Died without lymphoma development. Post-mortem not possible. Cause of death unknown.
1163	MEC04	A-1331852	Tumour-free survival Tumour weight Spleen weight Haematology (death)	Died without lymphoma development. Other illness endpoint criteria reached.

Throughout the course of the experiment, blood was analysed using the ADVIA automated haematology system. Bleeds were taken pre-xenograft, pre- and post-treatment and immediately before death. The tumour burdened mice showed no difference in platelet counts between the control and drug treatment groups at the time of death (**figure 4.17B**). However, SNK6 cell transplanted mice receiving A-1331852 did present with a clear decrease in platelet counts (mean 2.48 x 10^5 cells per uL) compared to control mice (mean 1.76 x 10^6 cells per uL) immediately post drug treatment (**figure 4.17B**). A similar decrease in platelets was observed for MEC04 cell transplanted mice immediately following completion of the treatment course — 1.86 x 10^6 and 4.48x10^5 cells per uL in A-1331852-treated and vehicle-treated mice, respectively (**Figure 4.18B**). Notably, at the point of death, there was an increase in monocyte numbers in A-1331852 treated SNK6-mice

compared to vehicle (**figure 4.17E**). This difference was not present in MEC04-mice (**figure 4.18E**). This suggests a possible difference in the immune response to the two cell lines. It can therefore be concluded that A-1331852 induced platelet death in mice, however, this depletion was temporary as platelet counts had later recovered and the transient depletion in platelets was not the cause of death in these mice.

Overall, the xenograft models show that the BCL-X_L inhibitor A-1331852 was capable of inducing a delay in tumour latency in SNK6 cell but not in SNT15 cell or MEC04 cell xenotransplanted mice. A-1331852 induced transient thrombocytopenia, but platelet numbers recovered and were not significantly different to vehicle-treated mice at the point of death. Therefore, BCL-X_L inhibition in a xenotransplant model of EBV-associated NK and T cell lymphoma was tolerable and, in certain circumstances, efficacious.

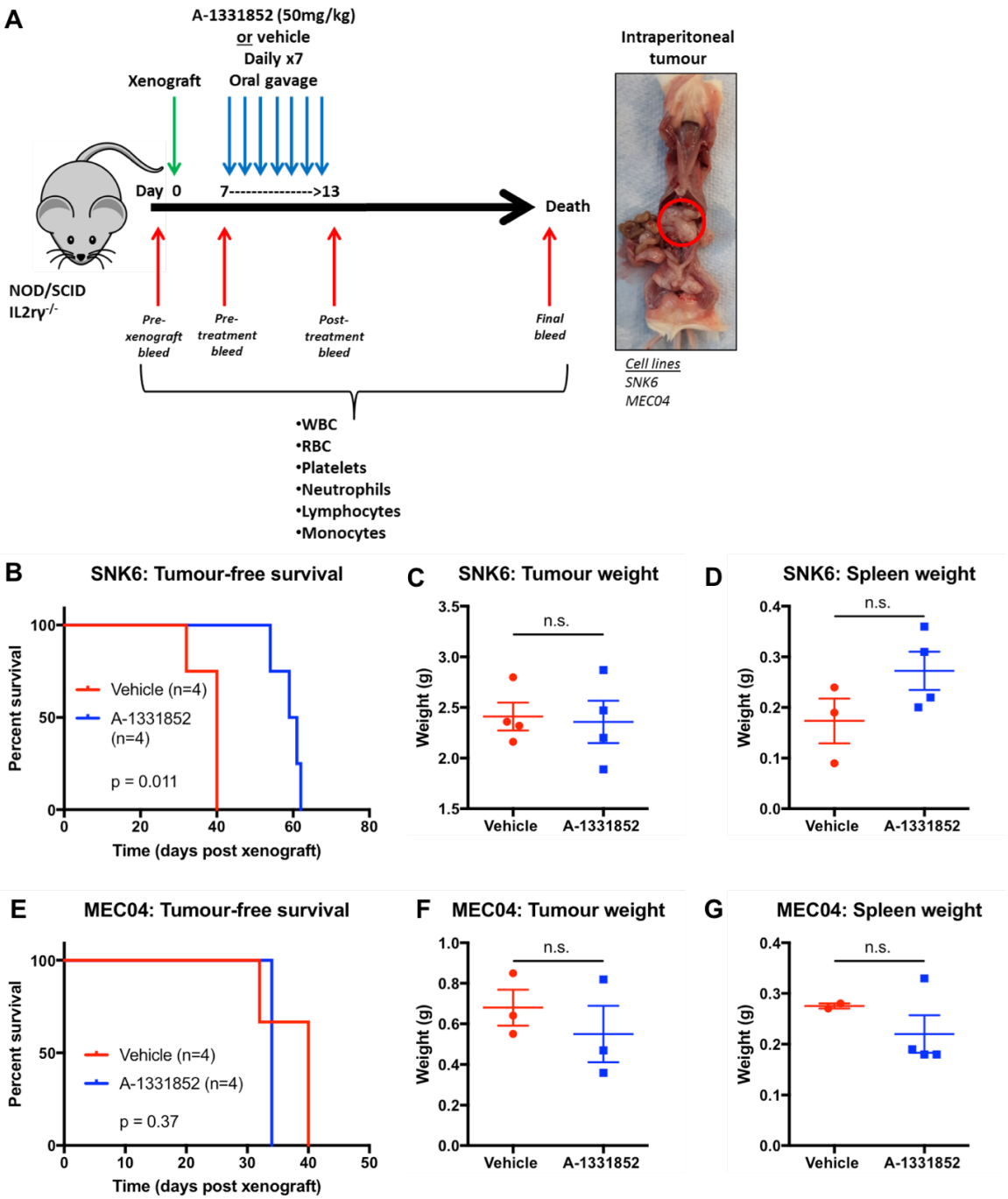


Figure 4.16 Tumour latency of A-1331852-treated NSG mice in intraperitoneal models. NSG mice were injected with $5x10^6$ SNK6 cells or MEC04 cells in 200 uL PBS at day 0. Oral gavage delivery of either A-1331852 (50 mg/kg body weight) or DMSO occurred daily between day 7 and 13 inclusive. Mice were monitored for endpoint illness criteria for up to 180 days. Mice were bled immediately before sacrifice for haematological analysis. Tumour and spleen were surgically harvested and weighed post-mortem. (n) Number of mice per treatment group.

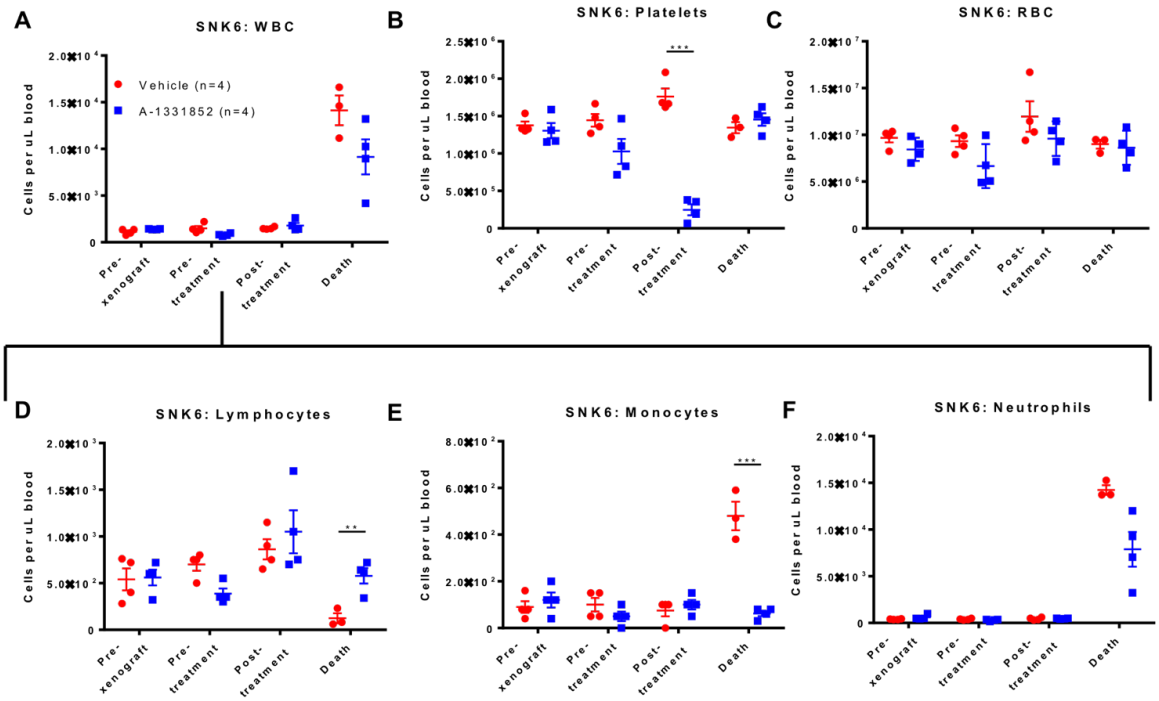


Figure 4.17 Haematological analysis of A-1331852-treated NSG mice with subcutaneous SNK6 tumours. The experiment was performed as outlined in **figure 4.16A.** Blood samples were taken at time points indicated from tumour-burdened NSG mice xenotransplanted with SNK6 cells. Peripheral blood cell populations were determined by the ADVIA blood analyser system. Each experimental arm included 3 mice.

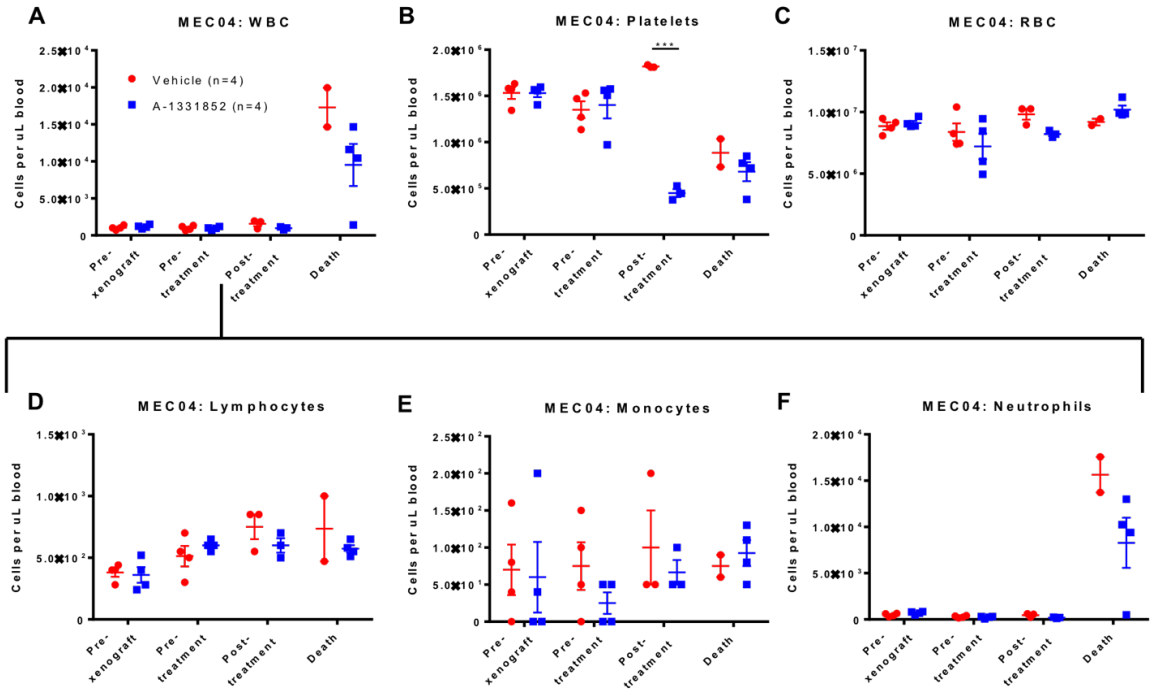


Figure 4.18 Haematological analysis of A-1331852-treated NSG mice with subcutaneous SNT15 tumours. The experiment was performed as outlined in **figure 5.9 (top).** Blood samples were taken at time points indicated from tumour-burdened NSG mice xenotransplanted with SNK6 cells. Peripheral blood cell populations were determined by the ADVIA blood analyser system. Each experimental arm included 3 mice.

4.7.3 Tumour cell dissemination in intraperitoneal models

In human lymphomas, malignant cells can infiltrate local tissues and spread to multiple organs, although typically to the spleen and bone marrow. The novel engraftment protocols for EBV-positive T and NK cell lines into NSG mice described above have proved that such cells can form tumours at the sites of injection. However, no data exist with respect to dissemination of these malignant cells to other tissues within the recipient animal. To address this unknown element of our model, immunohistochemistry (IHC) was performed on multiple organs harvested post-mortem from tumour transplanted mice. This allows the identification of infiltration sites. The organs assessed included spleen, kidney, lung, heart and sternum (for bone marrow infiltrate), and they were chosen based on common sites of infiltration. The preliminary histological examinations using H&E stains alone were inconclusive for tumour cell infiltrate, into the spleen in particular, due to the irregular structure of lymphoid tissue in immune-deficient NSG mice — as judged by clinical haematologist Dr Brandon Aubrey, WEHI. Therefore, we incorporated an antibody against human CD45, a general lymphocyte marker, into the IHC protocol to specifically identify the human lymphoma cells in the mouse organs. Using this method, we also aimed to determine if treatment of the lymphoma xenotransplanted mice with A-1331852 could kill or prevent cells from establishing growth in other organs. To investigate this, we applied the IHC staining for human CD45 to organs collected from recipient NSG mice intraperitoneally injected with SNK6 cells or MEC04 cells and treated with either A-1331852 or vehicle (control). Representative tissue sections from selected mice are presented in **figure 4.19**.

Positive staining for human CD45 presented as dark brown staining at the cellular membrane of tissue sections. As shown in **figure 4.19**, substantial tumour infiltrates were observed in the spleen, sternum and kidney of mice injected with SNK6 cells or MEC04 cells. MEC04 cells also migrated into the liver and lung but this was not observed in mice that had been injected with SNK6 cells, although some non-specific staining was evident within the liver. However, no tumour cells had disseminated to the heart in either SNK6 cell or MECO4 cell transplanted mice. The presence of tumour cells in the spleen, sternum, kidney, liver and lungs did not differ between mice treated with the BCL-X_L inhibitor or with vehicle. This suggests that A-1331852 treatment could not prevent tumour cell metastasis in any of the analysed organs.

The data presented here suggest that MEC04 cells have a greater ability to spread to a wider range of organs compared to SNK6 cells. MEC04 cells migrated to 5 of 6 organs analysed, whereas SNK6 cells only migrated to 3 of 6. No difference in the number of organs infiltrated by tumour cells was found between A-1331852-treated vs vehicle-treated mice although the extensiveness of infiltrate was not quantitated.

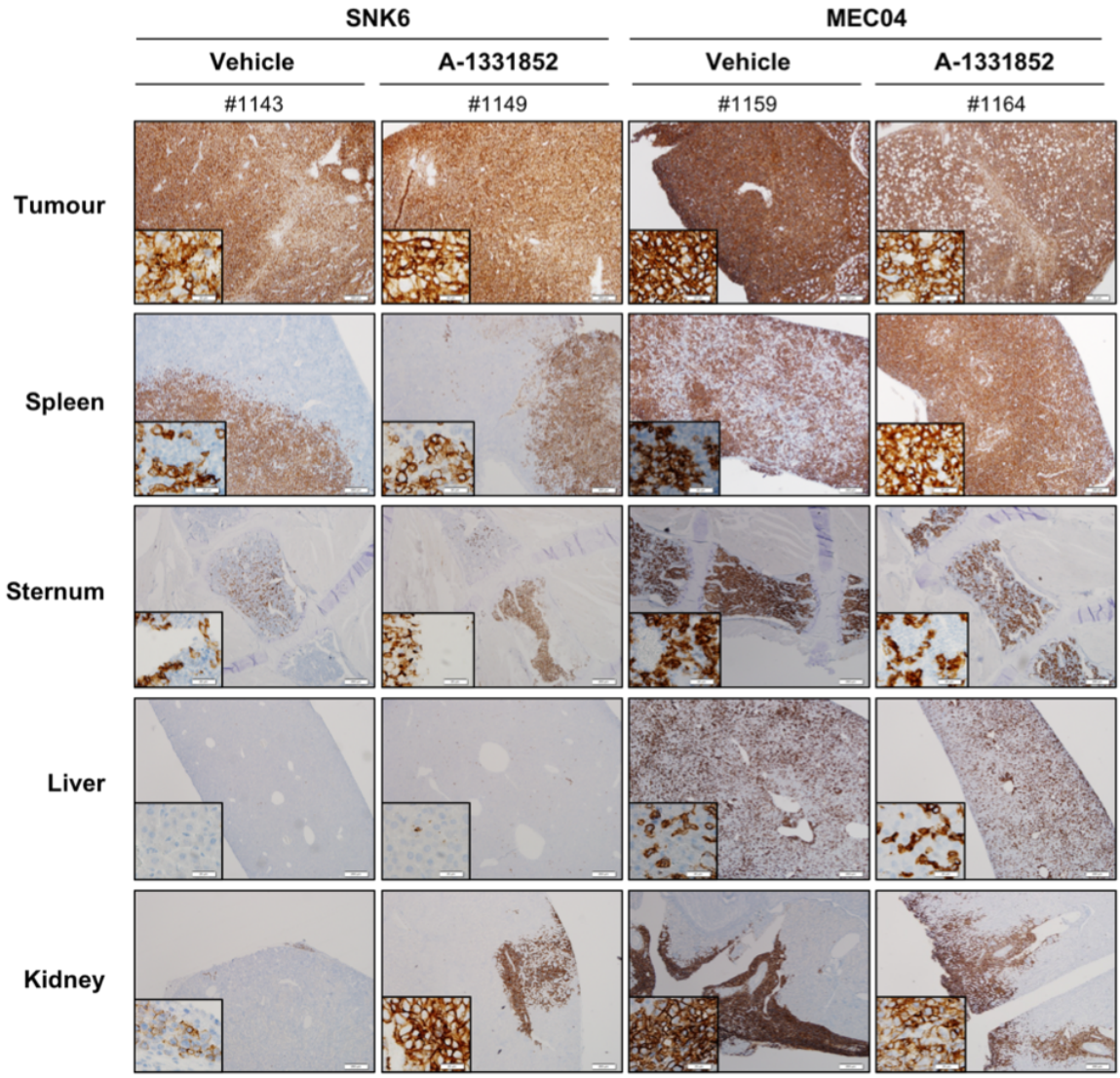


Figure 4.19 Histological analysis of A-1331852-treated NSG mice with intraperitoneal injection of SNK6 or MEC04 tumours. The experiment was performed as outlined in **figure 4.16A**. Organs were harvested from sick mice post-mortem, fixed and stained with human CD45 specific antibody. Data shown are stained sections representative of entire organs and of representative mice for each treatment arm. Positive control demonstrated by brown staining of tumour sections (top row).

4.8 The effect of IL-2 depletion on the sensitivity to BH3 mimetic drugs

4.8.1 Expression of BCL-2 family members and LMP1

Various members of the BCL-2 family can be regulated by signalling pathways activated by cytokine-cytokine receptor interactions — a consideration we next investigated in order to understand the different sensitivities to the BCL-X_L inhibitor A-1331852 observed *in vitro* and *in vivo*. More specifically, the IL-2-rich environment in which the EBV-positive T and NK cells are cultured *in vitro* is not representative of their *in vivo* growth conditions in NSG mice. NSG mice lack mature mouse lymphocytes capable of producing IL-2 (Shultz et al., 2005). Therefore, lymphoma cells injected into NSG mice are growing in an IL-2-depleted environment and we hypothesised that this may affect the expression of the pro-survival BCL-2 family members and consequently the response of these lymphoma cells to BCL-X_L inhibition. After 48 hours of IL-2 depletion, cell viability remains at approximately 50-80% (depending on the cell line) relative to control cells grown in media containing IL-2 (L. George, unpublished).

In order to mimic the loss of IL-2 that occurs *in vivo*, EBV-positive T and NK cells were grown *in vitro* in the absence of IL-2, then assessed for BCL-2 family member expression by Western blotting at 24, 48 and 72 hours (**figure 4.20** and **supplementary figure 2**). At 72 hours, all 8 cell lines displayed a decrease in BCL-X_L and BCL-2 expression. At varying time points, MCL-1 protein expression increased in 6 of 8 cell lines: SNK1, SNT8, SNT13, NKC1 cells and most notably in SNT15 and MEC04 cells.

The expression of viral LMP1 has been reported to be regulated by IL-2 in EBV-positive T and NK cell line panel (Takahara et al., 2006). The level of LMP1 protein was therefore also monitored by Western blotting over the time course of the experiment (**figure 4.20**). In all cell lines in which LMP1 could be detected (with the exception of $LMP1^{low/-}$ MEC04 cells), its expression decreased by 24 hours post-IL-2 removal and continued to do so until 72 hours.

Collectively, these data suggest that IL-2, a cytokine previously demonstrated to be required for *in vitro* survival and proliferation of EBV-positive T and NK cell lines, influences the BCL-2 family member expression profile and viral LMP1 expression in a potentially interlinked signalling axis. The change in expression levels of the BCL-2 pro-survival proteins following IL-2 depletion may be anticipated to affect sensitivity to BH3 mimetic drugs.

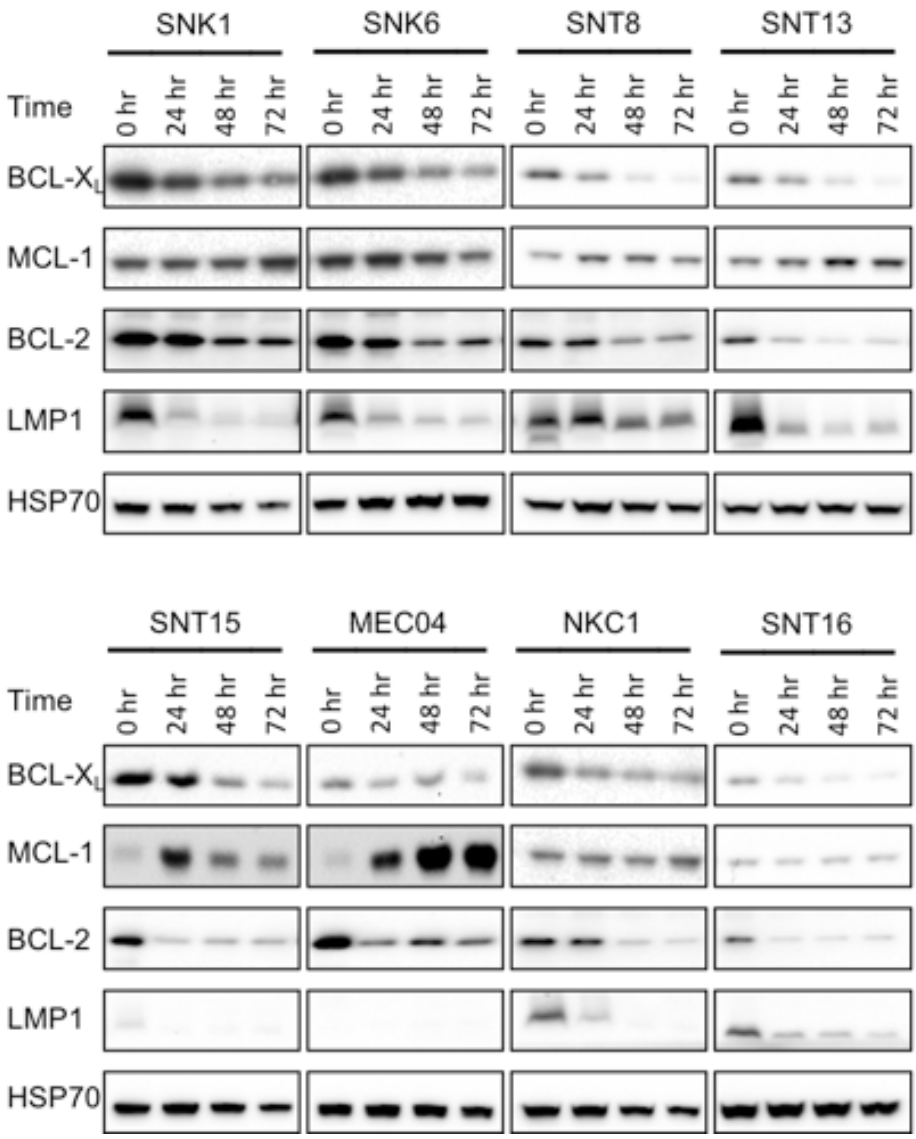


Figure 4.20 Expression of pro-survival BCL-2 family members and viral LMP1 after IL-2 withdrawal. A time course experiment was performed on EBV-positive T and NK cell lines at 24, 48 and 72 hours post IL-2 withdrawal. Pro-survival BCL-2 family members BCL-X_L, MCL-1 and BCL-2 and the viral oncoprotein LMP1 were detected by Western blotting. Probing for HSP70 was used as a loading control. IL-2-deprived lymphoma cells were treated with 25 uM QVD-OPH (broad spectrum caspase inhibitor) at 0 h to prevent degradation of proteins due to apoptosis. Data are representative of two independent experiments.

4.8.2 Response to BH3 mimetic drugs

As described above, the reduction of IL-2 leads to alterations in the expression of BCL-2 family members. It could thus be predicted that such changes in expression alter responses to treatment with BH3 mimetic drugs. To test this hypothesis, EBV-positive T and NK cells were cultured *in vitro* in the absence of IL-2 for 48 hours, treated with selected BH3 mimetic drugs for 24 hours and the survival of the cells analysed (**figure 4.21**). The BH3 mimetic drugs A-1331852, ABT-199 and S63845 were selected for treatment of the cell lines due to their individual specificities for BCL-X_L, BCL-2 and MCL-1, respectively. The cell lines SNK6, SNT15 and MEC04 were selected for examination due to their use in the NSG xenograft models and *in vivo* A-1331852 treatment experiments. Under IL-2-deprived conditions, the absolute viability of untreated MEC04 cells was less than approximately 30%, and therefore too low to interpret the additional effect of treatment with the BH3 mimetic drugs. Therefore, only data from the experiments with SNK6 and SNT15 cells are shown.

In the absence of IL-2, SNK6 cells demonstrated a statistically significant increase in sensitivity to A-1331852, ABT199 and most dramatically to MCL-1 inhibition by S63845 (**figure 4.21A, -C** and **-E**). SNT15 cells depleted of IL-2, conversely became less sensitive to BCL-X_L inhibition by A-1331852 (**figure 4.21B**) but dramatically more sensitive to MCL-1 inhibition by S63845, particularly at the lowest concentration of 0.2 uM (mean 4.2% viability in the absence of IL-2 vs 72.8% viability in the presence of IL-2) (**figure 4.21D**).

These results potentially explain the difference in sensitivity to the BCL-X_L inhibitor A-1331852 observed in mice xenotansplanted with SNK6 cells or SNT15 cells. BCL-X_L inhibition was effective at delaying tumour growth in mice transplanted with SNK6 cells, consistent with these cells becoming more BCL-X_L dependent in the absence of IL-2. Conversely A-1331852 treatment of mice transplanted with SNT15 cells could not delay tumour growth, consistent with these cells becoming less dependent on BCL-X_L in the absence of IL-2. The *in vitro* data would suggest that treatment of the SNT15 cell xenotransplanted mice with S63845 would be more effective at delaying tumour growth *in vivo* since these malignant cells were much more MCL-1 dependent following withdrawal of IL-2.

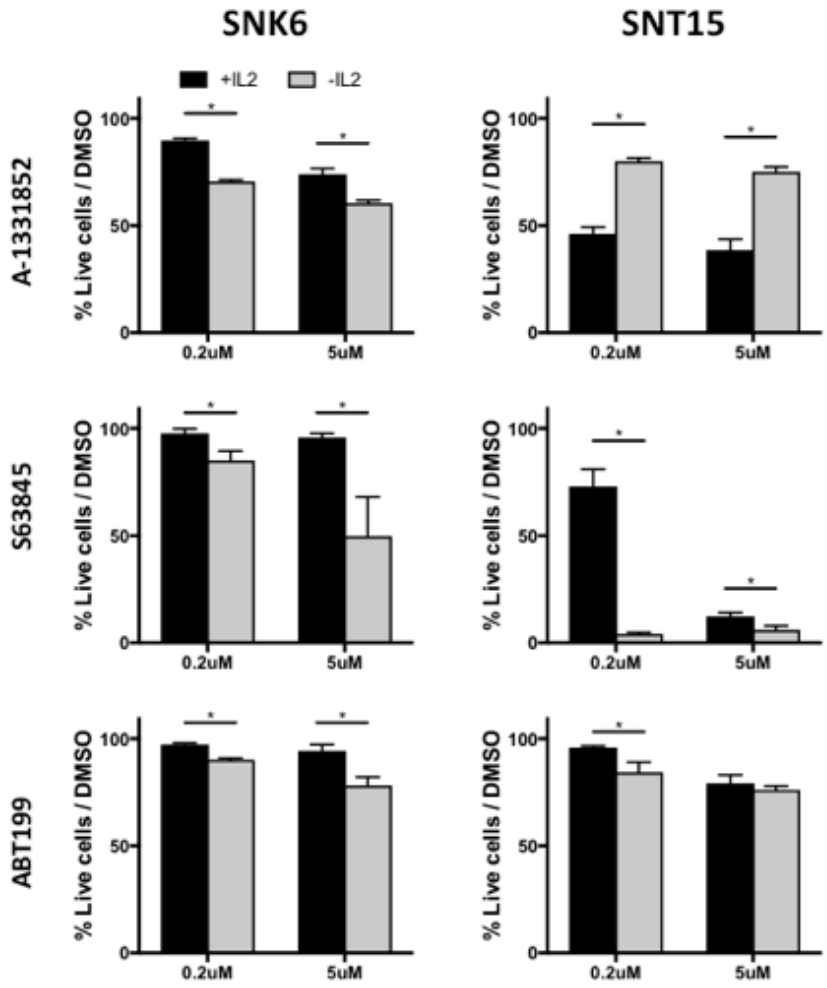


Figure 4.21 Cell survival analysis of IL-2 deprived SNK6 cells and SNT15 cells following treatment with BH3 mimetic drugs. Cells were deprived of IL-2 for 48 hours then treated with BH3 mimetic drugs for 24 hours. Cells were then stained with Annexin V and PI to determine survival where PI_/Annexin V- double negative populations were normalised to DMSO-only controls and then plotted. Cells were treated with either ABT-199, A-1331852 or S63845 at the indicated concentrations for 24 hours. Data presented are mean ±SE of three independent experiments performed in triplicate. *p<0.05.

4.9 Discussion

ENKTL exhibits a poor response to chemotherapy and high rates of relapse are common in those patients that do show initial remission (Au et al., 2009, Wang et al., 2012). ENKTL patients have traditionally been treated with the CHOP chemotherapy regimen although recently there has been an adoption of the SMILE regimen. This adjustment was made following suggestions that CHOP resistance was mediated via the expression of the multi-drug efflux pump, p-glycoprotein (Yamaguchi et al., 1995, Yoshimori et al., 2015). The three questions we intended to answer in this results chapter are: 1) Is SMILE an effective anti-tumour treatment regimen? 2) How do EBV-positive T and NK cells evade cell death induced by genotoxic anti-cancer agents? 3) Which therapeutic options are effective in inducing cell death?

To answer the above questions, we first assessed the ability of clinically relevant anti-cancer agents to induce cell death in the available panel of cell lines. Secondly, we attempted to determine the mechanism of resistance to cell death by assessing multiple factors: drug efflux by p-glycoprotein; deregulation of the p53 pathway; and deregulation of the BCL-2 family of apoptosis regulators. Finally, we assessed the susceptibility of the lymphoma cells to therapeutic targeting of the BCL-2 family with BH3 mimetic drugs *in vitro* and *in vivo*.

As mentioned, the SMILE regimen was adopted to treat ENKTL due to the expression of *ABCB1*/p-glycoprotein. However, two key components of the regimen, the genotoxic agents etoposide and methotrexate, have unclear relationships with the drug efflux pump.

Etoposide was included in the regimen due to its ability to induce apoptosis in the ENKTL cell line NK-YS despite the demonstration that etoposide is a substrate for p-glycoprotein mediated efflux (Uno et al., 2001, Leu and Huang, 1995). However, mutational studies suggest that *ABCB1* mutations are not a factor in etoposide resistance in cell lines (Jaffrezou et al., 1994). With regards to methotrexate, selected clones from human leukaemic cell lines that showed methotrexate resistance had increased *ABCB1* expression. Methotrexate susceptibility was then partially restored by treatment with a p-glycoprotein-targeting monoclonal antibody (Norris et al., 1996). Although it appears agreed that methotrexate is a p-glycoprotein substrate, its method of cellular entry (diffusion or transporter) affects its likelihood of interacting with p-glycoprotein and therefore cellular efflux (de Graaf et al., 1996).

The effectiveness of etoposide and methotrexate in a broad range of ENKTL (or CAEBV) cell lines has not been demonstrated previous to this study. Although susceptibilities were variable across the cell line panel, we show that even high concentrations of either compound did not induce extensive cell killing. P-glycoprotein expression/functionality was only demonstrable in 4 of 8 ENKTL/CAEBV cell lines tested, suggesting that this was not the primary resistance mechanism. The literature appears to favour the argument that both etoposide and methotrexate are substrates of p-glycoprotein-mediated efflux. We would have therefore predicted to see etoposide/methotrexate susceptibility in the p-glycoprotein-negative cell lines. However, this was not the case. It could be concluded that resistance to such compounds is not mediated by p-glycoprotein but instead by deregulation in cellular signalling processes. However, it is plausible that the p-

glycoprotein-negative cell lines may have acquired additional mutations to facilitate their resistance to such compounds. Clinical data comparing the response to chemotherapy in patients with p-glycoprotein-positive versus -negative tumours would prove insightful.

Although SMILE therapy for ENKTL appears to be the direction that the field is moving towards, its effectiveness is still unclear based on early clinical trials. A study of 27 newly diagnosed stage IV ENKTL patients combined SMILE therapy with autologous stem cell transplantation reported a median overall survival of 10.6 months (Kim et al., 2015). A phase II study from 2011 reported 19 patients who were treated with SMILE therapy with autologous/allogeneic stem cell transplant reported a 55% overall survival at 1 year (Yamaguchi et al., 2011). These reports involve small cohorts of patients but do provide modest improvements compared to CHOP therapy, which had a median survival of 7.8 months (Vose et al., 2008). Perhaps the alteration of chemotherapy regimens has provided slight improvements in patient outcomes, but it is unlikely that these improvements have occurred due to the avoidance of p-glycoprotein action. From the *in vitro* data generated here, we would predict that these reported patient improvements will be limited by the infectiveness of etoposide and methotrexate in this disease background.

As the mechanism of resistance to cell death remained elusive, we turned our attention to the p53 pathway — the deregulation of which can maintain survival in the presence of many genotoxic drugs. P53 sequencing of our cell lines revealed a potentially complex issue with respect to EBV infected T and NK cells. Interestingly, only 1 of 8 cell lines contained a mutation in the DNA binding domain of the p53 gene. However, sequencing of the entire gene is required to completely rule out mutations that occur elsewhere in the gene.

Despite WT p53 sequences, only 2 cell lines showed clear susceptibility to non-genotoxic p53 activation by the MDM2 inhibitor, nutlin-3a. Therefore, a full profile of p53 signalling within these cells is required to elucidate the functionality of the pathway.

Given their role in cell death, investigation into the BCL-2 family of apoptosis regulators was required. The role of the BCL-2 protein family in maintaining cell survival in EBV-positive T and NK cells had not been explored to date. Initially, we showed by protein expression analysis that all of the examined ENKTL/CAEBV cell lines appeared capable of undergoing apoptosis as each cell line expressed the pro-apoptotic effector proteins BAK and BAX. All cell lines also expressed pro-survival BCL-2, BCL-X_L and MCL-1 proteins at variable levels. Following treatment with BH3 mimetic drugs, either individually or in combinations, it was apparent that the cell lines primarily showed a dependency on BCL-X_L for survival, and a dependency on MCL-1 was secondary. It was surprising that no dependency on BCL-2 was demonstrated since BCL-2 protein was expressed at the highest levels across these cell lines.

Following a series of optimisation experiments, we showed that the engraftment of multiple human EBV-positive T and NK cell lines into NSG mice was possible. This is the first description of such subcutaneous and intraperitoneal injection protocols for this panel of cell lines. Only the SNK6 cell line had previously been described to form subcutaneous tumours in NOG mice, and this was the basis for these experiments (Siddiquey et al., 2014). The models developed in this thesis chapter were used to test the *in vivo* efficacy of the BCL-X_L specific BH3 mimetic drug, A-1331852.

A-1331852 was selected for *in vivo* examination due to its ability to induce apoptosis in all 8 EBV-positive T and NK cell lines. Although the combination of A-1331852 plus S63845 was shown to be the most effective method of inducing the highest level of killing in these cell lines, this combination has been poorly tolerated in mouse leukaemia models (G. Kelly, unpublished). Therefore, single treatment with A-1331852 was the next logical preference. Also, A-1331852 has previously demonstrated efficacy in xenograft models of SCLC, breast and ovarian cancer (Leverson et al., 2015a).

A delay in tumour latency was observed with SNK6 cell-transplanted NSG mice compared to DMSO-only controls in both subcutaneous and intraperitoneal models. However, the changes in tumour latency between the two treatment groups were not significant with SNT15 cell or MEC04 cell transplanted mice. We speculated that this is due to the changes in IL-2 availability to the cells. NSG mice lack the IL-2 receptor gamma chain and therefore cannot produce mature $CD4^+$ T cells, the major source of IL-2 (Shultz et al., 2005, Nelson, 2004). Therefore, xenografted ENKTL/CAEBV cells were rapidly starved of this cytokine. We therefore predicted that this change would alter the expression of key BCL-2 family members as well as the viral oncogene LMP1, as has been previously reported (Lord et al., 1998, Takahara et al., 2006). Consistently across the cell line panel, the levels of BCL-X_L decreased upon IL-2 deprivation and in some cell lines, importantly the SNT15 cells and MEC04 cells, the levels of MCL-1 increased. These changes were important as SNT15 cells became less sensitive to BCL-X_L inhibition and switched their survival dependency to MCL-1, as demonstrated by increased sensitivity to S63845. The concept of switching of dependency from one to another pro-survival BCL-2 family member has previously been

reported in NSCLC cell lines where inhibition of BCL-2 or BCL-X_L by siRNA was only capable of inducing cell death when MCL-1 was also silenced (Zhang et al., 2011). In non-disease settings, intracellular BH3 profiling was used to demonstrate a switching of dependency from BCL-2 to a combination of MCL-1 plus BCL-X_L in proliferating B cells when stimulated with either CD40/IL-4 or CpG DNA (Dai and Luftig, 2018). We report that, in EBV-positive T and NK cell backgrounds, MCL-1 inhibition by S63845 is only an effective strategy of cell killing when BCL-X_L has also been targeted.

In SNK6 cells where no increase in MCL-1 was observed following IL-2 removal, the sensitivity to BCL-X_L inhibition remained intact and therefore a delay in tumour latency was observed. The determining factor that decides whether a cell will switch its dependency from BCL-X_L to MCL-1 is currently unknown. It is however, known that inhibition of both pro-survival proteins will lead to extensive cell killing *in vitro*, although this has not yet been demonstrated *in vivo*.

In conclusion, our findings suggest that the SMILE regimen may not be a solution for EBV-positive T and NK cell disease due to the limited effectiveness of etoposide and methotrexate. The P-glycoprotein status or p53 mutational status may not be definitive factors when predicting resistance to chemotherapy. Instead, cellular survival is mediated by the pro-survival proteins BCL-X_L and MCL-1. The therapeutic targeting of BCL-X_L has shown potential here in animal models of EBV-associated T and NK cell disease.

5. Results III: Towards the development of novel therapies

5.1 Introduction

ENKTL patients have largely been empirically treated based upon the chemotherapy regimens used in other non-Hodgkins lymphomas (Young, 1992). Such regimens heavily rely on cytotoxic agents that target replicating DNA (e.g. the topoisomerase II inhibitor, etoposide). These treatments are accompanied by toxic side effects and have a small therapeutic window (Kobayashi and Ratain, 1994). The combination of autologous stem cell transplantation with chemoradiation has proved a successful treatment in many incidences of ENKTL (Fox et al., 2015, Teshima et al., 1996, Takami et al., 1998, Sasaki et al., 2000). However, most patients fail to achieve complete remission with such therapies and median survival of ENKTL patients remains at less than a year and therefore a targeted therapeutic approach is desired (Vose et al., 2008).

It has been suggested that p-glycoprotein/multidrug resistance protein 1 (MDR-1) was a route of drug resistance in ENKTL, and this led to the application of the non-anthracyline-based regimen, SMILE, which has improved short term survival rates (Yamaguchi et al., 1995, Yamaguchi et al., 2011). The contribution of p-glycoprotein to the poor ENKTL patient responses to CHOP has been disputed in the previous chapter of this thesis. SMILE remains a difficult to tolerate chemotherapy regimen that includes the cytotoxic compounds, etoposide and methotrexate, which the field would ideally like to depart from.

The identification of novel therapeutic compounds/regimens for use in the treatment of ENKTL has only been attempted to a limited degree. The histone deacetylase inhibitor, suberoylanilide hydroxamic acid (SAHA), has shown efficacy in an ENKTL mouse xenograft model where the compound acted to diminish JAK-STAT signalling (Siddiquey et al., 2014, Karube et al., 2013). *In vitro* studies targeting the EBV antigen LMP1 have also been attempted, either directly by use of an LMP1-specific monoclonal antibody or indirectly via heat shock protein 90 inhibition, to induce tumour cell death (Mao et al., 2012, Suzuki et al., 2015).

To thoroughly examine an array of clinically viable compounds, high-throughput screening (HTS) approaches can be employed. HTS approaches can repurpose drugs currently designed and approved for use in other disease types. The repurposing of previously approved compounds for use in the ENKTL setting can alleviate the need for extensive toxicity and safety studies and thus lead to quicker implementation in patients. The extensive number of compounds in an HTS compound library, which target vast numbers of proteins, can also reveal important details into which signalling pathways are important for the sustained growth and survival of the tumour cells.

In this chapter, we describe an HTS to test 4079 compounds on a panel of T and NK cell lines. The selected cell lines have been screened with three compound libraries: 1) The kinase library – this contains 276 agents that inhibit various kinases; 2) The targeted agents library – this contains 73 compounds with high affinity to specified targets and; 3) The known drugs library – this contains approximately 3700 compounds that have been either clinically approved, failed in clinical trials or are currently involved in clinical trials. The data

generated were used to identify susceptibilities in signalling pathways and to compare these cell lines via shared hit analysis. Also, the most potent compounds were used to make suggestions for further validation and to speculate on potential therapeutic avenues for ENKTL and CAEBV.

5.2 Assay optimisation

The purpose of performing HTS is two-fold. Firstly, the process allows the identification of compounds for novel use in EBV-associated T and NK cell disease. Secondly, the mechanisms of action of potent compounds collectively reveal information regarding which signalling pathways are required for sustained growth and survival in ENKTL and CAEBV. A total of 6 cell lines (SNK6, SNT8, SNT13, SNT15, NKC1 and MEC04 cells) were able to be screened. A series of optimisation experiments were designed and performed in order to determine how to set up the screen, considering factors such as the cell density at plating, variability between assay plates and maximum DMSO tolerance. These are conditions that may impact upon the read-out of cell viability, CellTiter-Glo (CTG) luminescence.

5.2.1 Cell number

To select a cell density suitable for each cell line that would not be limiting to CTG luminescence, cells were titrated at increasing densities then lysed after 48 hours and stained with CTG. A cell density of 2,500 cells per well in 50 uL final volume was deemed

suitable for each cell line as this density was below the maximal luminescence signal (**figure 5.1**).

5.2.2 DMSO tolerance

In order to determine the DMSO tolerance of each cell line, which would ultimately impact on the dose of drug that could be used, 2,500 cells were treated with increasing concentrations of DMSO and cell viability was determined by CTG luminescence after 48 hours, as performed previously (**figure 5.2**). This experiment indicated that the HTS should be performed at less than 0.5% DMSO, a concentration where no cell lines exhibited a difference in viability compared to the 0% DMSO control. The primary screen requires that cells can tolerate 0.2% DMSO, which falls below the maximum tolerance of 0.5% demonstrated here.

5.2.3 Assay variability

The HTS was to be performed using several drug-coated multi-well plates. To ensure that variability in luminescence readings were not introduced by different plates, two entire plates were examined per cell line and then compared. To do this, each plate was seeded with 2,500 DMSO-treated cells for 48 hours followed by lysis and measurement of the CTG luminescence of each well. For each of the 6 cell lines, no significant difference in luminescence between the two plates was observed (**figure 5.3**).

5.2.4 Control compounds

The measure of cell death from the HTS was calculated as a percentage of luminescence relative to a positive control capable of inducing near-complete death (>98%) of the cell population. To determine such a condition, cells were subjected to treatment with BH3 mimetic drugs with demonstrated efficacy as shown in the previous chapter of this thesis. The BCL-X_L inhibitor A-1331852 was the most effective single agent and the A-1331852 plus S63845 combination was the most effective treatment tested (**chapter 4**). Cells were seeded at 2,500 cells per well and treated with either 10 uM A-1331852 or 10 uM A-1331852 plus 10 uM S63845 with a final DMSO concentration of 0.2% (**figure 5.4**). The combination treatment with both BH3 mimetic drugs was capable of inducing >98% killing in all 6 cell lines compared to DMSO-treatment controls. The increased sensitivity of these cell lines to the tested BH3 mimetics relative to data shown in chapter 4 (**figures 4.10** and **4.11**) is likely due to differences in time course (24 hours versus 48 hours), drug concentration (5 µM versus 10 µM) and a difference in viability read out (AV/PI negativity versus relative CTG luminescence). An increase in drug treatment time and concentration was performed in the experiments of this chapter as the aim was to induce maximal cell death whereas previously the aim was to identify differences in sensitivity between different compounds.

Collectively, these experiments identified the optimal conditions to be taken forward to the primary screen of the HTS assay. For each cell line, 2,500 cells per well in 50 uL is not luminescence-limiting. Furthermore, at these doses of DMSO, there was no DMSO toxicity and therefore no interference in luminescence would occur. No variation occurred

between assay plates, which removed this as a variable. Finally, the combination of A-1331852 plus S63845 acted as a suitable positive-control.

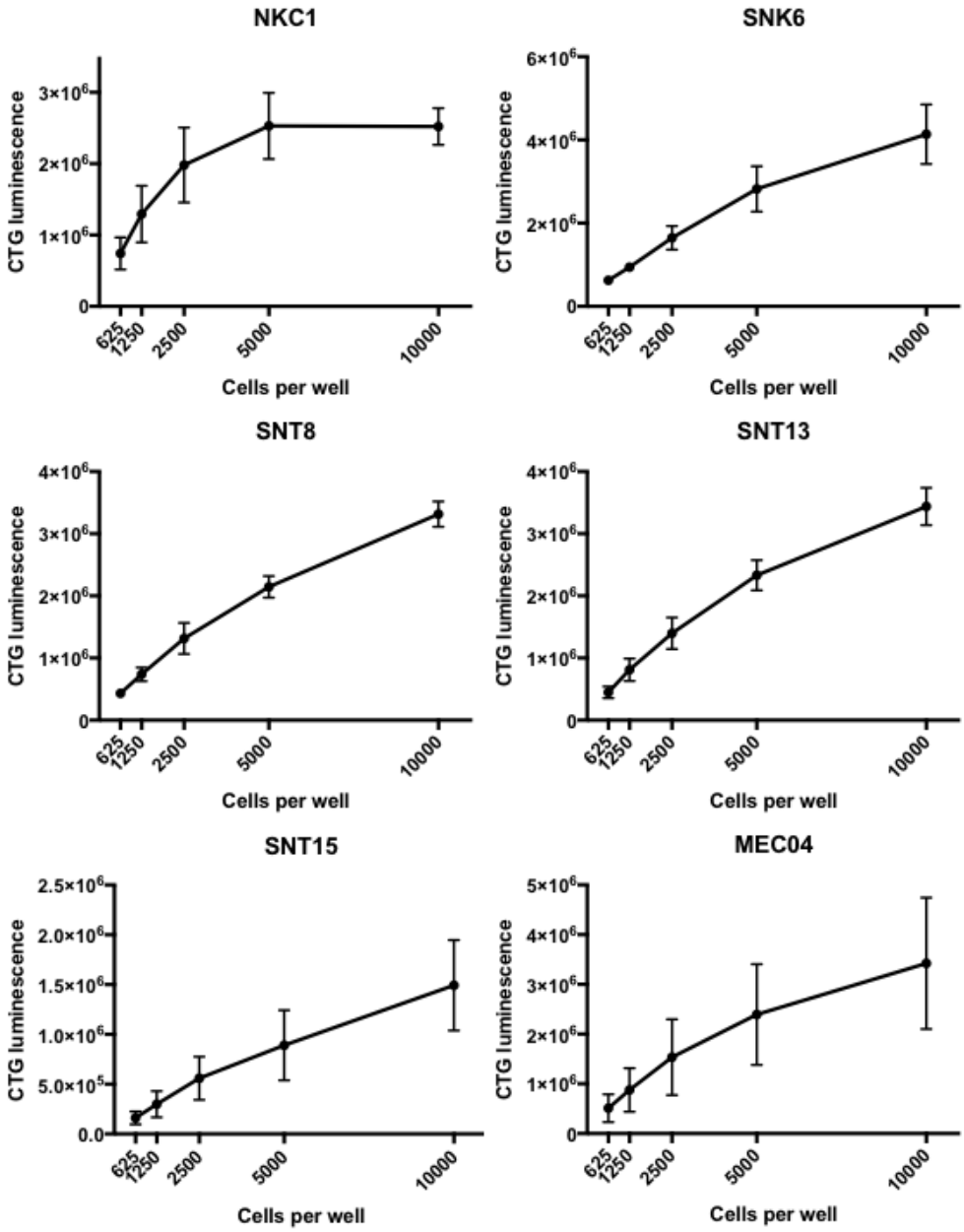


Figure 5.1 Cell number optimisation. NKC1, SNK6, SNT8, SNT13, SNT15 and MEC04 cells were seeded at the indicated densities in 384-well plates After 48 hours, cells were lysed by shaking and stained with CTG before luminescence detection. Raw values are plotted. Data presented are mean ±SD of three independent experiments performed in triplicate. CTG, Cell-titre Glo; SD, standard deviation.

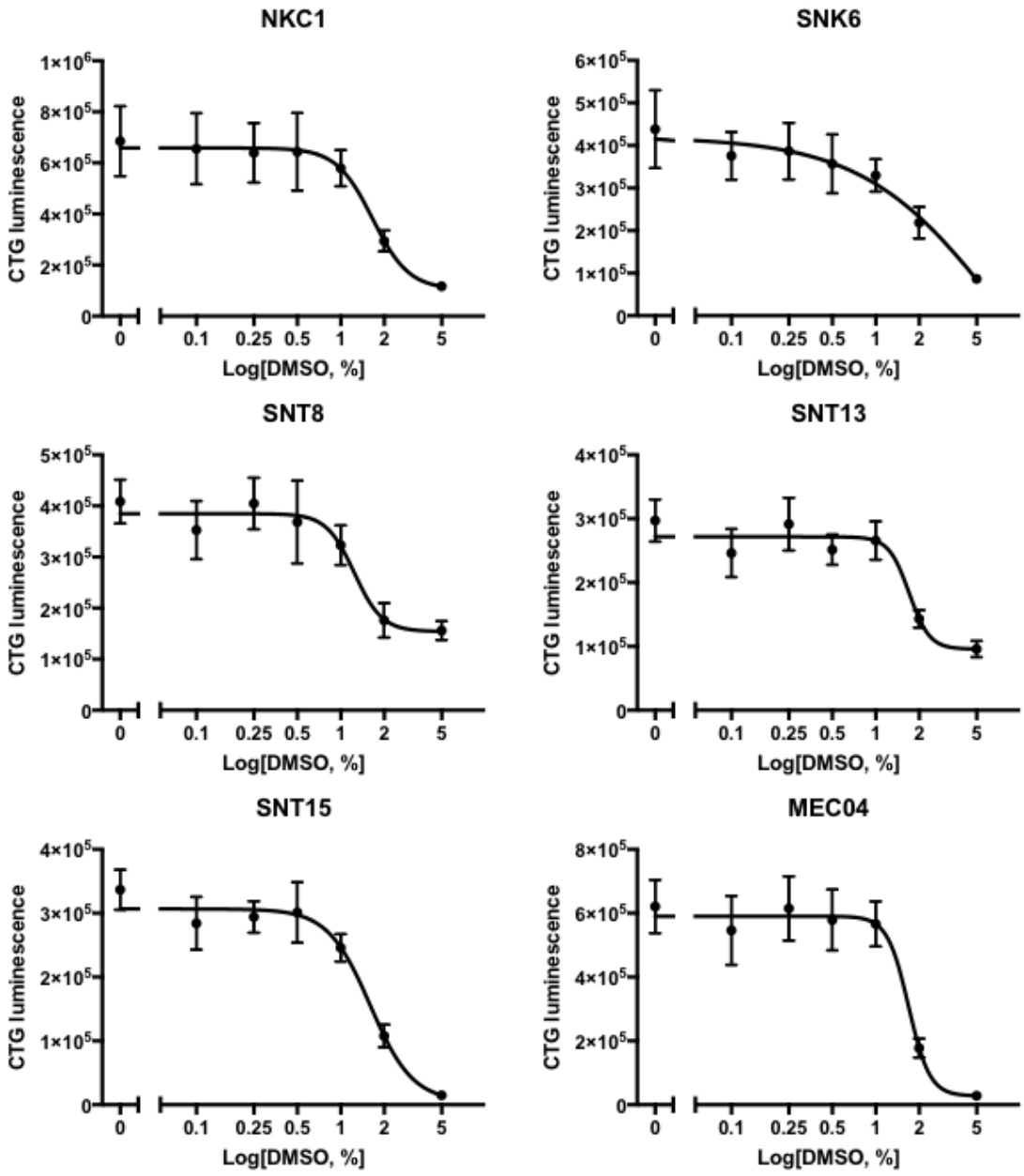


Figure 5.2 DMSO tolerance. NKC1, SNK6, SNT8, SNT13, SNT15 and MEC04 cells were seeded at 2,500 cells per well in 384-well plates After 48 hours, cells were lysed by shaking and stained with CTG before luminescence detection and raw values are plotted. Data presented are mean ±SD of three independent experiments performed in triplicate.

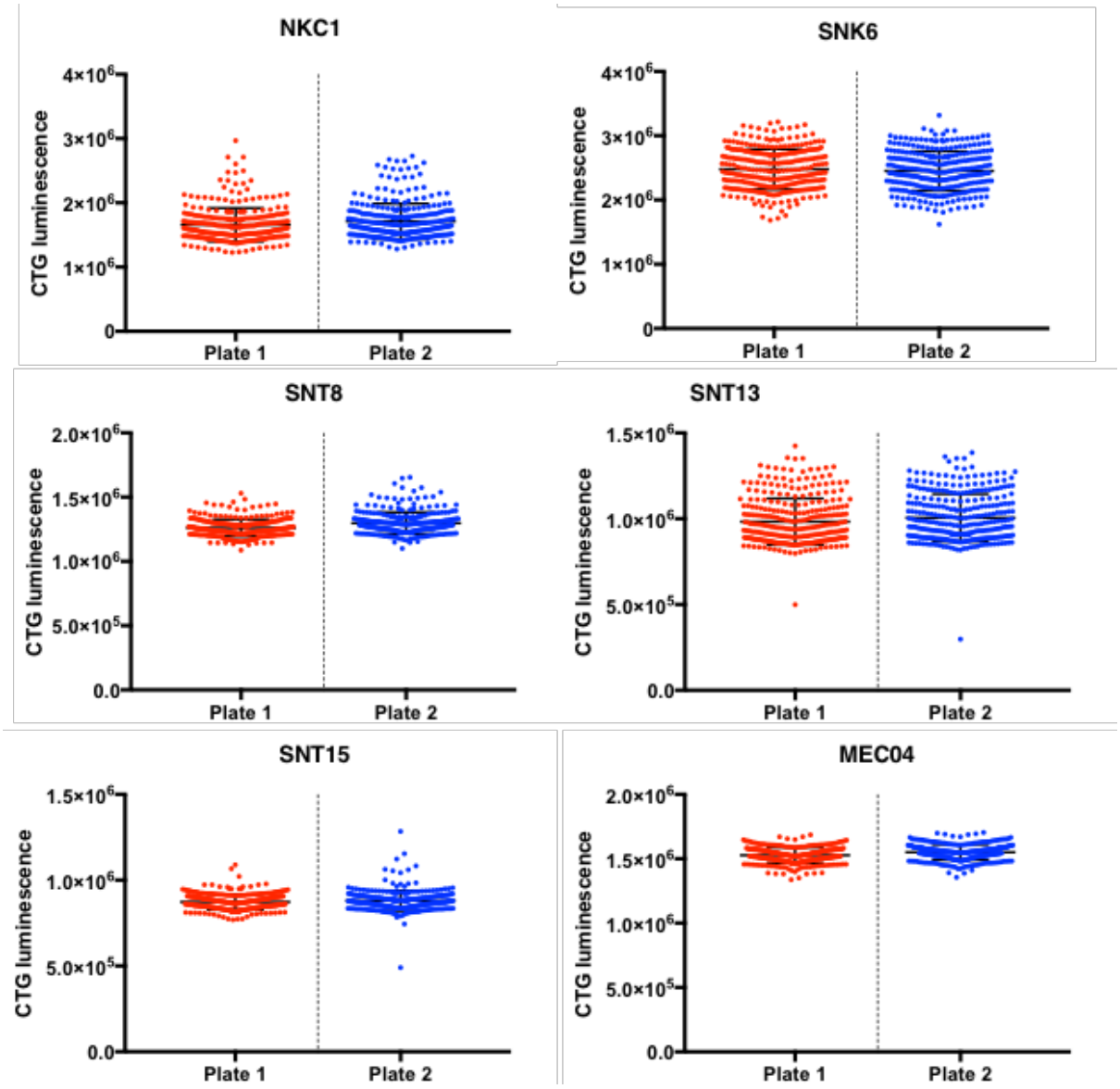


Figure 5.3 Plate variability. NKC1, SNK6, SNT8, SNT13, SNT15 and MEC04 cells were seeded at 2,500 cells per well (in 0.2% DMSO-containing media) into all wells of two 384-well drug-screening plates. Data presented are mean ±SD of three independent experiments performed in triplicate.

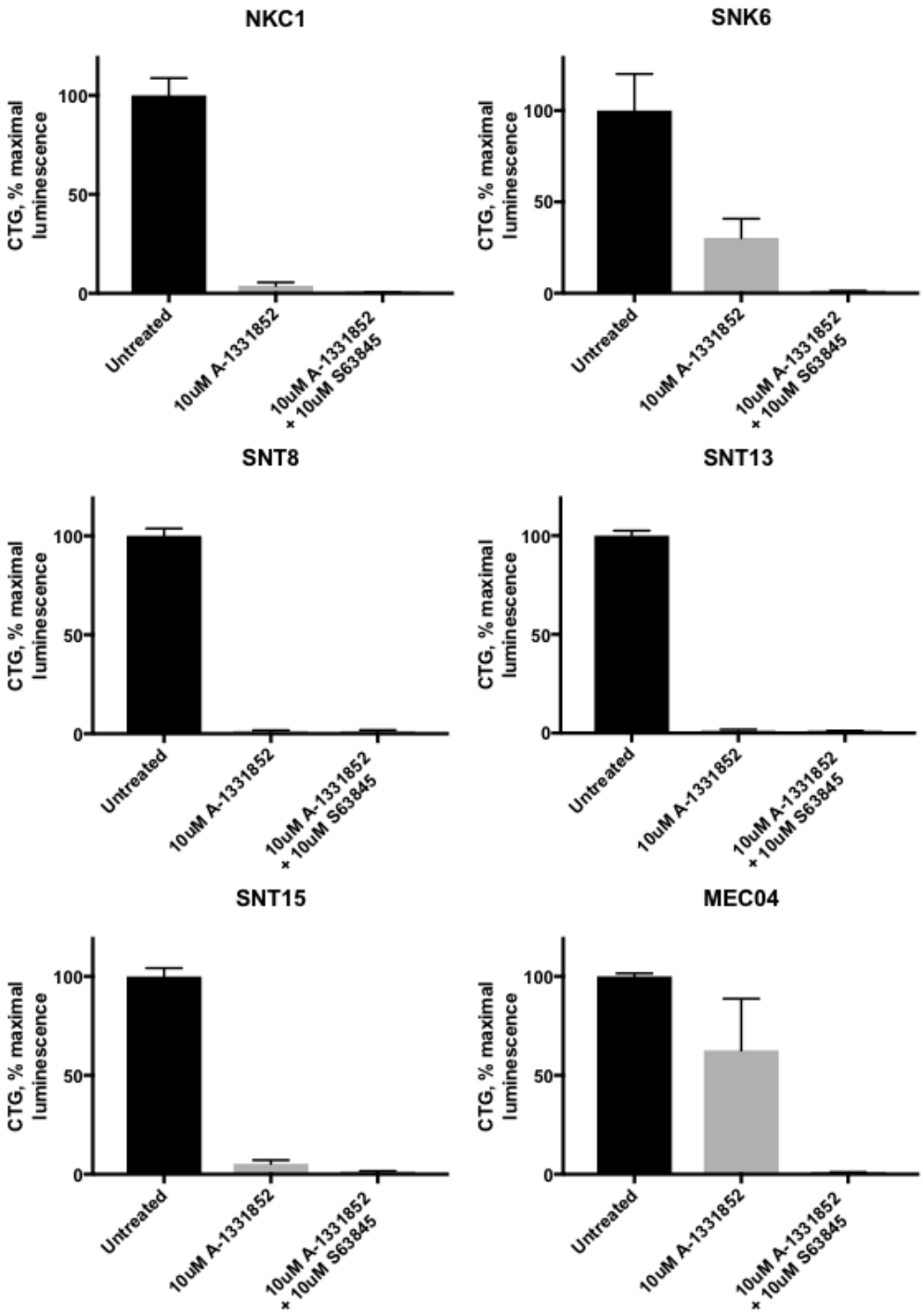


Figure 5.4 Combination of the BH3 mimetic drugs A-1331852 and S63845 induces extensive killing of ENKTL and CAEBV cell lines. The indicated cell lines were either left untreated (DMSO-only), treated with 10 uM A-1331852 alone or 10 uM A-1331852 combined with 10 uM S63845 for 48 hours. Cells were then lysed by shaking and stained with CTG before luminescence detection. Luminescence data are normalised to untreated cells (100%). Data presented are mean ±SE of three independent experiments performed in triplicate.

5.3 Primary screen: Data quality

Following the optimisation of the HTS protocol for the EBV-positive T and NK cell lines, the primary screen of 4079 compounds was performed. Here, each cell line was treated for 48 hours with either DMSO, control compounds (10 uM A-1331852 plus 10 uM S63845) or test compounds, followed by CTG luminescence measurement as described above. The luminescence readings from the DMSO-treated and control compound-treated cells were used to determine the statistical robustness of the screen. The robustness of the primary screen was confirmed, where each assay plate of each cell line was statistically assessed using Z prime (Z') and robust Z prime (RZ') analysis (**table 5.1**). The Z' score was calculated from the mean and standard deviation of positive and negative control wells as previously described for HTS assays (Zhang et al., 1999), in order to determine the likelihood of false-positive hits. Similarly, a modified calculation was performed, as previously described (Birmingham et al., 2009), to determine the RZ' score which removes outliers that may produce apparently unfavourable Z' scores. For both measures and in all cell lines, scores exceeded the value of 0 (an acceptable range considered a marginal assay) and most assay plates exceeded a score of 0.5 (considered a very good assay) (Zhang et al., 1999).

Luminescence readings from test-drug treated cells were converted to survival percentages calculated from the mean luminescence values of DMSO-treated cells (normalised as 100% viable) and the mean luminescence values of control-drug treated cells (0% viable) (**figure 5.5**). This was required as subsequent analysis relied on comparison

between cell lines which exhibit varying maximal luminescence due to different levels of ATP between cell lines.

Table 5.1 Primary screen: Z prime and robust Z prime values. The mean value for each cell line is the mean of all assay plates. Minimum and maximum values are the lowest and highest scoring assay plates. Z', Z prime; RZ', robust Z prime.

	Z'			RZ'		
	Mean	**Min**	**Max**	**Mean**	**Min**	**Max**
NKC1	0.486	0.404	0.627	0.655	0.475	0.867
SNK6	0.474	0.414	0.569	0.633	0.500	0.776
SNT8	0.608	0.518	0.704	0.726	0.636	0.818
SNT13	0.560	0.500	0.662	0.674	0.535	0.827
SNT15	0.640	0.551	0.752	0.772	0.692	0.868
MEC04	0.875	0.813	0.920	0.921	0.900	0.956

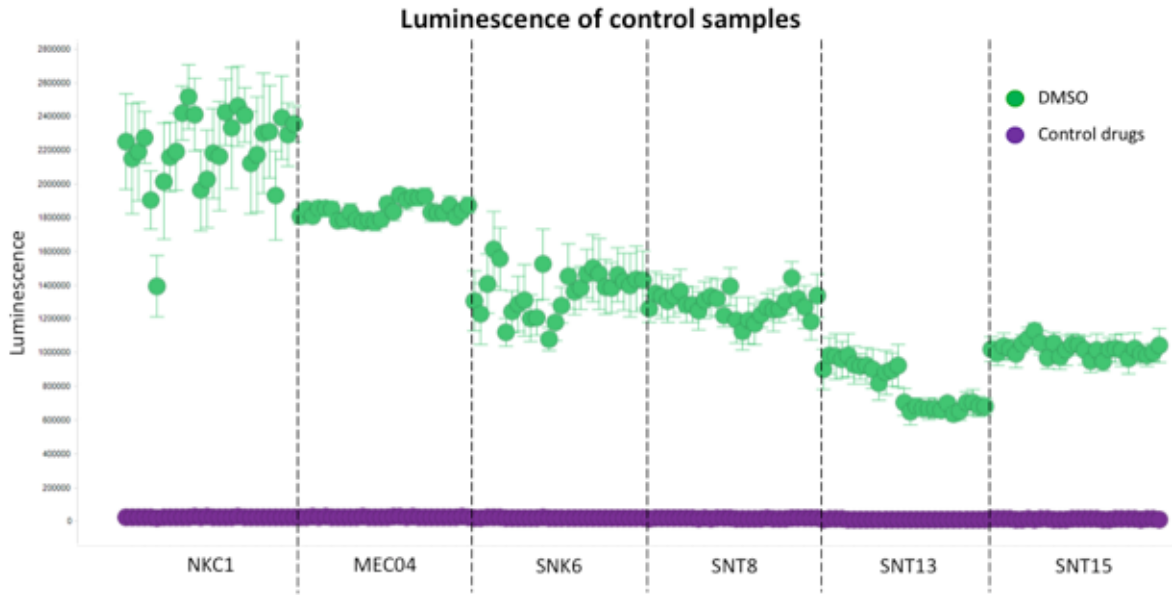


Figure 5.5 Control compounds successfully induce killing of ENKTL and CAEBV cell lines in the primary screen. The indicated cell lines were treated with either DMSO (0.2%) or control drugs (10 uM A-1331852 + 10 uM S63845) for 48 hours. Cells were then lysed by shaking and stained with CTG before luminescence detection and raw values are plotted. Data presented are mean ±SE of 14 individual plates for each cell line.

5.4 Primary screen: Hit analysis

The data generated from the primary screen were used to answer two key questions: to what extent are the cell lines similar with their overall response to drug treatments and also to identify specific compounds that may be of therapeutic benefit. To answer these questions, effective compounds must first be identified. During initial analysis, a tested compound qualified as an effective compound (or 'hit') if it was able to induce at least 70% cell killing in a given cell line. Correlation between the two replicates of the experiment increased with increasing potency of the compounds (**supplementary figure 3**). A cut-off

of 70% was chosen in order to maximise the number of hits for future analysis while maintaining confidence in the effectiveness of the compound.

The total number of hits across the cell line panel ranged from 277 (SNT8 cells) to 492 (SNT15 cells) (**table 5.3**). A subsequent analysis identified compounds that induced >70% cell killing in more than one cell line. Encouragingly, 152 compounds induced substantial cell killing in all 6 tested cell lines and a total of 563 unique compounds were effective in one cell line or more (**table 5.3**). The overlap of cytotoxic compounds between the cell lines was made in **figure 5.6**. NKC1 cells and SNT15 cells exhibited the highest hit rates (number of effective compounds as a percentage of total compounds) and accordingly demonstrated the highest number of unique hits, whereas no compounds were uniquely toxic to SNT8 cells (**figure 5.6A**). SNK6 cells ranked last in shared hits when compared to each of the other cell lines and showed the lowest level of overlap (184 compounds) with MEC04 cells, whereas the highest level of overlap was between NKC1 cells and SNT15 cells (368 compounds) (**figure 5.6B**).

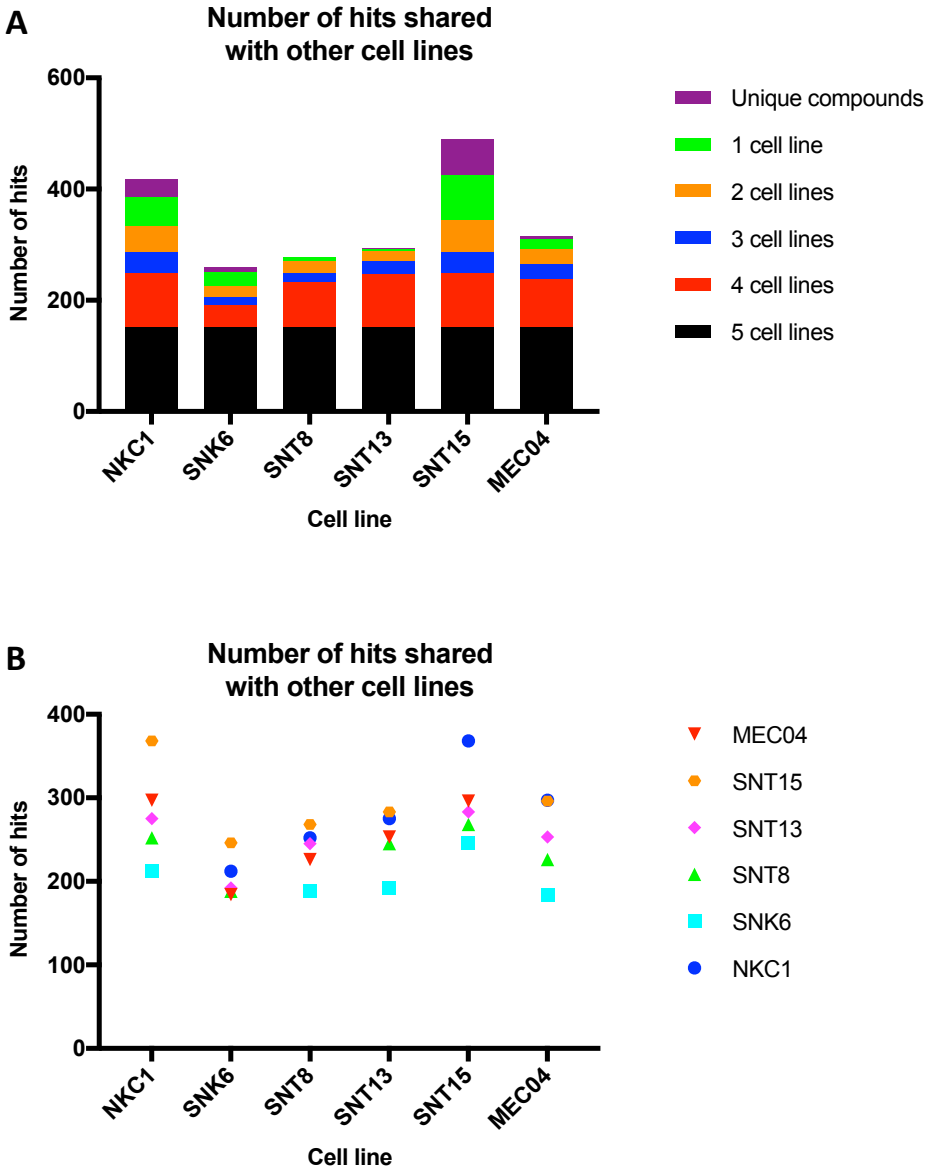


Figure 5.6 Comparison of hits between cell lines. Data were extracted from the primary screen of the HTS where all 6 ENKTL or CAEBV cell lines were treated in duplicate with the 4079 compound library for 48 hours. Cells were then lysed and stained with CTG and luminescence was measured as relative to positive and negative controls. Hits were defined as compounds that induced at least 70% cell killing in a given cell line. **A)** The total number of hits for each cell line are presented with the number of cell lines in which the hits are shared. **B)** The number of hits shared with other cell lines.

Table 5.2 Hits per cell line. Total number of compounds that induced at least 70% cell killing and number of hits as a percentage of all tested compounds.

	Total number of hits	Hit rate (%)
NKC1	417	10.22
SNK6	260	6.37
SNT8	277	6.79
SNT13	293	7.18
SNT15	492	12.06
MEC04	316	7.75

Table 5.3 Total primary screen hits. Total number of compounds that could induce at least 70% cell killing in multiple cell lines.

Number of cell lines with >70% death	Number of compounds
6	152
≥5	250
≥4	290
≥3	354
≥2	448
≥1	563
0	3516

Ultimately, the positive hits identified from the primary screen will need to be taken forward for an additional screen during which the concentrations of the compounds are titrated to allow for IC50 calculation, a value indicative of potency. The number of compounds that will be taken forward to such a secondary screen will be limited by our follow-up capacity. Therefore, compounds that were deemed effective in ≥3 cell lines (354 compounds) will be assessed further. The IC50 values generated will reveal which compounds are effective in multiple cell lines and to which targets are the cells most susceptible.

At this point, our analysis was limited to absolute effectiveness at 10 uM. The most effective compounds — that averaged more than 99% cell killing across all 6 cell lines — have been listed in **table 5.4.** The most common therapeutic group of drugs in the list are tyrosine kinase inhibitors, mostly with broad specificities. This suggests that such compounds are potent against the ENKTL/CAEBV cell lines of interest. All tyrosine kinase inhibitors tested in the primary screen were assessed for their ability to induce cell killing in all 6 cell lines (**figure 5.7A**). A mean of 27.2 (S.D. 6.7) compounds out of 97 reached the 70% cell killing threshold. Due to the broad specificities of these compounds, the vital kinases cannot be accurately identified. A second therapeutic group within the list of top compounds in **table 5.4** are JAK inhibitors (represented by the JAK2 inhibitor, TG101348/Fedratinib) — a group that contains compounds with greater degrees of specificity. All JAK inhibitors included in the primary screen were labelled for their specific targets and assessed for their ability to induce cell killing in all 6 cell lines (**figure 5.7B**). The 70% cell killing threshold was reached for all 5 JAK2 inhibitors present in the compound

library when tested against NKC1 cells and SNT15 cells. Four out of five JAK2 inhibitors reached the threshold in SNK6, SNT13 and MEC04 cells and 3 out of 5 in SNT8 cells. Neither of the two JAK3 inhibitors induced greater than 32% cell killing in any of the cell lines examined.

Table 5.4 Most effective compounds from global hit list. Compounds included in this list induced greater than 99% cell killing in all 6 cell lines. Compounds are ranked by the average percentage of cell killing induced across all 6 cell lines.

Compound	Average cell death	Drug class
Auranofin	99.8	Antirheumatic Agent
Cediranib (AZD2171)	99.76	Kinase inhibitor
TOVOK (BIBW-2992 Afatinib)	99.67	Kinase inhibitor
Aurora A Inhibitor I	99.56	Kinase inhibitor
PD-166285 hydrate	99.55	Kinase inhibitor
JNJ-26481585	99.48	Histone deacetylase inhibitor
IKK 16	99.47	Kinase inhibitor
WZ8040	99.43	Kinase inhibitor
UNC1999	99.39	Methyltransferase inhibitor
LBH589 (Panobinostat)	99.37	Histone deacetylase inhibitor
PHA 665752	99.34	Kinase inhibitor
Thimerosal	99.26	Antifungal agent
Pyrvinium pamoate	99.25	Antithelmintic agent
SB590885	99.24	Kinase inhibitor
Bosutinib (SKI-606)	99.23	Kinase inhibitor
Hesperadin	99.17	Kinase inhibitor
SGI-1776	99.15	Kinase inhibitor
TG101348	99.05	Kinase inhibitor
Sunitinib (Sutent SU11248)	99.04	Kinase inhibitor
BIX-01294	99.03	Methyltransferase inhibitor

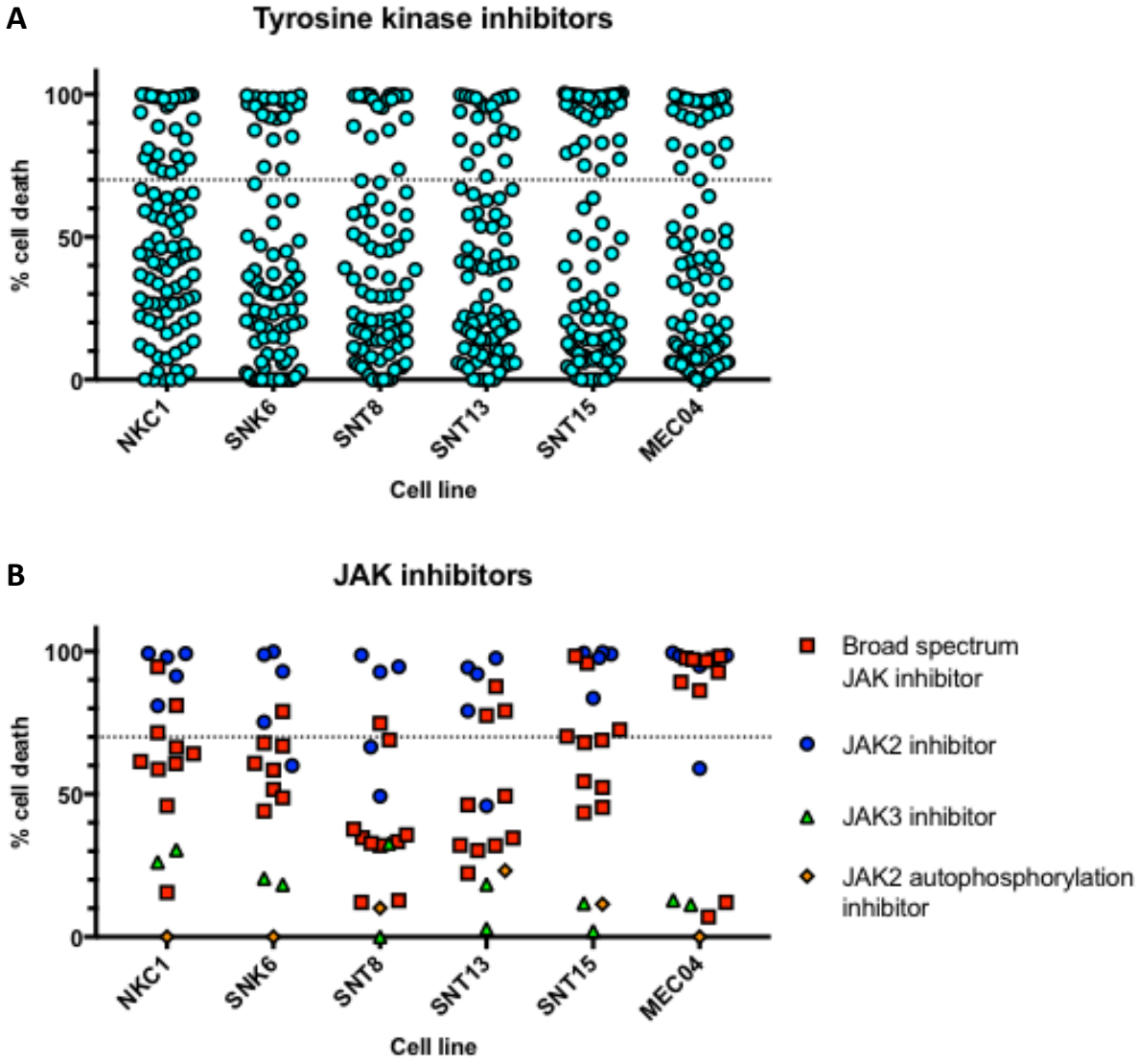


Figure 5.7 JAK2 inhibitors induce cell killing across the cell line panel. Data plotted are the mean percentage cell killing induced by individual compounds from duplicate experiments of the HTS primary screen. Percentages were calculated relative to DMSO-treated cells. 70% cell killing (indicated by dotted line) considered a positive hit. **A)** TKIs with wide-ranging activity crossed the positive-hit threshold. **B)** Multiple JAK inhibitors that primarily target JAK2 crossed the positive-hit threshold. HTS, high throughput screen; TKI, tyrosine kinase inhibitor; JAK, Janus kinase.

5.6 Discussion

The poor survival rates of ENKTL patients can be attributed to disease aggressiveness and feebleness of current treatment regimens. Chemotherapy regimens such as CHOP or SMILE have induced initial tumour regression however relapse is common (Au et al., 2009, Wang et al., 2012). In addition, the cytotoxic agents within each regimen, such as etoposide and methotrexate, have toxic side effects, narrow therapeutic windows and are therefore poorly tolerated by patients in particular the elderly. Therefore, there is a need to better understand the disease pathogenesis and try to identify more effective and tolerable therapeutics. We chose to perform an HTS of 4079 compounds, with either clinical or research utility, as a method that can provide information that will assist with such needs.

The effective combination treatment using the BH3 mimetic drugs A-1331852 and S63845 (targeting BCL-X_L and MCL-1, respectively) was identified in the previous chapter of this thesis. This combination was used as a control in an HTS screen that sought to compare the effectiveness of over 4000 other compounds to induce cell death in the panel of EBV-positive NK and T cell lymphoma derived cell lines. HTS approaches can be used as a non-biased method of repurposing drugs for the treatment of other diseases.

The analysis of the primary HTS screen to identify drugs that could induce >70% killing in >1 cell line revealed multiple therapeutic drug groups. Interestingly, tyrosine kinase inhibitors were the most abundant drug group in the top hits list (**table 5.4**). At this stage, our ability to ascertain which individual target(s) was most critical to cell survival was limited due to the broad-spectrum nature of the TKIs. However, greater specificities could

be found within the JAK-targeting compounds — a therapeutic group appearing in **table 5.4** via the JAK2 inhibitor, TG101348.

JAK2 inhibition by TG101348 led to extensive cell killing in all 6 cell lines. We speculate that such cell death was induced by interference with the IL-6/JAK2/STAT3/LMP1 axis, which potentially impacted cell survival via reduced NF-kB activity. An autoregulatory loop of LMP1 via IL-6/IL-6 receptor/JAK driven phosphorylation of STAT3 has previously been described (Chen et al., 2003). This is supported by the presence of functional STAT3-binding sites in the LMP1 promoters, L1-TR and L1-ED (Chen et al., 2001). It has also long been established that LMP1 expression leads to NF-kB activity, which can upregulate expression of pro-survival BCL-2 (Paine et al., 1995, Rowe et al., 1994). An increase in BCL-X_L expression, although it has not yet been shown to occur as a result of LMP1 activity, can also be upregulated by NF-kB activity, such as when induced by CD40 ligation (Wang et al., 1995, Lee et al., 1999). With such pathways in mind, it is not surprising to see JAK2 inhibition, the primary JAK kinase associated with the IL-6 receptor, lead to cell death in the cell line panel examined here. We speculate that the mechanism of the observed cell killing is due to a reduction of activity in the LMP1/IL-6 feedback loop and therefore a reduction in the maintenance of pro-survival BCL-2 family members (i.e. BCL-X_L).

Although the BCL-X_L inhibitor A-1331852 was not included in the drug library used for the above drug screen, another BCL-X_L targeting BH3 mimetic compound, ABT-737, was included and did induce at least 70% cell killing in all 6 cell lines as would be predicted. Encouragingly, the BCL-2 targeting BH3 mimetic ABT-199 did not reach this cell killing

threshold in any of the 6 EBV-positive T and NK cell lines, which is in agreement with our previous data (**chapter 4, figure 4.9**).

Interestingly, drug inhibition of JAK3 had minimal impact on the viability of the ENKTL cell lines tested. Such compounds would interfere with the IL-2/JAK3/STAT5/BCL-X_L axis meaning that this pathway may not be as important as the IL-6/JAK2/STAT3/LMP1 axis discussed above. However, we showed that IL-2 is required for BCL-X_L maintenance in our cell lines, but this does not agree with the JAK3 inhibition data. This suggests that the cells require IL-2 for LMP1 maintenance more so than JAK3/STAT5-mediated regulation of BCL-X_L. IL-2 stimulation of EBV-positive T and NK cells is known to control the expression of LMP1 (Takahara et al., 2006). In models of CAEBV where both EBV-infected cells and patient-derived PBMCs were xenografted into NOG mice, EBV-positive T/NK cells did not proliferate when normal patient $CD4^+$ T cells were depleted by OKT-4 monoclonal antibody (Imadome et al., 2011). The authors of this report speculate that this may be due to the abrogation of the cytokine stimulation provided by $CD4^+$ T cells. This is consistent with our findings as such immune cells are the major producers of IL-2 (Nelson, 2004). From the data presented here, it can be inferred that EBV-positive T and NK cells require both IL-6 (autoregulated) and IL-2 (provided by local $CD4^+$ T cells or exogenously *in vitro*) to maintain LMP1 expression for cell survival that is primarily mediated by BCL-X_L.

The requirement for inhibition of both BCL-X_L and MCL-1 but the improbability that these BH3 mimetic drugs can be used in a safe manner presents an interesting problem. An answer to this could be found within the HTS data. The inhibition of BCL-X_L activity/expression may be indirectly achieved via treatment with alternative compounds

(such as a JAK2 inhibitors) which could then be used in combination with the MCL-1 inhibitor, S63845. This would be the more attractive BH3 mimetic to be used in this context, due to its progress into phase I clinical trials (study ID: CL1-64315-001). The combination of JAK2 inhibition with BH3 mimetic drugs, such as ABT-737 (BCL-2, BCL-X_L and BCL-W-targeting compound) has successfully induced apoptosis in erythro-leukaemia cells that contained a JAK2 V617F activating mutation (Will et al., 2010). Such cell killing via JAK2 inhibition was greatly reduced following BIM knockdown, however, this dependence on BIM induction could be overcome by treatment with ABT-737. This finding is encouraging in the context of EBV-positive T and NK cells, as most cell lines express low levels of BIM (**chapter 4, figure 4.8**).

In conclusion, our data support the concept of targeting both BCL-X_L and MCL-1 to induce significant levels of cell killing in EBV-infected T and NK cells. Therapeutic strategies could be designed to target both proteins with BH3 mimetic drugs if this develops into a clinically viable option. Alternatively, the silencing of BCL-X_L indirectly (via the disruption of its regulation) could be effective if combined with the MCL-1 inhibitor, S63845. A combined therapeutic approach is recommended to avoid development of resistance to BH3 mimetic drugs through switching dependency of malignant cells between different pro-survival BCL-2 family members.

6. Final discussion and future directions

The focus of this thesis has been on the pathogenesis of the EBV-associated T and NK cell lymphoproliferative diseases, ENKTL and CAEBV. As discussed in previous chapters, the low survival rates in patients receiving standard chemotherapy-based treatments has demanded investigation into the mechanism(s) behind such resistance and into novel alternative therapeutic strategies (Vose et al., 2008, Au et al., 2009). The limited literature available on ENKTL and CAEBV has been a result of the relative rarity of these diseases compared to other EBV-associated disease of B cell or epithelial cell origin. Consequently, the availability of fewer cell lines, mouse models and primary patient material has curbed our knowledge on disease pathogenesis. Hence, my broad research aims were defined as follows:

1) To characterise and validate the use of currently available ENKTL and CAEBV cell lines as the primary disease model within the field.

2) To determine the mechanism of resistance of ENKTLs and CAEBVs to current chemotherapeutics.

3) To identify novel susceptibilities of ENKTL and CAEBV derived cell lines that could be exploited therapeutically in the future.

Firstly, a comprehensive collection of ENKTL/CAEBV cell lines was acquired and then characterised for cellular and viral gene expression patterns. These cell lines were reported

to be a representative cross-section of the disease in terms of cellular phenotypes, including tumours of NK cell, αβ T cell or γδ T cell origin. We confirmed that the cell lines satisfactorily represented published clinical observations for the tumours in terms of cellular phenotype. Furthermore, such T and NK cell lines were validated as EBV infected and displaying a latency II phenotype, in accordance with the literature (Harabuchi et al., 1996, van Gorp et al., 1996, Chiang et al., 1996). The viral oncogene, LMP1, which is likely a major contributor to pathogenesis, was found to be expressed at varying levels across the cell line panel.

Secondly, these cells demonstrated resistance to apoptotic induction when treated with clinically relevant genotoxic compounds. Although the literature favoured the hypothesis that the multi-drug efflux pump, p-glycoprotein, was implicated in the resistance to such compounds, we found that p-glycoprotein expression and function was inconsistent across the cell lines and therefore could not be entirely responsible for the universal resistance to chemotherapeutics observed in all cell lines. Given the cell lines did not respond to chemotherapeutics that induce p53 or induction of p53 using the MDM2 antagonist nutlin-3a, we examined the mutational status of the p53 gene in the ENKTL/CAEBV cell lines. Surprising we found mutations in the DNA binding domain of p53 in only the MEC04 cell line and therefore we hypothesised that the p53 tumour suppressor pathway was inactivated by other, as yet, unidentified mechanisms. Given the p53 pathway appeared non-functional in the cell lines, we decided to examine the role of the downstream BCL-2 family of proteins in the sustained survival of the panel of cell lines using several BH3-mimetics that have specificity for the different BCL-2 pro-survival proteins. Using the BCL-

X_L specific inhibitor, A-1331852, we found that the anti-apoptotic protein, BCL-X_L, was a major survival factor in ENKTL/CAEBV cell lines grown in culture. Following the establishment of a protocol for xenograft mouse models of ENKTL, treatment with A-1331852 was shown to be effective in delaying tumour latency *in vivo* for some transplanted cell lines. However, following transplantation of some cell lines into NSG mice, A-1331852 was less effective at delaying tumour growth and *in vitro* experiments showed that IL-2 withdrawal (as would occur following *in vivo* transplantation) reduced the dependency of the cells on BCL-X_L. In some cell backgrounds, the absence of IL-2 exposure led to the switching of survival dependency from BCL-X_L to the closely related anti-apoptotic protein, MCL-1. This raised the possibility that a more accurate xenograft mouse model would require constitutive human IL-2 signalling or alternatively combined inhibition of both BCL-X_L and MCL-1, by A-1331852 and S63845, would be most effective. Importantly, this combination of BH3 mimetics was shown to be highly potent *in vitro*.

Thirdly, a high-throughput screen (HTS) of over 4000 compounds was performed to identify compounds for novel use in ENKTL and CAEBV. A list of potent compounds were identified where, after validation studies, these can be applied in the pre-clinical models established earlier. The potency of a subset of kinase inhibitors, targeting JAK2, was clear across all tested cell lines where we speculate this could be due to the interference of a signalling axis centrally involving LMP1.

Collectively, these findings suggested that targeting of apoptotic pathways downstream of p53 would be a good therapeutic option. Select BH3 mimetics proved effective both *in vitro* and, to a certain degree, *in vivo* and therefore may hold clinical potential for ENKTL/CAEBV.

As discussed in previous chapters, the effective combination of both BCL-X_L-targeting and MCL-1-targeting agents may not be a clinically viable option. In fact, the potential for dose-limiting thrombocytopenia with BCL-X_L inhibitors even when used as monotherapy could be an obstacle (Lessene et al., 2013). Perhaps the future for ENKTL and CAEBV, as is the case with many other diseases and especially solid organ cancers, is in the combination of BH3 mimetics with other therapies.

There are numerous examples where BH3 mimetics have been combined with various anti-cancer treatments such as chemotherapy agents or oncogenic kinase inhibitors in cell lines and in animal models. For example, ABT-737 has been shown to be effective when combined with etoposide or cisplatin in mouse models of SCLC and NSCLC, respectively (Hann et al., 2008, Kim et al., 2017). The combination of ABT-737 with multiple kinase inhibitors targeting EGFR, MEK, JAK1 or JAK2 has proved effective in a broad range of cell lines of epithelial and haematopoietic origin (Cragg et al., 2007, Cragg et al., 2008, Will et al., 2010, Senkevitch et al., 2018). The MCL-1 targeting BH3-mimetic S63845 was also shown to effectively synergise with various kinase inhibitors to induce cell death in *in vitro* models of breast cancer, NSCLC and melanoma (Kotschy et al., 2016).

The pre-clinical studies are compelling and, as such, Phase I clinical trials using BH3 mimetics in combination with other chemotherapeutics have commenced. In human clinical trials, phase I studies have been completed using a combination of gemcitabine and ABT-263 (the orally bioavailable analogue of ABT-737) in various solid tumour settings including NSCLC, pancreatic and ovarian carcinoma (Cleary et al., 2014). Safety studies have been performed in CLL patients using ABT-199 in combination with the hypomethylating

agent, 5-azocytidine, and with the therapeutic monoclonal antibody, rituximab, which targets the B cell-specific marker CD20 (Seymour et al., 2017).

In terms of ENKTL/CAEBV, we hope that the results of the drug screen will identify novel drugs or identify critical pathways that could be exploited therapeutically for the treatment of these diseases. We will then test these drugs alone or in combination with BH3 mimetics in the pre-clinical models of ENKTL that we have established.

Whilst the xenograft model in immune-deficient mice that has been described in this thesis has been informative, certain technical limitations must be overcome if we want to extensively test the therapeutic potential of novel drug combinations. The importance of cytokine signalling in this disease has been demonstrated, firstly by our data regarding IL-2 withdrawal influencing BCL-X_L versus MCL-1 dependency and secondly the body of evidence in the literature that reports that EBV induces extensive cytokine induction in T and NK cells (Chuang et al., 2005, Lay et al., 2003). The supplementation of signalling factors, like IL-2, could be delivered to xenografted mice exogenously as has been done in other mouse models (Foussat et al., 2004, Ohnishi et al., 1990). Alternatively, the manipulation of the cell lines pre-transplantation, for example inducing the cells to overexpress IL-2 themselves from a lentivirus could be considered. Extending our models of disease to include patient-derived xenografts (PDX) into immune-deficient mice would also be useful and informative if sufficient patient material was available. However, these models may also be affected by the dependency of the tumour cells on human IL-2. Nevertheless, PDXs have been greatly utilised in cancers where patient material has not been limiting such as AML, large B cell lymphoma, pancreatic carcinoma and colorectal

carcinoma (Lai et al., 2017). The benefits of PDX models extend beyond pre-clinical drug studies, and have provided insights into tumour heterogeneity and metastasis, however it remains uncertain whether such methodologies could be adopted in the field of EBV-associated T and NK cell disease.

The experiments described in this thesis provide good preliminary evidence regarding the promising therapeutic potential of certain BH3 mimetics and the potential role of the viral protein LMP1 in maintaining cell survival. The data also indicate that the use of JAK2 inhibiting compounds warrants closer investigation. However, to truly achieve our overarching research goal of finding new effective therapeutic options for patients with ENKTL, we need to delve deeper into the underlying mechanistic details of these observations.

To achieve such goals, the adoption of new technologies, such as CRISPR/Cas9 gene-editing, could prove valuable. Investigations into the contribution of EBV in disease pathogenesis and/or cellular transformation has classically been performed by the generation of mutant viruses, lacking specific genes of interest, and then the transformation of readily infectible primary B cells *in vitro* (Kaye et al., 1993, Feederle et al., 2011a, Chen et al., 2006). However, due to our lack of understanding of the mechanism of EBV infection of T and NK cells, the adoption of this technique is not transferable. Also, various studies in T and NK cells have investigated the role of LMP1 in this disease and demonstrated that LMP1 can interfere with TNFα production and NF-□B signalling (Lay et al., 2003, Takada et al., 2017). However, these functional studies have artificially overexpressed LMP1 in established and already immortalised EBV-negative cell lines.

Although these experiments have proved to be informative, more can still be learned of the contribution of LMP1 and other latent viral genes in the context of EBV-dependent/transformed cells, such as the panel of ENKTL/CAEBV cell lines collected here, using more biologically relevant systems.

To this end, an alternate approach we would favour to investigate the role of EBV in infected tumour cells is to directly manipulate the EBV genome already residing within the ENKTL and CAEBV cells to induce genetic alterations. With encouraging results, CRISPR/Cas9 technology has been utilised to target EBV and other herpesviruses which was first described in 2014 (Wang and Quake, 2014). In this paper, the authors attempted to genetically target the EBV genome to eradicate it from cells as a therapeutic antiviral strategy. Typically, CRISPR/Cas9 gene-editing is performed by using either a single or a pair of small guide RNA (sgRNA) molecules which guide the Cas9 endonuclease to the intended location in the DNA. Here, Cas9 induces double stranded DNA breaks and subsequently insertions or deletions are introduced via the imperfect DNA repair process of non-homologous end joining (NHEJ). Interestingly, the above-mentioned report introduced 7 sgRNAs targeting different regions of the EBV genome, two of which targeted repeat regions, to induce numerous cleavage points throughout the viral DNA. This experimental design was intended to induce extensive and irreparable damage to the viral genome resulting in loss of EBV from the BL cells (Raji cell line) in which the experiment was performed. However, despite such an attack on the viral genome, only 65-85% of the viral genomes were cleared. This may be because infected cells carry multiple EBV episomes and this process is just not efficient enough to target every copy of the viral genome,

perhaps due to the expression of Cas9 and the sgRNAs being driven from a transfected expression plasmid as opposed to the more efficient method of lentiviral transduction. Other groups have used a lentiviral system to deliver CRISPR/CAS9 genome editing technology to EBV-infected BL cells to specifically disrupt the viral miRNA regions, BART5 and BART16 (van Diemen et al., 2016). They functionally demonstrated successful targeting of these miRNAs, however, it was not clear whether every viral genome within a given cell contained the disrupted sequence. In the future we would adapt previously reported methodology described (Aubrey et al., 2015), to analyse the contribution of different EBV genes, in particular LMP1 to the sustained growth and chemosensitivity of ENKTL and CAEBV cell lines. We have already quantitated the viral genome copy number of each of the cell lines and so we would initially set up this methodology on cells that had low viral loads, therefore we will have more chance to disrupt the target genes in every copy of the viral genome.

A genetic screen using CRISPR/CAS9 would also be useful to gain a greater understanding of the apoptotic response in ENKTL and CAEBV cells and help identify factors that confer resistance to drugs. To do this, we would infect our ENKTL/CAEBV cells with a whole human genome sgRNA library targeting 18,080 genes (Shalem et al., 2014) and treat the cells with drugs that we identified were effective at killing the cells. We would then rescue the small proportion of cells that do not die and sequence the guide RNAs to determine which genes, when knocked out/mutated, can confer resistance to potential drug combinations. These experiments will enable us to identify biomarkers that would confer innate resistance to

the therapeutics and help identify potential mediators of acquired resistance in treated patients.

The speed of future developments in the field of EBV-associated T and NK cell disease will be aided by the continuing improvement of accurate preclinical models and the development and implementation of new research technologies. In this thesis we have made a contribution to the ENKTL/CAEBV field by validating cell lines and developing a useful, although not yet ideal, xenograft model of disease. Whilst much remains to be understood in such intriguing diseases, we have made exciting discoveries regarding the therapeutic potential of targeting the pro-survival protein BCL-X_L and we hope, with future work, that these findings will have a positive impact on the treatment and prognosis of patients with this devastating disease.

7. References

ADAMS, C. M., KIM, A. S., MITRA, R., CHOI, J. K., GONG, J. Z. & EISCHEN, C. M. 2017a. BCL-W has a fundamental role in B cell survival and lymphomagenesis. *J Clin Invest,* 127**,** 635-650.

ADAMS, C. M., MITRA, R., GONG, J. Z. & EISCHEN, C. M. 2017b. Non-Hodgkin and Hodgkin Lymphomas Select for Overexpression of BCLW. *Clin Cancer Res,* 23**,** 7119-7129.

ADAMS, J. M. & CORY, S. 2007. Bcl-2-regulated apoptosis: mechanism and therapeutic potential. *Curr Opin Immunol,* 19**,** 488-496.

ADLDINGER, H. K., DELIUS, H., FREESE, U. K., CLARKE, J. & BORNKAMM, G. W. 1985. A putative transforming gene of Jijoye virus differs from that of Epstein-Barr virus prototypes. *Virology,* 141**,** 221.

AITKEN, C., SENGUPTA, S. K., AEDES, C., MOSS, D. J. & SCULLEY, T. B. 1994. Heterogeneity within the Epstein-Barr virus nuclear antigen 2 gene in different strains of Epstein-Barr virus. *Journal of General Virology,* 75**,** 95.

ALFIERI, C., BIRKENBACH, M. & KIEFF, E. 1991. Early events in Epstein-Barr virus infection of human B lymphocytes. *Virology,* 181**,** 595-608.

ALLES, J., MENEGATTI, J., MOTSCH, N., HART, M., EICHNER, N., REINHARDT, R., MEISTER, G. & GRASSER, F. A. 2016. miRNA expression profiling of Epstein-Barr virus-associated NKTL cell lines by Illumina deep sequencing. *FEBS Open Bio,* 6**,** 251-63.

AMUNDSON, S. A., MYERS, T. G., SCUDIERO, D., KITADA, S., REED, J. C. & FORNACE, A. J., JR. 2000. An informatics approach identifying markers of chemosensitivity in human cancer cell lines. *Cancer Res,* 60**,** 6101-6110.

ARBOUR, N., VANDERLUIT, J. L., LE GRAND, J. N., JAHANI-ASL, A., RUZHYNSKY, V. A., CHEUNG, E. C., KELLY, M. A., MACKENZIE, A. E., PARK, D. S., OPFERMAN, J. T. & SLACK, R. S. 2008. Mcl-1 is a key regulator of apoptosis during CNS development and after DNA damage. *J Neurosci,* 28**,** 6068-6078.

AU, W. Y., WEISENBURGER, D. D., INTRAGUMTORNCHAI, T., NAKAMURA, S., KIM, W. S., SNG, I., VOSE, J., ARMITAGE, J. O. & LIANG, R. 2009. Clinical differences between nasal and extranasal natural killer/T-cell lymphoma: a study of 136 cases from the International Peripheral T-Cell Lymphoma Project. *Blood,* 113**,** 3931-7.

AUBREY, B. J., KELLY, G. L., KUEH, A. J., BRENNAN, M. S., O'CONNOR, L., MILLA, L., WILCOX, S., TAI, L., STRASSER, A. & HEROLD, M. J. 2015. An inducible lentiviral guide RNA platform enables the identification of tumor-essential genes and tumor-promoting mutations in vivo. *Cell Rep,* 10**,** 1422-32.

AUSTIN, P. J., FLEMINGTON, E., YANDAVA, C. N., STROMINGER, J. L. & SPECK, S. H. 1988. Complex transcription of the Epstein-Barr virus BamHI fragment H rightward open reading frame 1 (BHRF1) in latently and lytically infected B lymphocytes. *Proc Natl Acad Sci U S A,* 85**,** 3678-82.

BAER, R., BANKIER, A. T., BIGGIN, M. D., DEININGER, P. L., FARRELL, P. J., GIBSON, T. J., HATFULL, G., HUDSON, G. S., SATCHWELL, S. C. & SEGUIN, C. 1984. DNA sequence and expression of the B95-8 Epstein-Barr virus genome. *Nature,* 310**,** 207-211.

BAGGSTROM, M. Q., QI, Y., KOCZYWAS, M., ARGIRIS, A., JOHNSON, E. A., MILLWARD, M. J., MURPHY, S. C., ERLICHMAN, C., RUDIN, C. M., GOVINDAN, R., MAYO PHASE, C. & CALIFORNIA, C. 2011. A phase II study of AT-101 (Gossypol) in chemotherapy-sensitive recurrent extensive-stage small cell lung cancer. *J Thorac Oncol,* 6**,** 1757-60.

BAILLY, J. D., MULLER, C., JAFFREZOU, J. P., DEMUR, C., GASSAR, G., BORDIER, C. & LAURENT, G. 1995. Lack of correlation between expression and function of P-glycoprotein in acute myeloid leukemia cell lines. *Leukemia,* 9**,** 799-807.

BASSIG, B. A., AU, W. Y., MANG, O., NGAN, R., MORTON, L. M., IP, D. K., HU, W., ZHENG, T., SEOW, W. J., XU, J., LAN, Q. & ROTHMAN, N. 2016. Subtype-specific incidence rates of lymphoid malignancies in Hong Kong compared to the United States, 2001-2010. *Cancer Epidemiol,* 42**,** 15-23.

BERNHARDT, K., HAAR, J., TSAI, M. H., POIREY, R., FEEDERLE, R. & DELECLUSE, H. J. 2016. A Viral microRNA Cluster Regulates the Expression of PTEN, p27 and of a bcl-2 Homolog. *PLoS Pathog,* 12**,** e1005405.

BEROUKHIM, R., MERMEL, C., PORTER, D., WEI, G., RAYCHAUDHURI, S., DONOVAN, J., BARRETINA, J., BOEHM, J., DOBSON, J., URASHIMA, M., MC HENRY, K., PINCHBACK, R., LIGON, A., CHO, Y.-J., HAERY, L., GREULICH, H., REICH, M., WINCKLER, W., LAWRENCE, M., WEIR, B., TANAKA, K., CHIANG, D., BASS, A., LOO, A., HOFFMAN, C., PRENSNER, J., LIEFELD, T., GAO, Q., YECIES, D., SIGNORETTI, S., MAHER, E., KAYE, F., SASAKI, H., TEPPER, J., FLETCHER, J., TABERNERO, J., BASELGA, J., TSAO, M.-S., DEMICHELIS, F., RUBIN, M., JANNE, P., DALY, M., NUCERA, C., LEVINE, R., EBERT, B., GABRIEL, S., RUSTGI, A., ANTONESCU, C., LADANYI, M., LETAI, A., GARRAWAY, L., LODA, M., BEER, D., TRUE, L., OKAMOTO, A., POMEROY, S., SINGER, S., GOLUB, T., LANDER, E., GETZ, G., SELLERS, W. & MEYERSON, M. 2010. The landscape of somatic copy-number alteration across human cancers. *Nature,* 463**,** 899-905.

BI, X. W., WANG, H., ZHANG, W. W., WANG, J. H., LIU, W. J., XIA, Z. J., HUANG, H. Q., JIANG, W. Q., ZHANG, Y. J. & WANG, L. 2016. PD-L1 is upregulated by EBV-driven LMP1 through NF-kappaB pathway and correlates with poor prognosis in natural killer/T-cell lymphoma. *J Hematol Oncol,* 9**,** 109.

BIRMINGHAM, A., SELFORS, L. M., FORSTER, T., WROBEL, D., KENNEDY, C. J., SHANKS, E., SANTOYO-LOPEZ, J., DUNICAN, D. J., LONG, A., KELLEHER, D., SMITH, Q., BEIJERSBERGEN, R. L., GHAZAL, P. & SHAMU, C. E. 2009. Statistical methods for analysis of high-throughput RNA interference screens. *Nat Methods,* 6**,** 569-75.

BLUME-JENSEN, P., JANKNECHT, R. & HUNTER, T. 1998. The kit receptor promotes cell survival via activation of PI 3-kinase and subsequent Akt-mediated phosphorylation of Bad on Ser136. *Curr Biol,* 8**,** 779-782.

BOLLARD, C. M., AGUILAR, L., STRAATHOF, K. C., GAHN, B., HULS, M. H., ROUSSEAU, A., SIXBEY, J., GRESIK, M. V., CARRUM, G., HUDSON, M., DILLOO, D., GEE, A., BRENNER, M. K. & ROONEY, C. M. 2004. Cytotoxic T Lymphocyte Therapy for Epstein-Barr Virus+ Hodgkin's Disease. *Journal of Experimental Medicine,* 200**,** 1623.

BOLLARD, C. M., GOTTSCHALK, S., HELEN HULS, M., LEEN, A. M., GEE, A. P. & ROONEY, C. M. 2011. Good manufacturing practice-grade cytotoxic T lymphocytes specific for latent membrane proteins (LMP)-1 and LMP2 for patients with Epstein-Barr virus-associated lymphoma. *Cytotherapy,* 13**,** 518-22.

BOLLARD, C. M., GOTTSCHALK, S., TORRANO, V., DIOUF, O., KU, S., HAZRAT, Y., CARRUM, G., RAMOS, C., FAYAD, L., SHPALL, E. J., PRO, B., LIU, H., WU, M. F., LEE, D., SHEEHAN, A. M., ZU, Y., GEE, A. P., BRENNER, M. K., HESLOP, H. E. & ROONEY, C. M. 2014. Sustained complete responses in patients with lymphoma receiving autologous cytotoxic T lymphocytes targeting Epstein-Barr virus latent membrane proteins. *J Clin Oncol,* 32**,** 798-808.

BORZA, C. M. & HUTT-FLETCHER, L. M. 2002. Alternate replication in B cells and epithelial cells switches tropism of Epstein-Barr virus. *Nature Medicine,* 8**,** 594.

BOUILLET, P., CORY, S., ZHANG, L.-C., STRASSER, A. & ADAMS, J. M. 2001. Degenerative disorders caused by Bcl-2 deficiency are prevented by loss of its BH3-only antagonist Bim. *Dev Cell,* 1**,** 645-653.

BOUILLET, P., METCALF, D., HUANG, D. C., TARLINTON, D. M., KAY, T. W., KONTGEN, F., ADAMS, J. M. & STRASSER, A. 1999. Proapoptotic Bcl-2 relative Bim required for certain apoptotic responses, leukocyte homeostasis, and to preclude autoimmunity. *Science,* 286**,** 1735-8.

BOUILLET, P., PURTON, J. F., GODFREY, D. I., ZHANG, L.-C., COULTAS, L., PUTHALAKATH, H., PELLEGRINI, M., CORY, S., ADAMS, J. M. & STRASSER, A. 2002. BH3-only Bcl-2 family member Bim is required for apoptosis of autoreactive thymocytes. *Nature,* 415**,** 922-926.

BRAEUNINGER, A., KUPPERS, R., STRICKLER, J. G., WACKER, H. H., RAJEWSKY, K. & HANSMANN, M. L. 1997. Hodgkin and Reed-Sternberg cells in lymphocyte predominant Hodgkin disease represent clonal populations of germinal center-derived tumor B cells. *Proceedings of the National Academy of Sciences of the United States of America,* 94**,** 9337-42.

BRAUNINGER, A., SCHMITZ, R., BECHTEL, D., RENNE, C., HANSMANN, M. L. & KUPPERS, R. 2006. Molecular biology of Hodgkin's and Reed/Sternberg cells in Hodgkin's lymphoma. *International Journal of Cancer,* 118**,** 1853-61.

BREDEL, M., BREDEL, C., JURIC, D., HARSH, G. R., VOGEL, H., RECHT, L. D. & SIKIC, B. I. 2005. High-resolution genome-wide mapping of genetic alterations in human glial brain tumors. *Cancer Res,* 65**,** 4088-96.

BRIEN, G., TRESCOL-BIEMONT, M. C. & BONNEFOY-BERARD, N. 2007. Downregulation of Bfl-1 protein expression sensitizes malignant B cells to apoptosis. *Oncogene,* 26**,** 5828-5832.

BROOKS, L., YAO, Q. Y., RICKINSON, A. B. & YOUNG, L. S. 1992. Epstein-Barr virus latent gene transcription in nasopharyngeal carcinoma cells: coexpression of EBNA1, LMP1, and LMP2 transcripts. *Journal of Virology,* 66**,** 2689-97.

CALIN, G. A., FERRACIN, M., CIMMINO, A., DI LEVA, G., SHIMIZU, M., WOJCIK, S. E., IORIO, M. V., VISONE, R., SEVER, N. I., FABBRI, M., IULIANO, R., PALUMBO, T., PICHIORRI, F., ROLDO, C., GARZON, R., SEVIGNANI, C., RASSENTI, L., ALDER, H., VOLINIA, S., LIU, C. G., KIPPS, T. J., NEGRINI, M. & CROCE, C. M. 2005. A MicroRNA signature associated with prognosis and progression in chronic lymphocytic leukemia. *N Engl J Med,* 353**,** 1793-1801.

CAMARGO, M. C., MURPHY, G., KORIYAMA, C., PFEIFFER, R. M., KIM, W. H., HERRERA-GOEPFERT, R., CORVALAN, A. H., CARRASCAL, E., ABDIRAD, A., ANWAR, M., HAO, Z., KATTOOR, J., YOSHIWARA-WAKABAYASHI, E., EIZURU, Y., RABKIN, C. S. & AKIBA, S. 2011. Determinants of Epstein-Barr virus-positive gastric cancer: an international pooled analysis. *Br J Cancer,* 105**,** 38-43.

CAMPBELL, K. J., BATH, M. L., TURNER, M. L., VANDENBERG, C. J., BOUILLET, P., METCALF, D., SCOTT, C. L. & CORY, S. 2010. Elevated Mcl-1 perturbs lymphopoiesis, promotes transformation of hematopoietic stem/progenitor cells, and enhances drug resistance. *Blood,* 116**,** 3197-207.

CARTRON, P. F., GALLENNE, T., BOUGRAS, G., GAUTIER, F., MANERO, F., VUSIO, P., MEFLAH, K., VALLETTE, F. M. & JUIN, P. 2004. The first alpha helix of Bax plays a necessary role in its ligand-induced activation by the BH3-only proteins Bid and PUMA. *Mol Cell,* 16**,** 807-818.

CASTLE, V. P., HEIDELBERGER, K. P., BROMBERG, J., OU, X., DOLE, M. & NUÑEZ, G. 1993. Expression of the apoptosis-suppressing protein *bcl*-2 in neuroblastoma is associated with unfavorable histology and N-*myc* amplification. *Am J Pathol,* 143**,** 1543-1550.

CHAI, J., DU, C., WU, J. W., KYIN, S., WANG, X. & SHI, Y. 2000. Structural and biochemical basis of apoptotic activation by Smac/DIABLO. *Nature,* 406**,** 855-862.

CHAN, C. W., CHIANG, A. K., CHAN, K. H. & LAU, A. S. 2003. Epstein-Barr virus-associated infectious mononucleosis in Chinese children. *Pediatr Infect Dis J,* 22**,** 974-8.

CHANG, T. K., WEBER, G. F., CRESPI, C. L. & WAXMAN, D. J. 1993. Differential activation of cyclophosphamide and ifosphamide by cytochromes P-450 2B and 3A in human liver microsomes. *Cancer Res,* 53**,** 5629-37.

CHEN, A., ZHAO, B., KIEFF, E., ASTER, J. C. & WANG, F. 2006. EBNA-3B- and EBNA-3C-regulated cellular genes in Epstein-Barr virus-immortalized lymphoblastoid cell lines. *J Virol,* 80**,** 10139-50.

CHEN, H., HUTT-FLETCHER, L., CAO, L. & HAYWARD, S. D. 2003. A positive autoregulatory loop of LMP1 expression and STAT activation in epithelial cells latently infected with Epstein-Barr virus. *J Virol,* 77**,** 4139-48.

CHEN, H., LEE, J. M., ZONG, Y., BOROWITZ, M., NG, M. H., AMBINDER, R. F. & HAYWARD, S. D. 2001. Linkage between STAT regulation and Epstein-Barr virus gene expression in tumors. *J Virol,* 75**,** 2929-37.

CHEN, S. Y., LU, J., SHIH, Y. C. & TSAI, C. H. 2002. Epstein-Barr virus latent membrane protein 2A regulates c-Jun protein through extracellular signal-regulated kinase. *J Virol,* 76**,** 9556-61.

CHESNOKOVA, L. S., NISHIMURA, S. L. & HUTT-FLETCHER, L. M. 2009. Fusion of epithelial cells by Epstein-Barr virus proteins is triggered by binding of viral glycoproteins gHgL to integrins alphavbeta6 or alphavbeta8. *Proc Natl Acad Sci U S A,* 106**,** 20464-9.

CHEUNG, W. C., KIM, J. S., LINDEN, M., PENG, L., VAN NESS, B., POLAKIEWICZ, R. D. & JANZ, S. 2004. Novel targeted deregulation of c-Myc cooperates with Bcl-X(L) to cause plasma cell neoplasms in mice. *J Clin Invest,* 113**,** 1763-1773.

CHIANG, A. K., TAO, Q., SRIVASTAVA, G. & HO, F. C. 1996. Nasal NK- and T-cell lymphomas share the same type of Epstein-Barr virus latency as nasopharyngeal carcinoma and Hodgkin's disease. *Int J Cancer,* 68**,** 285-90.

CHO-VEGA, J. H., RASSIDAKIS, G. Z., ADMIRAND, J. H., OYARZO, M., RAMALINGAM, P., PARAGUYA, A., MCDONNELL, T. J., AMIN, H. M. & MEDEIROS, L. J. 2004. MCL-1 expression in B-cell non-Hodgkin's lymphomas. *Hum Pathol,* 35**,** 1095-1100.

CHU, Y., YAHR, A., HUANG, B., AYELLO, J., BARTH, M. & M, S. C. 2017. Romidepsin alone or in combination with anti-CD20 chimeric antigen receptor expanded natural killer cells targeting Burkitt lymphoma in vitro and in immunodeficient mice. *Oncoimmunology,* 6**,** e1341031.

CHUANG, H. C., LAY, J. D., HSIEH, W. C., WANG, H. C., CHANG, Y., CHUANG, S. E. & SU, I. J. 2005. Epstein-Barr virus LMP1 inhibits the expression of SAP gene and upregulates Th1 cytokines in the pathogenesis of hemophagocytic syndrome. *Blood,* 106**,** 3090-6.

CHUANG, H. C., WANG, J. M., HSIEH, W. C., CHANG, Y. & SU, I. J. 2008. Up-regulation of activating transcription factor-5 suppresses SAP expression to activate T cells in hemophagocytic syndrome associated with Epstein-Barr virus infection and immune disorders. *Am J Pathol,* 173**,** 1397-405.

CIMMINO, A., CALIN, G. A., FABBRI, M., IORIO, M. V., FERRACIN, M., SHIMIZU, M., WOJCIK, S. E., AQEILAN, R. I., ZUPO, S., DONO, M., RASSENTI, L., ALDER, H., VOLINIA, S., LIU, C. G., KIPPS, T. J., NEGRINI, M. & CROCE, C. M. 2005. miR-15 and miR-16 induce apoptosis by targeting BCL2. *Proc Natl Acad Sci U S A,* 102**,** 13944-13949.

CLEARY, J. M., LIMA, C. M., HURWITZ, H. I., MONTERO, A. J., FRANKLIN, C., YANG, J., GRAHAM, A., BUSMAN, T., MABRY, M., HOLEN, K., SHAPIRO, G. I. & URONIS, H. 2014. A phase I clinical trial of navitoclax, a targeted high-affinity Bcl-2 family inhibitor, in combination with gemcitabine in patients with solid tumors. *Invest New Drugs,* 32**,** 937-45.

COHEN, J. I., JAFFE, E. S., DALE, J. K., PITTALUGA, S., HESLOP, H. E., ROONEY, C. M., GOTTSCHALK, S., BOLLARD, C. M., RAO, V. K., MARQUES, A., BURBELO, P. D., TURK, S. P., FULTON, R., WAYNE, A. S., LITTLE, R. F., CAIRO, M. S., EL-MALLAWANY, N. K., FOWLER, D., SPORTES, C., BISHOP, M. R., WILSON, W. & STRAUS, S. E. 2011. Characterization and treatment of chronic active Epstein-Barr virus disease: a 28-year experience in the United States. *Blood,* 117**,** 5835-49.

COLEMAN, C. B., DAUD, II, OGOLLA, S. O., RITCHIE, J. A., SMITH, N. A., SUMBA, P. O., DENT, A. E. & ROCHFORD, R. 2017. Epstein-Barr Virus Type 2 Infects T Cells in Healthy Kenyan Children. *J Infect Dis,* 216**,** 670-677.

COLEMAN, C. B., WOHLFORD, E. M., SMITH, N. A., KING, C. A., RITCHIE, J. A., BARESEL, P. C., KIMURA, H. & ROCHFORD, R. 2015. Epstein-Barr virus type 2 latently infects T cells, inducing an atypical activation characterized by expression of lymphotactic cytokines. *J Virol,* 89**,** 2301-12.

COPPO, P., GOUILLEUX-GRUART, V., HUANG, Y., BOUHLAL, H., BOUAMAR, H., BOUCHET, S., PERROT, C., VIEILLARD, V., DARTIGUES, P., GAULARD, P., AGBALIKA, F., DOUAY, L., LASSOUED, K. & GORIN, N. C. 2009. STAT3 transcription factor is constitutively activated and is oncogenic in nasal-type NK/T-cell lymphoma. *Leukemia,* 23**,** 1667-78.

COULTAS, L., BOUILLET, P., STANLEY, E. G., BRODNICKI, T. C., ADAMS, J. M. & STRASSER, A. 2004. Proapoptotic BH3-only Bcl-2 family member Bik/Blk/Nbk is expressed in hemopoietic and endothelial cells but is redundant for their programmed death. *Mol Cell Biol,* 24**,** 1570-1581.

COULTAS, L., TERZANO, S., THOMAS, T., VOSS, A., REID, K., STANLEY, E. G., SCOTT, C. L., BOUILLET, P., BARTLETT, P., HAM, J., ADAMS, J. M. & STRASSER, A. 2007. Hrk/DP5 contributes to the apoptosis of select neuronal populations but is dispensable for haematopoietic cell apoptosis. *J Cell Sci,* 120**,** 2044-2052.

CRAGG, M. S., JANSEN, E. S., COOK, M., STRASSER, A. & SCOTT, C. L. 2008. Treatment of B-RAF mutant human tumor cells with a MEK inhibitor requires Bim and is enhanced by a BH3 mimetic. *J Clin Invest,* 118**,** 3651-3659.

CRAGG, M. S., KURODA, J., PUTHALAKATH, H., HUANG, D. C. S. & STRASSER, A. 2007. Gefitinib-Induced Killing of NSCLC Cell Lines Expressing Mutant *EGFR* Requires Bim and Can Be Enhanced by BH3 Mimetics. *PLoS Med,* 4**,** 1681-89.

CRUZ-MUNOZ, W., JARAMILLO, M. L., MAN, S., XU, P., BANVILLE, M., COLLINS, C., NANTEL, A., FRANCIA, G., MORGAN, S. S., CRANMER, L. D., O'CONNOR-MCCOURT, M. D. & KERBEL, R. S. 2012. Roles for endothelin receptor B and BCL2A1 in spontaneous CNS metastasis of melanoma. *Cancer Res,* 72**,** 4909-19.

CUMBER, P. M., JACOBS, A., HOY, T., WHITTAKER, J. A., TSURUO, T. & PADUA, R. A. 1991. Increased drug accumulation ex vivo with cyclosporin in chronic lymphatic leukemia and its relationship to epitope masking of P-glycoprotein. *Leukemia,* 5**,** 1050-3.

D'ACQUISTO, F. & CROMPTON, T. 2011. CD3+CD4-CD8- (double negative) T cells: saviours or villains of the immune response? *Biochem Pharmacol,* 82**,** 333-40.

D'SOUZA, B., ROWE, M. & WALLS, D. 2000. The bfl-1 gene is transcriptionally upregulated by the Epstein-Barr virus LMP1, and its expression promotes the survival of a Burkitt's lymphoma cell line. *J Virol,* 74**,** 6652-8.

DAI, H., SMITH, A., MENG, X. W., SCHNEIDER, P. A., PANG, Y. P. & KAUFMANN, S. H. 2011. Transient binding of an activator BH3 domain to the Bak BH3-binding groove initiates Bak oligomerization. *J Cell Biol,* 194**,** 39-48.

DAI, J. & LUFTIG, M. A. 2018. Intracellular BH3 Profiling Reveals Shifts in Antiapoptotic Dependency in Human B Cell Maturation and Mitogen-Stimulated Proliferation. *J Immunol,* 200**,** 1727-1736.

DAIKOKU, T., KUDOH, A., FUJITA, M., SUGAYA, Y., ISOMURA, H., SHIRATA, N. & TSURUMI, T. 2005. Architecture of replication compartments formed during Epstein-Barr virus lytic replication. *J Virol,* 79**,** 3409-18.

DAMBAUGH, T., HENNESSY, K., CHAMNANKIT, L. & KIEFF, E. 1984. U2 region of Epstein-Barr virus DNA may encode Epstein-Barr nuclear antigen 2. *Proceedings of the National Academy of Sciences U.S.A.,* 81**,** 7632-7636.

DE GRAAF, D., SHARMA, R. C., MECHETNER, E. B., SCHIMKE, R. T. & RONINSON, I. B. 1996. P-glycoprotein confers methotrexate resistance in 3T6 cells with deficient carrier-mediated methotrexate uptake. *Proc Natl Acad Sci U S A,* 93**,** 1238-42.

DE MIGUEL, D., LEMKE, J., ANEL, A., WALCZAK, H. & MARTINEZ-LOSTAO, L. 2016. Onto better TRAILs for cancer treatment. *Cell Death Differ,* 23**,** 733-47.

DE PAOLI, P., GENNARI, D., MARTELLI, P., CAVARZERANI, V., COMORETTO, R. & SANTINI, G. 1990. Gamma delta T cell receptor-bearing lymphocytes during Epstein-Barr virus infection. *J Infect Dis,* 161**,** 1013-6.

DEBRINCAT, M. A., JOSEFSSON, E. C., JAMES, C., HENLEY, K. J., ELLIS, S., LEBOIS, M., BETTERMAN, K. L., LANE, R. M., ROGERS, K. L., WHITE, M. J., ROBERTS, A. W., HARVEY, N. L., METCALF, D. & KILE, B. T. 2012. Mcl-1 and Bcl-x(L) coordinately regulate megakaryocyte survival. *Blood,* 119**,** 5850-8.

DELECLUSE, H. J., HILSENDEGEN, T., PICH, D., ZEIDLER, R. & HAMMERSCHMIDT, W. 1998. Propagation and recovery of intact, infectious Epstein-Barr virus from prokaryotic to human cells. *Proc Natl Acad Sci U S A,* 95**,** 8245-50.

DENG, J., CARLSON, N., TAKEYAMA, K., DAL CIN, P., SHIPP, M. & LETAI, A. 2007. BH3 profiling identifies three distinct classes of apoptotic blocks to predict response to ABT-737 and conventional chemotherapeutic agents. *Cancer Cell,* 12**,** 171-185.

DEVERAUX, Q. L., TAKAHASHI, R., SALVESEN, G. S. & REED, J. C. 1997. X-linked IAP is a direct inhibitor of cell-death proteases. *Nature,* 388**,** 300-304.

DEWSON, G., KRATINA, T., SIM, H. W., PUTHALAKATH, H., ADAMS, J. M., COLMAN, P. M. & KLUCK, R. M. 2008. To trigger apoptosis, Bak exposes its BH3 domain and homodimerizes via BH3:groove interactions. *Mol Cell,* 30**,** 369-80.

DHARNIDHARKA, V. R., WEBSTER, A. C., MARTINEZ, O. M., PREIKSAITIS, J. K., LEBLOND, V. & CHOQUET, S. 2016. Post-transplant lymphoproliferative disorders. *Nat Rev Dis Primers,* 2**,** 15088.

EADIE, L. N., HUGHES, T. P. & WHITE, D. L. 2014. Interaction of the efflux transporters ABCB1 and ABCG2 with imatinib, nilotinib, and dasatinib. *Clin Pharmacol Ther,* 95**,** 294-306.

EADIE, L. N., HUGHES, T. P. & WHITE, D. L. 2016. ABCB1 Overexpression Is a Key Initiator of Resistance to Tyrosine Kinase Inhibitors in CML Cell Lines. *PLoS One,* 11**,** e0161470.

EGLE, A., HARRIS, A. W., BOUILLET, P. & CORY, S. 2004. Bim is a suppressor of Myc-induced mouse B cell leukemia. *Proc Natl Acad Sci U S A,* 101**,** 6164-6169.

EISCHEN, C. M., WEBER, J. D., ROUSSEL, M. F., SHERR, C. J. & CLEVELAND, J. L. 1999. Disruption of the ARF-Mdm2-p53 tumor suppressor pathway in Myc-induced lymphomagenesis. *Genes and Development,* 13**,** 2658-2669.

ELIOPOULOS, A. G. & YOUNG, L. S. 2001. LMP1 structure and signal transduction. *Semin Cancer Biol,* 11**,** 435-44.

EPSTEIN, M. A., BARR, Y. M. & ACHONG, B. G. 1964. Virus particles in cultured lymphoblasts from Burkitt's lymphoma. *Lancet,* i**,** 702.

ERLACHER, M., LAABI, V., MANZL, C., BOCK, G., TZANKOV, A., HAECKER, G., STRASSER, A. & VILLUNGER, A. 2006. Puma cooperates with Bim, the rate-limiting BH3-only protein in cell death during lymphocyte development, in apoptosis induction. *J Exp Med,* 203**,** 2939-2951.

ESTEVE-ARENYS, A. & ROUE, G. 2018. BFL-1 expression determines the efficacy of venetoclax in MYC+/BCL2+ double hit lymphoma. *Oncoscience,* 5**,** 59-61.

FAHRAEUS, R., FU, H. L., ERNBERG, I., FINKE, J., ROWE, M., KLEIN, G., FALK, K., NILSSON, E., YADAV, M., BUSSON, P., TURSZ, T. & KALLIN, B. 1988. Expression of Epstein-Barr virus-encoded proteins in nasopharyngeal carcinoma. *International Journal of Cancer,* 42**,** 329-338.

FANG, W., MUELLER, D. L., PENNELL, C. A., RIVARD, J. J., LI, Y. S., HARDY, R. R., SCHLISSEL, M. S. & BEHRENS, T. W. 1996. Frequent aberrant immunoglobulin gene rearrangements in pro-B cells revealed by a bcl-x_L transgene. *Immunity,* 4**,** 291-299.

FEEDERLE, R., HAAR, J., BERNHARDT, K., LINNSTAEDT, S. D., BANNERT, H., LIPS, H., CULLEN, B. R. & DELECLUSE, H. J. 2011a. The members of an Epstein-Barr virus microRNA cluster cooperate to transform B lymphocytes. *J Virol,* 85**,** 9801-10.

FEEDERLE, R., LINNSTAEDT, S. D., BANNERT, H., LIPS, H., BENCUN, M., CULLEN, B. R. & DELECLUSE, H. J. 2011b. A viral microRNA cluster strongly potentiates the transforming properties of a human herpesvirus. *PLoS Pathog,* 7**,** e1001294.

FINGEROTH, J. D., WEIS, J. J., TEDDER, T. F., STROMINGER, J. L., BIRO, P. A. & FEARON, D. T. 1984. Epstein-Barr virus receptor of human B lymphocytes is the C3d receptor CR2. *Proceedings of the National Academy of Sciences of the United States of America,* 81**,** 4510-4.

FLINN, I. W., BRUNVAND, M., CHOI, M. Y., DYER, M. J. S., GRIBBEN, J., HILLMEN, P., JONES, J., LI, Y., MOBASHER, M., VOSGANIAN, G. & KIPPS, T. J. 2015. Safety and Efficacy of a Combination of Venetoclax (GDC-0199/ABT-199) and Obinutuzumab in Patients with Relapsed/Refractory or Previously Untreated Chronic Lymphocytic Leukemia - Results from a Phase 1b Study (GP28331). *Blood,* 126**,** 494--494.

FORBES, S. A., BEARE, D., GUNASEKARAN, P., LEUNG, K., BINDAL, N., BOUTSELAKIS, H., DING, M., BAMFORD, S., COLE, C., WARD, S., KOK, C. Y., JIA, M., DE, T., TEAGUE, J. W., STRATTON, M. R., MCDERMOTT, U. & CAMPBELL, P. J. 2015. COSMIC: exploring the world's knowledge of somatic mutations in human cancer. *Nucleic Acids Res,* 43**,** D805-11.

FORTUNE, J. M. & OSHEROFF, N. 2000. Topoisomerase II as a target for anticancer drugs: when enzymes stop being nice. *Prog Nucleic Acid Res Mol Biol,* 64**,** 221-53.

FOUSSAT, A., BOUCHET-DELBOS, L., COUDERC, J., BERREBI, D., GERMAN-FATTAL, M., MAILLOT, M. C., DURAND-GASSELIN, I., GALANAUD, P., DI SANTO, J. P. & EMILIE, D. 2004. Effects of exogenous IL-2 administration on the homeostasis of CD4+ T lymphocytes. *J Clin Immunol,* 24**,** 503-14.

FOX, C. P., BOUMENDIL, A., SCHMITZ, N., FINEL, H., LUAN, J. J., SUCAK, G., BLAISE, D., FINKE, J., PFLUGER, K. H., VEELKEN, H., GORIN, N. C., POIRE, X., GANSER, A., DREGER, P. & SUREDA, A. 2015. High-dose therapy and autologous stem cell transplantation for extra-nodal NK/T lymphoma in patients from the Western hemisphere: a study from the European Society for Blood and Marrow Transplantation. *Leuk Lymphoma,* 56**,** 3295-300.

FOX, C. P., HAIGH, T. A., TAYLOR, G. S., LONG, H. M., LEE, S. P., SHANNON-LOWE, C., O'CONNOR, S., BOLLARD, C. M., IQBAL, J., CHAN, W. C., RICKINSON, A. B., BELL, A. I. & ROWE, M. 2010. A novel latent membrane 2 transcript expressed in Epstein-Barr virus-positive NK- and T-cell lymphoproliferative disease encodes a target for cellular immunotherapy. *Blood,* 116**,** 3695-704.

FRENZEL, A., LABI, V., CHMELEWSKIJ, W., PLONER, C., GELEY, S., FIEGL, H., TZANKOV, A. & VILLUNGER, A. 2010. Suppression of B-cell lymphomagenesis by the BH3-only proteins Bmf and Bad. *Blood,* 115**,** 995-1005.

FUKUDA, M. & LONGNECKER, R. 2004. Latent membrane protein 2A inhibits transforming growth factor-beta 1-induced apoptosis through the phosphatidylinositol 3-kinase/Akt pathway. *J Virol,* 78**,** 1697-705.

FULDA, S. & DEBATIN, K. M. 2006. Extrinsic versus intrinsic apoptosis pathways in anticancer chemotherapy. *Oncogene,* 25**,** 4798-811.

GARRISON, S. P., JEFFERS, J. R., YANG, C., NILSSON, J. A., HALL, M. A., REHG, J. E., YUE, W., YU, J., ZHANG, L., ONCIU, M., SAMPLE, J. T., CLEVELAND, J. L. & ZAMBETTI, G. P. 2008. Selection against PUMA gene expression in Myc-driven B-cell lymphomagenesis. *Mol Cell Biol,* 28**,** 5391-402.

GEORGE, N. M., EVANS, J. J. & LUO, X. 2007. A three-helix homo-oligomerization domain containing BH3 and BH1 is responsible for the apoptotic activity of Bax. *Genes Dev,* 21**,** 1937-1948.

GESBERT, F. & GRIFFIN, J. D. 2000. Bcr/Abl activates transcription of the *Bcl-X* gene through STAT5. *Blood,* 96**,** 2269-2276.

GHETIE, M. A., PODAR, E. M., GORDON, B. E., PANTAZIS, P., UHR, J. W. & VITETTA, E. S. 1996. Combination immunotoxin treatment and chemotherapy in SCID mice with advanced, disseminated Daudi lymphoma. *Int J Cancer,* 68**,** 93-6.

GLASER, S., LEE, E. F., TROUNSON, E., BOUILLET, P., WEI, A., FAIRLIE, W. D., IZON, D. J., ZUBER, J., RAPPAPORT, A. R., HEROLD, M. J., ALEXANDER, W., LOWE, S. W., ROBB, L. & STRASSER, A. 2012. Anti-apoptotic Mcl-1 is essential for the development and sustained growth of acute myeloid leukemia. *Genes Dev,* 26**,** 120-125.

GOLDSTEIN, L. J., GALSKI, H., FOJO, A., WILLINGHAM, M., LAI, S. L., GAZDAR, A., PIRKER, R., GREEN, A., CRIST, W., BRODEUR, G. M. & ET AL. 1989. Expression of a multidrug resistance gene in human cancers. *J Natl Cancer Inst,* 81**,** 116-24.

GRABOW, S., DELBRIDGE, A. R., VALENTE, L. J. & STRASSER, A. 2014. MCL-1 but not BCL-XL is critical for the development and sustained expansion of thymic lymphoma in p53-deficient mice. *Blood,* 124**,** 3939-46.

GUIKEMA, J. E., SCHUURING, E. & KLUIN, P. M. 2008. Structure and consequences of IGH switch breakpoints in Burkitt lymphoma. *J Natl Cancer Inst Monogr***,** 32-6.

HANADA, M., DELIA, D., AIELLO, A., STADMAUER, E. & REED, J. C. 1993. *bcl*-2 gene hypomethylation and high-level expression in B-cell chronic lymphocytic leukemia. *Blood,* 82**,** 1820-1828.

HANAHAN, D. & WEINBERG, R. A. 2000. The hallmarks of cancer. *Cell,* 100**,** 57-70.

HANAHAN, D. & WEINBERG, R. A. 2011. Hallmarks of cancer: the next generation. *Cell,* 144**,** 646-74.

HANN, C. L., DANIEL, V. C., SUGAR, E. A., DOBROMILSKAYA, I., MURPHY, S. C., COPE, L., LIN, X., HIERMAN, J. S., WILBURN, D. L., WATKINS, D. N. & RUDIN, C. M. 2008. Therapeutic efficacy of ABT-737, a selective inhibitor of BCL-2, in small cell lung cancer. *Cancer Res,* 68**,** 2321-8.

HAPPO, L., PHIPSON, B., SMYTH, G. K., STRASSER, A. & SCOTT, C. L. 2012. Neither loss of Bik alone, nor combined loss of Bik and Noxa, accelerate murine lymphoma development or render lymphoma cells resistant to DNA damaging drugs. *Cell Death Dis,* 3**,** e306.

HARABUCHI, Y., IMAI, S., WAKASHIMA, J., HIRAO, M., KATAURA, A., OSATO, T. & KON, S. 1996. Nasal T-cell lymphoma causally associated with Epstein-Barr virus: clinicopathologic, phenotypic, and genotypic studies. *Cancer,* 77**,** 2137-49.

HARABUCHI, Y., TAKAHARA, M., KISHIBE, K., MORIAI, S., NAGATO, T. & ISHII, H. 2009. Nasal natural killer (NK)/T-cell lymphoma: clinical, histological, virological, and genetic features. *Int J Clin Oncol,* 14**,** 181-90.

HARRIS, A. W., PINKERT, C. A., CRAWFORD, M., LANGDON, W. Y., BRINSTER, R. L. & ADAMS, J. M. 1988. The E mu-myc transgenic mouse. A model for high-incidence spontaneous lymphoma and leukemia of early B cells. *J Exp Med,* 167**,** 353-71.

HARRIS, S. L. & LEVINE, A. J. 2005. The p53 pathway: positive and negative feedback loops. *Oncogene,* 24**,** 2899-908.

HATAKEYAMA, S., HAMASAKI, A., NEGISHI, I., LOH, D. Y., SENDO, F. & NAKAYAMA, K. 1998. Multiple gene duplication and expression of mouse bcl-2-related genes, A1. *Int Immunol,* 10**,** 631-637.

HAVERKOS, B. M., COLEMAN, C., GRU, A. A., PAN, Z., BRAMMER, J., ROCHFORD, R., MISHRA, A., OAKES, C. C., BAIOCCHI, R. A., FREUD, A. G. & PORCU, P. 2017. Emerging insights on the pathogenesis and treatment of extranodal NK/T cell lymphomas (ENKTL). *Discov Med,* 23**,** 189-199.

HAVERKOS, B. M., PAN, Z., GRU, A. A., FREUD, A. G., RABINOVITCH, R., XU-WELLIVER, M., OTTO, B., BARRIONUEVO, C., BAIOCCHI, R. A., ROCHFORD, R. & PORCU, P. 2016. Extranodal NK/T Cell Lymphoma, Nasal Type (ENKTL-NT): An Update on Epidemiology, Clinical Presentation, and Natural History in North American and European Cases. *Curr Hematol Malig Rep,* 11**,** 514-527.

HEMANN, M. T., ZILFOU, J. T., ZHAO, Z., BURGESS, D. J., HANNON, G. J. & LOWE, S. W. 2004. Suppression of tumorigenesis by the p53 target PUMA. *Proc Natl Acad Sci U S A,* 101**,** 9333-9338.

HENDERSON, E., MILLER, G., ROBINSON, J. & HESTON, L. 1977. Efficiency of transformation of lymphocytes by Epstein-Barr virus. *Virology,* 76**,** 152.

HENDERSON, S., ROWE, M., GREGORY, C., CROOM CARTER, D., WANG, F., LONGNECKER, R., KIEFF, E. & RICKINSON, A. 1991. Induction of *bcl*-2 expression by Epstein-Barr virus latent membrane protein 1 protects infected B cells from programmed cell death. *Cell,* 65**,** 1107-1115.

HERSHKO, T. & GINSBERG, D. 2004. Up-regulation of Bcl-2 homology 3 (BH3)-only proteins by E2F1 mediates apoptosis. *J Biol Chem,* 279**,** 8627-8634.

HIND, C. K., CARTER, M. J., HARRIS, C. L., CHAN, H. T., JAMES, S. & CRAGG, M. S. 2015. Role of the pro-survival molecule Bfl-1 in melanoma. *Int J Biochem Cell Biol,* 59**,** 94-102.

HINO, R., UOZAKI, H., INOUE, Y., SHINTANI, Y., USHIKU, T., SAKATANI, T., TAKADA, K. & FUKAYAMA, M. 2008. Survival advantage of EBV-associated gastric carcinoma: survivin up-regulation by viral latent membrane protein 2A. *Cancer Res,* 68**,** 1427-35.

HISLOP, A. D., TAYLOR, G. S., SAUCE, D. & RICKINSON, A. B. 2007. Cellular responses to viral infection in humans: lessons from Epstein-Barr virus. *Annual Review of Immunology,* 25**,** 587-617.

HONDA, R., TANAKA, H. & YASUDA, H. 1997. Oncoprotein MDM2 is a ubiquitin ligase E3 for tumor suppressor p53. *FEBS Lett,* 420**,** 25-7.

HONGYO, T., HOSHIDA, Y., NAKATSUKA, S., SYAIFUDIN, M., KOJYA, S., YANG, W. I., MIN, Y. H., CHAN, H., KIM, C. H., HARABUCHI, Y., HIMI, T., INUYAMA, M., AOZASA, K. & NOMURA, T. 2005. p53, K-ras, c-kit and beta-catenin gene mutations in sinonasal NK/T-cell lymphoma in Korea and Japan. *Oncol Rep,* 13**,** 265-71.

HOQUE, M. O., BEGUM, S., SOMMER, M., LEE, T., TRINK, B., RATOVITSKI, E. & SIDRANSKY, D. 2003. PUMA in head and neck cancer. *Cancer Lett,* 199**,** 75-81.

HOUMANI, J. L., DAVIS, C. I. & RUF, I. K. 2009. Growth-promoting properties of Epstein-Barr virus EBER-1 RNA correlate with ribosomal protein L22 binding. *J Virol,* 83**,** 9844-53.

HSIEH, J. J. & HAYWARD, S. D. 1995. Masking of the CBF1/RBPJ kappa transcriptional repression domain by Epstein-Barr virus EBNA2. *Science,* 268**,** 560-3.

HSIEH, P. P., TUNG, C. L., CHAN, A. B., LIAO, J. B., WANG, J. S., TSENG, H. H., SU, H. H., CHANG, K. C. & CHANG, C. C. 2007. EBV viral load in tumor tissue is an important prognostic indicator for nasal NK/T-cell lymphoma. *Am J Clin Pathol,* 128**,** 579-84.

HSU, S. Y., KAIPIA, A., MCGEE, E., LOMELI, M. & HSUEH, A. J. W. 1997. Bok is a pro-apoptotic Bcl-2 protein with restricted expression in reproductive tissues and heterodimerizes with selective anti-apoptotic Bcl-2 family members. *Proc Natl Acad Sci U S A,* 94**,** 12401-12406.

HUANG, Y., DE REYNIES, A., DE LEVAL, L., GHAZI, B., MARTIN-GARCIA, N., TRAVERT, M., BOSQ, J., BRIERE, J., PETIT, B., THOMAS, E., COPPO, P., MARAFIOTI, T., EMILE, J. F., DELFAU-LARUE, M. H., SCHMITT, C. & GAULARD, P. 2010. Gene expression profiling identifies emerging oncogenic pathways operating in extranodal NK/T-cell lymphoma, nasal type. *Blood,* 115**,** 1226-37.

HUANG, Y. T., SHEEN, T. S., CHEN, C. L., LU, J., CHANG, Y., CHEN, J. Y. & TSAI, C. H. 1999. Profile of cytokine expression in nasopharyngeal carcinomas: A distinct expression of interleukin 1 in tumour and CD4(+) T cells. *Cancer Research,* 59**,** 1599.

HUDNALL, S. D., GE, Y., WEI, L., YANG, N. P., WANG, H. Q. & CHEN, T. 2005. Distribution and phenotype of Epstein-Barr virus-infected cells in human pharyngeal tonsils. *Mod Pathol,* 18**,** 519-27.

IAN, M. X., LAN, S. Z., CHENG, Z. F., DAN, H. & QIONG, L. H. 2008. Suppression of EBNA1 expression inhibits growth of EBV-positive NK/T cell lymphoma cells. *Cancer Biol Ther,* 7**,** 1602-6.

IKEGAKI, N., KATSUMATA, M., MINNA, J. & TSUJIMOTO, Y. 1994. Expression of bcl-2 in small cell lung carcinoma cells. *Cancer Res,* 54**,** 6-8.

IMADOME, K., YAJIMA, M., ARAI, A., NAKAZAWA, A., KAWANO, F., ICHIKAWA, S., SHIMIZU, N., YAMAMOTO, N., MORIO, T., OHGA, S., NAKAMURA, H., ITO, M., MIURA, O., KOMANO, J. & FUJIWARA, S. 2011. Novel mouse xenograft models reveal a critical role of CD4+ T cells in the proliferation of EBV-infected T and NK cells. *PLoS Pathog,* 7**,** e1002326.

IMAIZUMI, K., TSUDA, M., IMAI, Y., WANAKA, A., TAKAGI, T. & TOHYAMA, M. 1997. Molecular cloning of a novel polypeptide, DP5, induced during programmed neuronal death. *J Biol Chem,* 272**,** 18842-18848.

IQBAL, J., KUCUK, C., DELEEUW, R. J., SRIVASTAVA, G., TAM, W., GENG, H., KLINKEBIEL, D., CHRISTMAN, J. K., PATEL, K., CAO, K., SHEN, L., DYBKAER, K., TSUI, I. F., ALI, H., SHIMIZU, N., AU, W. Y., LAM, W. L. & CHAN, W. C. 2009. Genomic analyses reveal global functional

alterations that promote tumor growth and novel tumor suppressor genes in natural killer-cell malignancies. *Leukemia,* 23**,** 1139-51.

ISHII, H., TAKAHARA, M., NAGATO, T., KIS, L. L., NAGY, N., KISHIBE, K., HARABUCHI, Y. & KLEIN, E. 2012. Monocytes enhance cell proliferation and LMP1 expression of nasal natural killer/T-cell lymphoma cells by cell contact-dependent interaction through membrane-bound IL-15. *Int J Cancer,* 130**,** 48-58.

ISOBE, Y., SUGIMOTO, K., YANG, L., TAMAYOSE, K., EGASHIRA, M., KANEKO, T., TAKADA, K. & OSHIMI, K. 2004. Epstein-Barr virus infection of human natural killer cell lines and peripheral blood natural killer cells. *Cancer Research,* 64**,** 2167-74.

IWATA, S., WADA, K., TOBITA, S., GOTOH, K., ITO, Y., DEMACHI-OKAMURA, A., SHIMIZU, N., NISHIYAMA, Y. & KIMURA, H. 2010. Quantitative analysis of Epstein-Barr virus (EBV)-related gene expression in patients with chronic active EBV infection. *J Gen Virol,* 91**,** 42-50.

JAFFREZOU, J. P., CHEN, G., DURAN, G. E., KUHL, J. S. & SIKIC, B. I. 1994. Mutation rates and mechanisms of resistance to etoposide determined from fluctuation analysis. *J Natl Cancer Inst,* 86**,** 1152-8.

JEFFERS, J. R., PARGANAS, E., LEE, Y., YANG, C., WANG, J., BRENNAN, J., MACLEAN, K. H., HAN, J., CHITTENDEN, T., IHLE, J. N., MCKINNON, P. J., CLEVELAND, J. L. & ZAMBETTI, G. P. 2003. Puma is an essential mediator of p53-dependent and -independent apoptotic pathways. *Cancer Cell,* 4**,** 321-328.

JONES, J. F., SHURIN, S., ABRAMOWSKY, C., TUBBS, R. R., SCIOTTO, C. G., WAHL, R., SANDS, J., GOTTMAN, D., KATZ, B. Z. & SKLAR, J. 1988. T-cell lymphomas containing Epstein-Barr viral DNA in patients with chronic Epstein-Barr virus infections. *New England Journal of Medicine,* 318**,** 733-741.

JOSEFSSON, E. C., JAMES, C., HENLEY, K. J., DEBRINCAT, M. A., ROGERS, K. L., DOWLING, M. R., WHITE, M. J., KRUSE, E. A., LANE, R. M., ELLIS, S., NURDEN, P., MASON, K. D., O'REILLY, L. A., ROBERTS, A. W., METCALF, D., HUANG, D. C. & KILE, B. T. 2011. Megakaryocytes possess a functional intrinsic apoptosis pathway that must be restrained to survive and produce platelets. *J Exp Med,* 208**,** 2017-31.

JOST, P. J., GRABOW, S., GRAY, D., MCKENZIE, M. D., NACHBUR, U., HUANG, D. C., BOUILLET, P., THOMAS, H. E., BORNER, C., SILKE, J., STRASSER, A. & KAUFMANN, T. 2009. XIAP discriminates between type I and type II FAS-induced apoptosis. *Nature,* 460**,** 1035-9.

JUNYING, J., HERRMANN, K., DAVIES, G., LISSAUER, D., BELL, A., TIMMS, J., REYNOLDS, G. M., HUBSCHER, S. G., YOUNG, L. S., NIEDOBITEK, G. & MURRAY, P. G. 2003. Absence of Epstein-Barr virus DNA in the tumor cells of European hepatocellular carcinoma. *Virology,* 306**,** 236-43.

KALKAVAN, H. & GREEN, D. R. 2018. MOMP, cell suicide as a BCL-2 family business. *Cell Death Differ,* 25**,** 46-55.

KALLA, M. & HAMMERSCHMIDT, W. 2012. Human B cells on their route to latent infection--early but transient expression of lytic genes of Epstein-Barr virus. *Eur J Cell Biol,* 91**,** 65-9.

KALLIOLIAS, G. D. & IVASHKIV, L. B. 2016. TNF biology, pathogenic mechanisms and emerging therapeutic strategies. *Nat Rev Rheumatol,* 12**,** 49-62.

KAMADA, S., SHIMONO, A., SHINTO, Y., TSUJIMURA, T., TAKAHASHI, T., NODA, T., KITAMURA, Y., KONDOH, H. & TSUJIMOTO, Y. 1995. *bcl-2* deficiency in mice leads to pleiotropic abnormalities: accelerated lymphoid cell death in thymus andspleen, polycystic kidney, hair hypopigmentation, and distorted small intestine. *Cancer Res,* 55**,** 354-359.

KANEMITSU, N., ISOBE, Y., MASUDA, A., MOMOSE, S., HIGASHI, M., TAMARU, J., SUGIMOTO, K. & KOMATSU, N. 2012. Expression of Epstein-Barr virus-encoded proteins in extranodal NK/T-cell Lymphoma, nasal type (ENKL): differences in biologic and clinical behaviors of LMP1-positive and -negative ENKL. *Clin Cancer Res,* 18**,** 2164-72.

KARST, A. M., DAI, D. L., MARTINKA, M. & LI, G. 2005. PUMA expression is significantly reduced in human cutaneous melanomas. *Oncogene,* 24**,** 1111-1116.

KARUBE, K., TSUZUKI, S., YOSHIDA, N., ARITA, K., KATO, H., KATAYAMA, M., KO, Y. H., OHSHIMA, K., NAKAMURA, S., KINOSHITA, T. & SETO, M. 2013. Comprehensive gene expression profiles of NK cell neoplasms identify vorinostat as an effective drug candidate. *Cancer Lett,* 333**,** 47-55.

KASAHARA, Y., YACHIE, A., TAKEI, K., KANEGANE, C., OKADA, K., OHTA, K., SEKI, H., IGARASHI, N., MARUHASHI, K., KATAYAMA, K., KATOH, E., TERAO, G., SAKIYAMA, Y. & KOIZUMI, S. 2001. Differential cellular targets of Epstein-Barr virus (EBV) infection between acute EBV-associated hemophagocytic lymphohistiocytosis and chronic active EBV infection. *Blood,* 98**,** 1882-8.

KAUFMANN, S. H. 1996. gamma/delta and other unconventional T lymphocytes: what do they see and what do they do? *Proc Natl Acad Sci U S A,* 93**,** 2272-9.

KAUFMANN, T., TAI, L., EKERT, P. G., HUANG, D. C., NORRIS, F., LINDEMANN, R. K., JOHNSTONE, R. W., DIXIT, V. M. & STRASSER, A. 2007. The BH3-Only Protein Bid Is Dispensable for DNA Damage- and Replicative Stress-Induced Apoptosis or Cell-Cycle Arrest. *Cell,* 129**,** 423-433.

KAWA, K., SAWADA, A., SATO, M., OKAMURA, T., SAKATA, N., KONDO, O., KIMOTO, T., YAMADA, K., TOKIMASA, S., YASUI, M. & INOUE, M. 2011. Excellent outcome of allogeneic hematopoietic SCT with reduced-intensity conditioning for the treatment of chronic active EBV infection. *Bone Marrow Transplant,* 46**,** 77-83.

KAYE, K. M., IZUMI, K. M. & KIEFF, E. 1993. Epstein-Barr virus latent membrane protein 1 is essential for B- lymphocyte growth transformation. *Proceedings of the National Academy of Sciences U.S.A.,* 90**,** 9150.

KE, F., GRABOW, S., KELLY, G. L., LIN, A., O'REILLY, L. A. & STRASSER, A. 2015. Impact of the combined loss of BOK, BAX and BAK on the hematopoietic system is slightly more severe than compound loss of BAX and BAK. *Cell Death Dis,* 6**,** e1938.

KE, F. F. S., VANYAI, H. K., COWAN, A. D., DELBRIDGE, A. R. D., WHITEHEAD, L., GRABOW, S., CZABOTAR, P. E., VOSS, A. K. & STRASSER, A. 2018. Embryogenesis and Adult Life in the Absence of Intrinsic Apoptosis Effectors BAX, BAK, and BOK. *Cell,* 173**,** 1217-1230.e17.

KEATING, S., PRINCE, S., JONES, M. & ROWE, M. 2002. The lytic cycle of Epstein-Barr virus is associated with decreased expression of cell surface major histocompatibility complex class I and class II molecules. *Journal of Virology,* 76**,** 8179.

KELLY, G. L., GRABOW, S., GLASER, S. P., FITZSIMMONS, L., AUBREY, B. J., OKAMOTO, T., VALENTE, L. J., ROBATI, M., TAI, L., FAIRLIE, W. D., LEE, E. F., LINDSTROM, M. S., WIMAN, K. G., HUANG,

D. C., BOUILLET, P., ROWE, M., RICKINSON, A. B., HEROLD, M. J. & STRASSER, A. 2014. Targeting of MCL-1 kills MYC-driven mouse and human lymphomas even when they bear mutations in p53. *Genes Dev,* 28**,** 58-70.

KELLY, G. L., LONG, H. M., STYLIANOU, J., THOMAS, W. A., LEESE, A., BELL, A. I., BORNKAMM, G. W., MAUTNER, J., RICKINSON, A. B. & ROWE, M. 2009. An Epstein-Barr virus anti-apoptotic protein constitutively expressed in transformed cells and implicated in burkitt lymphomagenesis: the Wp/BHRF1 link. *PLoS Pathog,* 5**,** e1000341.

KELLY, P. N. & STRASSER, A. 2011. The role of Bcl-2 and its pro-survival relatives in tumourigenesis and cancer therapy. *Cell Death Differ,* 18**,** 1414-24.

KELLY-ROGERS, J., MADRIGAL-ESTEBAS, L., O'CONNOR, T. & DOHERTY, D. G. 2006. Activation-induced expression of CD56 by T cells is associated with a reprogramming of cytolytic activity and cytokine secretion profile in vitro. *Hum Immunol,* 67**,** 863-73.

KERR, J. F., WYLLIE, A. H. & CURRIE, A. R. 1972. Apoptosis: a basic biological phenomenon with wide-ranging implications in tissue kinetics. *Br J Cancer,* 26**,** 239-57.

KIEFF, E. & RICKINSON, A. B. 2007. Epstein-Barr Virus and its Replication. *Fields Virology.* Philadelphia: Lippincott-Williams and Wilkins Publishers.

KIM, B. S., KIM, T. Y., KIM, C. W., KIM, J. Y., HEO, D. S., BANG, Y. J. & KIM, N. K. 2003. Therapeutic outcome of extranodal NK/T-cell lymphoma initially treated with chemotherapy--result of chemotherapy in NK/T-cell lymphoma. *Acta Oncol,* 42**,** 779-83.

KIM, E. Y., JUNG, J. Y., KIM, A., CHANG, Y. S. & KIM, S. K. 2017. ABT-737 Synergizes with Cisplatin Bypassing Aberration of Apoptotic Pathway in Non-small Cell Lung Cancer. *Neoplasia,* 19**,** 354-363.

KIM, H., RAFIUDDIN-SHAH, M., TU, H. C., JEFFERS, J. R., ZAMBETTI, G. P., HSIEH, J. J. & CHENG, E. H. 2006. Hierarchical regulation of mitochondrion-dependent apoptosis by BCL-2 subfamilies. *Nat Cell Biol,* 8**,** 1348-1358.

KIM, H., TU, H. C., REN, D., TAKEUCHI, O., JEFFERS, J. R., ZAMBETTI, G. P., HSIEH, J. J. & CHENG, E. H. 2009. Stepwise activation of BAX and BAK by tBID, BIM, and PUMA initiates mitochondrial apoptosis. *Mol Cell,* 36**,** 487-99.

KIM, J. Y., AHN, H. J., RYU, J. H., SUK, K. & PARK, J. H. 2004. BH3-only protein Noxa is a mediator of hypoxic cell death induced by hypoxia-inducible factor 1alpha. *J Exp Med,* 199**,** 113-124.

KIM, M. S., KIM, S. S., YOO, N. J. & LEE, S. H. 2012. Rare somatic mutation of pro-apoptotic BAX and BAK genes in common human cancers. *Tumori,* 98**,** 149e-51e.

KIM, S. J., PARK, S., KANG, E. S., CHOI, J. Y., LIM, D. H., KO, Y. H. & KIM, W. S. 2015. Induction treatment with SMILE and consolidation with autologous stem cell transplantation for newly diagnosed stage IV extranodal natural killer/T-cell lymphoma patients. *Ann Hematol,* 94**,** 71-8.

KIM, W. S., SONG, S. Y., AHN, Y. C., KO, Y. H., BAEK, C. H., KIM, D. Y., YOON, S. S., LEE, H. G., KANG, W. K., LEE, H. J., PARK, C. H. & PARK, K. 2001. CHOP followed by involved field radiation: is it optimal for localized nasal natural killer/T-cell lymphoma? *Ann Oncol,* 12**,** 349-52.

KIM, W. Y., JUNG, H. Y., NAM, S. J., KIM, T. M., HEO, D. S., KIM, C. W. & JEON, Y. K. 2016. Expression of programmed cell death ligand 1 (PD-L1) in advanced stage EBV-associated extranodal NK/T cell lymphoma is associated with better prognosis. *Virchows Arch,* 469**,** 581-590.

KIMURA, H., HOSHINO, Y., HARA, S., SUGAYA, N., KAWADA, J., SHIBATA, Y., KOJIMA, S., NAGASAKA, T., KUZUSHIMA, K. & MORISHIMA, T. 2005. Differences between T cell-type and natural killer cell-type chronic active Epstein-Barr virus infection. *Journal of Infectious Disease,* 191**,** 531-9.

KIMURA, H., HOSHINO, Y., KANEGANE, H., TSUGE, I., OKAMURA, T., KAWA, K. & MORISHIMA, T. 2001. Clinical and virologic characteristics of chronic active Epstein-Barr virus infection. *Blood,* 98**,** 280-6.

KIMURA, H., MORISHIMA, T., KANEGANE, H., OHGA, S., HOSHINO, Y., MAEDA, A., IMAI, S., OKANO, M., MORIO, T., YOKOTA, S., TSUCHIYA, S., YACHIE, A., IMASHUKU, S., KAWA, K. & WAKIGUCHI, H. 2003. Prognostic factors for chronic active Epstein-Barr virus infection. *J Infect Dis,* 187**,** 527-33.

KIRITO, K., WATANABE, T., SAWADA, K., ENDO, H., OZAWA, K. & KOMATSU, N. 2002. Thrombopoietin regulates *Bcl-xL* gene expression through Stat5 and phosphatidylinositol 3-kinase activation pathways. *J Biol Chem,* 277**,** 8329-8337.

KITADA, S., ANDERSEN, J., AKAR, S., ZAPATA, J. M., TAKAYAMA, S., KRAJEWSKI, S., WANG, H.-G., ZHANG, X., BULLRICH, F., CROCE, C. M., RAI, K., HINES, J. & REED, J. C. 1998. Expression of apoptosis-regulating proteins in chronic lymphocytic leukemia: correlations with *in vitro* and *in vivo* chemoresponses. *Blood,* 91**,** 3379-3389.

KNUDSON, C. M., TUNG, K. S. K., TOURTELLOTTE, W. G., BROWN, G. A. J. & KORSMEYER, S. J. 1995. Bax-deficient mice with lymphoid hyperplasia and male germ cell death. *Science,* 270**,** 96-99.

KOBAYASHI, K. & RATAIN, M. J. 1994. Pharmacodynamics and long-term toxicity of etoposide. *Cancer Chemother Pharmacol,* 34 Suppl**,** S64-8.

KOBAYASHI, S., WERNEBURG, N. W., BRONK, S. F., KAUFMANN, S. H. & GORES, G. J. 2005. Interleukin-6 contributes to Mcl-1 up-regulation and TRAIL resistance via an Akt-signaling pathway in cholangiocarcinoma cells. *Gastroenterology,* 128**,** 2054-2065.

KOMABAYASHI, Y., KISHIBE, K., NAGATO, T., UEDA, S., TAKAHARA, M. & HARABUCHI, Y. 2014. Downregulation of miR-15a due to LMP1 promotes cell proliferation and predicts poor prognosis in nasal NK/T-cell lymphoma. *Am J Hematol,* 89**,** 25-33.

KONOPLEVA, M., WATT, J., CONTRACTOR, R., TSAO, T., HARRIS, D., ESTROV, Z., BORNMANN, W., KANTARJIAN, H., VIALLET, J., SAMUDIO, I. & ANDREEFF, M. 2008. Mechanisms of antileukemic activity of the novel Bcl-2 homology domain-3 mimetic GX15-070 (obatoclax). *Cancer Res,* 68**,** 3413-20.

KOSS, B., MORRISON, J., PERCIAVALLE, R. M., SINGH, H., REHG, J. E., WILLIAMS, R. T. & OPFERMAN, J. T. 2013. Requirement for antiapoptotic MCL-1 in the survival of BCR-ABL B-lineage acute lymphoblastic leukemia. *Blood,* 122**,** 1587-98.

KOTSCHY, A., SZLAVIK, Z., MURRAY, J., DAVIDSON, J., MARAGNO, A. L., LE TOUMELIN-BRAIZAT, G., CHANRION, M., KELLY, G. L., GONG, J. N., MOUJALLED, D. M., BRUNO, A., CSEKEI, M., PACZAL, A., SZABO, Z. B., SIPOS, S., RADICS, G., PROSZENYAK, A., BALINT, B., ONDI, L.,

BLASKO, G., ROBERTSON, A., SURGENOR, A., DOKURNO, P., CHEN, I., MATASSOVA, N., SMITH, J., PEDDER, C., GRAHAM, C., STUDENY, A., LYSIAK-AUVITY, G., GIRARD, A. M., GRAVE, F., SEGAL, D., RIFFKIN, C. D., POMILIO, G., GALBRAITH, L. C., AUBREY, B. J., BRENNAN, M. S., HEROLD, M. J., CHANG, C., GUASCONI, G., CAUQUIL, N., MELCHIORE, F., GUIGAL-STEPHAN, N., LOCKHART, B., COLLAND, F., HICKMAN, J. A., ROBERTS, A. W., HUANG, D. C., WEI, A. H., STRASSER, A., LESSENE, G. & GENESTE, O. 2016. The MCL1 inhibitor S63845 is tolerable and effective in diverse cancer models. *Nature,* 538**,** 477-482.

KUCUK, C., HU, X., JIANG, B., KLINKEBIEL, D., GENG, H., GONG, Q., BOUSKA, A., IQBAL, J., GAULARD, P., MCKEITHAN, T. W. & CHAN, W. C. 2015. Global promoter methylation analysis reveals novel candidate tumor suppressor genes in natural killer cell lymphoma. *Clin Cancer Res,* 21**,** 1699-711.

KUPPERS, R. 2009. The biology of Hodgkin's lymphoma. *Nat Rev Cancer,* 9**,** 15-27.

KWONG, Y. L., KIM, W. S., LIM, S. T., KIM, S. J., TANG, T., TSE, E., LEUNG, A. Y. & CHIM, C. S. 2012. SMILE for natural killer/T-cell lymphoma: analysis of safety and efficacy from the Asia Lymphoma Study Group. *Blood,* 120**,** 2973-80.

LABI, V., ERLACHER, M., KIESSLING, S., MANZL, C., FRENZEL, A., O'REILLY, L., STRASSER, A. & VILLUNGER, A. 2008. Loss of the BH3-only protein Bmf impairs B cell homeostasis and accelerates gamma irradiation-induced thymic lymphoma development. *J Exp Med,* 205**,** 641-655.

LAI, Y., WEI, X., LIN, S., QIN, L., CHENG, L. & LI, P. 2017. Current status and perspectives of patient-derived xenograft models in cancer research. *J Hematol Oncol,* 10**,** 106.

LAICHALK, L. L. & THORLEY-LAWSON, D. A. 2005. Terminal differentiation into plasma cells initiates the replicative cycle of Epstein-Barr virus in vivo. *J Virol,* 79**,** 1296-307.

LAUX, G., PERRICAUDET, M. & FARRELL, P. J. 1988. A spliced Epstein-Barr virus gene expressed in immortalized lymphocytes is created by circularization of the linear viral genome. *EMBO Journal,* 7**,** 769-774.

LAY, J. D., CHUANG, S. E., ROWE, M. & SU, I. J. 2003. Epstein-barr virus latent membrane protein-1 mediates upregulation of tumor necrosis factor-alpha in EBV-infected T cells: implications for the pathogenesis of hemophagocytic syndrome. *J Biomed Sci,* 10**,** 146-55.

LE GOUILL, S., PODAR, K., HAROUSSEAU, J. L. & ANDERSON, K. C. 2004. Mcl-1 regulation and its role in multiple myeloma. *Cell Cycle,* 3**,** 1259-62.

LEE, H. H., DADGOSTAR, H., CHENG, Q., SHU, J. & CHENG, G. 1999. NF-kappaB-mediated up-regulation of Bcl-x and Bfl-1/A1 is required for CD40 survival signaling in B lymphocytes. *Proc Natl Acad Sci U S A,* 96**,** 9136-41.

LEE, J. H., SOUNG, Y. H., LEE, J. W., PARK, W. S., KIM, S. Y., CHO, Y. G., KIM, C. J., SEO, S. H., KIM, H. S., NAM, S. W., YOO, N. J., LEE, S. H. & LEE, J. Y. 2004. Inactivating mutation of the pro-apoptotic gene BID in gastric cancer. *J Pathol,* 202**,** 439-45.

LEE, N., MOSS, W. N., YARIO, T. A. & STEITZ, J. A. 2015a. EBV noncoding RNA binds nascent RNA to drive host PAX5 to viral DNA. *Cell,* 160**,** 607-18.

LEE, S., YIN, C., AYELLO, J., MORRIS, E., CONNELL, T., HARRISON, L., VAN DE VEN, C., BARTH, M. J., MILES, R. R., GALARDY, P. J., GOLDMAN, S., LIM, M. S., HERMISTON, M. L., MCALLISTER-LUCAS, L., GIULINO-ROTH, L., PERKINS, S. L. & CAIRO, M. S. 2015b. Ibrutinib Significantly

Prolonged Survival in a Human Burkitt Lymphoma (BL) Xenograft NSG Mouse Model: Ibrutinib May be a Potential Adjuvant Agent in the Treatment of BL. *Blood,* 126**,** 5117--5117.

LEE, S. H., AHN, Y. C., KIM, W. S., KO, Y. H., KIM, K. & PARK, K. 2006. The effect of pre-irradiation dose intense CHOP on anthracyline resistance in localized nasal NK/T-cell lymphoma. *Haematologica,* 91**,** 427-8.

LEE, S. H., SOUNG, Y. H., LEE, J. W., KIM, H. S., LEE, J. H., PARK, J. Y., CHO, Y. G., KIM, C. J., KIM, S. Y., PARK, W. S., KIM, S. H., LEE, J. Y. & YOO, N. J. 2003. Mutational analysis of Noxa gene in human cancers. *Apmis,* 111**,** 599-604.

LEIGHT, E. R. & SUGDEN, B. 2000. EBNA-1: a protein pivotal to latent infection by Epstein-Barr virus. *Rev Med Virol,* 10**,** 83-100.

LESSENE, G., CZABOTAR, P. E., SLEEBS, B. E., ZOBEL, K., LOWES, K. L., ADAMS, J. M., BAELL, J. B., COLMAN, P. M., DESHAYES, K., FAIRBROTHER, W. J., FLYGARE, J. A., GIBBONS, P., KERSTEN, W. J. A., KULASEGARAM, S., MOSS, R. M., PARISOT, J. P., SMITH, B. J., STREET, I. P., YANG, H., HUANG, D. C. S. & WATSON, K. G. 2013. Structure-guided design of a selective BCL-XL inhibitor. *Nat Chem Biol,* 9**,** 390-397.

LESTOU, V. S., STREHL, S., LION, T., GADNER, H. & AMBROS, P. F. 1996. High-resolution FISH of the entire integrated Epstein-Barr virus genome on extended human DNA. *Cytogenet Cell Genet,* 74**,** 211-7.

LETAI, A., BASSIK, M., WALENSKY, L., SORCINELLI, M., WEILER, S. & KORSMEYER, S. 2002. Distinct BH3 domains either sensitize or activate mitochondrial apoptosis, serving as prototype cancer therapeutics. *Cancer Cell,* 2**,** 183-192.

LEU, B. L. & HUANG, J. D. 1995. Inhibition of intestinal P-glycoprotein and effects on etoposide absorption. *Cancer Chemother Pharmacol,* 35**,** 432-6.

LEVERSON, J. D., PHILLIPS, D. C., MITTEN, M. J., BOGHAERT, E. R., DIAZ, D., TAHIR, S. K., BELMONT, L. D., NIMMER, P., XIAO, Y., MA, X. M., LOWES, K. N., KOVAR, P., CHEN, J., JIN, S., SMITH, M., XUE, J., ZHANG, H., OLEKSIJEW, A., MAGOC, T. J., VAIDYA, K. S., ALBERT, D. H., TARRANT, J. M., LA, N., WANG, L., TAO, Z. F., WENDT, M. D., SAMPATH, D., ROSENBERG, S. H., TSE, C., HUANG, D. C., FAIRBROTHER, W. J., ELMORE, S. W. & SOUERS, A. J. 2015a. Exploiting selective BCL-2 family inhibitors to dissect cell survival dependencies and define improved strategies for cancer therapy. *Sci Transl Med,* 7**,** 279ra40.

LEVERSON, J. D., ZHANG, H., CHEN, J., TAHIR, S. K., PHILLIPS, D. C., XUE, J., NIMMER, P., JIN, S., SMITH, M., XIAO, Y., KOVAR, P., TANAKA, A., BRUNCKO, M., SHEPPARD, G. S., WANG, L., GIERKE, S., KATEGAYA, L., ANDERSON, D. J., WONG, C., EASTHAM-ANDERSON, J., LUDLAM, M. J., SAMPATH, D., FAIRBROTHER, W. J., WERTZ, I., ROSENBERG, S. H., TSE, C., ELMORE, S. W. & SOUERS, A. J. 2015b. Potent and selective small-molecule MCL-1 inhibitors demonstrate on-target cancer cell killing activity as single agents and in combination with ABT-263 (navitoclax). *Cell Death Dis,* 6**,** e1590.

LEVITSKAYA, J., CORAM, M., LEVITSKY, V., IMREH, S., STEIGERWALD-MULLEN, P. M., KLEIN, G., KURILLA, M. G. & MASUCCI, M. G. 1995. Inhibition of antigen processing by the internal repeat region of the Epstein-Barr virus nuclear antigen 1. *Nature,* 375**,** 685.

LI, H., ZHU, H., XU, C.-J. & YUAN, J. 1998. Cleavage of BID by caspase 8 mediates the mitochondrial damage in the Fas pathway of apoptosis. *Cell,* 94**,** 491-501.

LI, Y. X., YAO, B., JIN, J., WANG, W. H., LIU, Y. P., SONG, Y. W., WANG, S. L., LIU, X. F., ZHOU, L. Q., HE, X. H., LU, N. & YU, Z. H. 2006. Radiotherapy as primary treatment for stage IE and IIE nasal natural killer/T-cell lymphoma. *J Clin Oncol,* 24**,** 181-9.

LIANG, R. 2009. Advances in the management and monitoring of extranodal NK/T-cell lymphoma, nasal type. *Br J Haematol,* 147**,** 13-21.

LIMA, M. 2015. Extranodal NK/T cell lymphoma and aggressive NK cell leukaemia: evidence for their origin on CD56+bright CD16-/+dim NK cells. *Pathology,* 47**,** 503-14.

LIN, J. H. & YAMAZAKI, M. 2003. Role of P-glycoprotein in pharmacokinetics: clinical implications. *Clin Pharmacokinet,* 42**,** 59-98.

LINDSTEN, T., ROSS, A. J., KING, A., ZONG, W., RATHMELL, J. C., SHIELS, H. A., ULRICH, E., WAYMIRE, K. G., MAHAR, P., FRAUWIRTH, K., CHEN, Y., WEI, M., ENG, V. M., ADELMAN, D. M., SIMON, M. C., MA, A., GOLDEN, J. A., EVAN, G., KORSMEYER, S. J., MACGREGOR, G. R. & THOMPSON, C. B. 2000. The combined functions of proapoptotic Bcl-2 family members Bak and Bax are essential for normal development of multiple tissues. *Mol Cell,* 6**,** 1389-1399.

LIU, P. & SPECK, S. H. 2003. Synergistic autoactivation of the Epstein-Barr virus immediate-early BRLF1 promoter by Rta and Zta. *Virology,* 310**,** 199-206.

LLAMBI, F., WANG, Y. M., VICTOR, B., YANG, M., SCHNEIDER, D. M., GINGRAS, S., PARSONS, M. J., ZHENG, J. H., BROWN, S. A., PELLETIER, S., MOLDOVEANU, T., CHEN, T. & GREEN, D. R. 2016. BOK Is a Non-canonical BCL-2 Family Effector of Apoptosis Regulated by ER-Associated Degradation. *Cell,* 165**,** 421-33.

LONG, H. M., TAYLOR, G. S. & RICKINSON, A. B. 2011. Immune defence against EBV and EBV-associated disease. *Curr Opin Immunol,* 23**,** 258-64.

LORD, J. D., MCINTOSH, B. C., GREENBERG, P. D. & NELSON, B. H. 1998. The IL-2 receptor promotes proliferation, *bcl-2* and *bcl-x* induction, but not cell viability through the adapter molecule Shc. *J Immunol,* 161**,** 4627-4633.

LUNEMANN, A., VANOAICA, L. D., AZZI, T., NADAL, D. & MUNZ, C. 2013. A distinct subpopulation of human NK cells restricts B cell transformation by EBV. *J Immunol,* 191**,** 4989-95.

LUO, B., WANG, Y., WANG, X. F., LIANG, H., YAN, L. P., HUANG, B. H. & ZHAO, P. 2005. Expression of Epstein-Barr virus genes in EBV-associated gastric carcinomas. *World J Gastroenterol,* 11**,** 629-33.

LUO, X., BUDLHARDJO, I., ZOU, H., SLAUGHTER, C. & WANG, X. 1998. Bid, a Bcl-2 interacting protein, mediates cytochrome *c* release from mitochondria in response to activation of cell surface death receptors. *Cell,* 94**,** 481-490.

MA, A., PENA, J. C., CHANG, B., MARGOSIAN, E., DAVIDSON, L., ALT, F. W. & THOMPSON, C. B. 1995. Bclx regulates the survival of double-positive thymocytes. *Proc Natl Acad Sci U S A,* 92**,** 4763-7.

MALLADI, S., CHALLA-MALLADI, M., FEARNHEAD, H. O. & BRATTON, S. B. 2009. The Apaf-1*procaspase-9 apoptosome complex functions as a proteolytic-based molecular timer. *Embo j,* 28**,** 1916-25.

MANCAO, C. & HAMMERSCHMIDT, W. 2007. Epstein-Barr virus latent membrane protein 2A is a B-cell receptor mimic and essential for B-cell survival. *Blood,* 110**,** 3715-21.

MANDELBAUM, J., BHAGAT, G., TANG, H., MO, T., BRAHMACHARY, M., SHEN, Q., CHADBURN, A., RAJEWSKY, K., TARAKHOVSKY, A., PASQUALUCCI, L. & DALLA-FAVERA, R. 2010. BLIMP1 is a tumor suppressor gene frequently disrupted in activated B cell-like diffuse large B cell lymphoma. *Cancer Cell,* 18**,** 568-79.

MAO, Y., ZHANG, D. W., WEN, J., CAO, Q., CHEN, R. J., ZHU, J. & FENG, Z. Q. 2012. A novel LMP1 antibody synergizes with mitomycin C to inhibit nasopharyngeal carcinoma growth in vivo through inducing apoptosis and downregulating vascular endothelial growth factor. *Int J Mol Sci,* 13**,** 2208-18.

MASON, K. D., CARPINELLI, M. R., FLETCHER, J. I., COLLINGE, J. E., HILTON, A. A., ELLIS, S., KELLY, P. N., EKERT, P. G., METCALF, D., ROBERTS, A. W., HUANG, D. C. & KILE, B. T. 2007. Programmed anuclear cell death delimits platelet life span. *Cell,* 128**,** 1173-1186.

MATSUO, T., HELLER, M., PETTI, L., O'SHIRO, E. & KIEFF, E. 1984. Persistence of the entire Epstein-Barr virus genome integrated into human lymphocyte DNA. *Science,* 226**,** 1322-5.

MATSUSAKA, K., KANEDA, A., NAGAE, G., USHIKU, T., KIKUCHI, Y., HINO, R., UOZAKI, H., SETO, Y., TAKADA, K., ABURATANI, H. & FUKAYAMA, M. 2011. Classification of Epstein-Barr virus-positive gastric cancers by definition of DNA methylation epigenotypes. *Cancer Res,* 71**,** 7187-97.

MERINO, D., GIAM, M., HUGHES, P. D., SIGGS, O. M., HEGER, K., O'REILLY, L. A., ADAMS, J. M., STRASSER, A., LEE, E. F., FAIRLIE, W. D. & BOUILLET, P. 2009. The role of BH3-only protein Bim extends beyond inhibiting Bcl-2-like prosurvival proteins. *J Cell Biol,* 186**,** 355-62.

MESTRE-ESCORIHUELA, C., RUBIO-MOSCARDO, F., RICHTER, J. A., SIEBERT, R., CLIMENT, J., FRESQUET, V., BELTRAN, E., AGIRRE, X., MARUGAN, I., MARIN, M., ROSENWALD, A., SUGIMOTO, K. J., WHEAT, L. M., KARRAN, E. L., GARCIA, J. F., SANCHEZ, L., PROSPER, F., STAUDT, L. M., PINKEL, D., DYER, M. J. & MARTINEZ-CLIMENT, J. A. 2007. Homozygous deletions localize novel tumor suppressor genes in B-cell lymphomas. *Blood,* 109**,** 271-280.

METCALFE, A. D., HUNTER, H. R., BLOOR, D. J., LIEBERMAN, B. A., PICTON, H. M., LEESE, H. J., KIMBER, S. J. & BRISON, D. R. 2004. Expression of 11 members of the BCL-2 family of apoptosis regulatory molecules during human preimplantation embryo development and fragmentation. *Mol Reprod Dev,* 68**,** 35-50.

MICHALAK, E. M., JANSEN, E. S., HAPPO, L., CRAGG, M. S., TAI, L., SMYTH, G. K., STRASSER, A., ADAMS, J. M. & SCOTT, C. L. 2009. Puma and to a lesser extent Noxa are suppressors of Myc-induced lymphomagenesis. *Cell Death Differ,* 16**,** 684-96.

MIQUEL, C., BORRINI, F., GRANDJOUAN, S., AUPERIN, A., VIGUIER, J., VELASCO, V., DUVILLARD, P., PRAZ, F. & SABOURIN, J. C. 2005. Role of bax mutations in apoptosis in colorectal cancers with microsatellite instability. *Am J Clin Pathol,* 123**,** 562-70.

MOHAMMAD, R. M., WANG, S., ABOUKAMEEL, A., CHEN, B., WU, X., CHEN, J. & AL-KATIB, A. 2005. Preclinical studies of a nonpeptidic small-molecule inhibitor of Bcl-2 and Bcl-X(L) [(-)-gossypol] against diffuse large cell lymphoma. *Mol Cancer Ther,* 4**,** 13-21.

MOLYNEUX, E. M., ROCHFORD, R., GRIFFIN, B., NEWTON, R., JACKSON, G., MENON, G., HARRISON, C. J., ISRAELS, T. & BAILEY, S. 2012. Burkitt's lymphoma. *Lancet,* 379**,** 1234-44.

MORA, J., CHEUNG, N. K., CHEN, L., QIN, J. & GERALD, W. 2001. Loss of heterozygosity at 19q13.3 is associated with locally aggressive neuroblastoma. *Clin Cancer Res,* 7**,** 1358-61.

MORALES, A. A., OLSSON, A., CELSING, F., OSTERBORG, A., JONDAL, M. & OSORIO, L. M. 2005. High expression of bfl-1 contributes to the apoptosis resistant phenotype in B-cell chronic lymphocytic leukemia. *Int J Cancer,* 113**,** 730-7.

MOSS, W. N. & STEITZ, J. A. 2013. Genome-wide analyses of Epstein-Barr virus reveal conserved RNA structures and a novel stable intronic sequence RNA. *BMC Genomics,* 14**,** 543.

MOTOYAMA, N., WANG, F., ROTH, K. A., SAWA, H., NAKAYAMA, K., NAKAYAMA, K., NEGISHI, I., SENJU, S., ZHANG, Q., FUJII, S. & ET AL. 1995. Massive cell death of immature hematopoietic cells and neurons in Bcl-x-deficient mice. *Science,* 267**,** 1506-10.

MUCHMORE, S. W., SATTLER, M., LIANG, H., MEADOWS, R. P., HARLAN, J. E., YOON, H. S., NETTESHEIM, D., CHANG, B. S., THOMPSON, C. B., WONG, S.-L., NG, S.-C. & FESIK, S. W. 1996. X-ray and NMR structure of human Bcl-x_L, an inhibitor of programmed cell death. *Nature,* 381**,** 335-341.

MULLER, P. A. & VOUSDEN, K. H. 2013. p53 mutations in cancer. *Nat Cell Biol,* 15**,** 2-8.

MUNZ, C. 2017. Humanized mouse models for Epstein Barr virus infection. *Curr Opin Virol,* 25**,** 113-118.

MUTHALAGU, N., JUNTTILA, M. R., WIESE, K. E., WOLF, E., MORTON, J., BAUER, B., EVAN, G. I., EILERS, M. & MURPHY, D. J. 2014. BIM is the primary mediator of MYC-induced apoptosis in multiple solid tissues. *Cell Rep,* 8**,** 1347-53.

NAGATA, H., KONNO, A., KIMURA, N., ZHANG, Y., KIMURA, M., DEMACHI, A., SEKINE, T., YAMAMOTO, K. & SHIMIZU, N. 2001. Characterization of novel natural killer (NK)-cell and gammadelta T-cell lines established from primary lesions of nasal T/NK-cell lymphomas associated with the Epstein-Barr virus. *Blood,* 97**,** 708-13.

NAKAMURA, M., ISHIDA, E., SHIMADA, K., NAKASE, H., SAKAKI, T. & KONISHI, N. 2005. Frequent HRK inactivation associated with low apoptotic index in secondary glioblastomas. *Acta Neuropathol,* 110**,** 402-10.

NAKANO, K. & VOUSDEN, K. H. 2001. *PUMA*, a novel proapoptotic gene, is induced by p53. *Mol Cell,* 7**,** 683-694.

NAKAYAMA, K., NAKAYAMA, K.-I., NEGISHI, I., KUIDA, K., SAWA, H. & LOH, D. Y. 1994. Targeted disruption of bcl-2ab in mice: occurrence of gray hair, polycystic kidney disease, and lymphocytopenia. *Proc Natl Acad Sci U S A,* 91**,** 3700-3704.

NELSON, B. H. 2004. IL-2, regulatory T cells, and tolerance. *J Immunol,* 172**,** 3983-8.

NIEBOROWSKA-SKORSKA, M., HOSER, G., KOSSEV, P., WASIK, M. A. & SKORSKI, T. 2002. Complementary functions of the antiapoptotic protein A1 and serine/threonine kinase pim-1 in the BCR/ABL-mediated leukemogenesis. *Blood,* 99**,** 4531-4539.

NORBURY, C. J. & ZHIVOTOVSKY, B. 2004. DNA damage-induced apoptosis. *Oncogene,* 23**,** 2797-808.

NORRIS, M. D., DE GRAAF, D., HABER, M., KAVALLARIS, M., MADAFIGLIO, J., GILBERT, J., KWAN, E., STEWART, B. W., MECHETNER, E. B., GUDKOV, A. V. & RONINSON, I. B. 1996. Involvement of MDR1 P-glycoprotein in multifactorial resistance to methotrexate. *Int J Cancer,* 65**,** 613-9.

O'REILLY, R. J., SMALL, T. N., PAPADOPOULOS, E. B., LUCAS, K. G., LACERDA, J. F. & KOULOVA, L. 1997. Biology and adoptive cell therapy of Epstein-Barr virus-associated lymphoproliferative disorders in recipients of marrow allgorafts. *Immunological Reviews,* 157**,** 195.

ODA, E., OHKI, R., MURASAWA, H., NEMOTO, J., SHIBUE, T., YAMASHITA, T., TOKINO, T., TANIGUCHI, T. & TANAKA, N. 2000. Noxa, a BH3-only member of the bcl-2 family and candidate mediator of p53-induced apoptosis. *Science,* 288**,** 1053-1058.

OGEMBO, J. G., KANNAN, L., GHIRAN, I., NICHOLSON-WELLER, A., FINBERG, R. W., TSOKOS, G. C. & FINGEROTH, J. D. 2013. Human complement receptor type 1/CD35 is an Epstein-Barr Virus receptor. *Cell Rep,* 3**,** 371-85.

OHNISHI, H., LIN, K. M. & CHU, T. M. 1990. Prolongation of serum half-life of interleukin 2 and augmentation of lymphokine-activated killer cell activity by pepstatin in mice. *Cancer Res,* 50**,** 1107-12.

OKANO, M. 2002. Overview and problematic standpoints of severe chronic active Epstein-Barr virus infection syndrome. *Crit Rev Oncol Hematol,* 44**,** 273-82.

OKUNO, Y., MURATA, T., SATO, Y., MURAMATSU, H., MURAKAMI, N., OKUNO, T., YOSHIDA, K., ITO, Y., SAWADA, A., OHSHIMA, K., SHIRAISHI, Y., CHIBA, K., TANAKA, K., MIYANO, S., TAKAHASHI, Y., KOJIMA, S., OGAWA, S. & KIMURA, H. 2017. Genetic Background of Chronic Active Epstein–Barr Virus Disease. *The American Society of Hematology 59th Annual Meeting & Exposition.* Atlanta, GA.

OLIVER, C. L., MIRANDA, M. B., SHANGARY, S., LAND, S., WANG, S. & JOHNSON, D. E. 2005. (-)-Gossypol acts directly on the mitochondria to overcome Bcl-2- and Bcl-X(L)-mediated apoptosis resistance. *Mol Cancer Ther,* 4**,** 23-31.

OLIVIER, M., HOLLSTEIN, M. & HAINAUT, P. 2010. TP53 mutations in human cancers: origins, consequences, and clinical use. *Cold Spring Harb Perspect Biol,* 2**,** a001008.

OLTERSDORF, T., ELMORE, S. W., SHOEMAKER, A. R., ARMSTRONG, R. C., AUGERI, D. J., BELLI, B. A., BRUNCKO, M., DECKWERTH, T. L., DINGES, J., HAJDUK, P. J., JOSEPH, M. K., KITADA, S., KORSMEYER, S. J., KUNZER, A. R., LETAI, A., LI, C., MITTEN, M. J., NETTESHEIM, D. G., NG, S., NIMMER, P. M., O'CONNOR, J. M., OLEKSIJEW, A., PETROS, A. M., REED, J. C., SHEN, W., TAHIR, S. K., THOMPSON, C. B., TOMASELLI, K. J., WANG, B., WENDT, M. D., ZHANG, H., FESIK, S. W. & ROSENBERG, S. H. 2005. An inhibitor of Bcl-2 family proteins induces regression of solid tumours. *Nature,* 435**,** 677-681.

OPFERMAN, J., IWASAKI, H., ONG, C. C., SUH, H., MIZUNO, S., AKASHI, K. & KORSMEYER, S. J. 2005. Obligate role of anti-apoptotic MCL-1 in the survival of hematopoietic stem cells. *Science,* 307**,** 1101-1104.

OPFERMAN, J. T., LETAI, A., BEARD, C., SORCINELLI, M. D., ONG, C. C. & KORSMEYER, S. J. 2003. Development and maintenance of B and T lymphocytes requires antiapoptotic MCL-1. *Nature,* 426**,** 671-676.

OUDEJANS, J. J., JIWA, M., VAN DEN BRULE, A. J., GRASSER, F. A., HORSTMAN, A., VOS, W., KLUIN, P. M., VAN DER VALK, P., WALBOOMERS, J. M. & MEIJER, C. J. 1995. Detection of heterogeneous Epstein-Barr virus gene expression patterns within individual post-transplantation lymphoproliferative disorders. *American Journal of Pathology,* 147**,** 923-33.

OYOSHI, M. K., NAGATA, H., KIMURA, N., ZHANG, Y., DEMACHI, A., HARA, T., KANEGANE, H., MATSUO, Y., YAMAGUCHI, T., MORIO, T., HIRANO, A., SHIMIZU, N. & YAMAMOTO, K. 2003. Preferential expansion of Vgamma9-JgammaP/Vdelta2-Jdelta3 gammadelta T cells in nasal T-cell lymphoma and chronic active Epstein-Barr virus infection. *Am J Pathol,* 162**,** 1629-38.

PAIK, P. K., RUDIN, C. M., BROWN, A., RIZVI, N. A., TAKEBE, N., TRAVIS, W., JAMES, L., GINSBERG, M. S., JUERGENS, R., MARKUS, S., TYSON, L., SUBZWARI, S., KRIS, M. G. & KRUG, L. M. 2010. A phase I study of obatoclax mesylate, a Bcl-2 antagonist, plus topotecan in solid tumor malignancies. *Cancer Chemother Pharmacol,* 66**,** 1079-85.

PAIK, P. K., RUDIN, C. M., PIETANZA, M. C., BROWN, A., RIZVI, N. A., TAKEBE, N., TRAVIS, W., JAMES, L., GINSBERG, M. S., JUERGENS, R., MARKUS, S., TYSON, L., SUBZWARI, S., KRIS, M. G. & KRUG, L. M. 2011. A phase II study of obatoclax mesylate, a Bcl-2 antagonist, plus topotecan in relapsed small cell lung cancer. *Lung Cancer,* 74**,** 481-5.

PAINE, E., SCHEINMAN, R. I., BALDWIN, A. S., JR. & RAAB-TRAUB, N. 1995. Expression of LMP1 in epithelial cells leads to the activation of a select subset of NF-kappa B/Rel family proteins. *J Virol,* 69**,** 4572-6.

PAL, A. D., BASAK, N. P., BANERJEE, A. S. & BANERJEE, S. 2014. Epstein-Barr virus latent membrane protein-2A alters mitochondrial dynamics promoting cellular migration mediated by Notch signaling pathway. *Carcinogenesis,* 35**,** 1592-601.

PARDOLL, D. M. 2012. The blockade of immune checkpoints in cancer immunotherapy. *Nat Rev Cancer,* 12**,** 252-64.

PARK, I. C., LEE, S. H., WHANG, D. Y., HONG, W. S., CHOI, S. S., SHIN, H. S., CHOE, T. B. & HONG, S. I. 1997. Expression of a novel Bcl-2 related gene, Bfl-1, in various human cancers and cancer cell lines. *Anticancer Res,* 17**,** 4619-4622.

PARK, S. & KO, Y. H. 2014. Epstein-Barr virus-associated T/natural killer-cell lymphoproliferative disorders. *J Dermatol,* 41**,** 29-39.

PARRISH, A. B., FREEL, C. D. & KORNBLUTH, S. 2013. Cellular mechanisms controlling caspase activation and function. *Cold Spring Harb Perspect Biol,* 5.

PAVLETICH, N. P., CHAMBERS, K. A. & PABO, C. O. 1993. The DNA-binding domain of p53 contains the four conserved regions and the major mutation hot spots. *Genes Dev,* 7**,** 2556-2564.

PEETERS, S. D., HOVENGA, S., ROSATI, S. & VELLENGA, E. 2005. Bcl-xl expression in multiple myeloma. *Med Oncol,* 22**,** 183-90.

PEPERZAK, V., VIKSTROM, I., WALKER, J., GLASER, S. P., LEPAGE, M., COQUERY, C. M., ERICKSON, L. D., FAIRFAX, K., MACKAY, F., STRASSER, A., NUTT, S. L. & TARLINTON, D. M. 2013. Mcl-1 is essential for the survival of plasma cells. *Nat Immunol,* 14**,** 290-7.

PEREZ-GALAN, P., ROUE, G., VILLAMOR, N., CAMPO, E. & COLOMER, D. 2007. The BH3-mimetic GX15-070 synergizes with bortezomib in mantle cell lymphoma by enhancing Noxa-mediated activation of Bak. *Blood,* 109**,** 4441-4449.

PETER, M. E., HADJI, A., MURMANN, A. E., BROCKWAY, S., PUTZBACH, W., PATTANAYAK, A. & CEPPI, P. 2015. The role of CD95 and CD95 ligand in cancer. *Cell Death Differ,* 22**,** 549-59.

PLONER, C., KOFLER, R. & VILLUNGER, A. 2008. Noxa: at the tip of the balance between life and death. *Oncogene,* 27 Suppl 1**,** S84-92.

PONGPRUTTIPAN, T., SUKPANICHNANT, S., ASSANASEN, T., WANNAKRAIROT, P., BOONSAKAN, P., KANOKSIL, W., KAYASUT, K., MITARNUN, W., KHUHAPINANT, A., BUNWORASATE, U., PUAVILAI, T., BEDAVANIJA, A., GARCIA-HERRERA, A., CAMPO, E., COOK, J. R., CHOI, J. & SWERDLOW, S. H. 2012. Extranodal NK/T-cell lymphoma, nasal type, includes cases of natural killer cell and alphabeta, gammadelta, and alphabeta/gammadelta T-cell origin: a comprehensive clinicopathologic and phenotypic study. *Am J Surg Pathol,* 36**,** 481-99.

PRINT, C. G., LOVELAND, K. L., GIBSON, L., MEEHAN, T., STYLIANOU, A., WREFORD, N., DE KRETSER, D., METCALF, D., KÖNTGEN, F., ADAMS, J. M. & CORY, S. 1998. Apoptosis regulator Bcl-w is essential for spermatogenesis but appears otherwise redundant. *Proc Natl Acad Sci U S A,* 95**,** 12424-12431.

PRYCZYNICZ, A., GRYKO, M., NIEWIAROWSKA, K., CEPOWICZ, D., USTYMOWICZ, M., KEMONA, A. & GUZINSKA-USTYMOWICZ, K. 2014. Bax protein may influence the invasion of colorectal cancer. *World J Gastroenterol,* 20**,** 1305-10.

PUTCHA, G. V., LE, S., FRANK, S., BESIRLI, C. G., CLARK, K., CHU, B., ALIX, S., YOULE, R. J., LAMARCHE, A., MARONEY, A. C. & JOHNSON, E. M., JR. 2003. JNK-mediated BIM phosphorylation potentiates BAX-dependent apoptosis. *Neuron,* 38**,** 899-914.

QUEIROGA, E. M., GUALCO, G., WEISS, L. M., DITTMER, D. P., ARAUJO, I., KLUMB, C. E., HARRINGTON, W. J., JR. & BACCHI, C. E. 2008. Burkitt lymphoma in Brazil is characterized by geographically distinct clinicopathologic features. *Am J Clin Pathol,* 130**,** 946-56.

RAAB-TRAUB, N. 2002. Epstein-Barr virus in the pathogenesis of NPC. *Semin Cancer Biol,* 12**,** 431-41.

RAAB-TRAUB, N. 2015. Nasopharyngeal Carcinoma: An Evolving Role for the Epstein-Barr Virus. *Curr Top Microbiol Immunol,* 390**,** 339-63.

RAAB-TRAUB, N., DAMBAUGH, T. & KIEFF, E. 1980. DNA of Epstein-Barr virus VIII: B95-8, the previous prototype, is an unusual deletion derivative. *Cell,* 22**,** 257-67.

RAMAKRISHNAN, R., DONAHUE, H., GARCIA, D., TAN, J., SHIMIZU, N., RICE, A. P. & LING, P. D. 2011. Epstein-Barr virus BART9 miRNA modulates LMP1 levels and affects growth rate of nasal NK T cell lymphomas. *PLoS One,* 6**,** e27271.

RANGER, A. M., ZHA, J., HARADA, H., DATTA, S. R., DANIAL, N. N., GILMORE, A. P., KUTOK, J. L., LE BEAU, M. M., GREENBERG, M. E. & KORSMEYER, S. J. 2003. *Bad*-deficient mice develop diffuse large B cell lymphoma. *Proc Natl Acad Sci U S A,* 100**,** 9324-9329.

RICKINSON, A. B., LONG, H. M., PALENDIRA, U., MUNZ, C. & HISLOP, A. D. 2014. Cellular immune controls over Epstein-Barr virus infection: new lessons from the clinic and the laboratory. *Trends Immunol,* 35**,** 159-69.

RICKINSON, A. B., YOUNG, L. S. & ROWE, M. 1987. Influence of the Epstein-Barr virus nuclear antigen EBNA 2 on the growth phenotype of virus-transformed B cells. *J Virol,* 61**,** 1310-7.

RIEDL, S. J. & SALVESEN, G. S. 2007. The apoptosome: signalling platform of cell death. *Nat Rev Mol Cell Biol,* 8**,** 405-13.

RIKER, A. I., ENKEMANN, S. A., FODSTAD, O., LIU, S., REN, S., MORRIS, C., XI, Y., HOWELL, P., METGE, B., SAMANT, R. S., SHEVDE, L. A., LI, W., ESCHRICH, S., DAUD, A., JU, J. & MATTA, J. 2008. The gene expression profiles of primary and metastatic melanoma yields a transition point of tumor progression and metastasis. *BMC Med Genomics,* 1**,** 13.

RILEY, K. J., RABINOWITZ, G. S., YARIO, T. A., LUNA, J. M., DARNELL, R. B. & STEITZ, J. A. 2012. EBV and human microRNAs co-target oncogenic and apoptotic viral and human genes during latency. *EMBO J,* 31**,** 2207-21.

RINKENBERGER, J. L., HORNING, S., KLOCKE, B., ROTH, K. & KORSMEYER, S. J. 2000. Mcl-1 deficiency results in peri-implantation embryonic lethality. *Genes Dev,* 14**,** 23-27.

ROBERTS, A. W., DAVIDS, M. S., PAGEL, J. M., KAHL, B. S., PUVVADA, S. D., GERECITANO, J. F., KIPPS, T. J., ANDERSON, M. A., BROWN, J. R., GRESSICK, L., WONG, S., DUNBAR, M., ZHU, M., DESAI, M. B., CERRI, E., HEITNER ENSCHEDE, S., HUMERICKHOUSE, R. A., WIERDA, W. G. & SEYMOUR, J. F. 2016. Targeting BCL2 with Venetoclax in Relapsed Chronic Lymphocytic Leukemia. *N Engl J Med,* 374**,** 311-22.

ROBERTS, A. W., SEYMOUR, J. F., BROWN, J. R., WIERDA, W. G., KIPPS, T. J., KHAW, S. L., CARNEY, D. A., HE, S. Z., HUANG, D. C., XIONG, H., CUI, Y., BUSMAN, T. A., MCKEEGAN, E. M., KRIVOSHIK, A. P., ENSCHEDE, S. H. & HUMERICKHOUSE, R. 2012. Substantial Susceptibility of Chronic Lymphocytic Leukemia to BCL2 Inhibition: Results of a Phase I Study of Navitoclax in Patients With Relapsed or Refractory Disease. *J Clin Oncol,* 30**,** 488-496.

ROONEY, C. M., ROWE, D. T., RAGOT, T. & FARRELL, P. J. 1989. The spliced BZLF1 gene of Epstein-Barr virus (EBV) transactivates an early EBV promoter and induces the virus productive cycle. *Journal of Virology,* 63**,** 3109.

ROOSWINKEL, R. W., VAN DE KOOIJ, B., VERHEIJ, M. & BORST, J. 2012. Bcl-2 is a better ABT-737 target than Bcl-xL or Bcl-w and only Noxa overcomes resistance mediated by Mcl-1, Bfl-1, or Bcl-B. *Cell Death Dis,* 3**,** e366.

ROSS, A. J., WAYMIRE, K. G., MOSS, J. E., PARLOW, A. F., SKINNER, M. K., RUSSELL, L. D. & MACGREGOR, G. R. 1998. Testicular degeneration in *Bclw*-deficient mice. *Nat Genet,* 18**,** 251-256.

ROWE, M., PENG-PILON, M., HUEN, D. S., HARDY, R., CROOM-CARTER, D., LUNDGREN, E. & RICKINSON, A. B. 1994. Upregulation of bcl-2 by the Epstein-Barr virus latent membrane protein LMP1: a B-cell-specific response that is delayed relative to NF-kappa B activation and to induction of cell surface markers. *Journal of Virology,* 68**,** 5602-12.

ROWE, M., YOUNG, L. S., CADWALLADER, K., PETTI, L., KIEFF, E. & RICKINSON, A. B. 1989. Distinction between Epstein-Barr virus type A (EBNA 2A) and type B (EBNA 2B) isolates extends to the EBNA 3 family of nuclear proteins. *Journal of Virology,* 63**,** 1031-9.

SAMPLE, J., YOUNG, L., MARTIN, B., CHATMAN, T., KIEFF, E., RICKINSON, A. & KIEFF, E. 1990. Epstein-Barr virus types 1 and 2 differ in their EBNA-3A, EBNA-3B, and EBNA-3C genes. *Journal of Virology,* 64**,** 4084-92.

SANZ, C., BENITO, A., INOHARA, N., EKHTERAE, D., NÚÑEZ, G. & FERNANDEZ-LUNA, J. L. 2000. Specific and rapid induction of the proapoptotic protein Hrk after growth factor withdrawal in hematopoietic progenitor cells. *Blood,* 95**,** 2742-2747.

SARIDAKIS, V., SHENG, Y., SARKARI, F., HOLOWATY, M. N., SHIRE, K., NGUYEN, T., ZHANG, R. G., LIAO, J., LEE, W., EDWARDS, A. M., ARROWSMITH, C. H. & FRAPPIER, L. 2005. Structure of the p53 binding domain of HAUSP/USP7 bound to Epstein-Barr nuclear antigen 1 implications for EBV-mediated immortalization. *Mol Cell,* 18**,** 25-36.

SASAKI, M., MATSUE, K., TAKEUCHI, M., MITOME, M. & HIROSE, Y. 2000. Successful treatment of disseminated nasal NK/T-cell lymphoma using double autologous peripheral blood stem cell transplantation. *Int J Hematol,* 71**,** 75-8.

SATOH, M., SEKI, S., HASHIMOTO, W., OGASAWARA, K., KOBAYASHI, T., KUMAGAI, K., MATSUNO, S. & TAKEDA, K. 1996. Cytotoxic gammadelta or alphabeta T cells with a natural killer cell marker, CD56, induced from human peripheral blood lymphocytes by a combination of IL-12 and IL-2. *J Immunol,* 157**,** 3886-92.

SCAFFIDI, C., FULDA, S., SRINIVASAN, A., FRIESEN, C., LI, F., TOMASELLI, K. J., DEBATIN, K.-M., KRAMMER, P. H. & PETER, M. E. 1998. Two CD95 (APO-1/Fas) signaling pathways. *EMBO J,* 17**,** 1675-1687.

SCHAEFER, B. C., PAULSON, E., STROMINGER, J. L. & SPECK, S. H. 1997. Constitutive activation of Epstein-Barr virus (EBV) nuclear antigen 1 gene transcription by IRF1 and IRF2 during restricted EBV latency. *Molecular and Cellular Biology,* 17**,** 873-86.

SCHENK, R. L., TUZLAK, S., CARRINGTON, E. M., ZHAN, Y., HEINZEL, S., TEH, C. E., GRAY, D. H., TAI, L., LEW, A. M., VILLUNGER, A., STRASSER, A. & HEROLD, M. J. 2017. Characterisation of mice lacking all functional isoforms of the pro-survival BCL-2 family member A1 reveals minor defects in the haematopoietic compartment. *Cell Death Differ,* 24**,** 534-545.

SCHERR, A. L., GDYNIA, G., SALOU, M., RADHAKRISHNAN, P., DUGLOVA, K., HELLER, A., KEIM, S., KAUTZ, N., JASSOWICZ, A., ELSSNER, C., HE, Y. W., JAEGER, D., HEIKENWALDER, M., SCHNEIDER, M., WEBER, A., ROTH, W., SCHULZE-BERGKAMEN, H. & KOEHLER, B. C. 2016. Bcl-xL is an oncogenic driver in colorectal cancer. *Cell Death Dis,* 7**,** e2342.

SCHMUTTE, C., TOMBLINE, G., RHIEM, K., SADOFF, M. M., SCHMUTZLER, R., VON DEIMLING, A. & FISHEL, R. 1999. Characterization of the human Rad51 genomic locus and examination of tumors with 15q14-15 loss of heterozygosity (LOH). *Cancer Res,* 59**,** 4564-4569.

SCHWARTZ, E. J., MOLINA-KIRSCH, H., ZHAO, S., MARINELLI, R. J., WARNKE, R. A. & NATKUNAM, Y. 2008. Immunohistochemical characterization of nasal-type extranodal NK/T-cell lymphoma using a tissue microarray: an analysis of 84 cases. *Am J Clin Pathol,* 130**,** 343-51.

SEGAWA, K., KURATA, S., YANAGIHASHI, Y., BRUMMELKAMP, T. R., MATSUDA, F. & NAGATA, S. 2014. Caspase-mediated cleavage of phospholipid flippase for apoptotic phosphatidylserine exposure. *Science,* 344**,** 1164-8.

SEHESTED, M., FRICHE, E., JENSEN, P. B. & DEMANT, E. J. 1992. Relationship of VP-16 to the classical multidrug resistance phenotype. *Cancer Res,* 52**,** 2874-9.

SENKEVITCH, E., LI, W., HIXON, J. A., ANDREWS, C., CRAMER, S. D., PAULY, G. T., BACK, T., CZARRA, K. & DURUM, S. K. 2018. Inhibiting Janus Kinase 1 and BCL-2 to treat T cell acute lymphoblastic leukemia with IL7-Ralpha mutations. *Oncotarget,* 9**,** 22605-22617.

SEYMOUR, J. F., MA, S., BRANDER, D. M., CHOI, M. Y., BARRIENTOS, J., DAVIDS, M. S., ANDERSON, M. A., BEAVEN, A. W., ROSEN, S. T., TAM, C. S., PRINE, B., AGARWAL, S. K., MUNASINGHE, W., ZHU, M., LASH, L. L., DESAI, M., CERRI, E., VERDUGO, M., KIM, S. Y., HUMERICKHOUSE, R. A., GORDON, G. B., KIPPS, T. J. & ROBERTS, A. W. 2017. Venetoclax plus rituximab in relapsed or refractory chronic lymphocytic leukaemia: a phase 1b study. *Lancet Oncol,* 18**,** 230-240.

SHAH, K. M., STEWART, S. E., WEI, W., WOODMAN, C. B., O'NEIL, J. D., DAWSON, C. W. & YOUNG, L. S. 2009. The EBV-encoded latent membrane proteins, LMP2A and LMP2B, limit the actions of interferon by targeting interferon receptors for degradation. *Oncogene,* 28**,** 3903-14.

SHALEM, O., SANJANA, N. E., HARTENIAN, E., SHI, X., SCOTT, D. A., MIKKELSON, T., HECKL, D., EBERT, B. L., ROOT, D. E., DOENCH, J. G. & ZHANG, F. 2014. Genome-scale CRISPR-Cas9 knockout screening in human cells. *Science,* 343**,** 84-87.

SHANNON-LOWE, C. & ROWE, M. 2014. Epstein Barr virus entry; kissing and conjugation. *Curr Opin Virol,* 4**,** 78-84.

SHENG, Y., SARIDAKIS, V., SARKARI, F., DUAN, S., WU, T., ARROWSMITH, C. H. & FRAPPIER, L. 2006. Molecular recognition of p53 and MDM2 by USP7/HAUSP. *Nat Struct Mol Biol,* 13**,** 285-91.

SHULTZ, L. D., LYONS, B. L., BURZENSKI, L. M., GOTT, B., CHEN, X., CHALEFF, S., KOTB, M., GILLIES, S. D., KING, M., MANGADA, J., GREINER, D. L. & HANDGRETINGER, R. 2005. Human lymphoid and myeloid cell development in NOD/LtSz-scid IL2R gamma null mice engrafted with mobilized human hemopoietic stem cells. *J Immunol,* 174**,** 6477-89.

SIDDIQUEY, M. N., NAKAGAWA, H., IWATA, S., KANAZAWA, T., SUZUKI, M., IMADOME, K., FUJIWARA, S., GOSHIMA, F., MURATA, T. & KIMURA, H. 2014. Anti-tumor effects of suberoylanilide hydroxamic acid on Epstein-Barr virus-associated T cell and natural killer cell lymphoma. *Cancer Sci,* 105**,** 713-22.

SINCLAIR, A. J., PALMERO, I., PETERS, G. & FARRELL, P. J. 1994. EBNA-2 and EBNA-LP cooperate to cause G0 to G1 transition during immortalization of resting human B lymphocytes by Epstein-Barr virus. *EMBO Journal,* 13**,** 3321-3328.

SKALSKY, R. L., CORCORAN, D. L., GOTTWEIN, E., FRANK, C. L., KANG, D., HAFNER, M., NUSBAUM, J. D., FEEDERLE, R., DELECLUSE, H. J., LUFTIG, M. A., TUSCHL, T., OHLER, U. & CULLEN, B. R. 2012. The viral and cellular microRNA targetome in lymphoblastoid cell lines. *PLoS Pathog,* 8**,** e1002484.

SOUERS, A. J., LEVERSON, J. D., BOGHAERT, E. R., ACKLER, S. L., CATRON, N. D., CHEN, J., DAYTON, B. D., DING, H., ENSCHEDE, S. H., FAIRBROTHER, W. J., HUANG, D. C., HYMOWITZ, S. G., JIN, S., KHAW, S. L., KOVAR, P. J., LAM, L. T., LEE, J., MAECKER, H. L., MARSH, K. C., MASON, K. D., MITTEN, M. J., NIMMER, P. M., OLEKSIJEW, A., PARK, C. H., PARK, C. M., PHILLIPS, D. C., ROBERTS, A. W., SAMPATH, D., SEYMOUR, J. F., SMITH, M. L., SULLIVAN, G. M., TAHIR, S. K., TSE, C., WENDT, M. D., XIAO, Y., XUE, J. C., ZHANG, H., HUMERICKHOUSE, R. A., ROSENBERG, S. H. & ELMORE, S. W. 2013. ABT-199, a potent and selective BCL-2 inhibitor, achieves antitumor activity while sparing platelets. *Nat Med,* 19**,** 202-8.

SPINNER, S., CRISPATZU, G., YI, J. H., MUNKHBAATAR, E., MAYER, P., HOCKENDORF, U., MULLER, N., LI, Z., SCHADER, T., BENDZ, H., HARTMANN, S., YABAL, M., PECHLOFF, K., HEIKENWALDER, M., KELLY, G. L., STRASSER, A., PESCHEL, C., HANSMANN, M. L., RULAND, J., KELLER, U., NEWRZELA, S., HERLING, M. & JOST, P. J. 2016. Re-activation of mitochondrial apoptosis inhibits T-cell lymphoma survival and treatment resistance. *Leukemia,* 30**,** 1520-30.

STAUD, F., CECKOVA, M., MICUDA, S. & PAVEK, P. 2010. Expression and function of p-glycoprotein in normal tissues: effect on pharmacokinetics. *Methods Mol Biol,* 596**,** 199-222.

STRASSER, A., HARRIS, A. W., BATH, M. L. & CORY, S. 1990. Novel primitive lymphoid tumours induced in transgenic mice by co-operation between myc and bcl-2. *Nature,* 348**,** 331.

STRASSER, A., HARRIS, A. W., HUANG, D. C. S., KRAMMER, P. H. & CORY, S. 1995. Bcl-2 and Fas/APO-1 regulate distinct pathways to lymphocyte apoptosis. *EMBO J,* 14**,** 6136-6147.

STRAUS, S. E. 1988. The chronic mononucleosis syndrome. *J Infect Dis,* 157**,** 405-12.

STURM, I., STEPHAN, C., GILLISSEN, B., SIEBERT, R., JANZ, M., RADETZKI, S., JUNG, K., LOENING, S., DORKEN, B. & DANIEL, P. T. 2006. Loss of the tissue-specific proapoptotic BH3-only protein Nbk/Bik is a unifying feature of renal cell carcinoma. *Cell Death Differ,* 13**,** 619-27.

SUZUKI, M., TAKEDA, T., NAKAGAWA, H., IWATA, S., WATANABE, T., SIDDIQUEY, M. N., GOSHIMA, F., MURATA, T., KAWADA, J., ITO, Y., KOJIMA, S. & KIMURA, H. 2015. The heat shock protein 90 inhibitor BIIB021 suppresses the growth of T and natural killer cell lymphomas. *Front Microbiol,* 6**,** 280.

SUZUKI, R., SUZUMIYA, J., NAKAMURA, S., KAGAMI, Y., KAMEOKA, J. I., SAKAI, C., MUKAI, H., TAKENAKA, K., YOSHINO, T., TSUZUKI, T., SUGIMORI, H., KAWA, K., KODERA, Y. & OSHIMI, K. 2006. Hematopoietic stem cell transplantation for natural killer-cell lineage neoplasms. *Bone Marrow Transplant,* 37**,** 425-31.

SUZUKI, R., SUZUMIYA, J., YAMAGUCHI, M., NAKAMURA, S., KAMEOKA, J., KOJIMA, H., ABE, M., KINOSHITA, T., YOSHINO, T., IWATSUKI, K., KAGAMI, Y., TSUZUKI, T., KUROKAWA, M., ITO, K., KAWA, K. & OSHIMI, K. 2010. Prognostic factors for mature natural killer (NK) cell neoplasms: aggressive NK cell leukemia and extranodal NK cell lymphoma, nasal type. *Ann Oncol,* 21**,** 1032-40.

SWERDLOW SH, CAMPO E & NL, H. 2008. WHO Classification of Tumours of Hematopoietic and Lymphoid Tissues. *4th IARC.* Lyon, France.

TAGAWA, H., KARNAN, S., SUZUKI, R., MATSUO, K., ZHANG, X., OTA, A., MORISHIMA, Y., NAKAMURA, S. & SETO, M. 2005. Genome-wide array-based CGH for mantle cell lymphoma: identification of homozygous deletions of the proapoptotic gene BIM. *Oncogene,* 24**,** 1348-1358.

TAKADA, H., IMADOME, K. I., SHIBAYAMA, H., YOSHIMORI, M., WANG, L., SAITOH, Y., UOTA, S., YAMAOKA, S., KOYAMA, T., SHIMIZU, N., YAMAMOTO, K., FUJIWARA, S., MIURA, O. & ARAI, A. 2017. EBV induces persistent NF-kappaB activation and contributes to survival of EBV-positive neoplastic T- or NK-cells. *PLoS One,* 12**,** e0174136.

TAKAHARA, M., KIS, L. L., NAGY, N., LIU, A., HARABUCHI, Y., KLEIN, G. & KLEIN, E. 2006. Concomitant increase of LMP1 and CD25 (IL-2-receptor alpha) expression induced by IL-10 in the EBV-positive NK lines SNK6 and KAI3. *Int J Cancer,* 119**,** 2775-83.

TAKAMI, A., NAKAO, S., YACHIE, A., KASAHARA, Y., OKUMURA, H., MIURA, Y., SUGIMORI, N., ZENG, W., WANG, H., KOTANI, T., SHIOBARA, S. & MATSUDA, T. 1998. Successful treatment of Epstein-Barr virus-associated natural killer cell large granular lymphocytic leukaemia using allogeneic peripheral blood stem cell transplantation. *Bone Marrow Transplant,* 21**,** 1279-82.

TAN, T. T., DEGENHARDT, K., NELSON, D. A., BEAUDOIN, B., NIEVES-NEIRA, W., BOUILLET, P., VILLUNGER, A., ADAMS, J. M. & WHITE, E. 2005. Key roles of BIM-driven apoptosis in epithelial tumors and rational chemotherapy. *Cancer Cell,* 7**,** 227-238.

TAO, Z. F., HASVOLD, L., WANG, L., WANG, X., PETROS, A. M., PARK, C. H., BOGHAERT, E. R., CATRON, N. D., CHEN, J., COLMAN, P. M., CZABOTAR, P. E., DESHAYES, K., FAIRBROTHER, W. J., FLYGARE, J. A., HYMOWITZ, S. G., JIN, S., JUDGE, R. A., KOEHLER, M. F., KOVAR, P. J., LESSENE, G., MITTEN, M. J., NDUBAKU, C. O., NIMMER, P., PURKEY, H. E., OLEKSIJEW, A., PHILLIPS, D. C., SLEEBS, B. E., SMITH, B. J., SMITH, M. L., TAHIR, S. K., WATSON, K. G., XIAO, Y., XUE, J., ZHANG, H., ZOBEL, K., ROSENBERG, S. H., TSE, C., LEVERSON, J. D., ELMORE, S. W. & SOUERS, A. J. 2014. Discovery of a Potent and Selective BCL-XL Inhibitor with in Vivo Activity. *ACS Med Chem Lett,* 5**,** 1088-93.

TEMPLE, R. M., ZHU, J., BUDGEON, L., CHRISTENSEN, N. D., MEYERS, C. & SAMPLE, C. E. 2014. Efficient replication of Epstein-Barr virus in stratified epithelium in vitro. *Proc Natl Acad Sci U S A,* 111**,** 16544-9.

TESHIMA, T., MIYAJI, R., FUKUDA, M. & OHSHIMA, K. 1996. Bone-marrow transplantation for Epstein-Barr-virus-associated natural killer cell-large granular lymphocyte leukaemia. *Lancet,* 347**,** 1124.

THOMAS, R. L., ROBERTS, D. J., KUBLI, D. A., LEE, Y., QUINSAY, M. N., OWENS, J. B., FISCHER, K. M., SUSSMAN, M. A., MIYAMOTO, S. & GUSTAFSSON, A. B. 2013. Loss of MCL-1 leads to impaired autophagy and rapid development of heart failure. *Genes Dev,* 27**,** 1365-77.

TIEN, H. F., SU, I. J., TANG, J. L., LIU, M. C., LEE, F. Y., CHEN, Y. C. & CHUANG, S. M. 1997. Clonal chromosomal abnormalities as direct evidence for clonality in nasal T/natural killer cell lymphomas. *Br J Haematol,* 97**,** 621-5.

TIERNEY, R. J., SHANNON-LOWE, C. D., FITZSIMMONS, L., BELL, A. I. & ROWE, M. 2015. Unexpected patterns of Epstein–Barr virus transcription revealed by a High throughput PCR array for absolute quantification of viral mRNA. *Virology,* 474**,** 117-130.

TSAI, C. N., TSAI, C. L., TSE, K. P., CHANG, H. Y. & CHANG, Y. S. 2002. The Epstein-Barr virus oncogene product, latent membrane protein 1, induces the downregulation of E-cadherin gene expression via activation of DNA methyltransferases. *Proc Natl Acad Sci U S A,* 99**,** 10084-9.

TSE, E. & KWONG, Y. L. 2013. How I treat NK/T-cell lymphomas. *Blood,* 121**,** 4997-5005.

TSUJIMOTO, Y., FINGER, L. R., YUNIS, J., NOWELL, P. C. & CROCE, C. M. 1984. Cloning of the chromosome breakpoint of neoplastic B cells with the t(14;18) chromosome translocation. *Science,* 226**,** 1097-1099.

TUZLAK, S., SCHENK, R. L., VASANTHAKUMAR, A., PRESTON, S. P., HASCHKA, M. D., ZOTOS, D., KALLIES, A., STRASSER, A., VILLUNGER, A. & HEROLD, M. J. 2017. The BCL-2 pro-survival protein A1 is dispensable for T cell homeostasis on viral infection. *Cell Death Differ,* 24**,** 523-533.

TWENTYMAN, P. R., RHODES, T. & RAYNER, S. 1994. A comparison of rhodamine 123 accumulation and efflux in cells with P-glycoprotein-mediated and MRP-associated multidrug resistance phenotypes. *Eur J Cancer,* 30a**,** 1360-9.

UCHIDA, J., YASUI, T., TAKAOKA-SHICHIJO, Y., MURAOKA, M., KULWICHIT, W., RAAB-TRAUB, N. & KIKUTANI, H. 1999. Mimicry of CD40 signals by Epstein-Barr virus LMP1 in B lymphocyte responses. *Science,* 286**,** 300-303.

UNO, M., TSUCHIYAMA, J., MORIWAKI, A., NOGUCHI, T., MIZOGUCHI, K., OGINO, T., YOSHINO, T., OKADA, S. & HARADA, M. 2001. In vitro induction of apoptosis for nasal angiocentric natural killer cell lymphoma-derived cell line, NK-YS, by etoposide and cyclosporine A. *Br J Haematol,* 113**,** 1009-14.

VALENTE, L. J., AUBREY, B. J., HEROLD, M. J., KELLY, G. L., HAPPO, L., SCOTT, C. L., NEWBOLD, A., JOHNSTONE, R. W., HUANG, D. C., VASSILEV, L. T. & STRASSER, A. 2016. Therapeutic Response to Non-genotoxic Activation of p53 by Nutlin3a Is Driven by PUMA-Mediated Apoptosis in Lymphoma Cells. *Cell Rep,* 14**,** 1858-66.

VALENTIN-VEGA, Y. A., WANG, Y. D., PARKER, M., PATMORE, D. M., KANAGARAJ, A., MOORE, J., RUSCH, M., FINKELSTEIN, D., ELLISON, D. W., GILBERTSON, R. J., ZHANG, J., KIM, H. J. & TAYLOR, J. P. 2016. Cancer-associated DDX3X mutations drive stress granule assembly and impair global translation. *Sci Rep,* 6**,** 25996.

VAN BEEK, J., ZUR HAUSEN, A., KLEIN KRANENBARG, E., VAN DE VELDE, C. J., MIDDELDORP, J. M., VAN DEN BRULE, A. J., MEIJER, C. J. & BLOEMENA, E. 2004. EBV-positive gastric adenocarcinomas: a distinct clinicopathologic entity with a low frequency of lymph node involvement. *J Clin Oncol,* 22**,** 664-70.

VAN DELFT, M. F., WEI, A. H., MASON, K. D., VANDENBERG, C. J., CHEN, L., CZABOTAR, P. E., WILLIS, S. N., SCOTT, C. L., DAY, C. L., CORY, S., ADAMS, J. M., ROBERTS, A. W. & HUANG, D. C. 2006. The BH3 mimetic ABT-737 targets selective Bcl-2 proteins and efficiently induces apoptosis via Bak/Bax if Mcl-1 is neutralized. *Cancer Cell,* 10**,** 389-99.

VAN DIEMEN, F. R., KRUSE, E. M., HOOYKAAS, M. J., BRUGGELING, C. E., SCHURCH, A. C., VAN HAM, P. M., IMHOF, S. M., NIJHUIS, M., WIERTZ, E. J. & LEBBINK, R. J. 2016. CRISPR/Cas9-Mediated Genome Editing of Herpesviruses Limits Productive and Latent Infections. *PLoS Pathog,* 12**,** e1005701.

VAN GORP, J., BRINK, A., OUDEJANS, J. J., VAN DEN BRULE, A. J., VAN DEN TWEEL, J. G., JIWA, N. M., DE BRUIN, P. C. & MEIJER, C. J. 1996. Expression of Epstein-Barr virus encoded latent genes in nasal T cell lymphomas. *J Clin Pathol,* 49**,** 72-6.

VASSILEV, L. T., VU, B. T., GRAVES, B., CARVAJAL, D., PODLASKI, F., FILIPOVIC, Z., KONG, N., KAMMLOTT, U., LUKACS, C., KLEIN, C., FOTOUHI, N. & LIU, E. A. 2004. In vivo activation of the p53 pathway by small-molecule antagonists of MDM2. *Science,* 303**,** 844-848.

VAUX, D. L., CORY, S. & ADAMS, J. M. 1988. Bcl-2 gene promotes haemopoietic cell survival and co-operates with c-myc to immortalise pre-B cells. *Nature,* 335**,** 440.

VEIS, D. J., SORENSON, C. M., SHUTTER, J. R. & KORSMEYER, S. J. 1993. Bcl-2-deficient mice demonstrate fulminant lymphoid apoptosis, polycystic kidneys, and hypopigmented hair. *Cell,* 75**,** 229-240.

VENTURA, A., YOUNG, A. G., WINSLOW, M. M., LINTAULT, L., MEISSNER, A., ERKELAND, S. J., NEWMAN, J., BRONSON, R. T., CROWLEY, D., STONE, J. R., JAENISCH, R., SHARP, P. A. & JACKS, T. 2008. Targeted deletion reveals essential and overlapping functions of the miR-17~92 family of miRNA clusters. *Cell,* 132**,** 875-886.

VERHOVEN, B., SCHLEGEL, R. A. & WILLIAMSON, P. 1995. Mechanisms of phosphatidylserine exposure, a phagocyte recognition signal, on apoptotic T lymphocytes. *J Exp Med,* 182**,** 1597-1601.

VIKSTROM, I., CAROTTA, S., LUETHJE, K., PEPERZAK, V., JOST, P. J., GLASER, S., BUSSLINGER, M., BOUILLET, P., STRASSER, A., NUTT, S. L. & TARLINTON, D. M. 2010. Mcl-1 is essential for germinal center formation and B cell memory. *Science,* 330**,** 1095-9.

VILLUNGER, A., MICHALAK, E. M., COULTAS, L., MULLAUER, F., BOCK, G., AUSSERLECHNER, M. J., ADAMS, J. M. & STRASSER, A. 2003a. p53- and drug-induced apoptotic responses mediated by BH3-only proteins puma and noxa. *Science,* 302**,** 1036-8.

VILLUNGER, A., SCOTT, C., BOUILLET, P. & STRASSER, A. 2003b. Essential role for the BH3-only protein Bim but redundant roles for Bax, Bcl-2, and Bcl-w in the control of granulocyte survival. *Blood,* 101**,** 2393-2400.

VOGLER, M., BUTTERWORTH, M., MAJID, A., WALEWSKA, R. J., SUN, X. M., DYER, M. J. & COHEN, G. M. 2009. Concurrent up-regulation of BCL-XL and BCL2A1 induces approximately 1000-fold resistance to ABT-737 in chronic lymphocytic leukemia. *Blood,* 113**,** 4403-13.

VOSE, J., ARMITAGE, J. & WEISENBURGER, D. 2008. International peripheral T-cell and natural killer/T-cell lymphoma study: pathology findings and clinical outcomes. *J Clin Oncol,* 26**,** 4124-30.

WAGNER, K. U., CLAUDIO, E., RUCKER, E. B., 3RD, RIEDLINGER, G., BROUSSARD, C., SCHWARTZBERG, P. L., SIEBENLIST, U. & HENNIGHAUSEN, L. 2000. Conditional deletion of the Bcl-x gene from erythroid cells results in hemolytic anemia and profound splenomegaly. *Development,* 127**,** 4949-4958.

WANG, B., LI, X. Q., MA, X., HONG, X., LU, H. & GUO, Y. 2008. Immunohistochemical expression and clinical significance of P-glycoprotein in previously untreated extranodal NK/T-cell lymphoma, nasal type. *Am J Hematol,* 83**,** 795-9.

WANG, J. & QUAKE, S. R. 2014. RNA-guided endonuclease provides a therapeutic strategy to cure latent herpesviridae infection. *Proc Natl Acad Sci U S A,* 111**,** 13157-62.

WANG, S., ROWE, M. & LUNDGREN, E. 1997. Expression of Epstein-Barr virus transforming protein LMP1 causes a rapid and transient stimulation of the bcl-2 homologue Mcl-1 levels in B cell lines. *Cancer Research,* 56**,** 4610-4613.

WANG, X. & HUTT-FLETCHER, L. M. 1998. Epstein-Barr virus lacking glycoprotein gp42 can bind to B cells but is not able to infect. *Journal of Virology,* 72**,** 158-63.

WANG, Z., KARRAS, J. G., HOWARD, R. G. & ROTHSTEIN, T. L. 1995. Induction of bcl-x by CD40 engagement rescues sIg-induced apoptosis in murine B cells. *J Immunol,* 155**,** 3722-5.

WANG, Z. Y., LIU, Q. F., WANG, H., JIN, J., WANG, W. H., WANG, S. L., SONG, Y. W., LIU, Y. P., FANG, H., REN, H., WU, R. Y., CHEN, B., ZHANG, X. M., LU, N. N., ZHOU, L. Q. & LI, Y. X. 2012. Clinical implications of plasma Epstein-Barr virus DNA in early-stage extranodal nasal-type NK/T-cell lymphoma patients receiving primary radiotherapy. *Blood,* 120**,** 2003-10.

WEBER, A., BOGER, R., VICK, B., URBANIK, T., HAYBAECK, J., ZOLLER, S., TEUFEL, A., KRAMMER, P. H., OPFERMAN, J. T., GALLE, P. R., SCHUCHMANN, M., HEIKENWALDER, M. & SCHULZE-BERGKAMEN, H. 2010. Hepatocyte-specific deletion of the antiapoptotic protein myeloid cell leukemia-1 triggers proliferation and hepatocarcinogenesis in mice. *Hepatology,* 51**,** 1226-36.

WESTPHAL, D., KLUCK, R. M. & DEWSON, G. 2014. Building blocks of the apoptotic pore: how Bax and Bak are activated and oligomerize during apoptosis. *Cell Death Differ,* 21**,** 196-205.

WIECH, M., OLSZEWSKI, M. B., TRACZ-GASZEWSKA, Z., WAWRZYNOW, B., ZYLICZ, M. & ZYLICZ, A. 2012. Molecular mechanism of mutant p53 stabilization: the role of HSP70 and MDM2. *PLoS One,* 7**,** e51426.

WILL, B., SIDDIQI, T., JORDA, M. A., SHIMAMURA, T., LUPTAKOVA, K., STABER, P. B., COSTA, D. B., STEIDL, U., TENEN, D. G. & KOBAYASHI, S. 2010. Apoptosis induced by JAK2 inhibition is mediated by Bim and enhanced by the BH3 mimetic ABT-737 in JAK2 mutant human erythroid cells. *Blood,* 115**,** 2901-9.

WILLIAMS, H., MCAULAY, K., MACSWEEN, K. F., GALLACHER, N. J., HIGGINS, C. D., HARRISON, N., SWERDLOW, A. J. & CRAWFORD, D. H. 2005. The immune response to primary EBV infection: a role for natural killer cells. *Br J Haematol,* 129**,** 266-74.

WILLIS, S. N., CHEN, L., DEWSON, G., WEI, A., NAIK, E., FLETCHER, J. I., ADAMS, J. M. & HUANG, D. C. 2005. Proapoptotic Bak is sequestered by Mcl-1 and Bcl-xL, but not Bcl-2, until displaced by BH3-only proteins. *Genes Dev,* 19**,** 1294-305.

WILSON, J. B., BELL, J. L. & LEVINE, A. J. 1996. Expression of Epstein-Barr virus nuclear antigen 1 induces B cell neoplasia in transgenic mice. *European Molecular Biology Organisation Journal,* 15**,** 3117.

WILSON, W. H., O'CONNOR, O. A., CZUCZMAN, M. S., LACASCE, A. S., GERECITANO, J. F., LEONARD, J. P., TULPULE, A., DUNLEAVY, K., XIONG, H., CHIU, Y. L., CUI, Y., BUSMAN, T., ELMORE, S. W., ROSENBERG, S. H., KRIVOSHIK, A. P., ENSCHEDE, S. H. & HUMERICKHOUSE, R. A. 2010. Navitoclax, a targeted high-affinity inhibitor of BCL-2, in lymphoid malignancies: a phase 1 dose-escalation study of safety, pharmacokinetics, pharmacodynamics, and antitumour activity. *Lancet Oncol,* 11**,** 1149-59.

WONG, K. B., DEDECKER, B. S., FREUND, S. M., PROCTOR, M. R., BYCROFT, M. & FERSHT, A. R. 1999. Hot-spot mutants of p53 core domain evince characteristic local structural changes. *Proc Natl Acad Sci U S A,* 96**,** 8438-42.

YAMAGUCHI, M., KITA, K., MIWA, H., NISHII, K., OKA, K., OHNO, T., SHIRAKAWA, S. & FUKUMOTO, M. 1995. Frequent expression of P-glycoprotein/MDR1 by nasal T-cell lymphoma cells. *Cancer,* 76**,** 2351-6.

YAMAGUCHI, M., KWONG, Y. L., KIM, W. S., MAEDA, Y., HASHIMOTO, C., SUH, C., IZUTSU, K., ISHIDA, F., ISOBE, Y., SUEOKA, E., SUZUMIYA, J., KODAMA, T., KIMURA, H., HYO, R., NAKAMURA, S., OSHIMI, K. & SUZUKI, R. 2011. Phase II study of SMILE chemotherapy for newly diagnosed stage IV, relapsed, or refractory extranodal natural killer (NK)/T-cell lymphoma, nasal type: the NK-Cell Tumor Study Group study. *J Clin Oncol,* 29**,** 4410-6.

YAMAGUCHI, M., SUZUKI, R., KWONG, Y. L., KIM, W. S., HASEGAWA, Y., IZUTSU, K., SUZUMIYA, J., OKAMURA, T., NAKAMURA, S., KAWA, K. & OSHIMI, K. 2008. Phase I study of dexamethasone, methotrexate, ifosfamide, L-asparaginase, and etoposide (SMILE) chemotherapy for advanced-stage, relapsed or refractory extranodal natural killer (NK)/T-cell lymphoma and leukemia. *Cancer Sci,* 99**,** 1016-20.

YIN, X.-M., WANG, K., GROSS, A., ZHAO, Y., ZINKEL, S., KLOCKE, B., ROTH, K. A. & KORSMEYER, S. J. 1999. Bid-deficient mice are resistant to Fas-induced hepatocellular apoptosis. *Nature,* 400**,** 886-891.

YONG, W. H., UEKI, K., CHOU, D., REEVES, S. A., VON DEIMLING, A., GUSELLA, J. F., MOHRENWEISER, H. W., BUCKLER, A. J. & LOUIS, D. N. 1995. Cloning of a highly conserved human protein

serine-threonine phosphatase gene from the glioma candidate region on chromosome 19q13.3. *Genomics,* 29**,** 533-6.

YOSHIMORI, M., TAKADA, H., IMADOME, K., KURATA, M., YAMAMOTO, K., KOYAMA, T., SHIMIZU, N., FUJIWARA, S., MIURA, O. & ARAI, A. 2015. P-glycoprotein is expressed and causes resistance to chemotherapy in EBV-positive T-cell lymphoproliferative diseases. *Cancer Med,* 4**,** 1494-504.

YOSHIOKA, M., ISHIGURO, N., ISHIKO, H., MA, X., KIKUTA, H. & KOBAYASHI, K. 2001. Heterogeneous, restricted patterns of Epstein-Barr virus (EBV) latent gene expression in patients with chronic active EBV infection. *J Gen Virol,* 82**,** 2385-92.

YOULE, R. J. & STRASSER, A. 2008. The BCL-2 protein family: opposing activities that mediate cell death. *Nat Rev Mol Cell Biol,* 9**,** 47-59.

YOUNG, L. S. & RICKINSON, A. B. 2004. Epstein-Barr virus: 40 years on. *Nature Reviews Cancer,* 4**,** 757-68.

YOUNG, R. C. 1992. Etoposide in the treatment of non-Hodgkin's lymphomas. *Semin Oncol,* 19**,** 19-25.

YU, J., FREUD, A. G. & CALIGIURI, M. A. 2013. Location and cellular stages of natural killer cell development. *Trends Immunol,* 34**,** 573-82.

YU, J. & ZHANG, L. 2008. PUMA, a potent killer with or without p53. *Oncogene,* 27 Suppl 1**,** S71-83.

ZHA, J., HARADA, H., YANG, E., JOCKEL, J. & KORSMEYER, S. J. 1996. Serine phosphorylation of death agonist BAD in response to survival factor results in binding to 14-3-3 not Bcl-x_L. *Cell,* 87**,** 619-628.

ZHANG, B., KRACKER, S., YASUDA, T., CASOLA, S., VANNEMAN, M., HOMIG-HOLZEL, C., WANG, Z., DERUDDER, E., LI, S., CHAKRABORTY, T., COTTER, S. E., KOYAMA, S., CURRIE, T., FREEMAN, G. J., KUTOK, J. L., RODIG, S. J., DRANOFF, G. & RAJEWSKY, K. 2012. Immune Surveillance and Therapy of Lymphomas Driven by Epstein-Barr Virus Protein LMP1 in a Mouse Model. *Cell,* 148**,** 739-51.

ZHANG, H., GUTTIKONDA, S., ROBERTS, L., UZIEL, T., SEMIZAROV, D., ELMORE, S. W., LEVERSON, J. D. & LAM, L. T. 2011. Mcl-1 is critical for survival in a subgroup of non-small-cell lung cancer cell lines. *Oncogene,* 30**,** 1963-8.

ZHANG, J. H., CHUNG, T. D. & OLDENBURG, K. R. 1999. A Simple Statistical Parameter for Use in Evaluation and Validation of High Throughput Screening Assays. *J Biomol Screen,* 4**,** 67-73.

ZHANG, Y., ADACHI, M., KAWAMURA, R. & IMAI, K. 2005. Bmf is a possible mediator in histone deacetylase inhibitors FK228 and CBHA-induced apoptosis. *Cell Death Differ,* 13**,** 129-140.

ZHANG, Y., NAGATA, H., IKEUCHI, T., MUKAI, H., OYOSHI, M. K., DEMACHI, A., MORIO, T., WAKIGUCHI, H., KIMURA, N., SHIMIZU, N. & YAMAMOTO, K. 2003. Common cytological and cytogenetic features of Epstein-Barr virus (EBV)-positive natural killer (NK) cells and cell lines derived from patients with nasal T/NK-cell lymphomas, chronic active EBV infection and hydroa vacciniforme-like eruptions. *Br J Haematol,* 121**,** 805-14.

ZHANG, Z., SUBRAMANIAM, S., KALE, J., LIAO, C., HUANG, B., BRAHMBHATT, H., CONDON, S. G., LAPOLLA, S. M., HAYS, F. A., DING, J., HE, F., ZHANG, X. C., LI, J., SENES, A., ANDREWS, D. W.

& LIN, J. 2016. BH3-in-groove dimerization initiates and helix 9 dimerization expands Bax pore assembly in membranes. *EMBO J,* 35**,** 208-36.

ZHAO, B., MARSHALL, D. R. & SAMPLE, C. E. 1996. A conserved domain of the Epstein-Barr virus nuclear antigens 3A and 3C binds to a discrete domain of J kappa. *Journal of Virology,* 70**,** 4228-4236.

ZHENG, J. H., GRACE, C. R., GUIBAO, C. D., MCNAMARA, D. E., LLAMBI, F., WANG, Y. M., CHEN, T. & MOLDOVEANU, T. 2018. Intrinsic Instability of BOK Enables Membrane Permeabilization in Apoptosis. *Cell Rep,* 23**,** 2083-2094 e6.

ZHOU, P., LEVY, N. B., XIE, H., QIAN, L., LEE, C. Y., GASCOYNE, R. D. & CRAIG, R. W. 2001. *MCL1* transgenic mice exhibit a high incidence of B-cell lymphoma manifested as a spectrum of histologic subtypes. *Blood,* 97**,** 3902-3909.

ZHU, J., YAMANE, H. & PAUL, W. E. 2010. Differentiation of effector CD4 T cell populations (*). *Annu Rev Immunol,* 28**,** 445-89.

ZINKEL, S. S., HUROV, K. E., ONG, C., ABTAHI, F. M., GROSS, A. & KORSMEYER, S. J. 2005. A Role for Proapoptotic BID in the DNA-Damage Response. *Cell,* 122**,** 579-591.

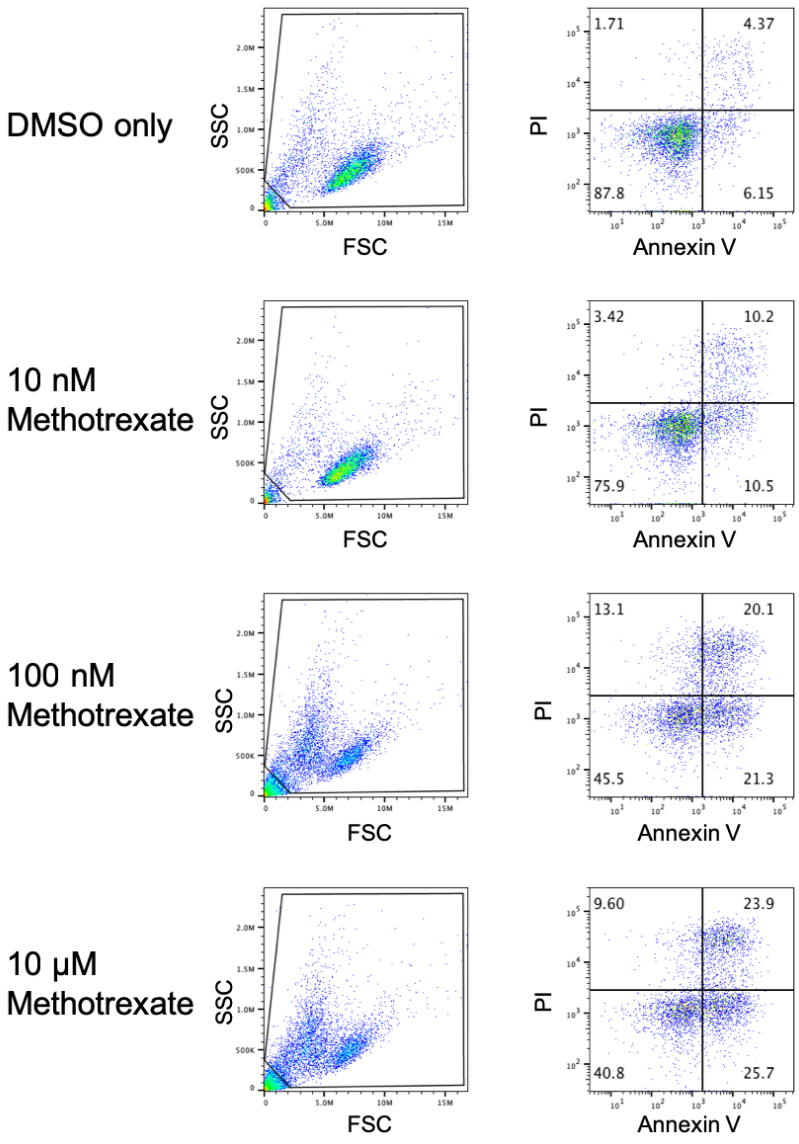
ZINKEL, S. S., ONG, C. C., FERGUSON, D. O., IWASAKI, H., AKASHI, K., BRONSON, R. T., KUTOK, J. L., ALT, F. W. & KORSMEYER, S. J. 2003. Proapoptotic BID is required for myeloid homeostasis and tumor suppression. *Genes Dev,* 17**,** 229-239.

ZONG, W. X., LINDSTEN, T., ROSS, A. J., MACGREGOR, G. R. & THOMPSON, C. B. 2001. BH3-only proteins that bind pro-survival Bcl-2 family members fail to induce apoptosis in the absence of Bax and Bak. *Genes Dev,* 15**,** 1481-1486.

ZUO, J., THOMAS, W. A., HAIGH, T. A., FITZSIMMONS, L., LONG, H. M., HISLOP, A. D., TAYLOR, G. S. & ROWE, M. 2011. Epstein-Barr virus evades CD4+ T cell responses in lytic cycle through BZLF1-mediated downregulation of CD74 and the cooperation of vBcl-2. *PLoS Pathog,* 7**,** e1002455.

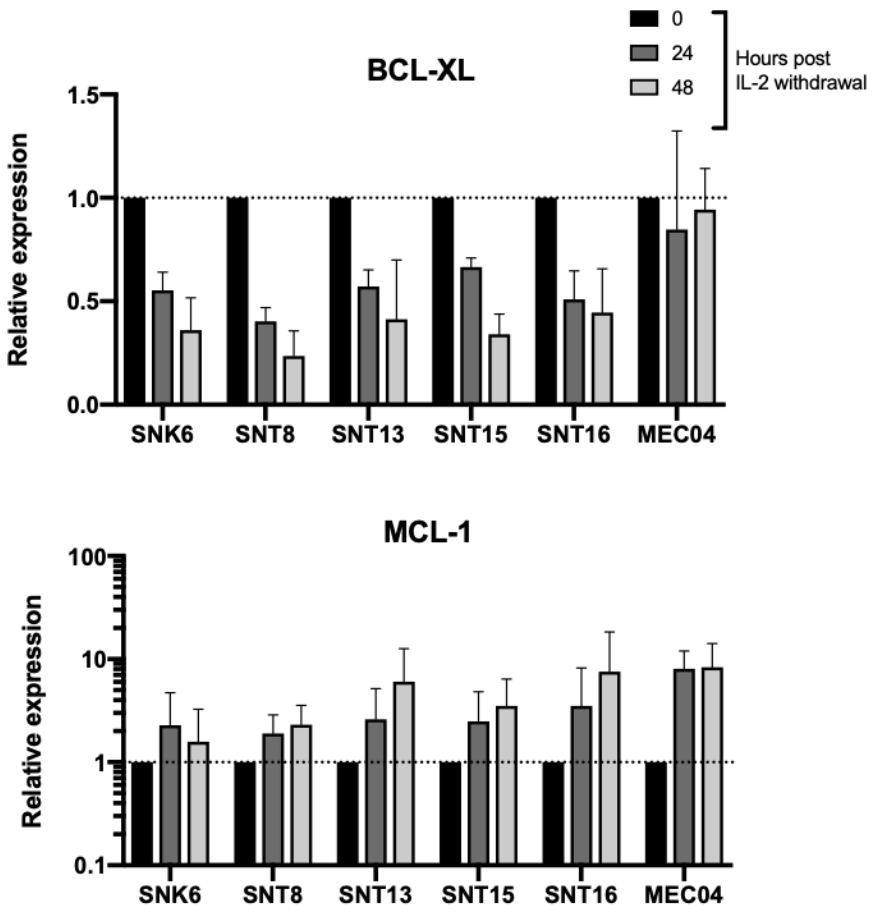
8. Appendices

8.1 Appendix I



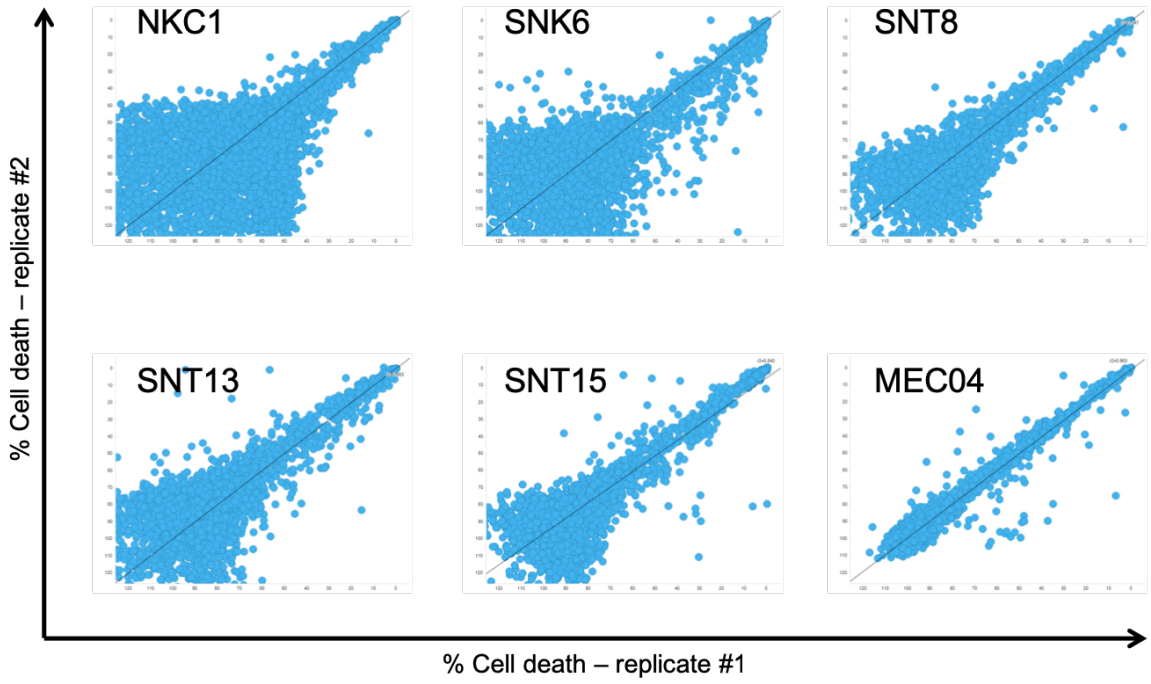
Supplementary figure 1 Viability of MEC04 cells following methotrexate treatment. MEC04 cells were treated with increasing concentrations of methotrexate for 48 hours then stained with Annexin V and propidium iodide (PI) prior to analysis by flow cytometry. Data shown here are representative flow cytometry plots from summary data presented in figure 4.1. Cells initially demonstrated sensitivity to methotrexate at low concentrations but lacked any further response above 100 nM.

8.2 Appendix II



Supplementary figure 2 Expression of pro-survival BCL-2 family members following IL-2 removal. A time course experiment was performed on EBV-positive T and NK cell lines at 24- and 48-hours post IL-2 withdrawal. IL-2-deprived cells were treated with 25 µM QVD-OPH (broad spectrum caspase inhibitor) at 0 h to prevent degradation of proteins due to apoptosis. Pro-survival proteins BCL-XL and MCL-1 were detected by Western blot analysis and quantified by densitometry. Data were normalised to loading control (HSP70) and the 0 hour control for each respective cell line. Data shown are the mean +/- standard deviation of three independent experiments.

8.3 Appendix III



Supplementary figure 3 Correlation between first and second replicates of primary screen for all compounds. 6 cell lines were subjected to the primary screen containing 4079 total compounds as described in Materials and Methods, **section 2.7**. CTG luminescence readings from positive (A-1331852 plus S63845) and negative controls (DMSO) were used to calculate minimum and maximum values for each cell line. CTG luminescence readings for test compounds were normalised using maximum and minimum values and viability percentages were plotted for both replicates. Cells were treated at a final drug concentration of 10 µM for 48 hours. CTG, CellTiter-Glo.

8.4 Appendix IV

Supplementary table 1 Detection of functional p-glycoprotein in EBV-positive T and NK cells

MFI of Rh-123 (mean of triplicates): Unstained cells, MFI-black

Biological replicate	SNK1	SNK6	SNT8	SNT13	SNT15	SNT16	MEC04	NKC1	Jurkat	KG-1
1	3997	2789	2620	1912	20300	9140	3723	2063	1532	1614
2	4252	4208	2064	3984	3535	9310	2174	3480	2121	27100
3	3727	2327	5402	1815	2333	1496	2770	1871	1837	1000

MFI of Rh-123 (mean of triplicates): Rh-123 stained cells with p-gp inhibitor (cyclosporin A), MFI-blue

Biological replicate	SNK1	SNK6	SNT8	SNT13	SNT15	SNT16	MEC04	NKC1	Jurkat	KG-1
1	1450000	785000	1180000	1310000	1370000	743000	594000	921000	603000	142000
2	852000	522000	1590000	871000	785000	750000	842000	682000	1260000	335000
3	2150000	992000	650000	1290000	1790000	1020000	615000	1330000	874000	140000

MFI of Rh-123 (mean of triplicates): Rh-123 stained cells, MFI-red

Biological replicate	SNK1	SNK6	SNT8	SNT13	SNT15	SNT16	MEC04	NKC1	Jurkat	KG-1
1	464000	67600	1150000	1390000	1250000	616000	116000	380000	484000	6264
2	343000	35000	1520000	667000	580000	624000	36600	324000	1200000	27500
3	883000	62500	542000	1230000	1640000	805000	35400	704000	637000	2201

Data shown here were used to generate normalised data presented in figure 4.3B. Raw median fluorescence intensity data was exported from flow cytometry analysis software. Mean values of technical replicates were calculated and shown above. Data were then processed using the following formula: (MFI-red x 100) / (MFI-blue – MFI-black); then the mean and standard deviation of the biological replicates were graphed in figure 4.3B.

8.5 Appendix V

Supplementary table 2 Binding affinities of BH3 mimetics to pro-survival BCL-2 family members

	Binding affinity, Ki (nM)				
BH mimetic	BCL-2	BCL-XL	BCL-W	MCL-1	Reference
ABT-199	< 0.010	48	245	> 444	Souers et al., 2013
ABT-737	≤ 1	≤ 1	≤ 1	> 1000	Oltersdorf et al., 2005
S63845	0.19 (Kd)	> 10,000	-	> 10,000	Kotschy et al., 2016
A1331852	6	< 0.010	4	142	Leverson et al., 2015a

Binding affinities are quoted as Ki values with the exception of S63845:MCL-1 which is quoted as Kd. The binding affinity of S63845 to BCL-W was not reported.